



UNIVERSITY *of the*
WESTERN CAPE

**Comparative Study of the Chemostratigraphic and Petrophysical characteristics of Wells
A-A1, A-L1, A-U1 and A-I1 in the Orange Basin, South Atlantic Margin, Offshore
South Africa.**

A Thesis in Petroleum Geosciences

By

CARLYNNE BAILEY

Submitted in partial fulfillment of the requirements for the degree of
Magister Scientiae in the Department of Earth Sciences,
University of the Western Cape

November 2009

Supervised by Professor Paul F. Carey
Co-Supervised by Prof Charles Okujeni



UNIVERSITY *of the*
WESTERN CAPE

UNIVERSITEIT VAN WES-KAAPLAND
BIBLIOTEEK
SS1.860968 BA1
LIBRARY
UNIVERSITY OF THE WESTERN CAPE

DECLARATION

I declare *Comparative Study of the Chemostratigraphic and Petrophysical characteristics of Wells A-A1, A-L1, A-U1 and A-II in the Orange Basin, South Atlantic Margin, Offshore South Africa* is my own work, that it has not been submitted before for any degree or examination in any other university, and that all the sources I have used or quoted have been indicated and acknowledged by means of complete references

Carlyne Bailey

November 2009



Signature

UNIVERSITY *of the*
WESTERN CAPE

**Comparative Study of Chemostratigraphy and the Petrophysical characteristics of
Wells A-A1, A-L1, A-U1 and A-I1 in the Orange Basin, South Atlantic Margin,
Offshore South Africa.**

Carlynnne Bailey

Keywords

Orange Basin, South Atlantic Margin

Chemostratigraphic modelling

Chemostratigraphic Indices

Principal Component Analysis

XRF Analysis

Well Logs

Neutron – Density Cross Plots

M-N plots

Geological Correlation



Abstract

Many hydrocarbon reservoirs are situated in barren sequences that display poor stratigraphic control. Correlation between the wells can become extremely difficult and traditional correlation techniques can prove to be inadequate. Past studies have shown that trace and major element concentrations can be used as a correlation tool. This practice of using geochemical fingerprints to characterize between wells is called Chemostratigraphic analysis. (Pearce et al, 1999)

Chemostratigraphy has been recognized as a very important correlation technique as it can be used for rocks of any age, in any geological setting as well as sequences that are traditionally defined as barren. Chemostratigraphic analyses can be used as a means of getting rid of ambiguities within data produced by traditional correlation methods such as Biostratigraphy, Lithostratigraphy and Geophysical Logging. In areas where stratigraphic data is not available it can be used to construct correlation frameworks for the sequences found in the area. The motivation behind this study is that the research is not only worthy of academic investigation, but can also provide the industry with new insights into areas that were previously misunderstood because traditional correlation methods were not adequate.

The study area, the Orange basin, is located offshore South Africa and is largely under-explored. The basin, that hosts two gas fields namely the Ibhubesi and the Kudu gas fields, has large potential but in the past has not been given due attention with only 34 wells being drilled in the area. The Orange basin has recently been the topic of investigation because of the belief that it may be hosts to more hydrocarbons.

This study will utilise Chemostratigraphy to attempt to provide geological information on this relatively under-explored basin. The aim of this research study is to produce a chemostratigraphic framework -scheme for the Orange Basin in order to facilitate reservoir scale interwell correlation. The Objectives of this research study will be to identify chemostratigraphic units or indices, to prove the adequate use of chemostratigraphy as an independent correlation technique and to integrate the chemostratigraphy and petrophysical characteristics of the four wells to facilitate lithological identification.

Element distribution Analysis was done on the data. This brought to the fore the dominance of SiO₂ across the samples for the four wells. Al₂O₃ concentrations were relatively high across the wells and were indicative of the clay rich nature of the samples. This also indicated that the samples were relatively immature.

Principal Component Analysis (PCA) plots were constructed for the purpose of identifying diametrical relationships between the elements or element clusters. These diametric relationships were in turn used to calculate the geochemical indices. The relative positions of the elements on the PCA plot highlighted the presence of alternating units of sandstone, feldspathic sandstone, calcareous clays and non calcareous clays within the samples. The PCA plots displayed diametric relationships between SiO_2 and the carbonate mineral clusters, SiO_2 and the clay mineral clusters, Nd and V, Nb and Ni, Zr and Co, Nb and Zn. SiO_2 and Co, Y and Pb, Zr and Sr, and lastly Nb and Rb.

Downhole plots were constructed to illustrate recognizable trends in the PCA plot and to relate this to the occurrence of various lithologies in the wells. Based on the element distribution patterns, PCA plots and Major and Trace element downhole profiles geochemical indices were calculated. They are grouped into three clusters, ratios indicative of the presence of clean sandstones (High $\text{SiO}_2/\text{Al}_2\text{O}_3$, SiO_2/Co , Zr/Co , Zr/Sr , Y/Pb and low Nd/V values); ratios indicative of the presence of clays (Low $\text{SiO}_2/\text{Al}_2\text{O}_3$, $\text{Fe}_2\text{O}_3/\text{Al}_2\text{O}_3$, SiO_2/Co , Zr/Co , Y/Pb and high Rb/Zn values); thirdly those indicative of the presence of feldspathic sandstones (High $\text{Na}_2\text{O}/\text{K}_2\text{O}$) and lastly those indicative of the presence of carbonates (low Zr/Sr).

Using the geochemical Indices six units were identified in Well A-A1, nine in A-I1 and 8 in Well A-U1 and A-L1. Four units (A-D) were found to correlate across the wells.

Well log interpretation for the Wells A-A1, A-I1, A-L1 and A-U1 started with a general overview of the log responses. The log responses for the four wells highlighted the presence of sandstones, argillaceous sandstones, shales and shale components. Geophysical units were identified using the logs responses. Six units were identified in Well A-A1, nine in Well A-I1 and eight in Wells A-L1 and A-U1. These units coincide with the units identified using Chemostratigraphic analysis. Neutron – Density cross plots were constructed for each unit across the four wells. The plotting of the points on the Neutron – Density cross plots for the wells A-A1, A-I1, A-L1 and A-U1 indicated the presence of sandstones, shales or greywackes and either limestones and dolomites but from the geochemistry it is known that neither limestone nor dolomite is present in the wells and it was thus inferred that the points plotting between the limestone and dolomite lithology curves indicated the presence of calcareous shales. M-N plots were constructed for each unit. The patterns exhibited by the points on the M-N plots for the wells was indicative of the presence calcareous clays, sandstones, greywacke and shales.

The Chemostratigraphic and Petrophysical results produced accurate and comparable results, however, the Chemostratigraphic analysis provided finer details regarding the lithology of the units. Based on the well log responses no distinction could be made between highly feldspathic sandstone, arkosic and argillaceous sandstone, while these distinctions were possible when analyzing the samples using Chemostratigraphy. The geochemistry was capable of providing signatures in areas where the wireline tools malfunctioned. The logs, on the other hand, sheds light on properties such as porosity and permeability of the rocks which cannot be obtained accurately from the geochemistry.

When comparing the correlation capabilities of these two techniques, the one based on geochemical signatures and the other based on the responses obtained from wireline tools, it is important to acknowledge that both these techniques has strengths and weaknesses. The best of both these techniques can only be fully utilised when either technique is used in conjunction with other techniques.

With respect to the Orange Basin, located offshore South Africa, it can be concluded that the dominant lithologies in the basin are sandstones, argillaceous sandstones, shales, feldspathic and arkosic sandstones and clays. In terms of petroleum prospectivity the sandstones in Wells A-A1, A-I1, A-U1 and A-L1 could possibly be considered to be reservoirs and the shales could be considered to be seals or source rocks, depending on the organic matter content. On the down side, the sandstones display relatively poor permeabilities and the porosities are variable. The density logs indicate that the sandstones are highly compacted and that could be an indication of poor porosities but more research needs to be done. Another factor highlighted from the research is the presence of alternating lithologies. This means that the reservoirs are compartmentalised and that the area has a high degree of heterogeneity.

ACKNOWLEDGEMENTS

I would like to express my sincere gratitude and appreciation to my supervisor, Prof Paul Carey. You have guided me through my studies and willingly shared your knowledge. Thank you for all your assistance and patience through the years.

My thanks to my co-supervisor Prof C. Okujeni for his unconditional assistance and constructive remarks through the duration of this research project.

My heartfelt thanks to my family for all their love, unconditional support and words of encouragement.

A special thanks to my dear friend, Miss Y. Hoosain for all your support and motivation through the years.



UNIVERSITY of the
WESTERN CAPE

Lastly, I would like to thank God for blessing me with the opportunity to pursue my studies and for carrying me through the years.

Table of Contents

DECLARATION.....	II
KEYWORDS.....	III
ABSTRACT.....	IV
ACKNOWLEDGEMENTS.....	VI
TABLE OF CONTENTS.....	VII

Chapter 1: General Introduction.....	2
1.1 Thesis Layout	2
1.2 Introduction	3
1.3 Rationale/Background	4
1.4 Aims and Objectives	5
1.5 Location of Study Area	5
1.6 Literature Review	6
1.6.1 Orange Basin	6
1.6.2 Chemostratigraphy	8
1.6.2.1 Introduction to Chemostratigraphy	8
1.6.2.2 Previous Work	9
Chapter 2: Regional Geology.....	10
2.1 Tectonic Setting	13



2.2 Depositional Environments and Stratigraphy	14
2.2.1 Depositional Environments	14
2.2.2 Stratigraphy of the Orange Basin	14
2.3 Petroleum Elements	17
2.3.1 Introduction to Petroleum Elements	17
2.3.1.1 Source Rocks	17
2.3.1.2 Reservoir Rocks	18
2.3.1.3 Traps	18
2.3.1.4 Seals	18
2.3.1.5 Petroleum System	18
2.3.2 Petroleum Elements of the Orange Basin	18
2.3.2.1 Source Rocks	18
2.3.2.2 Reservoir Rocks	19
2.3.2.3 Traps	19
2.3.2.4 Seals	19
2.3.3 Petroleum Systems in the Orange Basin	19
Chapter 3: Methodology	21
3.1 Well Selection	21
3.2 Sample Selection	22
3.3 Sample Preparation	23
3.4 Data Acquisition	23
3.5 Quality Control	23




3.6 Data Interpretation	24
3.6.1 Chemostratigraphy	24
3.6.2 Well log Interpretation	26
Chapter 4: Chemostratigraphy.....	28
4.1 Element Distributions Patterns	29
4.1.1 Results	29
4.1.1.1 Well A-A1	29
4.1.1.2 Well A-I1	31
4.1.1.3 Well A-L1	32
4.1.1.4 Well A-U1	34
4.1.1.5 Overview of Element Distribution Patterns	37
4.1.2 Discussion	39
4.1.1.1 Well A-A1	39
4.1.1.2 Well A-I1	39
4.1.1.3 Well A-L1	40
4.1.1.4 Well A-U1	40
4.2 Principal Component Analysis	41
4.2.1 Results	42
4.1.1.1 Well A-A1	42
4.1.1.2 Well A-I1	43
4.1.1.3 Well A-L1	44



4.1.1.4 Well A-U1	45
4.2.2 Discussion	46
4.1.1.1 Well A-A1	46
4.1.1.2 Well A-I1	47
4.1.1.3 Well A-L1	49
4.1.1.4 Well A-U1	50
4.2.3 Summary	52
4.3 Major and Trace Element Profiles	53
4.3.1 Results	53
4.3.1.1 Well A-A1	53
4.3.1.2 Well A-L1	57
4.3.1.3 Well A-U1	59
4.3.1.4 Well A-I1	64
4.3.2 Discussion	67
4.3.2.1 Well A-A1	67
4.3.2.2 Well A-L1	67
4.3.2.3 Well A-U1	68
4.3.2.4 Well A-I1	70
4.3.3 Summary	71
4.4 Element Ratio Profiles	72
4.4.1 Introduction	72



4.4.2 Results	6
4.4.2.1 Well A-A1	76
4.4.2.2 Well A-L1	78
4.4.2.3 Well A-U1	82
4.4.2.4 Well A-I1	85
4.4.2.5 Correlated Units	88
4.4.3 Discussion	91
4.4.3.1 Well A-A1	91
4.4.3.2 Well A-L1	93
4.4.3.3 Well A-U1	95
4.4.3.4 Well A-I1	97
4.4.3.5 Correlated Units	99
4.4.4 Summary	102
 UNIVERSITY of the WESTERN CAPE	
Chapter 5: Well Log Interpretation.....	104
5.1 Theoretical Background	104
5.1.1 Gamma Ray	105
5.1.2 Spontaneous Potential Log	105
5.1.3 Neutron Log	106
5.1.4 Density Log	107
5.1.5 Sonic Log	107

5.2 General Overview of Well Logs	108
5.2.1 Results	108
5.2.1.1 Well A-A1	108
5.2.1.2 Well A-I1	108
5.2.1.3 Well A-L1	111
5.2.1.4 Well A-U1	113
5.2.2 Discussions	115
5.2.1.1 Well A-A1	115
5.2.1.2 Well A-I1	115
5.2.1.3 Well A-L1	116
5.2.1.4 Well A-U1	117
5.3 Geophysical Units	118
5.3.1 Results	118
5.3.1.1 Well A-A1	118
5.3.1.2 Well A-I1	120
5.3.1.3 Well A-L1	122
5.3.1.4 Well A-U1	123
5.3.2 Discussions	126
5.3.2.1 Well A-A1	126
5.3.2.2 Well A-I1	127
5.3.2.3 Well A-L1	128
5.3.2.4 Well A-U1	129



UNIVERSITY *of the*
WESTERN CAPE

5.4 Neutron Density Cross Plots	131
5.4.1 Results	131
5.4.1.1 Well A-A1	131
5.4.1.2 Well A-I1	132
5.4.1.3 Well A-L1	134
5.4.1.4 Well A-U1	136
5.4.1.5 Correlated Units	138
5.4.1.5.1 Unit A	138
5.4.1.5.2 Unit B	139
5.4.1.5.3 Unit C	140
5.4.1.5.4 Unit D	141
5.4.2 Discussions	142
5.4.2.1 Well A-A1	142
5.4.2.2 Well A-I1	143
5.4.2.3 Well A-L1	143
5.4.2.4 Well A-U1	144
5.4.2.5 Correlated Units	146
5.4.2.5.1 Unit A	146
5.4.2.5.2 Unit B	146
5.4.2.5.3 Unit C	147
5.4.1.5.4 Unit D	147



UNIVERSITY *of the*
WESTERN CAPE

5.5 N/M PLOTS	148
5.5.1 Results	150
5.5.1.1 Well A-A1	150
5.5.1.2 Well A-I1	151
5.5.1.3 Well A-L1	154
5.5.1.4 Well A-U1	156
5.5.1.5 Correlated Units	158
5.5.1.5.1 Unit A	158
5.5.1.5.2 Unit B	160
5.5.1.5.3 Unit C	162
5.5.1.5.4 Unit D	164
5.5.2 Discussions	166
5.5.2.1 Well A-A1	166
5.5.2.2 Well A-I1	166
5.5.2.3 Well A-L1	167
5.5.2.4 Well A-U1	168
5.5.2.5 Correlated Units	169
5.5.2.5.1 Unit A	169
5.5.2.5.2 Unit B	169
5.5.2.5.3 Unit C	170
5.5.2.5.4 Unit D	170
5.6 Summary	172



UNIVERSITY *of the*
WESTERN CAPE

Chapter 6 Comparison of Chemostratigraphic and Petrophysical Results.....	174
6.1 General Overview and Comparison of the Chemostratigraphic and Petrophysical Characteristics of Wells A-A1, A-I1, A-L1 and A-U1	174
6.1.1 Results	
6.1.1.1 Well A-A1	
6.1.1.1.1 Chemostratigraphic Results	174
6.1.1.1.2 Petrophysical Results	175
6.1.1.2 Well A-I1	
6.1.1.2.1 Chemostratigraphic Results	175
6.1.1.2.2 Petrophysical Results	176
6.1.1.3 Well A-L1	
6.1.1.3.1 Chemostratigraphic Results	176
6.1.1.3.2 Petrophysical Results	177
6.1.1.4 Well A-U1	
6.1.1.4.1 Chemostratigraphic Results	177
6.1.1.4.2 Petrophysical Results	178
6.1.2 Discussion	179
6.1.2.1 Well A-A1	179
6.1.2.2 Well A-I1	179
6.1.2.3 Well A-L1	180
6.1.2.4 Well A-U1	180



**6.2 Comparison of the Chemostratigraphic and Petrophysical Units of Wells A-A1, A-I1
A-L1 and A-U1**

6.2.1 Well A-A1	182
6.2.2 Well A-I1	183
6.2.3 Well A-L1	188
6.2.4 Well A-U1	193
6.2.5 Correlated Units	198
6.2.5.1 Unit A	198
6.2.5.2 Unit B	19
6.2.5.3 Unit C	199
6.2.5.4 Unit D	199



6.3 Correlation Framework 201

Chapter 7 Conclusions and Recommendation..... 203

7.1 Conclusions 203

7.1.1 Chemostratigraphy 203

7.1.2 Petrophysical 204

7.1.3 Discussion of Chemostratigraphic and Petrophysical Conclusions 205

7.2 Recommendations 207

REFERENCES 209

APPENDICES 214

List of Figures

Chapter 1

- 1.1 Map illustrating the location of the Orange Basin along the southwestern margin of South Africa (*modified from van der Spuy et al, 2003*)..... 6

Chapter 2

- 2.1 Figure 2.1 Map illustrating the locations of South Africa's offshore basins.

A shows the position of the Orange Basin on the western offshore, B – Bredasdorp, Pletmos, Gamtoos, Algoa and Outeniqua basins found on the southern offshore area and C- Durban and Zululand Basins found on the eastern offshore.

(*Modified from van Der Spuy, 2003*).....11

- 2.2 Figure 2.2 Map illustrating the topography of South Africa's continental margin and sea floor. The map is derived from satellite-altimetry imagery.

(*Broad, 2007*).....12

- 2.3 Figure 2.3 Location of the Orange basin that formed as a result of rifting of the South American (left) and African plates (right).

(*Modified from van der Spuy et al, 2007*)..... 13

- 2.4 Schematic Cross Section through the Orange Basin (*modified from Junslager, 1999*)....14

- 2.5 Map showing the showing the locations of the Kudu arch in the north and

the Agulhas- Columbine Arch to the south. Also illustrated is the position of the Orange River, the main contributor of sediments to the Orange basin.

(Modified from van der Spuy, 2007)..... 15

2.6 Stratigraphic Column of the Orange Basin..... 17

Chapter 3

3.1 Map illustrating the locations of Wells A-A1, A-I1, A-U1 and A-L1 21

Chapter 4

4.2.1 PCA plot of the major and trace elements for Well A-A1 42

4.2.2 PCA plot of the major and trace elements for Well A-I1. 43

4.2.3 PCA plot of the major and trace elements for Well A-L1. 44

4.2.4 PCA plot of the major and trace elements for Well A-U1. 45

4.2.5 PCA plot of the major and trace elements for Well A-A1 with interpreted clusters. 46

4.2.6 PCA plot of the major and trace elements for Well A-I1 with interpreted clusters. 48

4.2.7 PCA plot of the major and trace elements for Well A-L1 with interpreted clusters. 49

4.2.8 PCA plot of the major and trace elements for Well A-U1 with interpreted clusters. 51

4.3.1 Major Element Profile for Well A-A1 55

4.3.2 Trace Element Profile for Well A-A1 56

4.3.3 Major Element Profile for Well A-L1 (section 1) 58

4.3.4 Major Element Profile for Well A-L1 (section 2) 58

4.3.5 Trace Element Profile for Well A-L1 (section 1) 60

4.3.6 Trace Element Profile for Well A-L1 (section 2)	60
4.3.7 Major Element Profile for Well A-U1 (section 1)	61
4.3.8 Major Element Profile for Well A-U1 (section 2)	61
4.3.9 Trace Element Profile for Well A-U1 (section 1)	63
4.3.10 Trace Element Profile for Well A-U1 (section 2)	63
4.3.11 Major Element Profile for Well A-I1	65
4.3.12 Trace Element Profile for Well A-I1	66
4.4.1 Element Ratio Profile for Well A-A1	77
4.4.2 Element Ratio Profile for Well A-L1 (section 1)	80
4.4.3 Element Ratio Profile for Well A-L1 (section 2)	80
4.4.4 Element Ratio Profile for Well A-U1 (section 1)	83
4.4.5 Element Ratio Profile for Well A-U1 (section 2)	83
4.4.6 Element Ratio Profile for Well A-I1	86

Chapter 5

5.2.1 General Overview of the well logs for Well A-A1	109
5.2.2 General Overview of the well logs for Well A-I1	110
5.2.3 General Overview of the well logs for Well A-L1 (section 1)	111
5.2.4 General Overview of the well logs for Well A-L1 (section 2)	112
5.2.5 General Overview of the well logs for Well A-U1 (section 1)	113
5.2.6 General Overview of the well logs for Well A-U1 (section 2)	114

5.3.1 Geophysical Units of Well A-A1	119
5.3.2 Geophysical Units of Well A-I1	121
5.3.3 Geophysical Units of Well A-L1 (section 1)	122
5.3.4 Geophysical Units of Well A-L1 (section 2)	123
5.3.5 Geophysical Units of Well A-U1 (section 1)	124
5.3.6 Geophysical Units of Well A-U1 (section 2)	125
5.4.1 Neutron – Density Cross Plots for (A) Unit 1 and (B) Unit 2 of Well A-A1.	131
5.4.2 Neutron – Density Cross Plots for (A) Unit 1 and (B) Unit 2 of Well A-I1.	132
5.4.3 Neutron – Density Cross Plots for (C) Unit 3, (D) Unit 4 and (E) Unit 5 of Well A- I1.	133
5.4.4 Neutron – Density Cross Plots for (A) Unit 1 and (B) Unit 2 of Well A-L1.	134
5.4.5 Neutron – Density Cross Plots for (C) Unit 3 and (D) Unit 4 of Well A-L1.	135
5.4.6 Neutron – Density Cross Plots for (A) Unit 1, (B) Unit 2, (C) Unit 3 and (D) Unit 4 of Well A-U1.	136
5.4.7 Neutron – Density Cross Plot for Unit A	138
5.4.8 Neutron – Density Cross Plot for Unit B	139
5.4.9 Neutron – Density Cross Plot for Unit C	140
5.4.10 Neutron – Density Cross Plot for Unit D	141
5.5 Figure 5.5: M-N Cross plots indicating the positions of minerals as defined by Schlumberger. (<i>Modified from Schlumberger, 1995</i>)	149
5.5.1 M/N Plots for Unit 1 (A) and Unit 2 (B) of Well A-A1.	150

5.5.2 M/N Plots for Unit 1 (A) and Unit 2 (B) of Well A-I1.	151
5.5.3 M/N Plots for Unit 3 (C) and Unit 4 (D) of Well A-I1.	152
5.5.4 M/N Plots for Unit 5 of Well A-I1	153
5.5.5 M/N Plots for Unit 1 (A) and Unit 2 (B) of Well A-I1.	154
5.5.6 M/N Plots for Unit 3 (C) and Unit 4 (D) of Well A-L1	155
5.5.7 M/N Plots for Unit 1 (A) and Unit 2 (B) of Well A-U1.	156
5.5.8 M/N Plots for Unit 3 (C) and Unit 4 (D) of Well A-U1.	157
5.5.9 M/N Plots for Well A-A1 (A) and Well A-L1 (B) of Unit A.	158
5.5.10 M/N Plots for Well A-I1 (C) and Well A-U1 (D) of Unit A.	159
5.5.11 M/N Plots for Well A-A1 (A) and Well A-L1 (B) of Unit B.	160
5.5.12 M/N Plots for Well A-I1 (C) and Well A-U1 (D) of Unit B.	161
5.5.13 M/N Plots for Well A-A1 (A) and Well A-I1 (B) of Unit C.	162
5.5.14 M/N Plot for Well A-L1 of Unit C.	163
5.5.15 M/N Plots for Well A-A1 (A) and Well A-L1 (B) of Unit D.	164
5.5.16 M/N Plots for Well A-I1 (C) and Well A-U1 (D) of Unit D.	165

Chapter 6

6.1. Comparison of the Chemostratigraphic Units (A) and the Petrophysical Units (B) for Well A-A1.	184
6.2. Comparison of the Chemostratigraphic Units (A) and the Petrophysical Units (B) for Well A-I1.	186
6.3. Comparison of the Chemostratigraphic Units (A) and the Petrophysical Units (B) for Well A-L1 (section 1).	189

6. 4. Comparison of the Chemostratigraphic Units (A) and the Petrophysical Units (B) for Well A-L1 (section 2).	191
6. 5. Comparison of the Chemostratigraphic Units (A) and the Petrophysical Units (B) for Well A-U1 (section 1).	194
6.6. Comparison of the Chemostratigraphic Units (A) and the Petrophysical Units (B) for Well A-U1 (section 1).	196
6.7 Schematic Correlation Framework for Wells A-A1, A-L1, A-U1 and A-I1 constructed using the Chemostratigraphic results.	201



UNIVERSITY *of the*
WESTERN CAPE

SECTION 1

Chapter 1 Introduction

Chapter 2 Geology of the Orange Basin

Chapter 3 Methodology



UNIVERSITY *of the*
WESTERN CAPE

CHAPTER 1 GENERAL INTRODUCTION

1.1 THESIS LAYOUT

The thesis is divided into 3 sections.

Section 1 serves as an introduction to the study, location and geology of the study area and the methodology to be followed. Part 1 is made up of Chapter 1, 2 and 3

- Chapter 1 gives an introduction to the study, the motivation behind the study, and the aims and objectives of the study. A summary of the location of the study area is also presented. This chapter ends with a synopsis of the literature consulted regarding the Orange basin and the process of Chemostratigraphy.
- Chapter 2 discusses the general geology of the Orange Basin. This chapter focuses on the tectonic setting, depositional history and Stratigraphy and petroleum elements of the Orange Basin. This chapter also provides a summary of the elements of petroleum systems.
- Chapter 3 discusses the materials and methods that are used during the project. It focuses on aspects such as well selection, sample selection, analytical procedures and quality control.

Section 2 focuses on the results and discussions pertaining to the study and is composed of Chapters 4, 5 and 6

- Chapter 4 deals with the Chemostratigraphic analysis
- Chapter 5 focuses on the integration of the Chemostratigraphic results with the wireline logs of the wells selected for this study. It also aims to explain the differences and/or similarities that may exist between the different correlation techniques.
- Chapter 6 focuses on the comparison of the Chemostratigraphic and Petrophysical results.

Section 3 of the thesis deals with the conclusions and recommendations and consists of Chapter 7.

- Chapter 7 discusses conclusions and recommendations regarding the use of Chemostratigraphy as a correlation tool as well as conclusions and recommendations on the petroleum prospectivity of this part of the Orange basin that are drawn from this study.

1.2 INTRODUCTION

Current oil reserves are rapidly becoming depleted due to an increase in the demand for petroleum products. This is accompanied by the fact that new petroleum plays are becoming increasingly arduous to unearth. This state of affairs has compelled the petroleum industry to turn to so called non traditional techniques that would enable them to discover, characterize and produce from new oil fields and also to characterize and augment production from existing oil fields within minimal time and also being cost effective.

An important part of reservoir characterization is the process of correlation. Correlation of the sedimentary successions can provide the geologist with information such as the lateral extent of the reservoir, and the precise chemical make up of the reservoir. This study focuses on a sub division of correlation, namely Chemostratigraphy. Chemostratigraphy uses the inorganic geochemistry of the rock type and then correlates on the basis of varying elemental composition.

Chemostratigraphy has been recognized as a very important correlation technique as it can be used for rocks of any age, in any geological setting as well as successions that are traditionally defined as barren. In the past Chemostratigraphy was not widely used due to technological restrictions. Elements are absorbed using Atomic Absorption Spectrometry, a process that allowed for the analysis of only one element at a time. This procedure is found to be both time-consuming and costly hence Chemostratigraphy is not widely used. Recent technological advances led to the development of the ICP-MS and X- Ray Fluorescence, both of which allow for the analysis of approximately 50 elements during a single run. This led to renewed interest in Chemostratigraphy as a correlation technique.

The study area, the Orange basin, is located offshore South Africa and is largely under-explored. The basin, that hosts two gas fields namely the Ibhubesi and the Kudu gas fields, has large potential but in the past has not been given due attention with only 34 wells being

drilled in the area. The Orange basin has recently been the topic of investigation because of the belief that it may be hosts to more hydrocarbons.

This study utilises Chemostratigraphy to attempt to provide information on this relatively under-explored basin. Another objective is to prove the adequate use of Chemostratigraphy as a correlation tool. The main outcome of this study will be a chemostratigraphic framework that will be generated for the reservoirs within the basin.

1.3 RATIONALE/ BACKGROUND

Many hydrocarbon reservoirs are situated in barren sequences that display poor stratigraphic control. Correlation between the wells can become extremely difficult and traditional correlation techniques can prove to be inadequate. Past studies (*see Bibliography*) have shown that trace and major element concentrations can be used as a correlation tool. This practice of using geochemical fingerprints to characterize between wells is called Chemostratigraphic analysis. (*Pearce et al, 1999*)

Chemostratigraphic analyses can be used as a means of getting rid of ambiguities within data produced by traditional correlation methods such as Biostratigraphy, Lithostratigraphy and Geophysical Logging. In areas where stratigraphic data is not available it can be used to construct correlation frameworks for the sequences found in the area.

The geochemical make up of sediments is highly variable and can be affected by the slightest change in their composition. This means that successions that appear to be uniform will display differences in the chemistry of their constituent minerals or in the ratios of heavy minerals and clay minerals. Each of the minerals possesses trace element content. The ability to identify and characterize the geochemical changes within uniform successions allows components these successions to be characterized and allows correlation between wells. (*Pearce et al, 1999*)

The motivation behind this study is that the research is not only worthy of academic investigation, but can also provide the industry with new insights into areas that are previously misunderstood because traditional correlation methods are not adequate.

1.4 AIMS AND OBJECTIVES

The aim of this research study is to produce a Chemostratigraphic framework for the Orange Basin in order to facilitate reservoir scale interwell correlation.

The objectives of this research study are to:

- ❖ Identify geochemical units
- ❖ Prove the use of Chemostratigraphy as an independent correlation tool.
- ❖ Comparison of the Chemostratigraphic and the petrophysical characteristics of these wells.

1.5 LOCATION OF STUDY AREA

The Orange basin is located on the Southern Atlantic margin offshore South Africa. The basin is the largest of the South African offshore basins and has an areal extent of approximately 160 000km².

The Orange basin is bounded on the north by the Kudu Arch and in the south western region by the Agulhas Columbine Arch. These arches are basement highs that are composed of sedimentary sediments, granites as well as metamorphic rocks (*Ransome et al, 1992*). The Orange basin is defined by the areal extent and thickness of the post – rift sedimentary successions that are found off the west coast of Namibia.

The basin is divided into the northern Orange Basin that reaches the coast of Namibia and hosts the Kudu gas field, and the southern Orange Basin, the location for this study, which is located along the western boundary of South Africa and hosts the Iubhesi gas field.

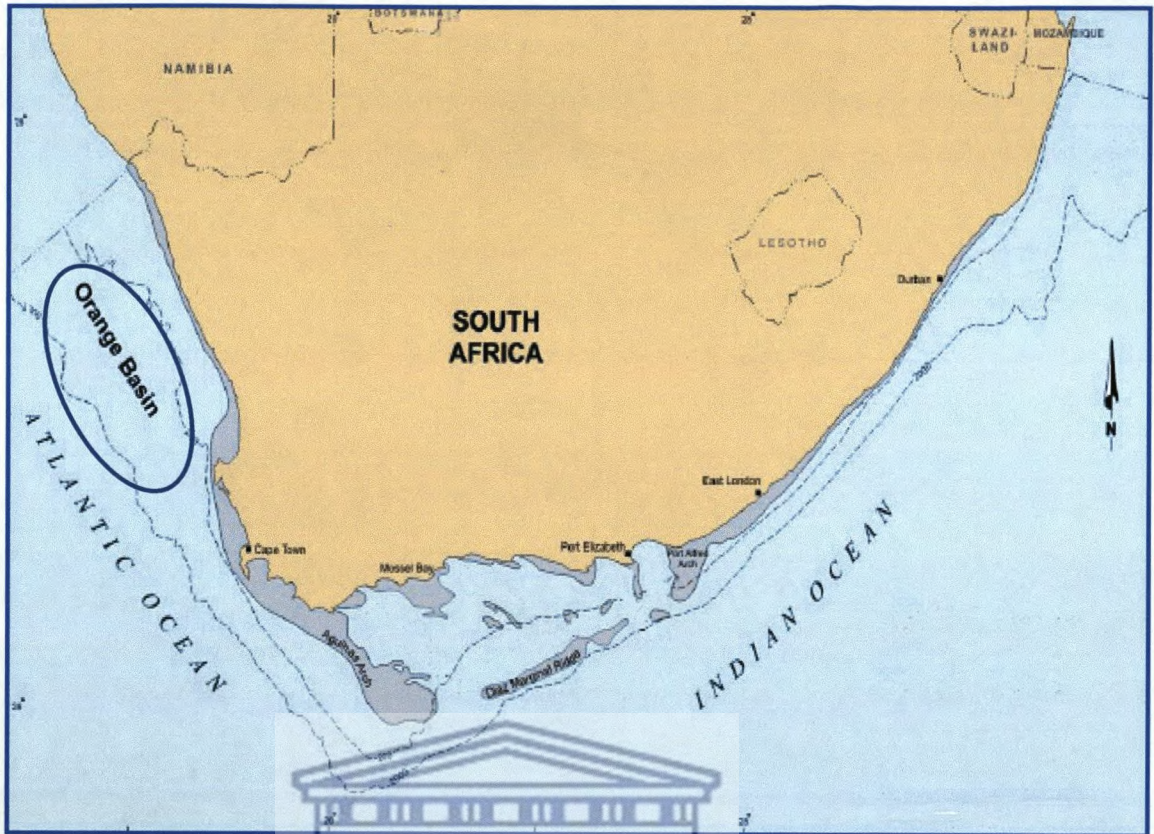


Figure 1.1: Map illustrating the location of the Orange Basin along the western margin of South Africa. (Modified from van Der Spuy, 2007)

1.6 Literature Review

1.6.1 ORANGE BASIN

Literature consulted for this topic discussed the geology, stratigraphy, palaeogeography, structural features and petroleum elements of the Orange Basin and the South Atlantic margin.

The South Atlantic margin is a divergent plate margin that formed as a result of rifting. According to *Clemson et al, 1997* three rifting phases occurred. The first phase of rifting is characterized by the occurrences of faulting and the presence of seismic packages that have been interpreted as moving in an easterly direction away from the direction of faulting. The second phase is characterized by seismic reflections that deviate from the hinge line in a westerly direction. The third phase is characterized by seismic packages that display trends of deviating in a westerly direction. Thickening of these seismic packages increases away from the hinge line.

Junslanger et al, 1999 recognized three sliding events of the paleo-shelf and slope. The first sliding event occurred during the early Turonian period, this is followed by the second event during the Campanian and the last sliding event occurred during the Cretaceous to Tertiary periods. These sliding events are important from a petroleum perspective as the detachments that originated during these slides may have led to the deposition of organic rich shales during the global anoxic event.

The margin is divided into four basins, namely the Orange Basin, Luderitz Basin, Walvis Basin and Namibe Basin. According to *Gallagher and Barton* the main depocentres of these basins contains thick successions of clastic sediments and volcanics. Sedimentation within these basins are dominated by oxidized, terrestrial, volcanoclastic sandstones, evaporates and subaerial volcanics.

The main structural controls on sedimentation along the continental margin of south-west Africa is the presence of graben and horsts that trends north-south and a large east-west trending graben and horst structure (*Dingle et al, 1993*).

According to *Dingle et al, 1993* the Orange basin extends for approximately 500km trending NNW-SSE on the continental crust and that it has spilled onto the COB. The Orange Basin contains approximately 4.2km of pre All strata. In the southern half of the basin the Orange basin is defined by two basinal areas namely the inner graben complex and the main basin.

The stratigraphy of the Orange Basin is discussed by *Dingle et al, 1993*. The proximal areas of the Orange Basin are characterized by isopach maps that display variable thicknesses and the sequences are composed of volcanoclastics that are interspersed with continental sediments. In the easterly direction the successions are composed of thin continental red beds, while in the westerly direction the successions are composed of grey restricted marine and lathstring sandstones. Within this basin a north south trending facies change is evident. The Barremian sequences are composed of continental sandstones interbedded with lava, and Albian-Maastrichtian sequences are composed of marine sandstones. The distal parts of the basin are composed of sequences of continental sandstones and shales interbedded with lava.

A total of 34 exploration wells have been drilled in the Orange Basin. This led to the discovery of two gas fields namely the Ihubesi and the Kudu gas fields. From a petroleum perspective, the source rocks in the Orange Basin ranges from dry gas prone, wet gas prone to oil prone. The source rocks have thicknesses ranging from 30m to approximately 90 m

with a maximum thickness of 140m and they display hydrocarbon potential ranging from 3kg/t to 11kg/t. (*Broad, 2007*) The reservoirs present within the Orange Basin possesses excellent porosity and permeability (*Broad, 2007*)

1.6.2 CHEMOSTRATIGRAPHY

1.6.2.1 INTRODUCTION TO CHEMOSTRATIGRAPHY

Chemostratigraphy is defined as the process of subdividing sedimentary sequences and modelling mineralogical changes using bulk inorganic chemistry (*Pearce et al, 1999*).

Interwell correlation using Chemostratigraphy is accomplished by the characterization of long term geochemical trends and the geochemical fingerprinting of sedimentary packages and individual sedimentary beds.

The bulk geochemistry of a rock will change in accordance to slight changes in the mineralogy of the sedimentary sequence. The mineralogical changes of a sequence/ lithology may be as a result of the following:

- (1) Changes in the composition of the source
- (2) Changes in the weathering processes that occurred
- (3) Changes in facies distribution
- (4) Changes in the diagenetic processes that took place

Chemostratigraphy makes use of a data array of approximately 50 elements. The vast number of elements that are used enables the determination of detailed geological information on provenance, climate and facies distribution. (www.chemostrat.com/methods)

Chemostratigraphy can be used under a variety of geological settings, rock ages and rock types, which results in Chemostratigraphy being an extremely useful correlation tool.

1.6.2.2 PREVIOUS WORK

Chemostratigraphy has been used as a correlation tool by the oil industry for a number of years but the work has been labelled propriety and therefore has not been released by the relevant companies. Available literature consulted discusses and emphasizes topics such as the use and volatility of the method as well as the advantages and disadvantages of the method.

The main research question of this study is the use and validity of Chemostratigraphy as a correlation technique in particular for reservoir-scale correlation. In a discussion by *Pearce et al, 1998* the validity of Chemostratigraphy is addressed. The Duckmantian-Stephanian sequences, located in the northern parts of the United Kingdom, are used as a case study. These successions are the onshore equivalent of the important hydrocarbon bearing Barren Red Measure sequences, hence much information regarding sedimentology, mineralogy and provenance of these successions are available and they provide the perfect setting to test the validity of Chemostratigraphy. Samples from cores, sidewall cores and cuttings are analyzed for 19 elements. Elemental concentrations obtained are compared with known elemental concentrations from mineralogical data. Correlation of geochemical data and previous lithostratigraphic subdivisions are found to coincide. The geochemical data had an advantage as it allowed the lithostratigraphic data to be further subdivided.

The use of chemostratigraphy as a correlation tool for reservoir-scale Interwell correlation is discussed by *Ratcliffe et al, 2003*. The reservoirs of the Argillo Greseux Inferieur field found in Algeria displays poor biostratigraphic control and lateral facies variation, for this reason reservoir characterization and reservoir management became a complex task to accomplish. Chemostratigraphy, carried out on approximately 800 core samples collected from thirteen wells, provided the basis for sub regional as well as field-scale correlation to be made. High resolution chemostratigraphy integrated with the sedimentology of the basin allowed for high resolution correlation to be achieved, in most cases bed to bed correlations are achieved, and also permitted the lateral extent of the reservoir zones to be highlighted.

In a discussion by *Dypvik et al, 2001* emphasis is placed on the use of inorganic geochemistry to correlate on fine grained siliciclastics. Geochemical ratios are used to construct correlation graphs. Element ratios are generated by elements that generate the best correlation co-efficient. The ratio of Zr/Zb is used to determine any variation in grain size. The grain sizes of the samples are very important as it will impact on the results. Coarser

grain sizes will have a lower overall elemental concentration than finer grain sizes. Other ratios used during the analysis includes (Zr/Rb)/Sr, which gives an indication of the percentage of siliciclastic components and carbonate components present within the sample. The reduction-oxidation conditions of the environment can also be determined by using the ratio Th/U. *Dypvik et al* used all of the above equations and then illustrated the fact that these geochemical ratios can be used to determine the sedimentological evolution of the depositional basin.

Statistical analysis has been chosen above the use of ternary diagrams for correlation purposes for this study. *Ehrenberg and Siring, 1992* undertook a study which is one of the first to use discriminant analysis of bulk geochemistry of sandstones as a stratigraphic correlation index. In the discussion two main advantages of using bulk chemical analysis are described, these advantages are firstly, that bulk chemical analysis are highly accurate and reproducible and secondly that these analysis are relatively inexpensive. The study is conducted in order to evaluate the correlation potential between cores based on bulk chemical analyses. Discriminant analyses are then performed in order to identify linear trends within the data sets. The results are validated using petrographical analysis. From the research conducted, the following pre cautions are noted,

Chemostratigraphy, as with any other correlation technique, has restrictions. In a discussion by *Ratcliffe et al, 2008* emphasis is placed on the fact that the technique is highly subjective and interpretative and that the large number of variables that affect the elemental concentrations of sediments will result in some sediments not falling within the range of typical geochemical signatures that are visible for samples from that zone.

Pearce et al, 1999 discussed the selection of elements. They emphasized the fact that only immobile elements should be used for analysis. Immobile elements or as they are alternatively termed stable elements, are more likely to resist modification or alteration due to weathering and diagenetic processes and hence will reflect changes related to sediment distribution and not as a result of diagenesis. Minerals such as feldspars and clay minerals are not used as they are more susceptible to alteration by diagenetic processes. They are thus more suited for research that focuses on correlation and provenance of areas. For the purpose of reservoir scale correlation, immobile elements such as Nb, Hf, Zr and Ta along with certain REE's are used. Review of this literature led to the development of one of the secondary aims of this study, namely the determination of the provenance of the study area using immobile elements concentrations.

CHAPTER 2 REGIONAL GEOLOGY

The basins found offshore along the margins of South Africa are divided into three distinct tectonostratigraphic zones.

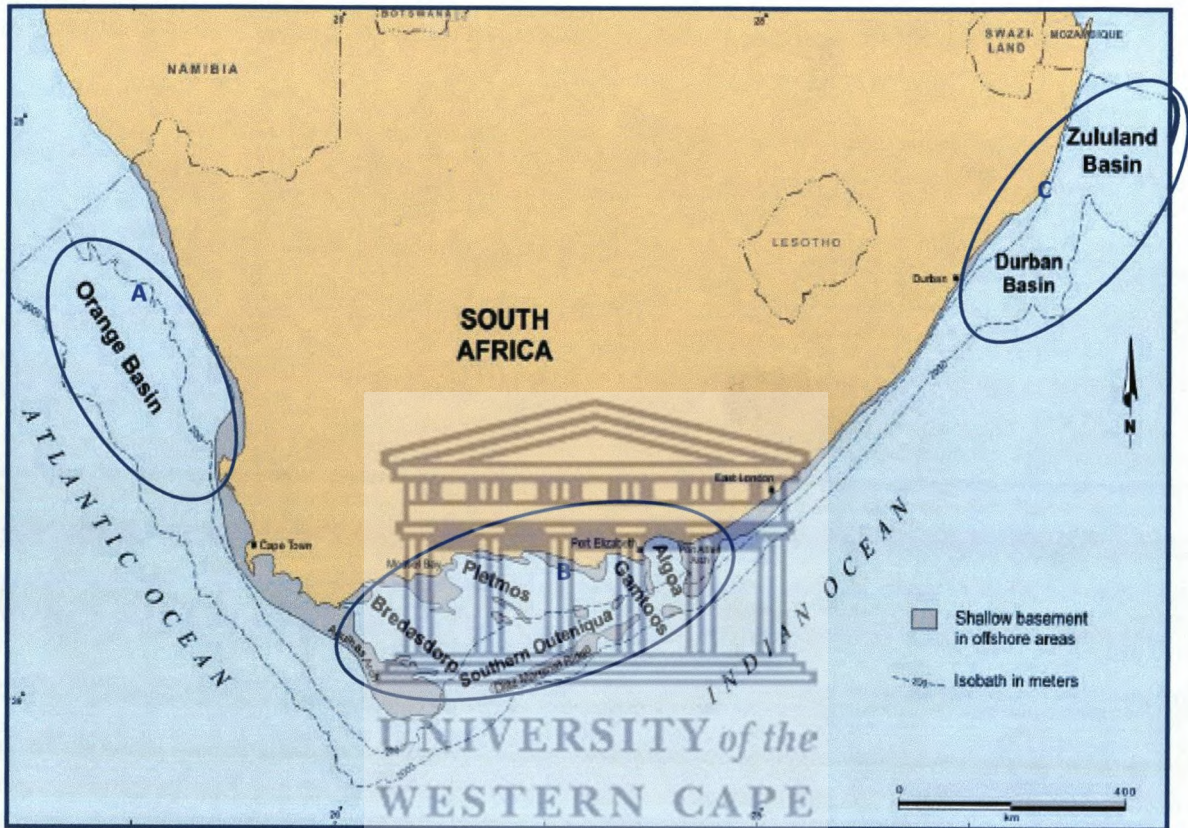


Figure 2.1 Map illustrating the locations of South Africa's offshore basins. A shows the position of the Orange Basin on the western offshore, B – Bredasdorp, Pletmos, Gamtoos, Algoa and Outeniqua basins found on the southern offshore area and C- Durban and Zululand Basins found on the eastern offshore. (Modified from van Der Spuy, 2005)

The eastern offshore areas are defined by passive margin settings that formed during the Jurassic as a result of the breakup of Africa, Madagascar and Antarctica. Deposition within these areas are restricted and only the Durban and Zululand basins display sedimentary sections.

The southern offshore area is defined by the Outeniqua basin which in turn is composed of a series of en echelon sub basins: Gamtoos, Pletmos, Bredasdorp and Algoa sub-basins.

The western offshore area is defined by the Orange basin. This area is described by a broad passive margin basin that is related to the opening of the South Atlantic during the Early Cretaceous. The Orange Basin is the largest of the South African offshore basins.

The coastline of South Africa covers an approximate length of 3000km of which 900km is covered by the west coast which stretches from the Orange River to Cape Point

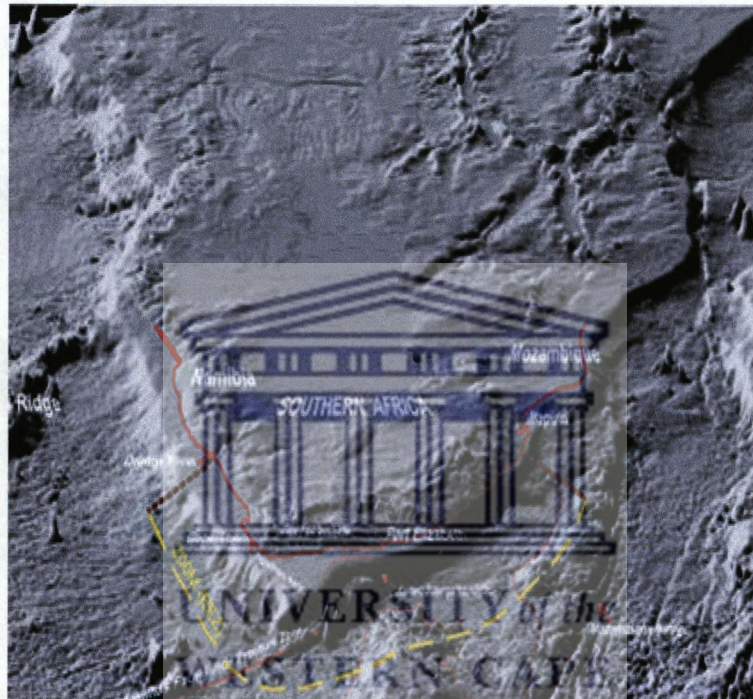


Figure 2.2 Map illustrating the topography of South Africa's continental margin and sea floor. The map is derived from satellite-altimetry imagery. (Broad, 2007)

The continental shelf and slope are found to display trends of being relatively wide along the west and south coast, being approximately 20-160km wide of the west coast and 50-200km of the south coast, but very narrow along the east coast with the only exception to this being the Durban Basin.

Within this paper only the Orange Basin will be discussed in detail.

2. 1 TECTONIC SETTING

The Orange Basin is situated along the South Atlantic margin on the west coast of South Africa. The margin is a divergent plate margin (Barton *et al*, 1993) that formed as a result of extensional stresses (Muntingh and Brown, 1991) that is generated by the rifting of the African and South American continental plates during the Late Jurassic and Lower Cretaceous. The margin is displaced by transverse marginal fractures. These fractures are correlated with faults that are produced during the rifting episodes that resulted in the crustal segmentation of the margin (Van der Spuy, 2007).

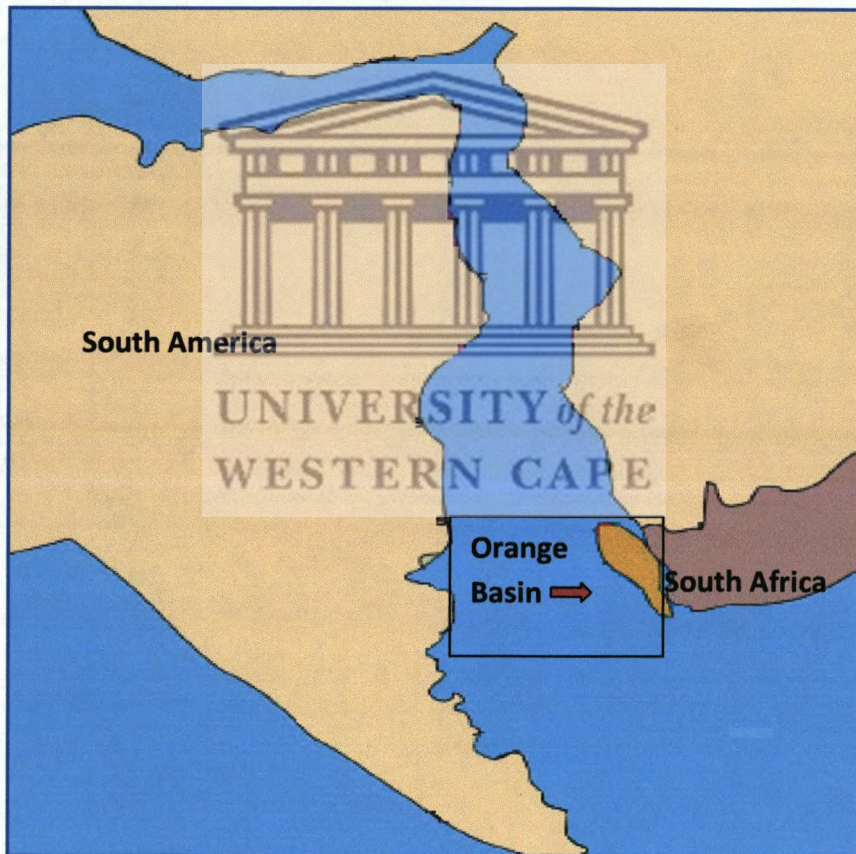


Figure 2.3 Location of the Orange basin, that formed as a result of rifting of the South American (left) and African plates (right). (Modified from Van der Spuy *et al*, 2007)

The Orange basin, the largest of the Mesozoic offshore basins, is elongated parallel to the coast and is found between coordinates $32^{\circ}30' S$ and $27^{\circ}30' S$). The Orange Basin is bound by the Kudu Arch to the north and the Agulhas- Columbine Arch in the south. (Dingle *et al*, 1983)

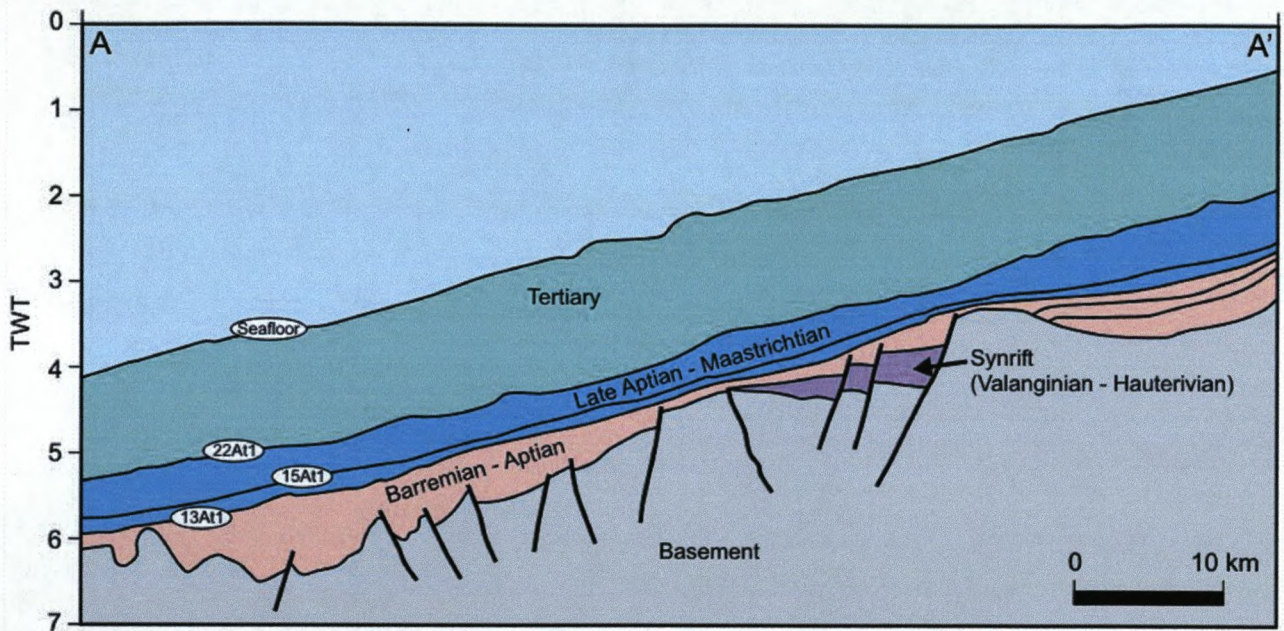


Figure 2.4: Schematic cross section through the Orange Basin (Van der Spuy, 2007)

2.2 DEPOSITIONAL ENVIRONMENTS AND STRATIGRAPHY

2.2.1 DEPOSITIONAL ENVIRONMENTS

Sedimentary input into the Orange Basin is controlled by the Orange River and to a lesser extent by the Olifants River (van der Spuy, 2007). Evidence to support this fact is the presence of major deltaic depocentres that are found adjacent to the mouths of the rivers (Dingle et al, 1993). The Orange River is the main contributor of sediments to the basin. The Olifants River contributed to filling the basin for approximately 13Ma from 117.5Ma to 103Ma (Brown et al, 1995) after which the Orange River is the sole contributor (van der Spuy, 2007).

2.2.2 STRATIGRAPHY OF THE ORANGE BASIN

The stratigraphy of the Orange Basin can be described in terms of the prerift, synrift, transitional, drift and tertiary to present day successions.

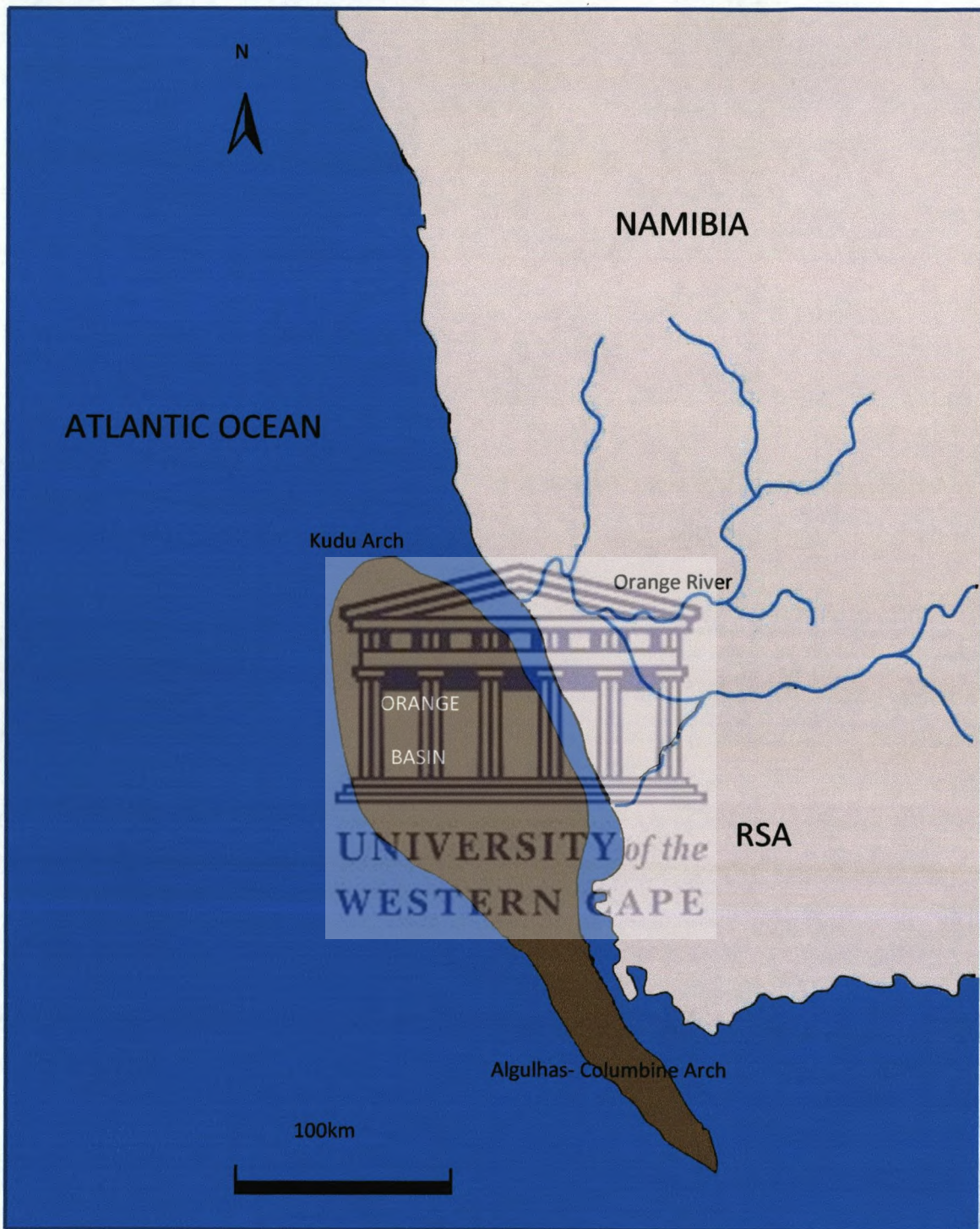


Figure 2.5: Map showing the showing the locations of the Kudu arch in the north and the Agulhas-Columbine Arch to the south. Also illustrated is the position of the Orange River, the main contributor of sediments to the Orange basin. (Modified from van der Spuy, 2007)

The Prerift or alternatively named basement rocks, of the Orange basin are composed in the southern part of high grade and low grade metamorphites and in the northern part of granitic plutons and alkaline intrusives (*Broad et al, 2007*)

The prerift rocks are overlain by Pre- Barremian synrift successions (*van der Spuy et al, 2005*) that have been intersected between horizons T and 6At. The succession is composed predominantly of basic lavas within the central rift sequences and coarse continental clastic, fluvial and lacustrine sediments along with volcanics within the marginal rift basins. (*Barton et al, 1993*)

The pre- Barremian synrift successions are overlain by the transitional succession of Barremian to Aptian age. This sequence is composed of alternating fluvial and marine rocks that are deposited as a result of transgression and regression of the sea level. (*van der Spuy et al, 2005*)

The stratigraphy of the drift successions are as follows:

- Barremian to early Aptian sediments includes continental red beds that are occasionally interbedded with basaltic lavas (*Barton et al, 1993*) and sandstones and shales of marine origin. Within the Kudu gas field Aeolian sandstones have also been intersected.
- During the Early to Middle Aptian extensive drowning of the margin occurred. This process may have caused an anoxic environment to be established that would favour the deposition of organic rich shales.
- Fluvio - deltaic sandstones are deposited during the Albian and Cenomanian periods. The Cenomanian to Turonian period is characterized by predominantly aggradational deposits. Progradational deposits are also found but to a lesser extent than aggradational deposits. (*Broad et al, 2007*)
- The tertiary to present day successions are composed of organic and chemical sediments that contain minimal amounts terrigenous material. (*Barton et al, 1993*)

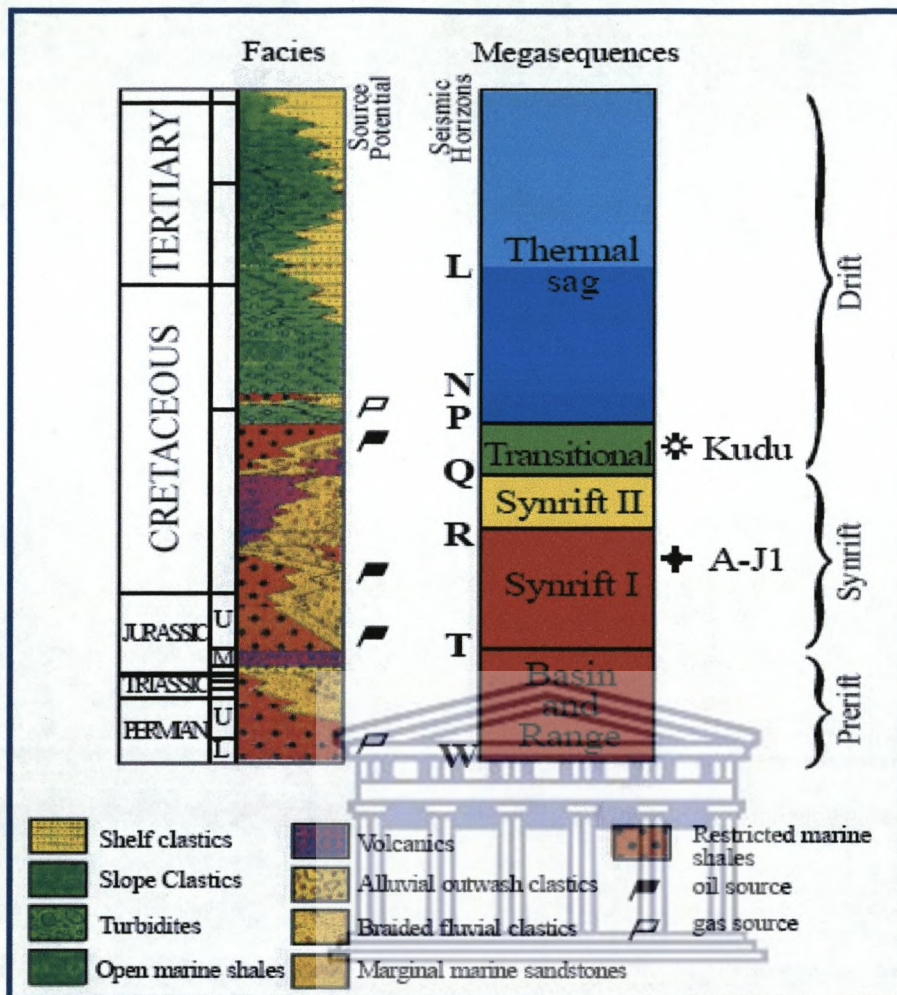


Figure 2.6: Stratigraphic Column of the Orange Basin

2.3 PETROLEUM ELEMENTS

2.3.1 INTRODUCTION TO PETROLEUM ELEMENTS

2.3.1.1 Source Rocks

Source rocks are anoxic deposits that are predominantly fine-grained and contain high percentages of organic matter and inhibit diffusion of oxidants into sediments to break down organic matter that is vital for the accumulation of petroleum. Shales are generally found to be excellent source rocks (Carey, 2007). There are three types of source rocks. Source rocks will be classified as either gas-prone or oil-prone on the basis of kerogen type. Kerogens are defined as reaction products and intermediaries of diagenesis that are no longer organic but are not yet petroleum. It is however the precursor to oil and gas. Source rocks are termed as gas prone if they are composed of either Type 1 Kerogens or Type 2 Kerogens. Type 1 kerogens have extremely high hydrogen to carbon ratios and are composed of marine algae. They are a very rich source of petroleum. Type 2 Kerogens, commonly called herbaceous kerogen, have an intermediate oil gas ratio and are most commonly found in rocks that are

deposited in marginal marine environments. Volumetrically this is the most important source rock for oil. Source rocks containing Type 3 Kerogens are gas prone. Type 3 Kerogens have low hydrogen to carbon ratios and are derived primarily from terrestrial plants. (*Laudon, 1996*)

2.3.1.2 Reservoir Rocks

A reservoir rock is defined as a rock that possesses sufficient porosity and permeability to hold economic quantities of oil. The porosity and permeability of the rocks depends on the depositional pore geometries as well as the subsequent diagenetic alteration that takes place. The most common reservoir rocks are sandstones and carbonates.

2.3.1.3 Traps

A trap is defined as any part of a reservoir that holds economic quantities of oil. The most common types of traps are structural traps and stratigraphic traps. Structural traps are formed when the space for petroleum is limited by the presence of a structural feature. Stratigraphic traps are created by the limits of the reservoir rock itself.

2.3.1.4 Seals

The seal is a relatively impermeable layer that is situated above the trap. In the presence of a stratigraphic trap the seal will be found below as well as above the trap. Common seals are shales and evaporites.

2.3.1.5 Petroleum System

A petroleum system is defined as a natural system an active source rock and all related oil and gas and all the geological elements and processes that are essential if a hydrocarbon accumulation is to exist. (*Junslanger, 1999*)

2.3.2 PETROLEUM ELEMENTS OF THE ORANGE BASIN

2.3.2.1 Source Rocks

Source rocks are found at three stratigraphic levels in the Orange Basin:

- Early Cretaceous Source rocks are encountered below the 6At1 unconformity (refer to figure 4). The source rock is oil prone and has an average thickness of 60m. (*Burden et al, 1989*)

- An Aptian source rock is present directly above the 13A horizon (refer to figure 4) (*Muntingh, 1993*). The source rock tends from dry-gas and wet-gas prone in the shelf to oil prone in the westerly direction.
- Source rocks are present above the 15A horizon (*Muntingh, 1993*), (refer to Figure 4). These source rocks are deposited during the Cenomanian/ Turonian Oceanic Anoxic event and are found to be immature over the shelfal region with its quality improving in the westerly direction (*Burden et al, 1989*).

2.3.2.2 Reservoir Rocks

Fluviodeltaic and lacustrine sandstones and conglomerates comprise the reservoirs within the marginal rift basins (*Barton et al, 1993*), (*Broad and Mills, 1994*) while sandstones of fluviodeltaic to deep marine origin constitute the reservoirs within the post rift succession. (*Broad and Mills, 1994*)

2.3.2.3 Traps

Both structural and stratigraphic traps are present in the Orange Basin where pinchouts and lowstand plays define the stratigraphic traps and dome and fault closures defines the structural traps (*Broad and Mills, 1994*).

2.3.2.4 Seals

The source rocks found above the 13A and 15A horizons have been defined as being a regional seal.

2.3.3 PETROLEUM SYSTEMS IN THE ORANGE BASIN

Petroleum Systems have been proven in the synrift, transitional and post rift successions of the Orange Basin:

- Within the synrift succession a lacustrine oil system has been encountered (*Junslager, 1999*) Evidence for this system is the AJ half graben.
- The presence of a lower Aptian – Barremian sourced gas system and a stratigraphic Barremian aeolian sandstone play (*Junslager, 1999*) that hosts the Kudu gas field has been proven (*Broad, 2007*). The gas within this system is stratigraphically trapped in

aeolian sandstones. The main reservoir in the system is found to be overlain by a gas charged shallow marine sandstone.

- The drift succession hosts the Barremian – Lower Aptian sourced gas system that is present within stratigraphically trapped sandstones of middle Albian – Cenomanian.



UNIVERSITY *of the*
WESTERN CAPE

CHAPTER 3 METHODOLOGY

3.1 WELL SELECTION

Well selection is done on the following basis

- Geographical and geological positions of the well
- They wells are chosen to demonstrate the depositional environments of the basin
- The wells selected display an east-west trend across the basin.

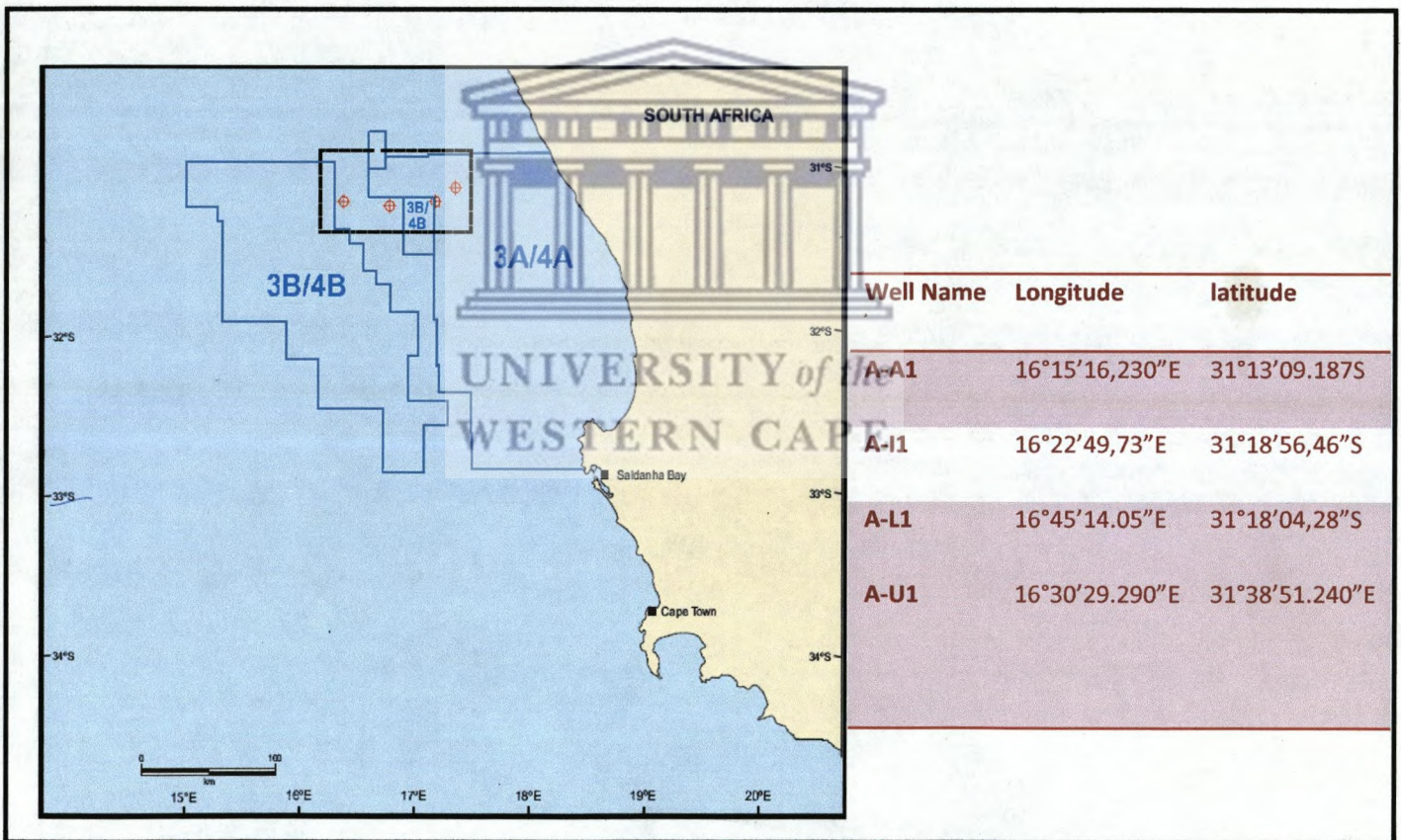


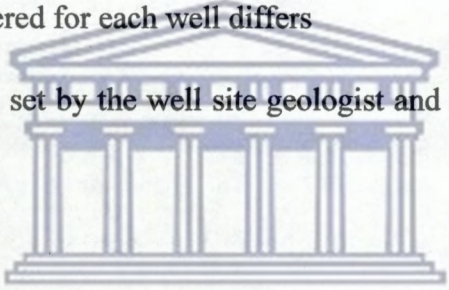
Figure 3.1 Map illustrating the locatons of Well A-A1, A-L1, A-U1 and A-I1 in Block 3 and Block 4 and in the Orange Basin, offshore South Africa

3.2 SAMPLE SELECTION

Sample selection is done on the basis of lithology, grain size as well as the depth. Only ditch cuttings of sandstone are used because the emphasis of the project is reservoir correlation. The grain size of sedimentary rocks has an enormous impact on the geochemistry of the rock and it will reflect the hydrodynamic sorting of the mineral components. The result of the above is that the element concentrations decrease in coarser grain sizes. It is therefore not feasible to use coarser grained sandstones and conglomerates. The sampling interval of ...m are set so that equal numbers of sample would be used from each zone.

The sampling interval and the number of samples collected for each well differs because of the following reasons:

- (1) The depth ranges covered for each well differs
- (2) The sampling interval set by the well site geologist and mud loggers differs for each well.



Well	Number of Samples
A-I1	34
A-A1	30
A-U1	35
A-Li	35

Table 3.2: Provides a summary of the sampling interval and the number of samples collected for each well

3.3 SAMPLE PREPARATION

The ditch cuttings are washed to remove any foreign objects and contamination that is caused by the drilling fluids. 2 litres of distilled water is used to wash each sample to ensure that the washing of the samples are done systematically. The samples are washed over a sieve of 106 Microns to ensure that only rock chips remained. The samples are dried in an oven at a temperature of 110°C for approximately 3 hours. The samples are crushed to a fine powder using a pulveriser for 2, 5 seconds. 9 grams of the dried sample is mixed with 2 grams of Hoerst wax (flux). This is done in order to prepare the samples to be pressed into pellets that have a thickness of 5mm. The Hoechst wax helps to bind the sediments so that it doesn't separate when being made into pellets. After pelletization the pellets are placed in an oven for approximately 45minutes to ensure that the sample is completely dry and all moisture has been removed.



3.4 DATA ACQUISITION

The pellets are inserted into the X-Ray fluorescence (XRF) machine. The XRF system uses an intense beam of X-rays of specified energy that strike and interact with constituent elements of the target specimens to produce characteristic X-rays of those elements.

The characteristic X-rays are detected with a wavelength spectrometer and scaled. The scaled signal is corrected for absorption and fluorescence effects and compared with standard specimens of known elemental concentrations. Unknown compositions ranging from major to trace amounts can be quantitatively determined in order to determine the percentage of the element that is lost as a result of the preparation of the sample.

3.5 QUALITY CONTROL

The percentage of concentration lost during preparation of the samples is referred to as loss of ignition.

The process to determine Loss on Ignition is as follows:

- The crucibles in which the powdered sediments are placed are measured.
- After this 1g of powdered sediments is measured.
- The crucibles containing 1gram of powdered sediments are firstly weighed together and is then placed in a furnace for approximately 45minutes.
- The crucibles are then removed and weighed again.
- The elemental concentrations given by the XRF is supposed to equal 100% but the concentrations never equal 100% because, as explained earlier, a percentage of the element is lost due to preparation of the sample.
- The initial weight of the crucible and sample (W_i), the final weight of the crucible and the sample (W_f), and the weight of the sample (W_s) are used to calculate the percentage of loss on ignition using the following formula:

$$LOI = (((W_i - W_f) * 100) / W_s)$$

- This process is repeated for each sample. The average of the two values obtained is taken as the final percentage of loss on ignition.
- The percentage of loss on ignition for each sample is added to the elemental concentrations obtained from the XRF for each of the samples. This process known as the correction for LOI

UNIVERSITY of the
WESTERN CAPE

3.6 DATA INTERPRETATION

3.6.1 CHEMOSTRATIGRAPHY

- The geochemical data is interrogated statistically to identify element distribution patterns
- Principal Component Analysis is performed on the data such that the mineralogical controls on chemical variation are highlighted. Principal component analysis is used to model elements, elemental relationships and element mineral relationships. The resultant plots and profiles obtained from statistical analysis describe the elemental relationships in terms of quartiles (1st, 2nd, 3rd and 4th quartiles) and are used to facilitate the construction of element ratios.

- Major and Trace Downhole profiles are constructed for the four wells such that element distribution and heterogeneity downhole could be observed. These in conjunction with the PCA plots are used to construct the element ratios.
- Element ratio patterns are constructed and used to identify Chemostratigraphic indices (geochemical units) that would be used for correlation purposes.

To enable the geochemical plots to be constructed certain elements known as Chemostratigraphic index elements have to be identified: These elements are identified on following basis:

- The mineralogical affinity of the elements – elements having simple affinities are more likely to preserve the detrital signature of the sediments
- The participation of elements in diagenetic activities – elements having little or no involvement in diagenetic processes are most suitable.
- Concentrations of refractory grains – High concentrations of refractory grains are desired.
- Each set of lithologies will be plotted as geochemical concentrations versus depth.
- Using the plots chemostratigraphic units are identified. This is achieved by identifying:
 - Elemental ratios
 - Systematic geochemical trends
- Interwell correlation, which is the scope of this study, is then achieved by the following:
 - The characterization of long term geochemical trends
 - The geochemical fingerprinting of sedimentary packages
 - The geochemical fingerprinting of individual beds

3.6.2 WELL LOG INTERPRETATION

The wire-line logs will be constructed using Interactive Petrophysics (IP). The wire-line logs will be used to identify signatures for the depths which have been sampled. The signatures obtained will be used to identify units that will then be correlated with the chemostratigraphic units that are obtained.

The following wireline logs will be used:

1. Gamma Ray log
2. Neutron Log
3. Density Log
4. Caliper Log



An overview of the pattern of the well logs for each well is constructed.

Geophysical Units are identified using the well logs by looking for distinct pattern changes.

Neutron Density Cross plots are constructed for each well to enable the identification of lithology. Neutron –Density cross plots are constructed using values obtained from the Neutron log on the x-axis and the Density plot on the y-axis. Three predefined curves indicating the presence of sandstone, dolomite and limestone are overlain on the plot.

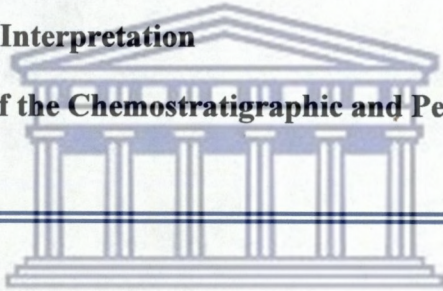
M/N plots are constructed for each unit identified to enable the recognition of minerals present within the unit. The M/N plots are constructed using the Neutron, Density and Sonic log. The Neutron log is plotted on the x-axis, Density log on the y-axis and the Sonic log on the z-axis. A predefined quartz- calcite- dolomite triangle is overlain on the plot. The mineral composition is identified in relation to the above triangle. The plotting of elements relative to the effects of secondary porosity, the shale effect and gas effect are also displayed on this plot.

SECTION 2

Chapter 4 Chemostratigraphy

Chapter 5 Petrophysical Interpretation

Chapter 6 Comparison of the Chemostratigraphic and Petrophysical Characteristics



UNIVERSITY *of the*
WESTERN CAPE

CHAPTER 4 CHEMOSTRATIGRAPHY

This chapter aims to present the results of the Chemostratigraphic framework for the wells A-A1, A-I1, A-L1 and A-U1 in the Orange basin. Chemostratigraphic analysis works on the basis of element pattern recognition. These patterns are used to identify geochemical units (chemostratigraphic indices) that facilitate reservoir scale interwell correlation. For this purpose the analytical data are evaluated using multivariate statistical techniques. This is completed in the order outlined below:

- A summary of the geochemical data (4.1) for the respective wells is first compiled, then compared and contrasted.
- Principal Component analysis (4.2) is performed on the data to define element groupings and suitable element ratios (4.4) that is used to facilitate the identification of the chemostratigraphic indices.
- Downhole major and trace element plots (4.3) are constructed using Earthworks. The resulting patterns are used to facilitate the identification of the chemostratigraphic indices.
- Element ratios (4.4) are calculated and plotted using Earthworks. Geochemical signatures are determined from the ensuing patterns and are used to correlate between the wells.
- The geochemical units (4.4) are identified, classified and their characteristics highlighted for the purpose of generating a chemostratigraphic framework for the wells studied and which may be applied to the Orange Basin.

4.1 ELEMENT DISTRIBUTION PATTERNS

This section presents a summary of the element distribution patterns for each well.

The components discussed are the:

1. Minimum concentrations
2. Maximum concentrations
3. Geometric mean of the elements.

The elements are grouped according to ranges developed using the geometric mean. The geometric mean provides a more realistic average than the arithmetic and the harmonic mean as it does not place emphasis on anomalies that exist within the data and therefore provides the best evaluation of a section. The major elements are expressed in percentages (%) as they constitute the bulk of the composition and the trace elements in parts per million (ppm) as they represent minute quantities. This section begins with the element distribution pattern for each well (**tables 4.1.1 to 4.1.4**) being analysed separately and ends with a general overview for the four wells (**table 4.1.5**).

UNIVERSITY of the
WESTERN CAPE

4.1.1 RESULTS

4.1.1.1 Well A-A1

The element distribution summary for the geochemical data resulted in the following classification (*refer to table 4.1.1*):

Major Elements

- MnO and P₂O₅ concentrations are in the range 0% - 1%.
- TiO₂, SO₃, Fe₂O₃, K₂O, MgO and CaO concentrations are in the range 1% - 5%.
- Al₂O₃ concentrations are in the range 10% - 20%.
- SiO₂ is the most dominant constituent with concentrations > 50%

The average elemental composition based on the geometric mean for Well A-A1 shows a dominance of SiO₂ (61.3%), Al₂O₃ (12.3%), Fe₂O₃ (4.9%), CaO (4.1%) and MgO (2.4%).

Trace elements:

- Co displays the lowest concentrations with a range of 4ppm – 27ppm
- Much higher concentrations are exhibited by Ni, V, Nb and Y (40ppm – 160ppm).
- Zr, Sr and Rb contents ranges between 160ppm – 350ppm.
- The highest average concentrations for these samples are a function of the elements Zn and Ba.

<i>Element</i>	<i>Minimum</i>	<i>Maximum</i>	<i>Std. deviation</i>	<i>Geo. Mean</i>
SiO ₂	51.8	73.4	5.8	61.3
Al ₂ O ₃	8.5	19.4	2.3	12.3
Fe ₂ O ₃	3.6	8.4	1.1	4.9
MnO	0.1	0.1	0.0	0.1
MgO	1.6	3.3	0.5	2.4
CaO	1.7	8.0	1.8	4.1
Na ₂ O	0.7	2.3	0.4	1.5
K ₂ O	2.4	5.0	0.7	1.4
TiO ₂	0.5	1.1	0.1	0.7
P ₂ O ₅	0.1	0.2	0.0	0.1
SO ₃	0.1	3.5	0.7	0.2
LOI	5.1	13.5	1.9	7.8
Co	4.0	27	5.6	13.2
Ni	40	157	31.9	84.7
V	77	149	19.9	101.3
Zr	188	321	33.5	263.2
Sr	126	318	40.9	180.2
Zn	116	8963	2506.3	557.1
Ba	423	3162	561.6	1126.8
Pb	9	1286	258.4	56.3
Ce	*nd	202	92.3	*nc
Nd	*nd	69	27.5	*nc
Nb	58	114	14.7	72.1
Y	37	100	15.2	61.2
Rb	116	259	37.5	164.5

Table 4.1.1: Summary statistics for minor elements of Well A-A1

*nd = not detected

*nc = not calculated

The average elemental compositions for the trace elements based on the geometric mean in Well A-A1 shows a dominance of Zn (557.1), Zr (263.2), Sr (180.2), Rb (164.5) and V (101.9). Cobalt (13.2) shows the lowest average elemental composition.

4.1.1.2 Well A-I1

The element distribution patterns for Well A-I1 (*refer to table 4.1.2*):

Major Elements

- MgO, Na₂O, TiO₂ and P₂O₅ contents are in the range 0 – 1%.
- Fe₂O₃, MnO, CaO, K₂O and SO₃ are included in the range 1% - 10%.
- Al₂O₃ concentrations are in the range of 10% - 20%
- SiO₂ is the dominant constituent with concentrations that are in the range > 40%

The average elemental compositions of the samples for Well a-I1 shows a dominance of SiO₂ (55.9), Al₂O₃ (13.2) and Fe₂O₃ (6.8).

UNIVERSITY of the
WESTERN CAPE

Trace Elements

- Ni concentrations range between 19ppm - 160ppm.
- V, Zr, Sr, and Rb contents are in the range 40ppm – 250ppm.
- Pb concentrations are in the range 16ppm – 294ppm while Nb concentrations fall in the range 38ppm – 61ppm.
- The high concentration of Ba (> 350ppm) as previously mentioned could be attributed to the fact that Ba forms a constituent of most drilling mud.

The average elemental composition of the trace elements for Well A-I1 shows a dominance of Zr (168.9), Rb (155.8), Sr (133.8), V (124.4) and Zn (120.3). The minimum values for Ce, Nd and Y fall below the detection limit of the XRF and as a result the geometric mean could not be calculated.

<i>Element</i>	<i>Minimum</i>	<i>Maximum</i>	<i>Std. deviation</i>	<i>Geo. Mean</i>
SiO ₂	43.8	83.1	10.2	55.9
Al ₂ O ₃	6.5	16.6	2.6	13.2
Fe ₂ O ₃	2.6	10.2	1.8	6.8
MnO	0.0	0.1	0.0	0.1
MgO	0.9	2.1	0.3	1.8
CaO	0.8	9.0	1.8	3.2
Na ₂ O	0.5	0.7	0.0	0.6
K ₂ O	1.6	5.8	1.0	4
TiO ₂	0.3	0.9	0.2	0.7
P ₂ O ₅	0.0	0.1	0.0	0.1
SO ₃	0.5	4.9	1.2	1.7
LOI	2.5	15.8	3.3	8.9
Co	0.0	63.0	12.0	
Ni	19.0	155.0	20.7	42.8
V	54.0	163.0	28.2	124.4
Zr	94.0	246.0	30.9	168.9
Sr	43.0	222.0	39.3	133.8
Zn	34.0	966.0	149.1	120.3
Ba	324.0	3859.0	851.9	651.1
Pb	16.0	294.0	44.8	32.7
Ce	*nd	200.0	90.8	*nc
Nd	*nd	65.0	26.5	*nc
Nb	38.0	61.0	6.0	53.1
Y	*nd	77.0	27.9	*nc
Rb	59.0	214.0	39.2	155.8

Table 4.1.2.: Summary statistics of the major elements for Well A-11

4.1.1.3 Well A –L1

The summary statistics for Well A-L1 resulted in the following classification (*refer to table 4.1.3*):

Major Elements

- MnO, Na₂O, TiO₂ and P₂O₅ concentrations fall in the range 0.1% - 1%.
- Al₂O₃ concentrations are in the range 3% - 16% while Fe₂O₃ concentrations range between 3% - 9.5%.

- MgO concentrations are in the range 1% - 10% and SO₃ concentrations ranges between 0.4% - 4%.
- Element concentrations for CaO and K₂O are in the ranges 0.6% - 17.5% and 0.7% - 5.5% respectively.
- SiO₂, as with previous wells, is the major constituent of the samples with concentrations measuring more than 50%.

The average elemental composition based on the geometric mean, for Well A-L1 shows a dominance of SiO₂ (67.3%), Al₂O₃ (8.4%) and Fe₂O₃ (6.1%). The elements MnO, Na₂O, TiO₂ and P₂O₅ shows the lowest average elemental composition (<1%).

Trace Elements

- Ni, V and Rb concentrations ranges between 18ppm – 156ppm, 53ppm – 144ppm and 26ppm -186ppm respectively.
- Zr concentrations are in the range 121ppm – 330ppm and Sr concentrations fall in the range of 56ppm – 332ppm.
- Zn and Pb concentrations are relatively high, falling in the range 51ppm -1718ppm and 17ppm – 423ppm respectively.
- Nb and Y have concentrations that fall in the range 36ppm - 60ppm and 1ppm – 77ppm respectively.

The average elemental concentrations of the samples for Well A-L1 show a dominance of Zr (216.7ppm), Sr (155.3ppm), Zn (111.3ppm) and Rb (92.7ppm). The minimum concentrations for Ce and Nd are not measured as they fall below the detection limit set for the equipment.

Variable	Minimum	Maximum	Std. deviation	Geo. Mean
SiO ₂	51.6	84.3	8.6	67.3
Al ₂ O ₃	3.3	16.2	2.9	8.4
Fe ₂ O ₃	3.3	9.5	1.7	6.1
MnO	0.0	0.2	0.0	0.1
MgO	0.6	2.1	0.3	1.1
CaO	0.6	17.5	3.2	2.5
Na ₂ O	0.1	0.6	0.1	0.3
K ₂ O	0.7	5.5	1.0	2.1
TiO ₂	0.2	0.9	0.2	0.5
P ₂ O ₅	0.0	0.1	0.0	0.1
SO ₃	0.4	4.1	0.8	1.3
LOI	3.9	12.9	2.2	7.8
Co	*nd	106.0	23.7	*nc
Ni	18.0	156.0	23.1	38.4
V	53.0	144.0	20.5	83.6
Zr	121.0	330.0	57.0	216.7
Sr	56.0	332.0	46.9	155.2
Zn	51.0	1718.0	353.6	111.3
Ba	149.0	1606.0	305.6	437.1
Pb	17.0	423.0	76.9	36.1
Ce	*nd	148.0	40.8	*nc
Nd	*nd	49.0	14.4	*nc
Nb	36.0	60.0	6.8	49.4
Y	1.0	77.0	22.5	37.8
Rb	26.0	186.0	54.1	92.7

Table 4.1.3.: Summary statistics for the minor elements of Well A-L1

4.1.1.4 Well A-U1

The element distribution patterns for A-U1 are as follows (*refer to table 4.1.4*)

Major Elements

- As with the previous wells, MnO, TiO₂ and P₂O₅ have the lowest concentrations, falling in the ranges 0.15 - 0.2%, 0.1% - 0.9% and 0.1% - 0.2% respectively.
- MgO concentrations are in the range 1.3% - 2.2% and K₂O concentrations fall in the range 1.7% - 4.3%.
- Well A-L1 is defined by Fe₂O₃ concentrations in the range 4.6% - 13.1% and Al₂O₃ concentrations in the range 7.4% - 17.7%

- CaO concentrations for Well A- U1 fall in the range 0.9% - 13.5%.
- SiO₂, as with the other wells, constitutes the bulk of the samples with an average concentration of more than 50%.

The average elemental composition of Well A-U1 shows a dominance of the elements SiO₂ (57.5%), Al₂O₃ (11.7%) and Fe₂O₃ (7%).

Trace Elements

- Ni has the lowest concentration falling in the range 22ppm – 62ppm.
- Nb concentrations ranges between 39ppm – 59ppm and Y concentrations ranges between 8ppm – 78ppm.
- Pb, Rb and Sr concentrations are in the ranges 19ppm - 251ppm, 42ppm – 204ppm and 67ppm – 242ppm respectively.
- V concentrations for these samples fall in the range 80ppm – 150ppm.
- Zr is found to have very high concentrations (165ppm – 492ppm).
- Ba, as with the previous wells, displays concentrations above 400ppm

The average elemental composition of these samples shows a dominance of Zr (279.7ppm), Zn (166ppm), Sr (142ppm), V (105.8ppm) and Rb (95ppm). The minimum values for Co, Ce and Nd could not be detected as they fall below the detection values set for the instrumentation.

<i>Element</i>	<i>Minimum</i>	<i>Maximum</i>	<i>Std. deviation</i>	<i>Geo. Mean</i>
SiO ₂	42.6	73.2	8.1	57.5
Al ₂ O ₃	7.4	17.7	2.6	11.7
Fe ₂ O ₃	4.6	13.1	2.1	7
MnO	0.1	0.2	0.0	0.1
MgO	1.3	2.2	0.3	1.7
CaO	0.9	13.5	3.0	3.8
Na ₂ O	0.5	1.2	0.2	1
K ₂ O	1.7	4.3	0.7	2.5
TiO ₂	0.5	0.9	0.1	0.7
P ₂ O ₅	0.1	0.2	0.0	0.1
SO ₃	0.8	5.1	1.2	1.8
LOI	4.1	23.1	3.6	9.3
Co	*nd	30.0	8.1	*nc
Ni	22.0	62.0	8.5	36.7
V	80.0	150.0	21.2	105.8
Zr	165.0	492.0	70.5	279.7
Sr	67.0	242.0	47.3	142
Zn	46.0	1251.0	278.4	166
Ba	210.0	3743.0	754.1	803.8
Pb	19.0	251.0	48.3	41.9
Ce	*nd	170.0	72.4	*nc
Nd	*nd	60.0	21.8	*nc
Nb	39.0	59.0	4.8	51
Y	8.0	78.0	22.3	42.6
Rb	42.0	204.0	38.7	95

UNIVERSITY of the
WESTERN CAPE

Table 4.1.4: Summary statistics for the major elements of Well A-U1

4.1.1.5 Overview of Element Distribution Patterns

Table 4.1.5 gives an overall view of the element distribution patterns based on the geometric mean.

- SiO_2 is the dominant element for each of the wells, thereby highlighting the siliceous nature of the samples.
- Wells A-A1, A-U1 and A-I1 shows Al_2O_3 concentrations in the range 10% - 15% while A-L1 concentrations are slightly lower (5% - 10%).
- Fe_2O_3 concentrations are slightly higher in Wells A-L1, A-U1 and A-I1 (5% - 10%) than in Well A-A1 (1% - 5%).
- Na_2O concentrations are slightly higher in Well A-U1 and A-I1, falling in the range 10% - 15%, than in Wells A-A1 (1% - 5%) and A-L1 (0 - 1%).
- The concentrations for the elements MgO, CaO, MnO, TiO_2 and P_2O_5 are constant across the four wells, with MgO and CaO falling in the range 1% - 5% and MnO, TiO_2 and P_2O_5 in the range 0% - 1%.
- SO_3 concentrations are lower in Well A-A1 (0 - 1%) than in the remaining wells (1% - 5%).
- The following trace elements fall in the same range for the four wells: Ni and Pb (0 - 50ppm), Sr (100 - 200ppm), Ba (> 400ppm) and Nb (0 - 50ppm).
- Well A-L1 shows a lower average V concentration (0 - 50ppm) than the remainder of the wells (100 - 200ppm).
- High Zr concentrations are found throughout and are consistent with the fact that sandstones are generally enriched in Zr.
- Zn concentrations are extremely high for Well A-A1 (>400ppm) but is slightly lower for Wells A-A1, A-L1 and A-I1 (200ppm - 300ppm).
- The geometric mean for Co, Ce and Nd could not be calculated as their minimum concentrations fall below the detection limit set for the equipment.

- The geometric mean for Y could not be calculated for Wells A- L1 and A-I1 while A-A1 and A-U1 fall in the range 50ppm – 100ppm.

	Well A-A1	Well A-L1	Well A-U1	Well A-I1
SiO ₂	★	★	★	★
Al ₂ O ₃	■	●	■	■
Fe ₂ O ₃	▲	●	●	●
MnO	⬢	⬢	⬢	⬢
MgO	▲	▲	▲	▲
CaO	▲	▲	▲	▲
Na ₂ O	▲	⬢	■	■
K ₂ O	▲	▲	▲	▲
TiO ₂	⬢	⬢	⬢	⬢
P ₂ O ₅	⬢	⬢	⬢	⬢
SO ₃	⬢	▲	▲	▲
LOI	●	●	●	●
Co	*nd	*nd	*nd	*nd
Ni	○	○	○	○
V	○	▲	○	○
Zr	□	□	□	○
Sr	○	○	○	○
Zn	★	□	□	□
Ba	★	★	★	★
Pb	○	○	○	○
Ce	*nd	*nd	*nd	*nd
Nd	*nd	*nd	*nd	*nd
Nb	▲	▲	▲	▲
Y	▲	*nd	▲	*nd
Rb	○	▲	▲	○

LEGEND	
⬢	0 - 1%
▲	1% - 5%
●	5% - 10%
■	10% - 15%
★	> 50%
○	0 - 50ppm
▲	50ppm - 100ppm
○	100ppm - 200ppm
□	200ppm - 300ppm
★	> 400ppm

Table 4.1.5: General Overview of the element distribution patterns for Wells A-A1, A-L1, A-I1 and A-U1.

4.1.2 DISCUSSION

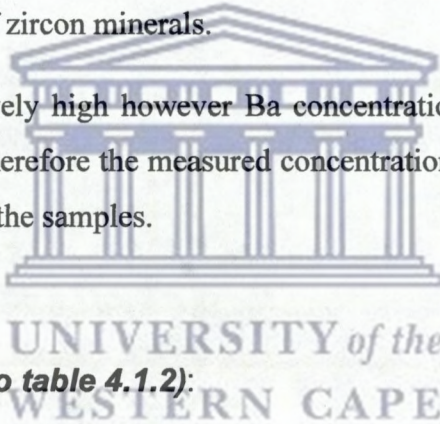
4.1.2.1 WELL A-A1 (refer to table 4.1.1):

The dominant constituent for this well is the element SiO_2 and is thus indicative of the siliceous nature of the samples. Al_2O_3 concentrations are relatively high and are seen as an indicator for the presence of clay minerals.

The concentration of CaO is suggestive of the presence of carbonate minerals within the samples while the high concentrations exhibited by vanadium is indicative of the abundance of detrital oxides and clay minerals that are present in the samples.

The relatively high contents of Sr could be attributed to the presence of calcite minerals in Well A-A1. The high concentrations of Zr may be supportive of the fact that the sandstones contain higher percentages of zircon minerals.

Ba concentrations are relatively high however Ba concentrations could be attributed to its presence in drilling muds. Therefore the measured concentration may not be a true reflection of the concentration of Ba in the samples.



4.1.2.2 WELL A-I1 (refer to table 4.1.2):

SiO_2 is the dominant constituent with concentrations above $> 40\%$ and thereby indicating the siliceous nature of the samples

The high concentrations of Fe_2O_3 may be indicative of the presence of iron minerals i.e. hematite. Al_2O_3 concentrations are in the range of $10\% - 20\%$ and are suggestive of the presence of clay minerals within these samples.

The Nb concentrations measured are relatively high and suggests that these samples could have a high concentration of clays and ferromagnesium silicates.

The high concentration of Zr indicates the siliceous nature of the sandstones while Sr concentrations are indicative of the presence of clay minerals

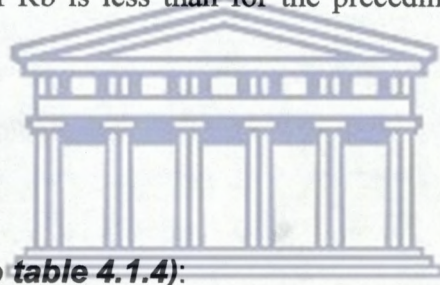
4.1.2.3 Well A-L1 (refer to table 4.1.3):

As with the previous wells SiO_2 is the dominant constituent and acts as an indicator of the siliceous nature of the samples. The high concentrations of Al_2O_3 are suggestive of the presence of clay minerals in the samples.

Fe_2O_3 concentrations are slightly less than for the preceding well but still relatively high and are assumed to be indicative of the presence of iron minerals, most probably hematite.

The elements Zr, Sr, Zn and Rb exhibit very high concentrations. Zr concentrations are indicative of the siliceous nature of the samples while the high concentrations exhibited by Sr are suggestive of the presence of carbonate minerals, most likely, calcite.

Zn and Rb concentrations are suggestive of the presence of clay minerals within the samples; however the concentration of Rb is less than for the preceding wells indicating that these samples are less argillaceous.



UNIVERSITY of the
WESTERN CAPE

4.1.2.4 Well A-U1 (refer to table 4.1.4):

As with the previous wells SiO_2 , Al_2O_3 and Fe_2O_3 are the dominant constituents. The high concentrations exhibited by SiO_2 and Zr are indicative of the feldspathic nature of the samples.

The concentrations exhibited by Al_2O_3 , Zn, V and Rb suggests that the samples are either feldspathic or arkose sandstones as these elements are normally associated with clay minerals.

The high Sr concentrations are indicative of the presence of calcite minerals, most likely, calcite.

4.2 PRINCIPAL COMPONENT ANALYSIS

The preceding section (4.1) focused on the element distribution patterns and brought to light the heterogeneity in the samples. This only highlighted element distribution patterns and the need arose for element grouping to be established. Hence, principal component analysis (PCA) is used to determine the patterns of element associations in the wells studied.

Principal Component Analysis is defined as the process of mathematically defining a set of variables that describes the variance present in the original data. These variables are independent of each other and correlation between the new variables will equal zero. These new variables are termed principal components. (*Harris, 1987*)

The principal components are defined from the eigenvectors of a square (*Murtagh, 2005*). Eigenvectors are expressed as vectors that are not rotated under a given linear transformation. The first component (F1), accounts for the largest proportion of variance and the second component (F2) accounts for the second largest proportion of variance in the data set (*Harris, 1987*). A detailed account of the principles and application of PCA in geology is given by *Wilkensen, 1999*.

The principal component analysis plot is divided into four quadrants. The elements plot in groups in either of these quadrants. These groups are termed element clusters or alternatively clusters. Elements that cluster together are usually associated with each other thus the PCA plots can be used to identify element associations such that 3dimensional correlation can be done.

The PCA plots are used in this study to:

- determine diametric relationships that are useful in the calculation of geochemical indices.
- facilitate the correlation of these chemostratigraphic indices across the four wells.

The PCA plots for these wells are plotted independently of each other to allow the different element association patterns in each well to be recognized and compared with each other.

4.2.1 RESULTS

4.2.1.1 Well A-A1

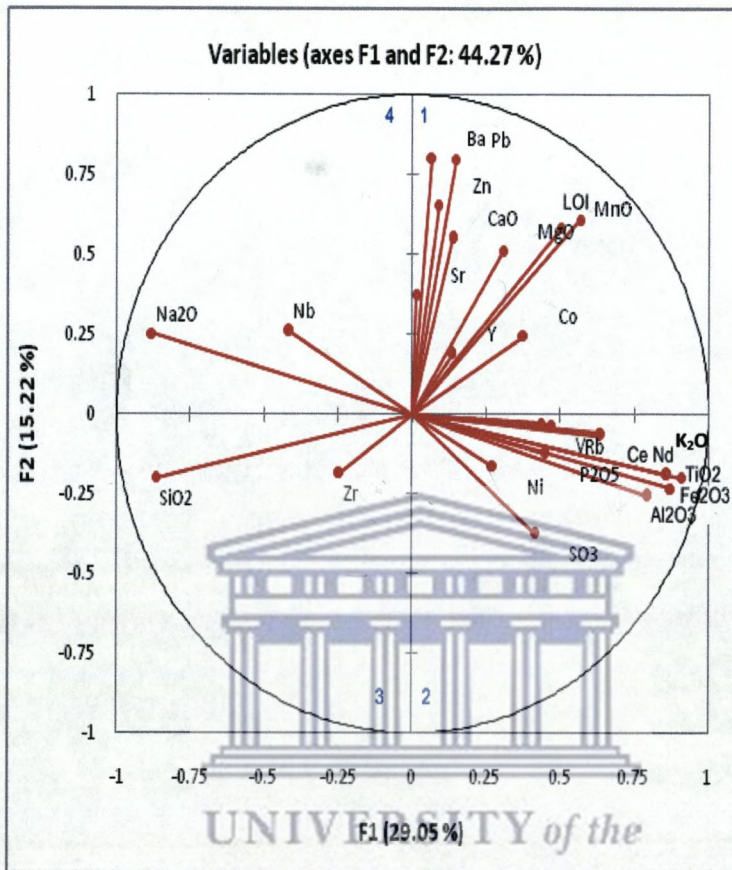


Figure 4.2.1.1: PCA plot of the major and minor elements for Well A-A1

The PCA plot for Well A-A1 displays four element clusters. SiO_2 and Zr plots in the 3rd quadrant. Na_2O and Nb plots in the fourth quadrant.

The third cluster is located in the 1st quadrant and is composed of the elements MnO, MgO, CaO Zn, Ba, Pb and Sr. Loss on ignition also plots in this cluster. The fourth element cluster is located in the 2nd quadrant and is composed of the major elements TiO_2 , Fe_2O_3 , P_2O_5 , K_2O , SO_3 and Al_2O_3 and trace elements V, Rb, Ce, Nd and Ni.

4.2.1.2 Well A-I1

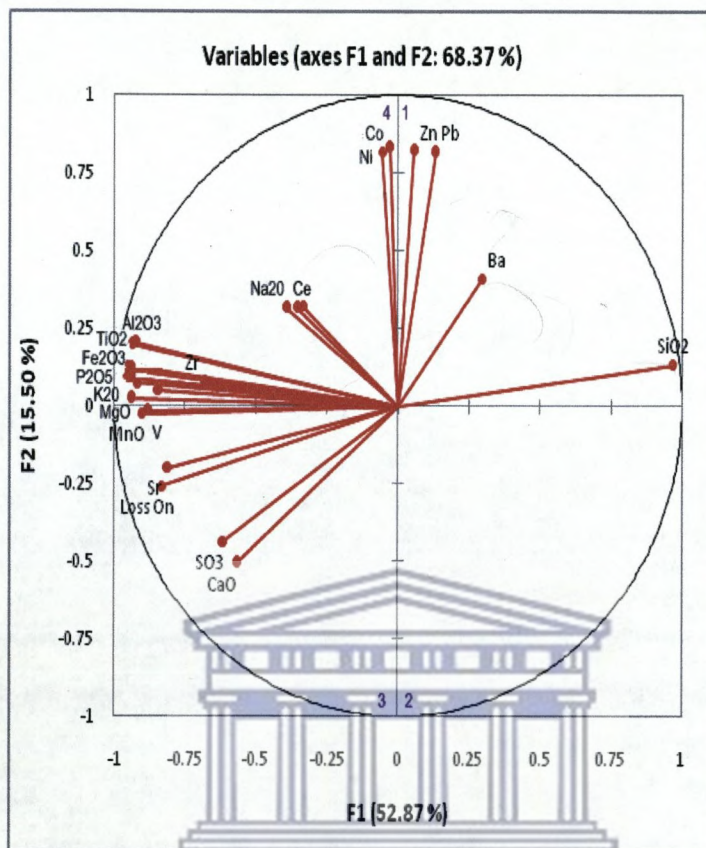


Figure 4.2.1.2: PCA plot of the major and minor elements for Well A-I1

The PCA plot for Well A-I1 displays three element clusters. The first cluster is located in the 4th quadrant of the PCA plot and consists of the major elements Al₂O₃, TiO₂, Fe₂O₃, K₂O, MnO, MgO, P₂O₅, and trace elements Ce, Nb, V, Zr and Sr.

The second cluster is located in the 1st quadrant of the plot and consists of the trace elements Ni, Co, Zn, Pb and Ba. The elements Ni and Co plots negatively on the axis F1. The remainder of the elements plot positive for axis F2.

The third cluster, that is located in the 3rd quadrant of the PCA plot, is composed of the elements CaO and SO₃. The elements in this cluster plot negative for both axes F1 and F2.

Loss of ignition (LOI) plots in the 3rd quadrant and is situated between cluster 1 and cluster 3. Na₂O plots in the 4th quadrant while SiO₂ plots in the 1st quadrant.

4.2.1.3 Well A-L1

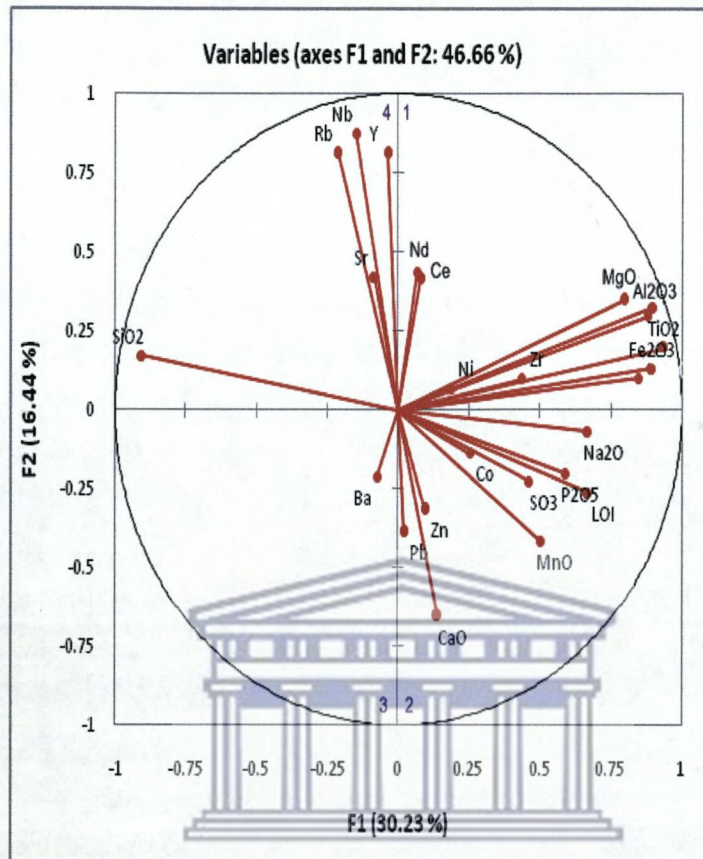


Figure 4.2.1.3: PCA plot of the major and minor elements for Well A-L1

Element cluster 1 of Well A-L1 plots in the 1st quadrant and is composed of the elements MgO, Al₂O₃, TiO₂, Fe₂O₃, K₂O, Ni and Zr. The elements display similar dispersion patterns.

The second element cluster is located in the 2nd quadrant. The cluster consists of the major elements MnO, SO₃, P₂O₅, and Na₂O and the trace element Co which displays similar dispersion trends.

The third cluster, that is located in the 4th quadrant, consists of the trace elements Rb, Nb, and Y. CaO is found in the 2nd quadrant and SiO₂ in the 4th quadrant.

4.2.1.4 Well A-U1

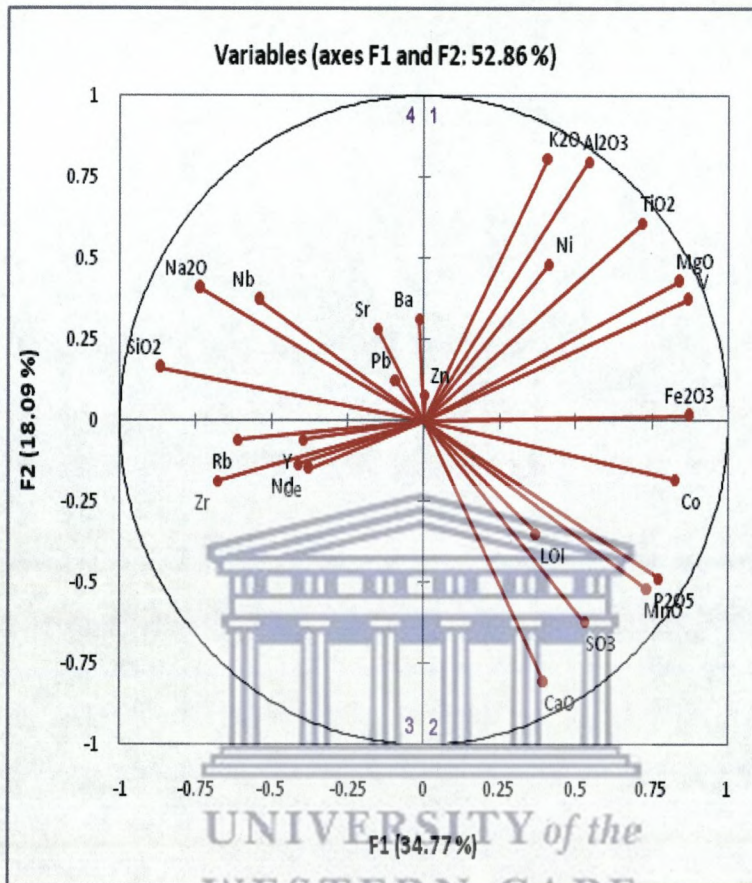


Figure 4.2.1.4: PCA plot of the major and minor elements for Well A-U1

The first element cluster for Well A-U1, located in the 1st quadrant of the PCA plot, consists of the major elements K_2O , Al_2O_3 , TiO_2 , MgO and trace elements Ni and V.

The second cluster is located in the 2nd quadrant and is composed of the major elements CaO , SO_3 , MnO , P_2O_5 , and the trace element Co.

The third cluster is located in the third quadrant and consists of the trace elements Rb, Zr, Nd, Ce, and Y.

The fourth cluster which is located in the 4th quadrant is comprised of the major elements Na_2O , SiO_2 and trace element Nb.

4.2.2 DISCUSSION

4.2.2.1 Well A-A1

The cluster composed of SiO_2 and Zr (C1) is suggestive of the siliceous nature of the sandstones. Na_2O and Nb (C2), in the 4th quadrant, are generally associated with feldspars (Pettijohn et al, 1987), (Brookfield et al, 2004). The third cluster (C3) is composed of the elements MnO, MgO and CaO, normally show an affinity to carbonate minerals. The presence of MgO and CaO if in lower concentrations may also be associated with clay minerals (Pettijohn et al, 1987). Loss on ignition also plotted in this cluster. This could be explained by the fact that carbonates contain a large amount of structurally bound water that is lost during the process.

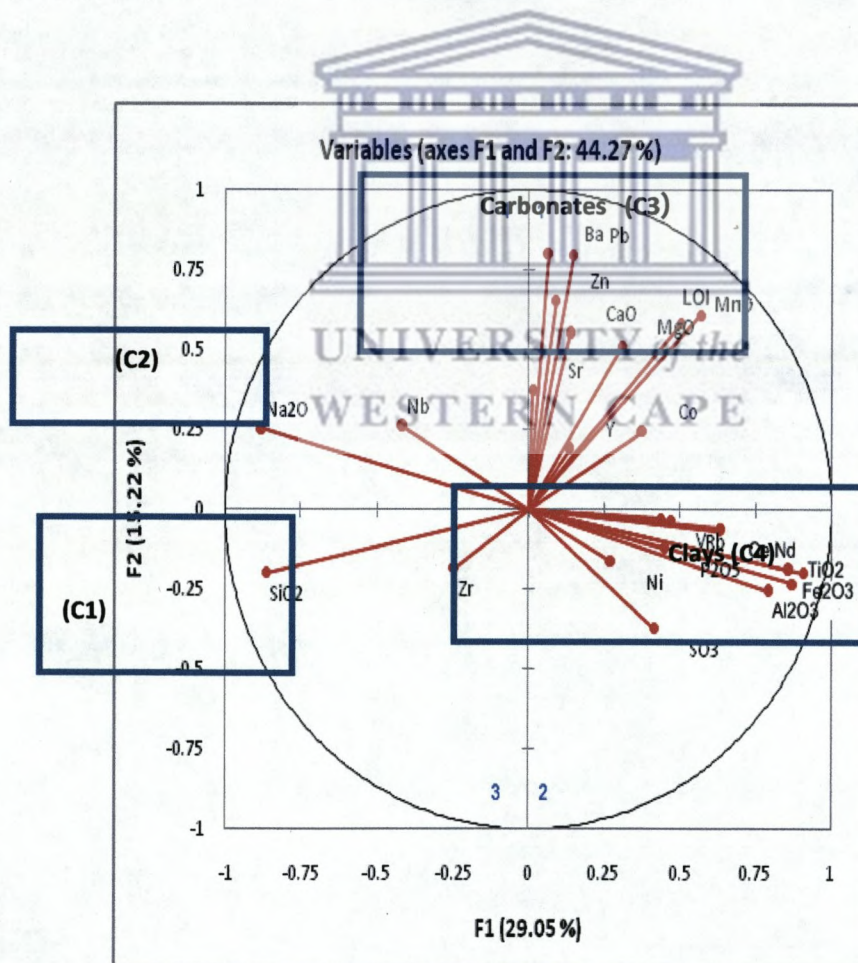


Figure 4.2.2.1: PCA plot of the major and minor elements for Well A-A1

The fourth cluster (C4), composed of the major elements TiO_2 , Fe_2O_3 , K_2O and Al_2O_3 , is normally associated with clay minerals. K_2O is normally associated with illite and mica while Al_2O_3 is associated with oxyhydroxides and kaolinite. (Pettijohn et al, 1987), (Brookfield et al, 2004)

Relationships that is evident in the well:

- Diametric relationship between SiO_2 and the elements associated with clays: This means that with increasing clay content, the siliceous nature of the rock decreases.
- Diametric relationship between SiO_2 and the elements associated with carbonate minerals. This indicates that an increase in the siliceous nature of the rock will result in a decrease in the concentration of carbonates.
- The clays display a diametric relationship with Na_2O . In other words, the clays have a low Na_2O concentration.



4.2.2.2 Well A-11

The first cluster (C1), located in the fourth quadrant of the PCA plot, consists of the major elements Al_2O_3 , TiO_2 , Fe_2O_3 , K_2O , MnO , MgO , P_2O_5 , and trace elements Ce, Nb, V, Zr and Sr. As mentioned previously this association of elements normally indicates the presence of clays (Pettijohn et al, 1987). To be more precise, Al_2O_3 could be associated with kaolinite or with the presence of feldspar (Deer et al, 1962), in this case it is most likely that it is found in association with clay minerals when considering the fact that the other elements in this cluster also displays strong affinities to clay minerals. K_2O has affinities with illite and mica. The presence of TiO_2 and high concentrations of MgO also indicates the presence of clay minerals (Pettijohn et al, 1987).

The second cluster (C2), located in the 1st quadrant of the plot, and consists of the trace elements Ni, Co, Zn, Pb and Ba. These elements are normally found in association with or are held in detrital ferromagnesium silicate minerals, detrital primary Fe oxides, hydrous Fe and Mn oxides and clay minerals. In the event where Fe is absent Zn is associated with minerals in carbon and silicate phases. Ba is also related to the abundance of feldspars (Pettijohn et al, 1987).

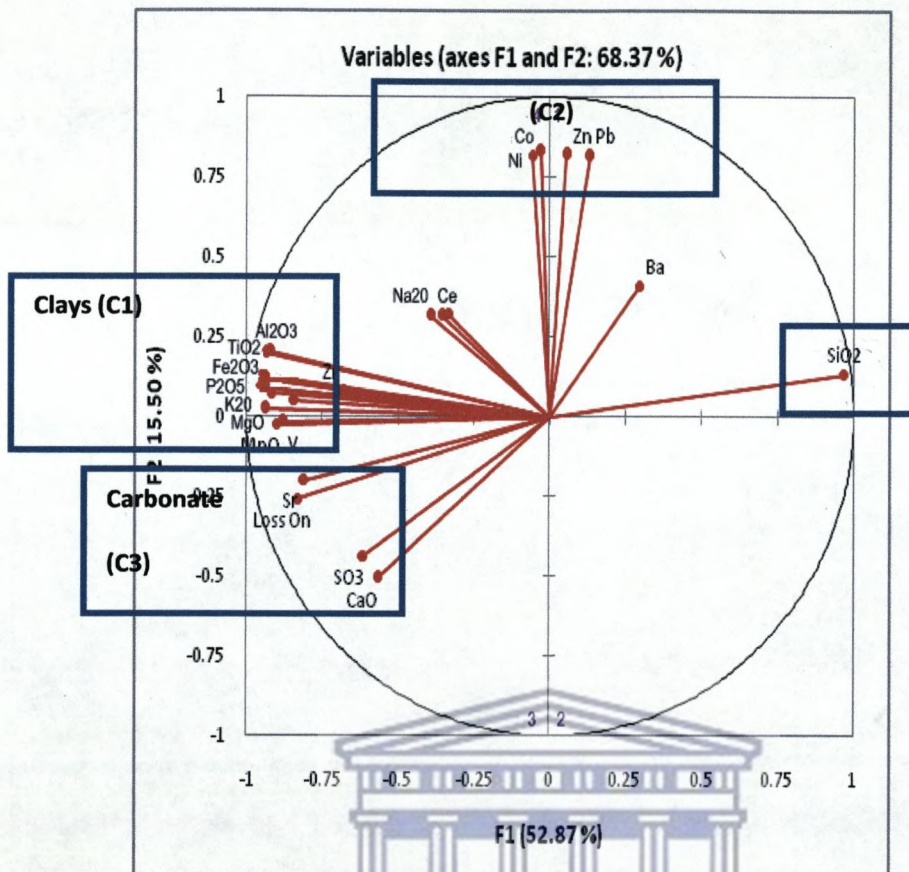


Figure 4.2.2.2 Principal Component Analysis plot of the major and minor elements for Well A-11

UNIVERSITY of the
WESTERN CAPE

The third cluster, which is located in the third quadrant of the PCA plot, is composed of the elements CaO and SO₃. The presence of the CaO in this cluster is indicative of the presence of carbonate minerals (*Brookfield et al, 2004*).

Loss of ignition (LOI) plots in the 3rd quadrant and lies between the clays (cluster 1) and the carbonates (cluster 3). This is expected as carbonates and clays lose a large amount of structurally bound water during the process. When this process takes place in clays it is referred to as dehydration or endothermic dehydroxylation. (*Sun,*)

Na₂O plots in the fourth quadrant and as discussed earlier is indicative of the presence of feldspar minerals. SiO₂ plots in the first quadrant and indicates the siliceous nature of the samples (*Pettijohn et al, 1987*), (*Deer et al, 1962*).

Relationships that are evident in the well:

- Diametric relationships between the elements associated with siliceous rocks and those associated with clays and the carbonates. In essence this means that an increase in silica will result in a decrease in clay minerals and carbonates.
- The position of the clay and carbonate clusters could indicate that some carbonates are also present in the clays.

4.2.2.3 Well A-L1

Element cluster 1 (C1) in the 1st quadrant is composed of Fe₂O₃, K₂O, Ni and Zr. As explained previously, these elements when found in association with each other is indicative of the presence of clays (*Pettijohn et al, 1987; Deer et al, 1962*).

The second element cluster (C2) consists of the major elements MnO, SO₃, P₂O₅, and Na₂O which display similar dispersion trends. These elements are associated with clay minerals and feldspars (*Deer et al, 1962*).

The third cluster consists of trace elements Rb, Nb, and Y. These elements are refractory elements. CaO is found in the third quadrant and is indicative of the presence of carbonates or carbonate minerals (*Deer et al, 1962*). SiO₂ is found in the fourth quadrant and its presence is suggestive of the siliceous nature of the samples.

Relationships that is evident from this well:

- Diametric relationship between the elements associated with those in sandstones (SiO₂) and those associated with clays. This implies a less siliceous nature of the lithologies with increasing clay content.
- SiO₂ displays a diametric relationship with the feldspar cluster; however the feldspar cluster and clay cluster are grouped very close together. It could thus be assumed that the feldspar minerals that are present are part of the clays and not the sandstone. The feldspar minerals in the clays may be either of an authigenic or secondary nature.

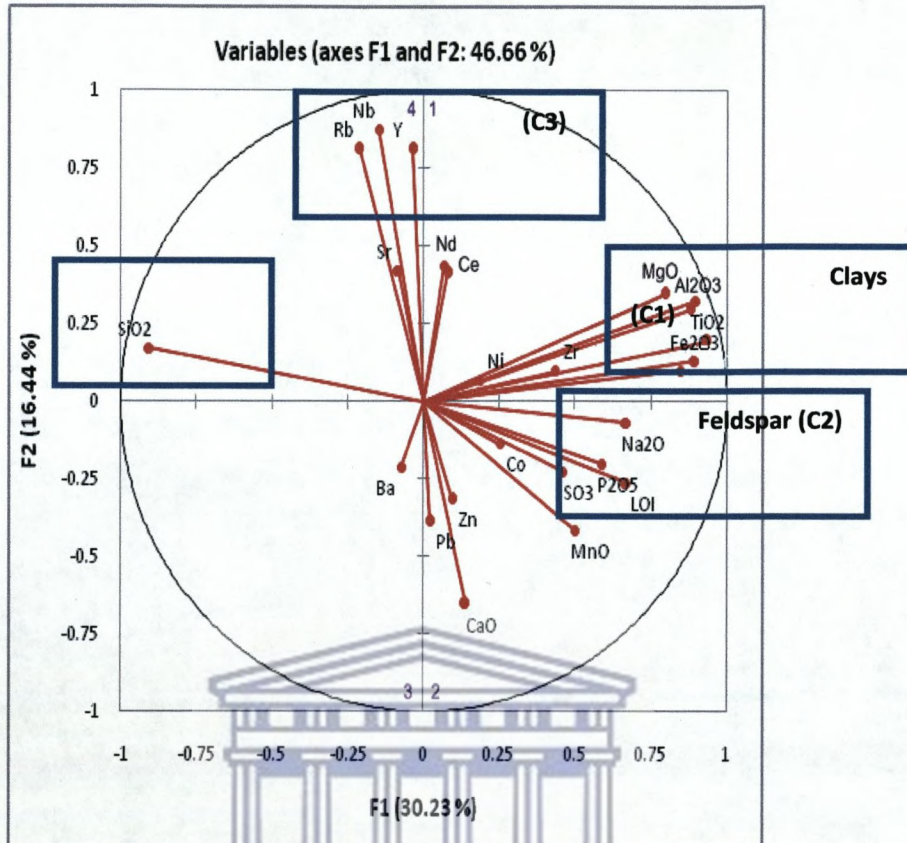


Figure 4.2.2.3 Principal Component Analysis plot of the major and minor elements for Well A-L1.

UNIVERSITY of the
WESTERN CAPE

4.2.2.4 Well A- U1

The first element cluster (C1) consists of the major elements K₂O, Al₂O₃, TiO₂, MgO and trace elements Ni and V. The major elements of this cluster have affinities for clay minerals, in particular kaolinite, illite and mica (Deer et al, 1962), (Pettijohn et al, 1987), (Trinidad et al, 2009). The trace elements Ni and V are both found in association with and reflect the abundance of detrital Fe oxides, clay minerals and hydrous oxides of Fe and Mn.

The second cluster (C2) is composed of the major elements CaO, SO₃, MnO, P₂O₅, and the trace element Co. CaO and MnO have affinities with carbonate minerals while P₂O₅ reflects the abundance of clay minerals in the samples (Pettijohn et al, 1987).

The third cluster (C3) is located in the 3rd quadrant and consists of the trace elements Rb, Zr, Nd, Ce, and Y. These elements are refractory elements.

The fourth cluster comprises major elements Na_2O , SiO_2 and trace element Nb. The presence of SiO_2 indicates the siliceous nature of the samples (Alberede et al, 2003) while Na_2O indicates the presence of feldspar minerals (Deer et al, 1962). Based on this it could be inferred that this cluster represents sandstone samples with high feldspar content or alternatively termed feldspathic sandstones.

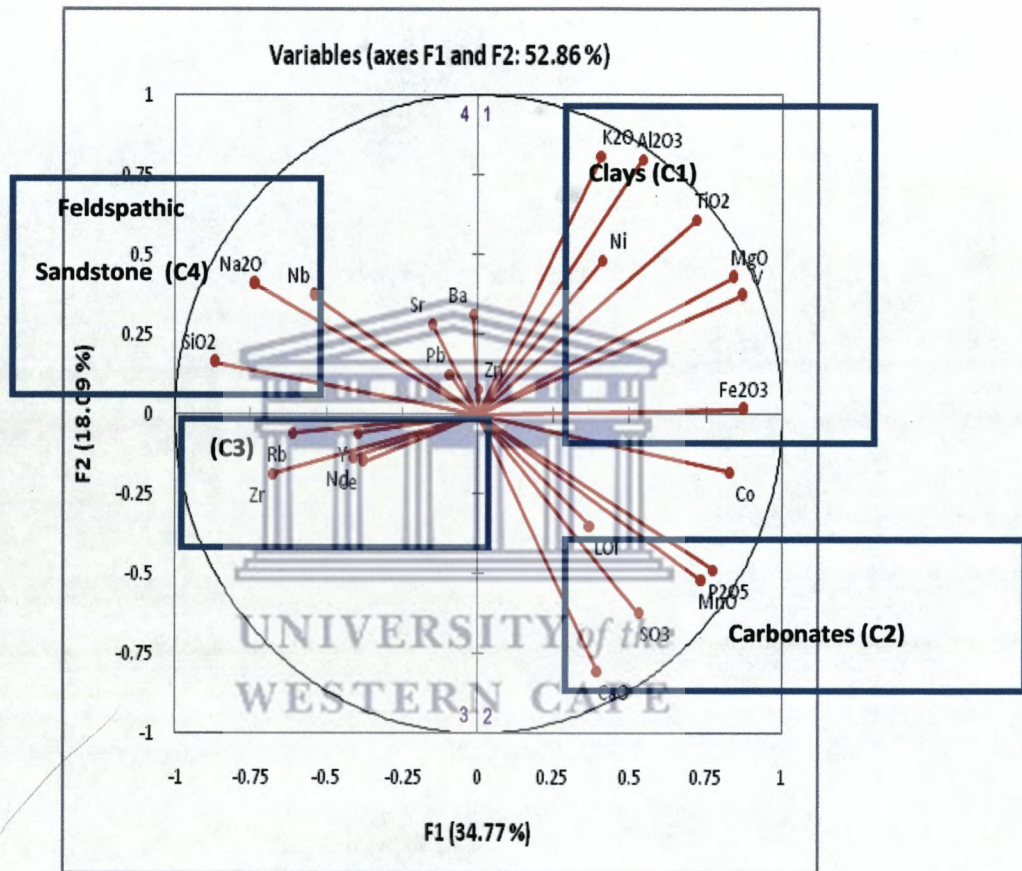


Figure 4.2.2.4 Principal Component Analysis plot of the major and minor elements for Well A-U1

Relationships evident from this well:

- Diametric relationship between the elements associated with sandstone (SiO_2) and those associated with carbonates.
- The clays and the carbonates, once again group very closely together.
- The relative positions of the three clusters indicates that this well could possibly be composed of alternating layers of calcareous clays, clays and sandstone units

4.2.3 SUMMARY

- The PCA plots for the wells produced element groupings that indicated that there are alternating units of sandstone, feldspathic sandstone, calcareous clays and clays present in the measured samples.
- The presence of SiO_2 indicates the siliceous nature of the samples.
- The wells display the following diametric relationships between:
 1. SiO_2 and the carbonate mineral cluster
 2. SiO_2 and clay mineral cluster
 3. Nd and V
 4. Nb and Ni
 5. Zr and Co
 6. Nb and Zn
 7. SiO_2 and Co
 8. Y and Pb
 9. Zr/Sr
 10. Nb/Rb
- Elements associated with Carbonate and clay minerals plotted close to each other for all the wells.
- The PCA plot for Well A-U1 indicated the presence of feldspathic sandstone while the plots for the other wells indicates that the feldspar minerals may be either in the carbonate phase or the clay phase.
- The elements that display diametric relationships are used to formulate element ratios (chemostratigraphic indices) whose signatures are used to identify chemostratigraphic units.

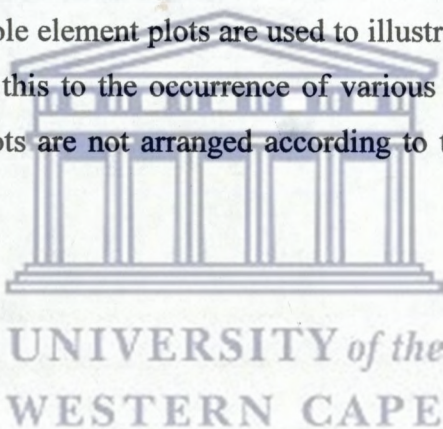


4.3. MAJOR AND TRACE ELEMENT GEOCHEMICAL PROFILES

4.3.1 RESULTS

The preceding results sections highlighted the following:

- The element distributions and associations patterns show slight differences in the wells that were samples. The treatment of the data from the various wells with principal component analysis established various element groupings. Some of these element groupings do however show common features that can be used to formulate geochemical indices for chemostratigraphy. These indices could be used to define the lithologies in all the wells.
- In this section downhole element plots are used to illustrate recognizable trends in the PCA plots and relate this to the occurrence of various lithologies in the wells. The downhole element plots are not arranged according to the clusters derived from the PCA plots.



4.3.1.1 Well A-A1

Major Element Profiles

- SiO_2 concentrations in the Well A-A1 vary between 60% - 75%. Three major concentration ranges were recognizable: <60%, 60% - 65% and above 65%. The latter clusters in the top and base of the samples section. **(Figure 4.3.1)**
- Al_2O_3 concentrations range from 10% to 16%. Three major concentration ranges are also recognizable: > 10%, 10% - 12% and above 12%. The latter coincides with zones featuring low SiO_2 contents. **(Figure 4.3.1)**
- Fe_2O_3 shows similar downhole trends as Al_2O_3 and varies in concentration that between 0.4% - 9%. Three concentration ranges are recognizable: < 4%, 4% - 5% and > 5%.
- CaO, MgO and MnO contents varies between 4% -7%, 2.1% - 2.9% and 0.08% - 0.12% respectively and displays similar downhole trends. Three concentration

categories were recognized for the three elements: CaO: > 3%, 3% - 5% and < 3%; MgO: < 1.9%, 1.9% - 2.3% and > 2.3%; MnO: < 0.01%, 0.01% - 0.09% and > 0.09%.(Figure 4.3.1)

- Na₂O contents ranges from 0.4% to 1.8%. The downhole trend for Na₂O is very similar to the trend displays by SiO₂.
- K₂O contents range between 1% to 5%. K₂O displays the same downhole trend as Al₂O₃ and Fe₂O₃.

Trace Element Profiles (Refer to Fig 4.3.2)

- Co concentrations show variation in the range of 3.5ppm – 22.5ppm. Three Co concentration ranges are identified: < 7.5ppm, 7.5ppm – 17.5ppm and > 17.5ppm. The latter range is found towards the bottom of the section. The element Co show similar downhole trends to Ni.
- Ni contents range from 10ppm to 140ppm and can be subdivided into three concentration ranges: < 60ppm, 60ppm – 80ppm and > 80ppm. The latter are concentrated between the depths of 3625m to 3650m.
- High Zr contents occur throughout the sampling interval and vary between 225ppm and 300ppm.
- Zn, Pb, Ba and Sr displays similar downhole dispersion patterns, with concentrations ranges of 116ppm – 8900ppm, 90ppm -1280ppm, 423ppm – 3150ppm and 100ppm – 225ppm respectively. These elements show an inverse trend when compared with the refractory elements Ni, Y, Nb and Rb in the downhole plots.

Major Element Profile: Well A-A1

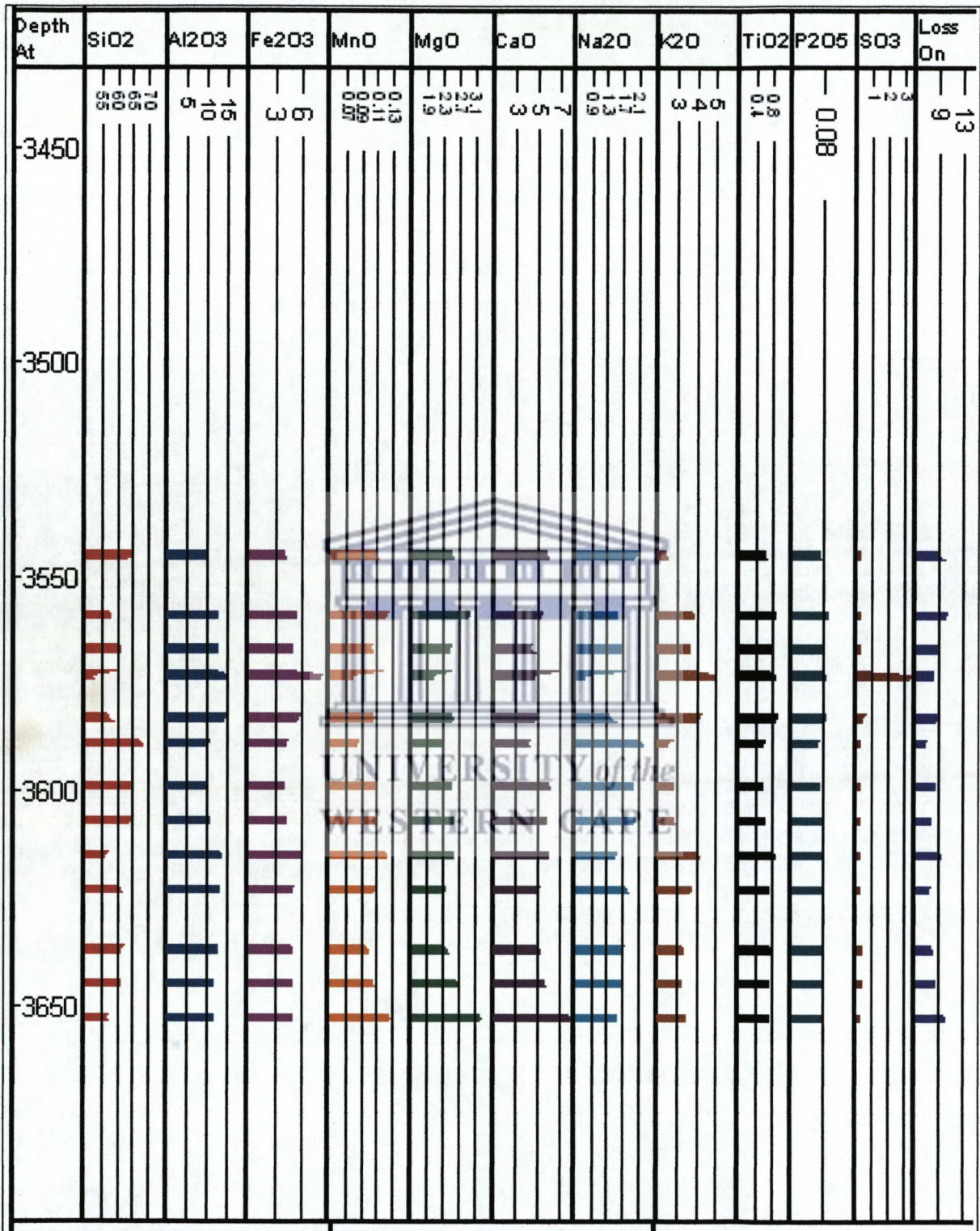


Figure 4.3.1: Major Element Profiles for Well A-A1

Minor Element Profile: Well A-A1

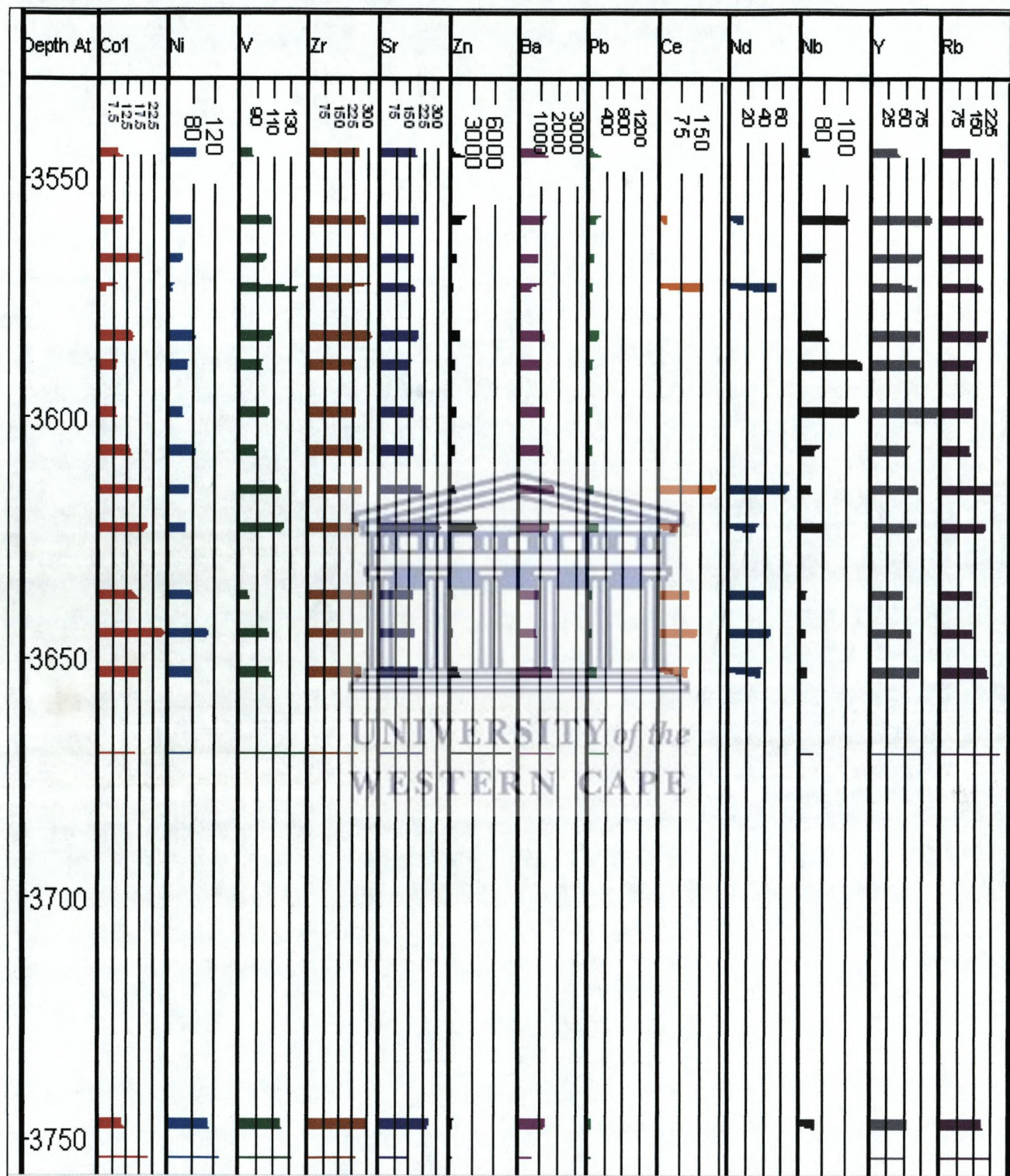


Figure 4.3.2: Minor Element Profile: Well A-A1

4.3.1.2 Well A-L1

Major Element Profiles (Refer to Figs 4.3.3 and 4.3.4)

The samples for this well comprise three different sampling intervals.

- SiO₂ concentrations for the Well A-L1 are in the range 50 % to 80% and three concentration ranges are identified: <55%, 55% - 70% and > 70%.
- Al₂O₃, Fe₂O₃, MnO and MgO contents varies between 6% to 12%, 4% to 10%, 0.14% and 0.18% and 1% to 2% respectively and display similar downhole trends. These elements display inverse trends with the element SiO₂.
- CaO concentrations are in the range 1% to 15% and can be subdivided into three concentration ranges: < 5%, 5% - 12% and >12%. The latter concentration range is concentrated at the top of the sampled section.
- Concentrations of Na₂O and MgO are in the range 0.1% -0.55% and 0.5% - 1.5% respectively and also display the similar downhole trends.
- K₂O and TiO₂ exhibits similar downhole trends and have concentrations in the range of 1% to 4% and 0.4% to 0.8% respectively.

Trace Element Profiles (Refer to Figs 4.3.5 and 4.3.6)

- Co concentrations are in the range 1ppm to 30ppm and occur in three concentration ranges: < 10ppm, 10ppm – 20ppm and > 20ppm. Co has inverse relationships with Sr, Zr, Zn and Pb. (Figure 4.3.2.3), (Figure 4.3.2.4)
- Ni and V contents vary between 10ppm – 75ppm and 30ppm – 120ppm respectively and follow similar downhole dispersion trends.

Major Element Profiles for Well A-L1

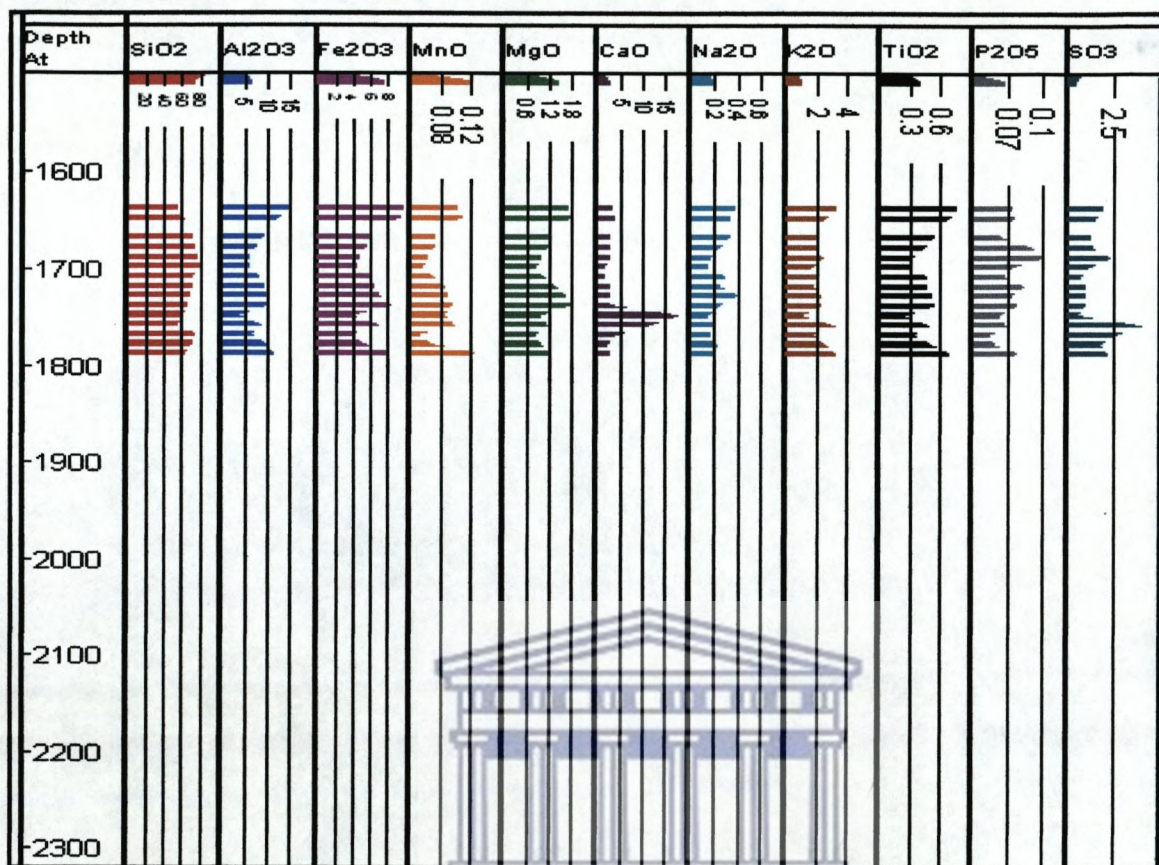


Figure 4.3.3: Major Element Profile: Well A-L1 (Section 1)

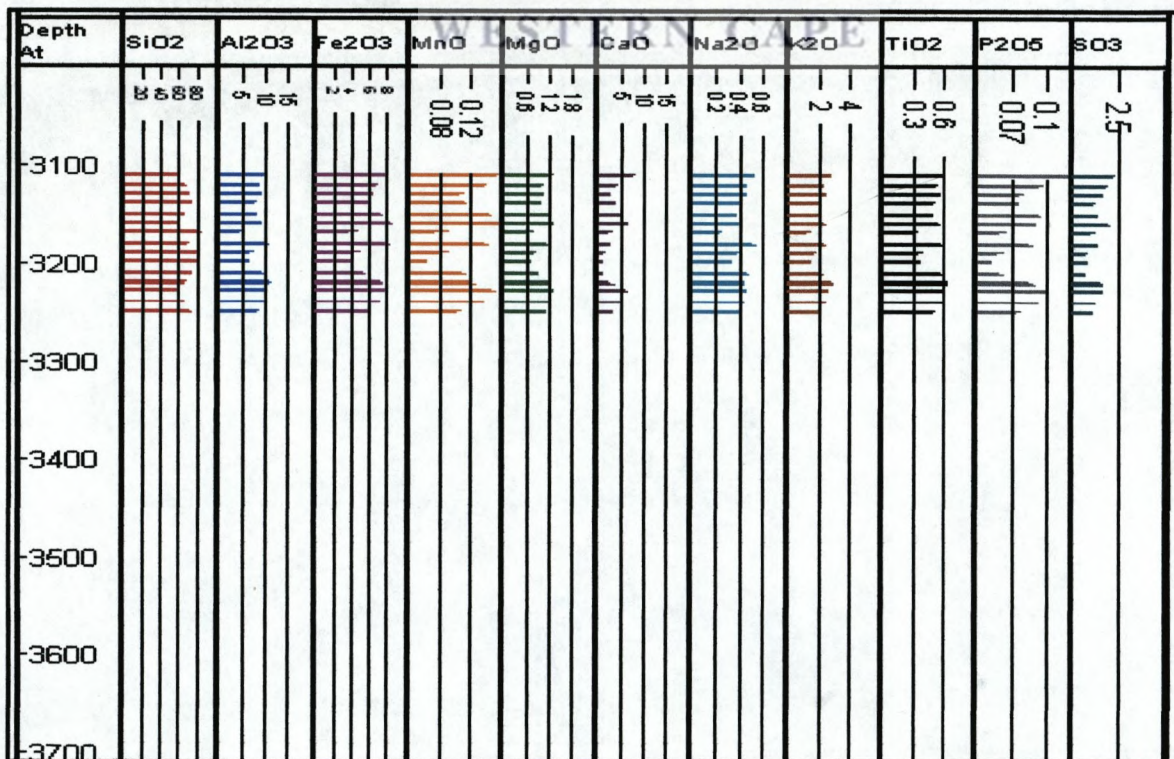
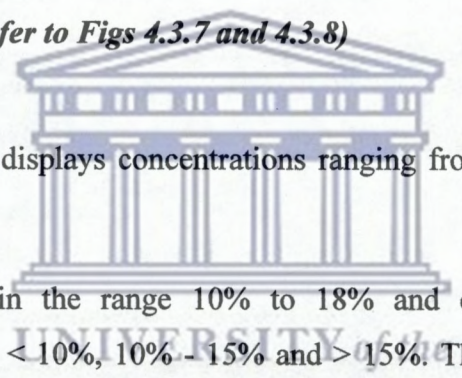


Figure 4.3.4: Major Element Profile: Well A-L1 (Section 2)

- Zr contents vary from 150ppm to 350ppm. Zr displays an inverse relationship with Co, Fe₂O₃, MnO and MgO.
- Nb, Rb and Y display similar downhole trends and have concentrations that are in the range 20ppm – 60ppm, 20ppm – 175ppm and 5ppm – 80ppm respectively. The highest concentrations for these elements are found at the top of the sampled section.
- The concentrations of Ce and Nd are in the ranges 25ppm to 100ppm and 5ppm to 40ppm respectively, and display similar downhole trends.

4.3.1.3 Well A-U1

Major Element Profiles (*Refer to Figs 4.3.7 and 4.3.8*)

- 
- SiO₂ for Well A-U1 displays concentrations ranging from approximately 60% to a maximum of 80%.
 - Al₂O₃ contents are in the range 10% to 18% and can be divided into three concentration ranges: < 10%, 10% - 15% and > 15%. The latter being concentrated towards the bottom of the section. Al₂O₃ displays an inverse trend with SiO₂.
 - The sampled interval displays high concentrations of Na₂O with a minimum of 0.6% and a maximum of 1.2%. This element displays the same downhole trend with SiO₂ as Al₂O₃.
 - CaO and MnO contents are in the range 3% to 13% and 0.04% - 0.01% respectively. CaO displays a peak of approximately 13% is found at a depth of 2750m. CaO and MnO displays the same downhole patterns
 - The concentrations of K₂O TiO₂ are in the ranges 2% - 4% and 0.4% - 0.9% respectively. These element display similar downhole trend as Al₂O₃

Minor Element Profiles for Well A-L1

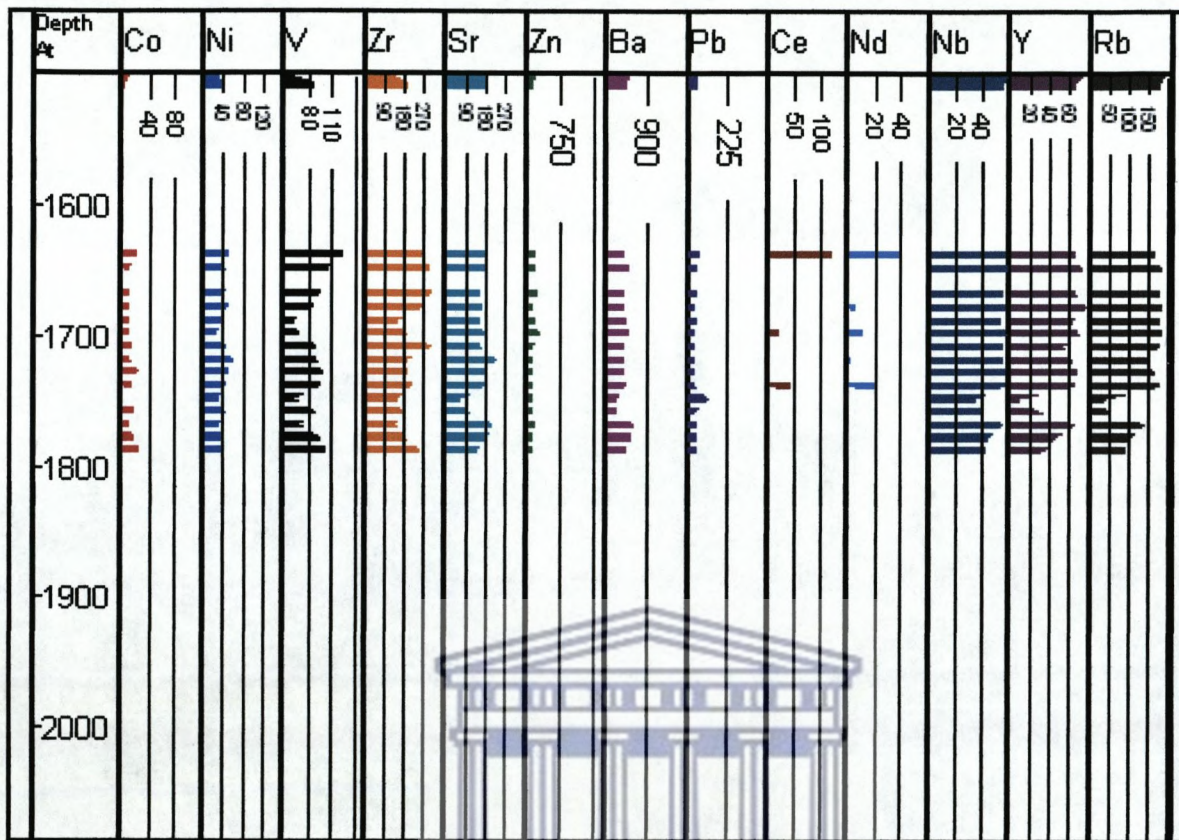


Figure 4.3.5 Minor Element Profile: Well A-L1 (Section 1)

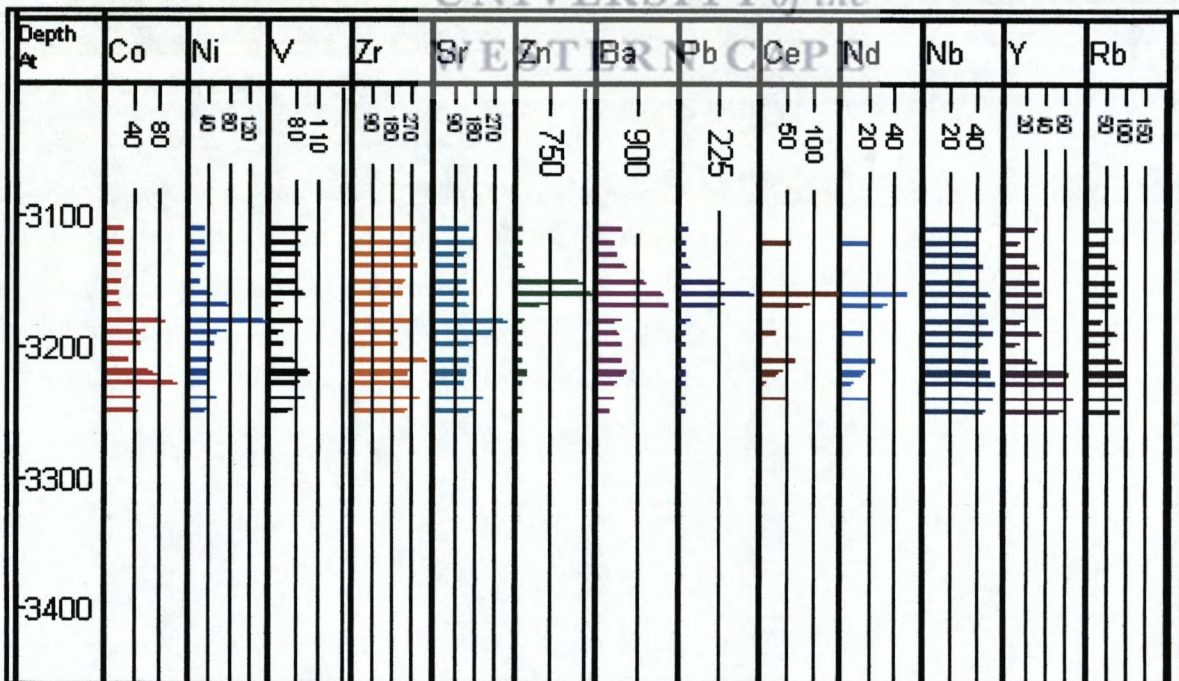


Figure 4.3.6 Minor Element Profile: Well A-L1 (Section 2)

Major Element Profiles for Well A-U1

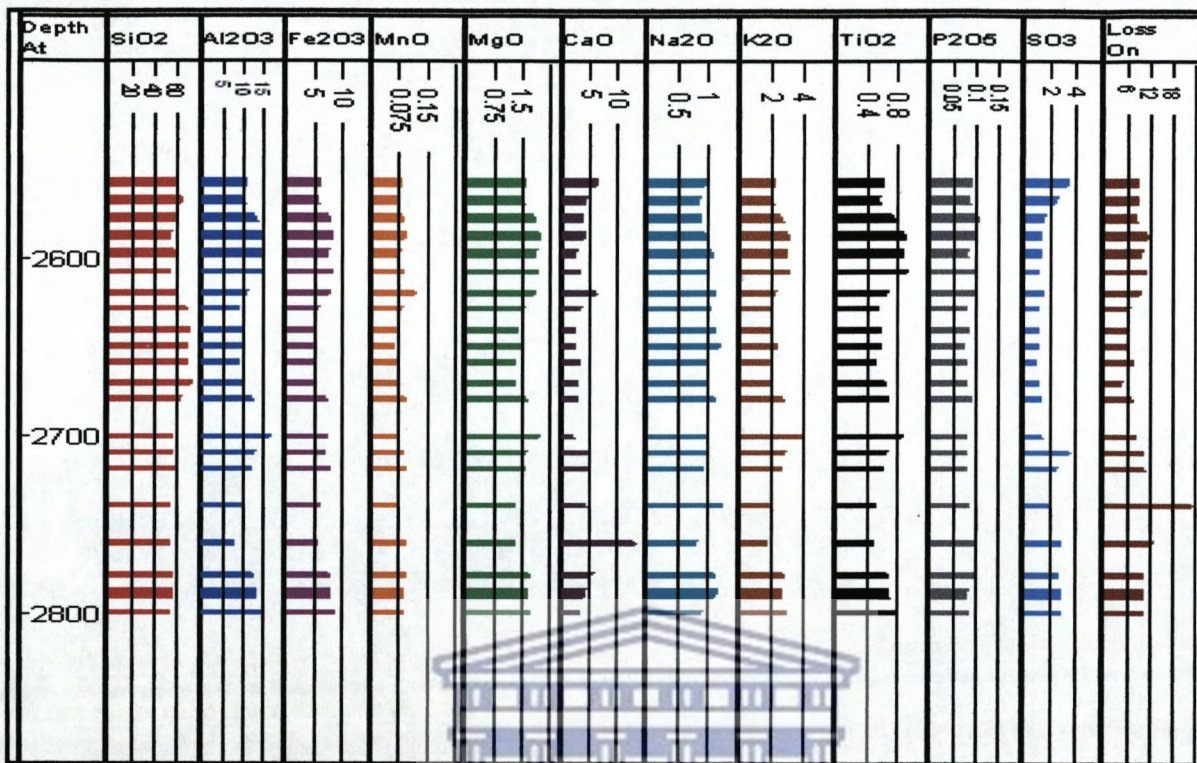


Figure 4.3.7 Major Element Profile: Well A-U1 (Section 1)

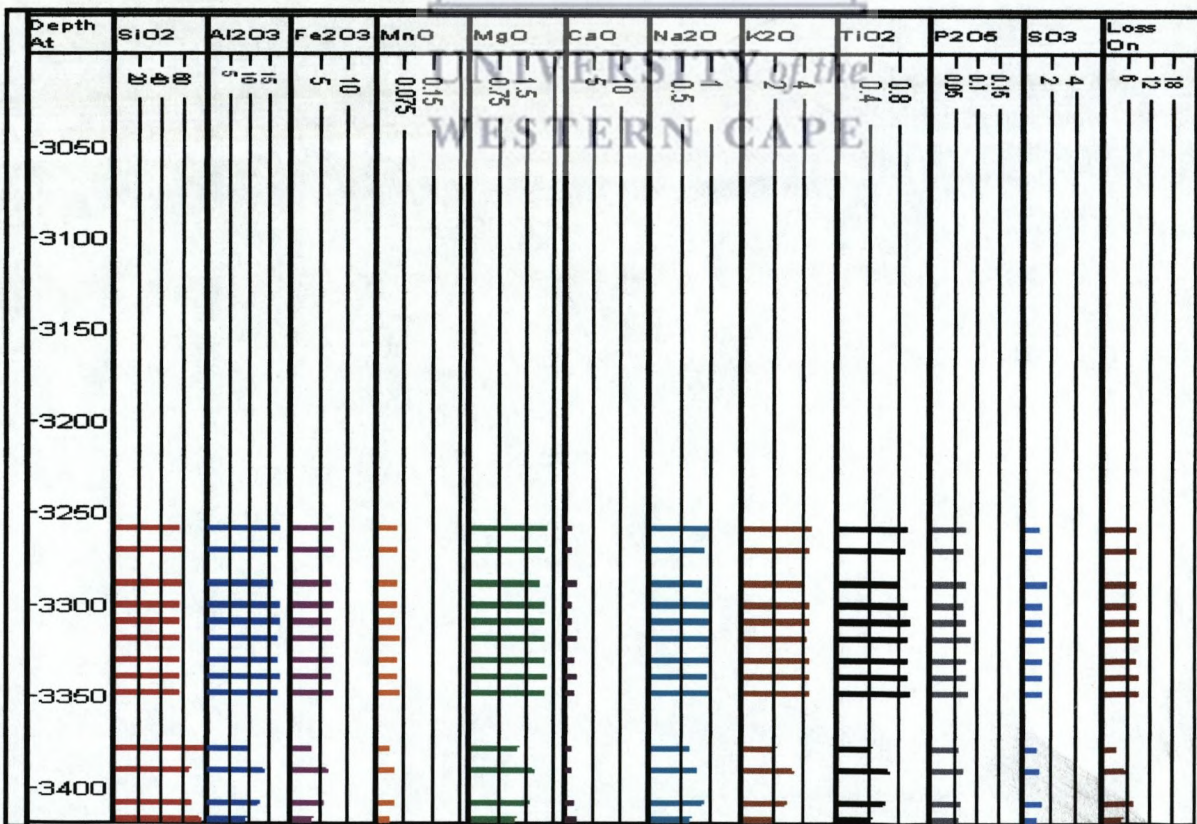


Figure 4.3.8 Major Element Profile: Well A-U1 (Section 2)

Trace Element Profiles (Refer to Fig 4.3.9 and 4.3.10)

- Co, Ni and V display similar downhole trends throughout the sampling interval and exhibit concentrations ranging from 10ppm to 30ppm, 50ppm to 60ppm and 100 to 150ppm respectively. Co and Ni both display an anomalous peak at the base of the unit reaching 50ppm and 170ppm respectively.
- Zr concentrations are in the range 200ppm – 400ppm and displays inverse downhole trends with the elements Co and Ni.
- Sr had concentrations fall in the range 100ppm – 300ppm displays the same trend as Co and Ni. The anomalous peak exhibited by Sr (approx 300ppm) correlated with that of Co and Ni.
- Zn (range: 100ppm – 1100ppm) displays relatively uniform concentrations (approximately 250ppm) except for a peak (approx 1000ppm) at a depth of 2750m. Zn, Pb (range: 20ppm – 280ppm) and Ba (100ppm – 3000ppm) displays similar dispersal trends. Pb displays peaks that corresponded to that of Zn.
- Ce concentrations for the sampled interval display variable concentrations ranging from very 0ppm to 100ppm.
- As with Well A-A1, the elements Nb, Y and Rb also displays similar trends throughout the interval.

Minor Element Profiles for Well A-U1

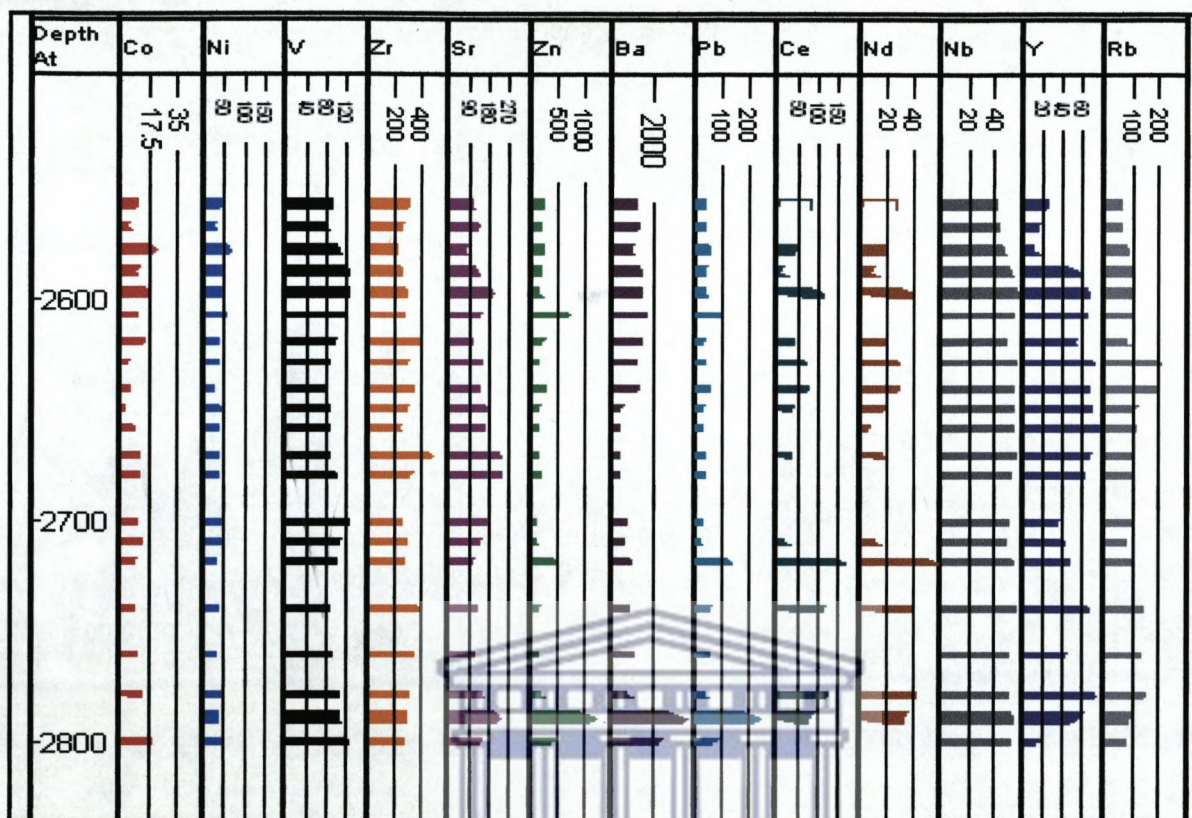


Figure 4.3.9: Minor Element Profile: Well A-U1 (Section 2)

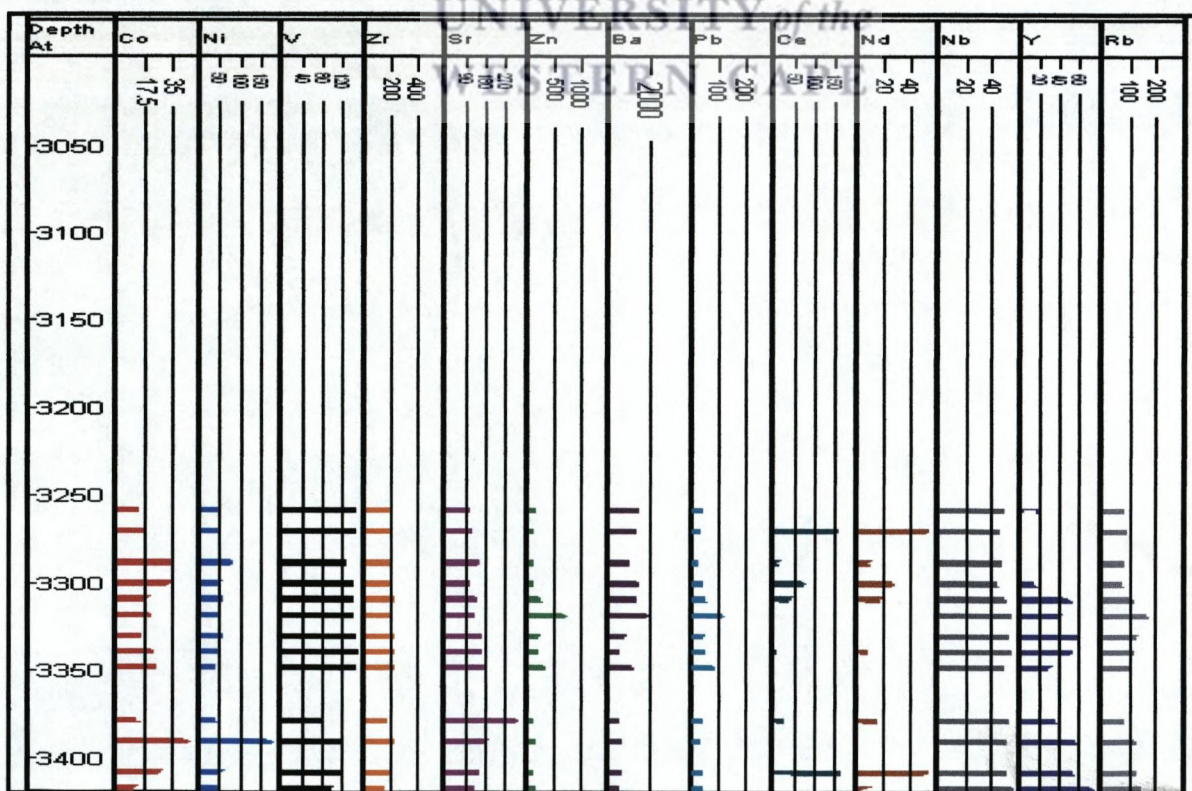


Figure 4.3.10 Minor Element Profile: Well A-U1 (Section 2)

3.3.1.4 Well A-11

Major Element Profiles (*Refer to Fig 4.3. 11*)

- SiO₂ concentrations for this well show concentrations in the range: 55% to 90%. Three element concentration clusters are recognized: < 50%, 50% - 70% and > 70%.
- Al₂O₃ (range: 8% to 12%), Fe₂O₃ (range: 5% to 10%), MnO (range: 0.02% to 0.09%), MgO (range: 0.9% to 2%) K₂O (range: 2% to 5%), and Ti₂O (range: 0.35% to 0.85%), as with the PCA, displays similar downhole dispersal patterns. These elements are generally associated with clay minerals. These elements display inverse relationships with SiO₂ thereby indicating alternating layers of pure sandstones with sandstones of a more argillaceous nature.
- CaO concentrations are in the range 1% - 9%. The concentrations are higher in the top part than in the lower part. This could indicate that the samples in the top part is composed of carbonate cements or possesses a carbonate matrix. CaO displays an inverse relationship with SiO₂ as seen on the PCA plot.
- Na₂O displays relatively uniform values falling in the range 0.5% - 0.6%. The downhole pattern exhibited by Na₂O indicates that the sandstones are of a more feldspathic nature than the rest.

Trace Element Profile (*Refer to Fig 4.3. 12*)

- Co and Ni, which displays similar dispersion patterns, have concentrations in the range 10ppm - 60ppm and 20ppm – 140ppm respectively. These elements are found in the same cluster on the PCA plot.
- V, Zr and Sr, much like the PCA, display the same dispersal patterns and have concentrations that fall in the ranges 60% - 80%ppm (except for an anomalous peak of 120ppm at a depth of 4000m), 75ppm – 225ppm and 75 – 225ppm respectively. All of the elements display distinctive changes in their trends below 4125m.
- The elements Co and Ni are characterized by sudden increases below 4125m while V, Zr, and Sr are characterized by decreases in their concentration.

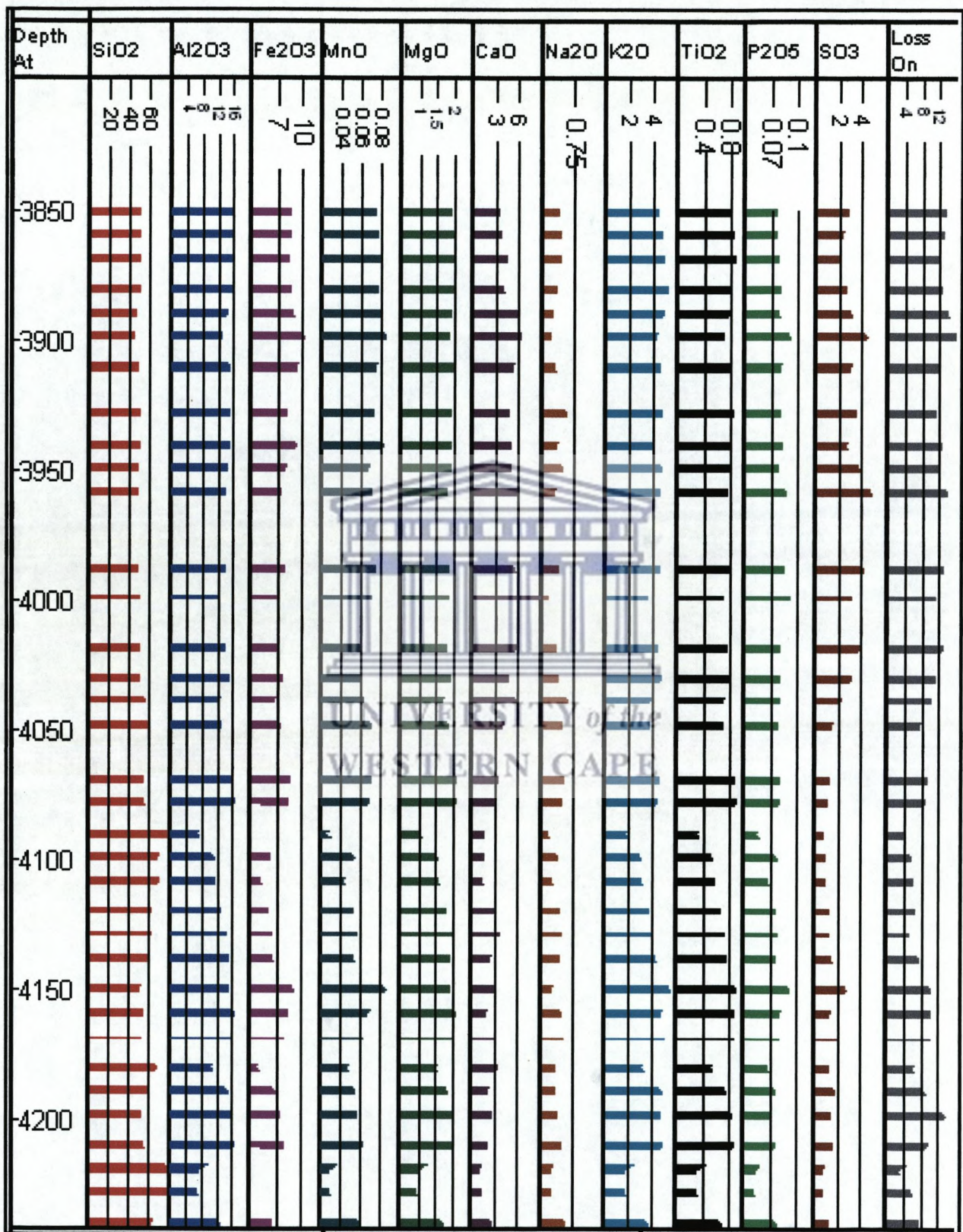


Figure 4.3.11: Major Element Profile: Well A-11

- The elements Ce and Nd plot in the same cluster on the PCA and shows similar dispersal patterns in the downhole profiles. They have concentrations that fall in the ranges 10ppm – 150ppm and 10ppm – 60ppm.
- Nb, Y and Rubidium followed similar downhole dispersal patterns. On the PCA these elements clustered together and their downhole trends substantiated the theory that these elements are associated. They display concentrations that fall in the following ranges: Nb: 40ppm -60ppm; Y: 20ppm – 80ppm; Rb: 60ppm – 200ppm.

Minor Element Profile for Well A-1

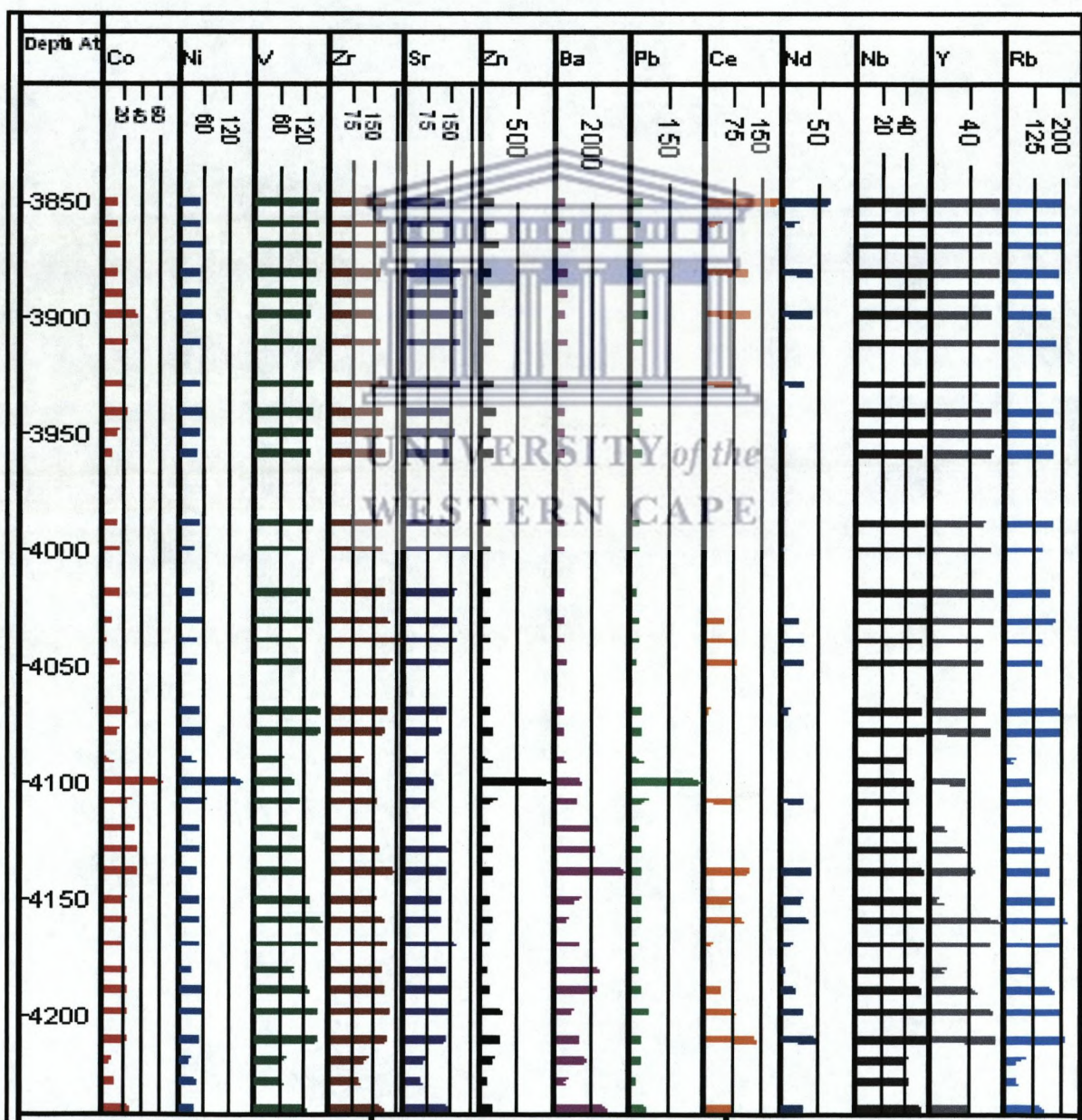


Figure 4.3.12 Minor Element Profile: Well A-1

4.3.2 DISCUSSION

4.3.2.1 Well A-A1 (Refer to Fig 4.3.1 and 4.3.2)

The high concentrations displayed by SiO_2 are suggestive of the siliceous nature of the samples. Al_2O_3 displays downhole trends that show an inverse relationship to SiO_2 and this could be suggestive of the presence of intervals composed of alternating layers of clean sandstone and more argillaceous layers. The downhole trend for Na_2O is very similar to those displayed by SiO_2 . Their strong association as depicted by the PCA plots and the similarities in the downhole trends suggests a variable feldspathic nature of the siliceous rocks.

Al_2O_3 , Fe_2O_3 and K_2O display similar downhole trends and thus explain their clustering on the PCA plots. This element association suggests the presence of clay minerals and the occurrence of argillaceous layers.

Furthermore, CaO , MgO , and MnO displays similar downhole trends and also cluster together on the PCA plots, which may be suggestive of the presence of carbonate minerals.

Co contents vary between 3.5ppm – 22.5ppm with three concentration ranges: < 7.5ppm, 7.5ppm – 17.5ppm and > 17.5ppm. The latter range is found towards the bottom of the section.

Ni contents vary from 10ppm to 140ppm with three concentration ranges identified namely, < 60ppm, 60ppm – 80ppm and > 80ppm. The latter concentration range occurs at depths 3625m to 3650m. The downhole patterns displays trends of cyclic increases and decreases.

Zn, Pb, Ba and Sr display similar downhole dispersion patterns and thus reflect their positive association in the PCA plot. The contents of these elements fall into the following concentration ranges: 116ppm – 8900ppm, 90ppm -1280ppm, 423ppm – 3150ppm and 100ppm – 225ppm respectively. This element association suggests the presence of carbonate rich zones. Zn displays diametric correlations with Ni and refractory elements Y, Nb and Rb.

4.3.2.2 Well A-L1

SiO_2 concentrations for the Well A-L1 are in the range 50 % to 80%. These relatively high concentrations are indicative of the siliceous layers downhole. Contrarily, Al_2O_3 , in line with

the PCA plots, displays an inverse relationship with SiO_2 , throughout the log section (**Figure 4.3.3**), (**Figure 4.3.4**). This indicated the presence of pure sands alternating with clay rich or feldspathic sands.

Na_2O and MgO displays the same downhole trends. The presence of these elements is normally suggestive of the presence of feldspar minerals. On the PCA plot Na_2O plots close to the clusters representing clay minerals as well as carbonates. CaO contents are in the range 1% to 15%. Highest concentrations are found at the top of the downhole section and are indicative of an increase in carbonate minerals at the top. (**Figure 4.3.3**) (**Figure 4.3.4**).

Fe_2O_3 , MnO and MgO all display downhole trends similar to Al_2O_3 . The fact that these elements are found to be abundant together suggested the occurrence of argillaceous components in the sandstone, as these elements have affinities to clay minerals (*see PCA plots*). K_2O and TiO_2 exhibited the same trend and areas of increase of K_2O coincide with areas of increase of Fe_2O_3 , MnO and MgO , further evidence of the presence of argillaceous units.

Co contents are in the range 1ppm to 30ppm and had inverse relationships with Sr , Zr , Zn and Pb (**Figure 4.3.5**), (**Figure 4.3.6**). Zr contents vary from 150ppm to 350ppm. Zr displays an inverse relationship with Co , Fe_2O_3 , MnO and MgO . Zr appears to be concentrated in siliceous rocks while high MnO and MgO occur in clays and carbonates.

Ni and V , as with the PCA plot, show similar dispersal trends. The bottom part of the sampled section has elevated values for Ni and Co which could indicate that the lower section is less siliceous than the preceding sections.

Nb , Rb and Y display similar downhole trends and also occur in the same cluster on the PCA plot. The highest contents of these elements occur at the top of the downhole section thereby indicating the argillaceous nature of the samples (**Figure 4.3.5**), (**Figure 4.3.6**).

4.3.2.3 Well A-U1

SiO_2 contents in Well A-U1 displays concentrations ranging from approximately 60% to a maximum of 80% thus indicating the siliceous nature of the underlying lithologies. The sampled interval displays very high concentrations of Na_2O up to 1.2% that displays inverse trends with SiO_2 . This corroborates the statement that there are alternating layers of clean and feldspathic sandstones present.

Al_2O_3 ranges between 10% and 18%. The highest concentrations occur at the top and the base of the sampled section. Al_2O_3 displays an inverse relationship with SiO_2 . An occurrence of alternating units of clean sandstones with feldspathic sandstones can therefore be assumed (**Figure 4.3.7**), (**Figure 4.3.8**).

CaO contents vary between 3% and 13%. A peak concentration of approximately 13% occurs at a depth of 2750m. CaO and MnO display the same downhole patterns and also cluster together on the PCA plot. As mentioned previously, these elements are associated with carbonate minerals.

K_2O , TiO_2 and Al_2O_3 , shows similar downhole patterns that are associated with the occurrence of clay minerals. (**Figure 4.3.7**), (**Figure 4.3.8**)

Co, Ni, Sr and V display similar downhole trends. Co, Sr and Ni both display high concentrations at the base of the section reaching 50ppm and 170ppm respectively and suggests that the bottom parts of the well is more argillaceous than the upper section (**Figure 4.3.7**), (**Figure 4.3.8**).

Zr displays diametric relationships with Co and Ni. The low Zr contents (200ppm) in the lower part of the well corroborate the above statement. Sr occurs in a concentration range between 100ppm – 300ppm and displays the same trend and peak concentrations (300ppm) as Co and Ni.

Zn, Pb and Ba display similar downhole trends with peaks that appear to coincide with feldspars or clays minerals in that section (**Figure 4.3.9**), (**Figure 4.3.10**).

Ce displays variable concentrations that range from 0ppm to 100ppm. Peak Ce concentrations most probably coincide with areas where cleaner sandstone units are present. Ce is predominantly associated with resistate minerals such as Zr and as described earlier sandstones are normally enriched in Zr. (www.gsfi/publ/foregsatlas/text/Ce.pdf). Ce and Zr also plot in the same cluster on the PCA plots.

4.3.2.4 Well A-11

SiO₂ concentrations in Well A-11 varied from: 55% to 90% with peak concentrations at the base of the well where siliceous rocks occur. (*Figure 4.3.12*)

Al₂O₃, Fe₂O₃, MnO, MgO, K₂O, and Ti₂O, as with the PCA, displays similar downhole trends and displays inverse relationships with SiO₂ thus suggesting alternating layers of pure sandstones and more argillaceous layers in the section. (*Figure 4.3.12*)

CaO concentrations are in the range 1% - 9%. The concentrations are higher in the top part of the section than in the lower part. This suggests that the samples in the top part are composed of carbonate cements or possesses a carbonate matrix. CaO displays an inverse relationship with SiO₂ as shown on the PCA plot.

Na₂O displays relatively uniform values falling in the range 0.5% -0.6%. The downhole pattern exhibited by Na₂O indicates that the sandstones are of a more feldspathic nature than the rest.

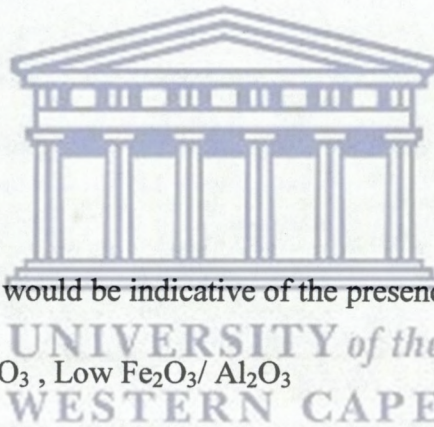
Co and Ni, displays similar downhole patterns and the elements clustered together on the PCA plot (*Figure 4.3.12*). This element association is indicative of the presence of clay minerals.

V, Zr and Sr, much like the PCA, display the same downhole patterns. All of the elements displays distinctive changes in their trends below 4125m (*Figure 4.3.12*). The elements Co and Ni are characterized by sudden increases below 4125m while V, Zr, and Sr are characterized by decreases in their concentration in the downhole section (*Fig 4.3.12*). This is suggestive of the fact that below that depth the samples are becoming increasingly argillaceous and less siliceous than the previous sections. The decrease in Sr also indicates a decrease in the concentration of carbonate minerals.

Nb, Y and Rubidium followed similar downhole dispersal patterns. On the PCA these elements clustered together and their downhole trend substantiated the theory that these elements are associated.

4.3.3 SUMMARY

- SiO_2 appeared to be a lead for sandstones while Al_2O_3 appeared to suggest the occurrence of clays along with Fe_2O_3 , MnO , MgO , K_2O , and Ti_2O that all shows similar downhole trends and cluster together on the PCA plot. Ca along with MnO , MgO and Sr suggests the presence of carbonates.
- Based on the above , the following indices would be indicative of clean sandstones:
 - High $\text{SiO}_2/\text{Al}_2\text{O}_3$
 - High SiO_2/Co
 - High Zr/Co
 - High Zr/Sr
 - Low Nd/V
 - High Y/Pb
- The following indices would be indicative of the presence of clays:
 - Low $\text{SiO}_2/\text{Al}_2\text{O}_3$, Low $\text{Fe}_2\text{O}_3/\text{Al}_2\text{O}_3$
 - Low SiO_2/Co , Low Zr/Co
 - High Rb/Zn
 - Low Y/Pb
- The following indices would be indicative of the presence of feldspathic sandstones:
 - High $\text{Na}_2\text{O}/\text{K}_2\text{O}$ and Low Zr/Sr



4.4 Element Ratios

4.4.1 INTRODUCTION

Chemostratigraphic analysis works on the basis of element pattern recognition. For this purpose element ratios are plotted. The element ratios help to enhance the geochemical signatures as well as provide information regarding the chemical composition of the samples

One of the functions of the PCA plots is to enable element ratios to be identified. Element ratios are normally chosen on the basis that the elements display diametric relationships with each other.

Element ratios are chosen on the basis that they met the above criteria as well as the fact that these ratios are common to all wells.

The following ratios are used for the analysis:

SiO₂/Al₂O₃

Silica is predominantly found as detrital material that is produced as a result of weathering in sedimentary rocks. Common source minerals of silica include quartz and feldspars. Sandstones and conglomerates typically contain silica in the range of 65% to 95%. (*Pettijohn et al, 1987*), (*Alberede et al, 2003*), (*Ratcliffe et al, 2008*)

Most sedimentary rocks with the exception of shale contain very little Al₂O₃. Shales contain high concentrations of Al₂O₃ as a result of the presence of clays such as kaolinite. Al₂O₃ is also a major constituent of rock forming minerals, such as feldspar and mica. Sandstones on average is said to contain an approximate concentration of 5% to 8% of Al₂O₃. (*Deer et al, 1962*)

The ratio of SiO₂/Al₂O₃ is therefore used to distinguish between so called cleaner sandstones and feldspathic or clay rich sandstones. A large ratio will be indicative of cleaner sandstones while a small ratio will be indicative of feldspathic sandstones or clay rich sandstones.

SiO₂/Co

As mentioned previously, Silica is predominantly found as detrital material that is produced as a result of weathering in sedimentary rocks. Common source minerals of silica include quartz and feldspars.

Cobalt is readily transferred to sedimentary rocks in which it is absorbed by manganese hydroxides and clays. Pure sandstones generally have very low Co concentrations. A high value for this ratio will be indicative of the presence of much more pure sandstone.

Zr/ Co

The concentration of Zr in sedimentary rocks is a function of the presence of detrital heavy minerals such as sphene and zircon and is used as a measure of the amount of coarse grained silicate siliciclastics that are present. (*Dypvik and Harris, 2001*)

Cobalt is readily transferred to sedimentary rocks in which it is absorbed by manganese hydroxides and clays. Pure sandstones generally have very low Co concentrations. The concentration of Co tends to vary with the iron and manganese content. Cobalt tends to be concentrated in finer grained fractions and arkose and greywacke are normally enriched in Co (*Pettijohn et al, 1987*).

A small value for this ratio thus indicates the presence of clays.

Rb/Zn

The ratio of Rb/Zn will be an indicator of the amount of feldspar to clay minerals that are present. A small value will be indicative of the sample being clean sandstone, while a higher value will indicate the presence clays.

Zr/Sr

The concentration of Zr in sedimentary rocks is a function of the presence of detrital heavy minerals such as sphene and zircon.

Sr is associated with the presence of carbonate minerals (*Gentaneh, 2002*) in particular calcite and aragonite. It may also be associated with feldspar and biotite but at much lower concentrations than in carbonate minerals. (*Dypvik and Harris, 2001*)

Nd/V

Nd is a rare earth element (REE) and they are generally depleted in sandstones (*Pettijohn et al, 1987*). The concentration of vanadium in sandstones is a reflection of the abundance of detrital oxides and clay minerals (*Pettijohn et al, 1987*). On this basis it can be concluded that a low ratio will be indicative of cleaner sandstone.

Y/Pb

The concentration of yttrium is principally determined by the abundance of heavy resistate minerals, such as zircon (*Vickery, 1960*), xenotime and garnet. In low energy environments yttrium may also occur in stable organic compounds. The concentration of Pb is controlled by the presence of primary detrital minerals such as feldspar, mica, sulphides and clay minerals.

Based on this it can be concluded that a high ratio is indicative of a pure sandstone.

Fe₂O₃/ K₂O

In sedimentary rocks Fe₂O₃ primarily as haematite grain coatings or cements.

The occurrence of K₂O is discussed under the ratio **Na₂O/K₂O**. A high value for this ratio indicates the presence of haematite while a small value will be indicative of the presence of feldspars or mica's.

Rb/Zn

Rubidium is concentrated in minerals where it substitutes for K-feldspar. It usually replaces for potassium in micas such as muscovite and in K-feldspars such as microcline and orthoclase. Rubidium is therefore present in K-feldspars, mica and clay minerals and is especially enriched in arkose and feldspathic sandstones (*Gentaneh, 2002*). The amount of Rb used as a measure of the concentration of fine grained siliciclastics that are present. (*Dypvik and Harris, 2001*).

The concentration of Zinc is controlled by the abundance of ferromagnesium silicates, detrital oxides and clay minerals. In the event that Fe is absent zinc will be present in carbonate and silicate phases. (*Deer et al, 1962*)

Nb/Ni

Nb is also found to be depleted in sandstones. Ni is mostly found in detrital ferromagnesium silicate minerals, detrital primary Fe oxides, hydrous Fe and Mg oxides as well as clay minerals (*Pettijohn et al, 1987*). A low value for this ratio is indicative of the presence of cleaner sandstones.

Nb/Zn

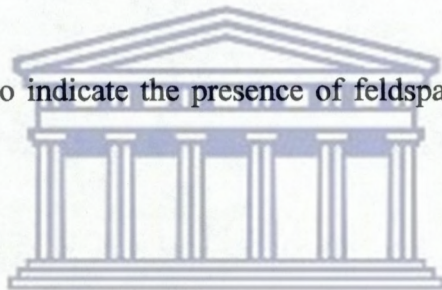
Niobium as discussed previously is much depleted in sandstones. Also, a high zinc concentration will be indicative of clay minerals, ferromagnesium silicates or detrital oxides (*Deer et al, 1962*). Thus a high value for the ratio will be indicative of any of the above.

Na₂O/K₂O

The main source of Na₂O in detrital sedimentary rocks is detrital feldspar. Sandstones on average will contain approximately 1.4% while shales show much greater variation and the concentration ranges between 0.1% and 9.2%. (*Pettijohn et al, 1987*), (*Brookfield et al, 2004*)

Sandstones most commonly contain on average less than 1% K₂O. The presence of K₂O in sedimentary rocks is commonly a function of the presence of K-feldspar, K- mica and glauconite (*Gentaneh, 2002*).

This ratio is used therefore to indicate the presence of feldspathic sandstone. A large ratio will be indicative of this.



UNIVERSITY of the
WESTERN CAPE

4.4.2 RESULTS

From the element ratios it is necessary to identify distinct chemical signatures or patterns and this is then assumed to represent a geochemical unit. All the element ratios will not be discussed further only those that enabled the recognition of geochemical patterns.

4.4.2.1 Well A-A1:

The following units are identified in Well A-A1 (*Refer to Fig 4.4.1*):

Geochemical Unit 1 (GU1) displays the following trends:

- $\text{SiO}_2/\text{Al}_2\text{O}_3$ values are in the range 3 to 8. This value became progressively smaller towards the base and $\text{Na}_2\text{O}/\text{K}_2\text{O}$ values are in the range 0.2 to 0.8. The highest values for the ratios are found at the top and it decreases progressively towards the base of the unit. The ratios $\text{Na}_2\text{O}/\text{K}_2\text{O}$ and $\text{SiO}_2/\text{Al}_2\text{O}_3$ display similar downhole trends.
- The ratio $\text{Fe}_2\text{O}_3/\text{K}_2\text{O}$ and $\text{K}_2\text{O}/\text{Rb}$ displays relatively uniform values of approximately 2 and 0.03 respectively for the entire unit.
- SiO_2/Co displays values of approximately 10. The ratio shows a decreasing trend towards the base of the unit and displays similar downhole trends as the ratios $\text{SiO}_2/\text{Al}_2\text{O}_3$ and $\text{Na}_2\text{O}/\text{K}_2\text{O}$.
- Zr/Co displays variable values that fall in the range 10 – 50. The highest values are found at the top and bottom of the unit. Zr/Co displays inverse downhole trends with $\text{Na}_2\text{O}/\text{K}_2\text{O}$ and $\text{SiO}_2/\text{Al}_2\text{O}_3$.
- Nb/Rb displays values that fall in the range 0.4 – 0.6 and as for the ratios $\text{Fe}_2\text{O}_3/\text{K}_2\text{O}$ and $\text{K}_2\text{O}/\text{Rb}$, they display relatively uniform trends for this unit,
- Nd/V display values in the range 0.05 – 0.2 and display an increasing trend towards the base of the unit.
- The ratio Y/Pb displays values in the range 0.05 – 0.2. The highest values are found at the top and the base of the unit.

- Zr/Sr depicts values that fall in the range 1 – 2 and displays a progressively increasing trend towards the base of the unit.
- Zn/ Rb displays values in the range: 5 – 10 and Zn/Nb displays values in the range: 5 – 20. These ratios display similar dispersion trends and the highest values are found in the middle of the unit.

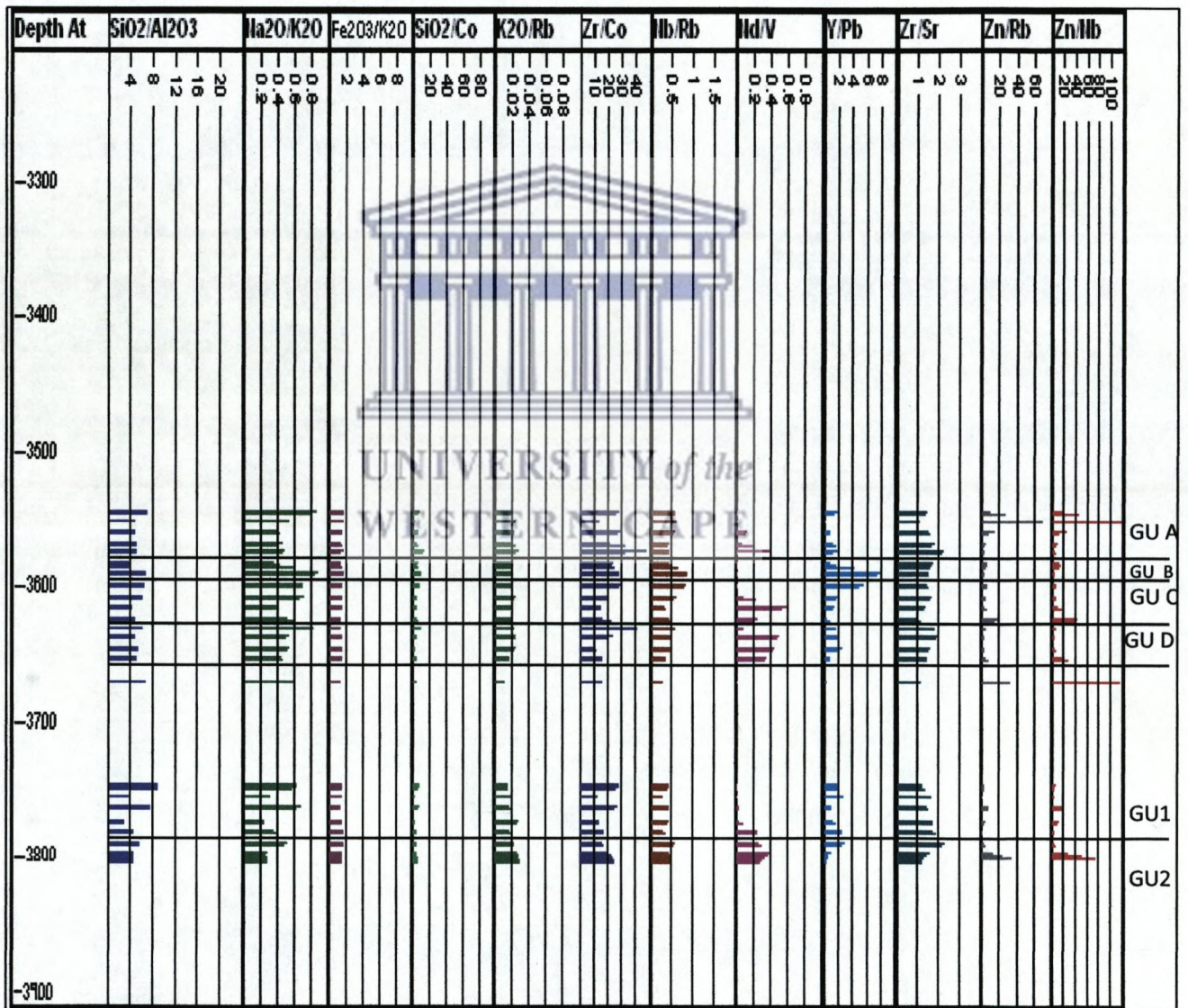


Figure 4.4.1 Element Ratio Profile for Well A-A1

Geochemical Unit 2 displays the following trends:

- $\text{SiO}_2/\text{Al}_2\text{O}_3$ values are in the range 3 to 9. This ratio increases slightly towards the base while $\text{Na}_2\text{O}/\text{K}_2\text{O}$ values are in the range 0.2% to 0.5%. The highest values for the ratios are found at the top of the unit and it decreases towards the base of the unit. The ratios $\text{Na}_2\text{O}/\text{K}_2\text{O}$ and $\text{SiO}_2/\text{Al}_2\text{O}_3$ display similar downhole trends.
- The ratio $\text{Fe}_2\text{O}_3/\text{K}_2\text{O}$ and Nb/Rb and displays uniform values of approximately 2 and 0.5 for the entire unit.
- SiO_2/Co displays values of approximately 10. The ratio shows an insignificant trend of increasing towards the base of the unit.
- Zr/Co displays variable values that fall in the ranges 15 – 25 and 0.02 – 0.03 respectively and displays similar downhole trends of decreasing towards the base.
- Nd/V displays values in the range 0.2 – 0.4 displays an increasing trend at the top of the unit and a decreasing trend toward the base of the unit.
- The ratio Y/Pb and Zr/Sr have values in the ranges 1– 3 and 1 – 2.5 and depicts a decreasing trend towards the base of the unit.
- Zn/Rb and Zn/Nb (have values in the ranges 10 – 40 and 10 – 60 respectively and display similar dispersion trends. They display increasing trends towards the base of the unit.

4.4.2.2 Well A-L1

Geochemical Unit 1 (GU1) displays the following trends (Refer to Fig. 4.4.2):

- Geochemical unit 1 is defined by $\text{SiO}_2/\text{Al}_2\text{O}_3$ values that range between 4 and 16. This ratio increases towards the base of the unit.
- $\text{Na}_2\text{O}/\text{K}_2\text{O}$ displays uniform values of approximately 0.2 for the entire unit.
- $\text{Fe}_2\text{O}_3/\text{K}_2\text{O}$ display values that fall in the range 3 – 4. The ratio decreases slightly towards the base of the unit.

- SiO_2/Co and Zr/Co have values in the ranges of 10 -15 and 25 – 50 respectively and follows similar downhole trends.
- $\text{K}_2\text{O}/\text{Rb}$ displays very slight decreases in value towards the base.
- Nd/V displays trends of increasing and decreasing slightly. The lowest values for this ratio are found at the base of the unit.
- Nb/Zn and most importantly Zr/Sr displays trends of recurring increases and decreases.

Geochemical Unit 2 (GU2) (Refer to Fig. 4.4.2)

- $\text{SiO}_2/\text{Al}_2\text{O}_3$ and SiO_2/Co displays values ranging between 8 and 14 and 10 and 20 respectively and displays increasing downhole trends.
- Values for $\text{Na}_2\text{O}/\text{K}_2\text{O}$ are below 0.2 and follow a trend of decreasing towards the base of the unit. $\text{Na}_2\text{O}/\text{K}_2\text{O}$ displays opposite downhole trends as $\text{SiO}_2/\text{Al}_2\text{O}_3$ and SiO_2/Co .
- $\text{Fe}_2\text{O}_3/\text{K}_2\text{O}$ and Zr/Co have values range from 2 – 3 and 10 – 50 respectively and display decreasing trends downhole. The downhole trends displays by $\text{Fe}_2\text{O}_3/\text{K}_2\text{O}$ and Zr/Co are opposite to those displays by $\text{SiO}_2/\text{Al}_2\text{O}_3$.
- Nd/V and Nb/Ni displays overall increasing trends.
- Zr/Sr and Rb/Zn all displays overall decreasing trends although very minor increases are noted at places.

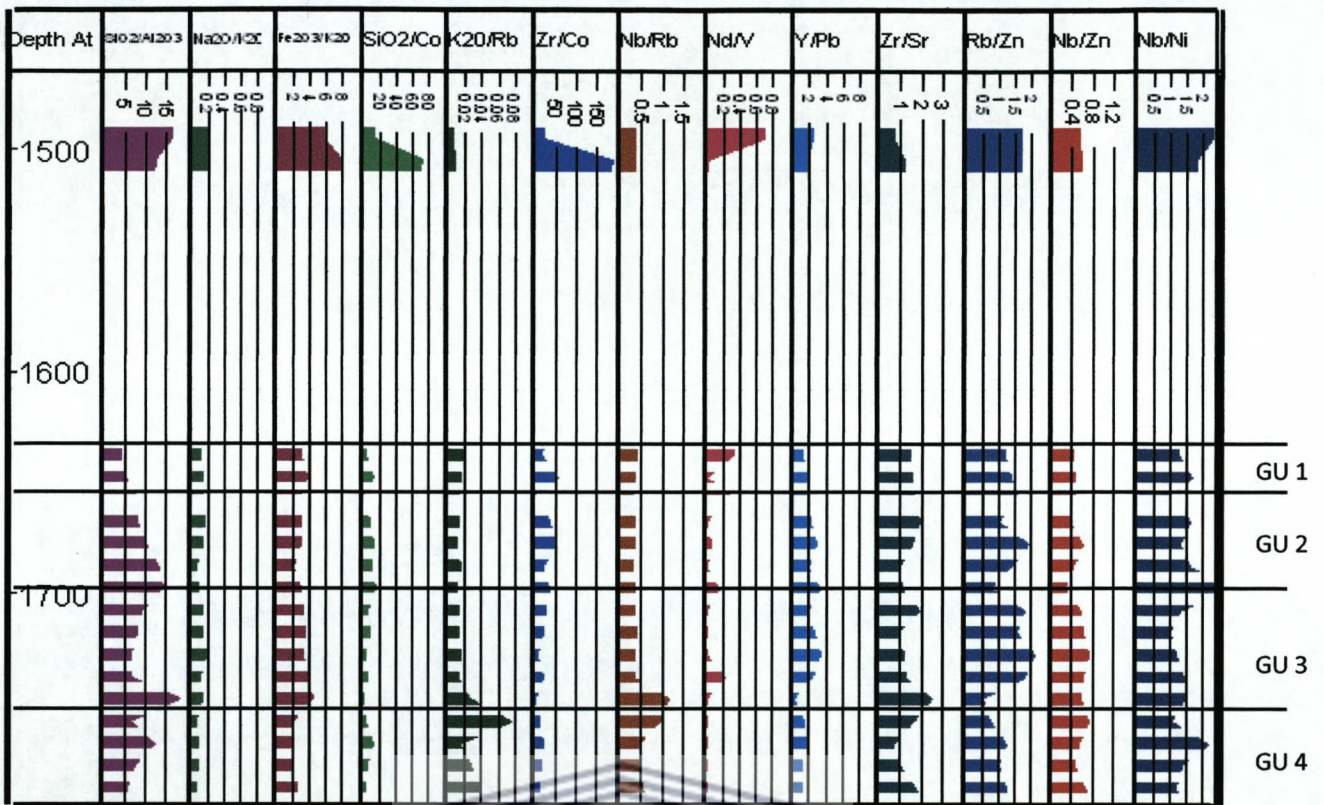


Figure 4.4.2: Element Ratio Profile for Well A-L1 (section1)

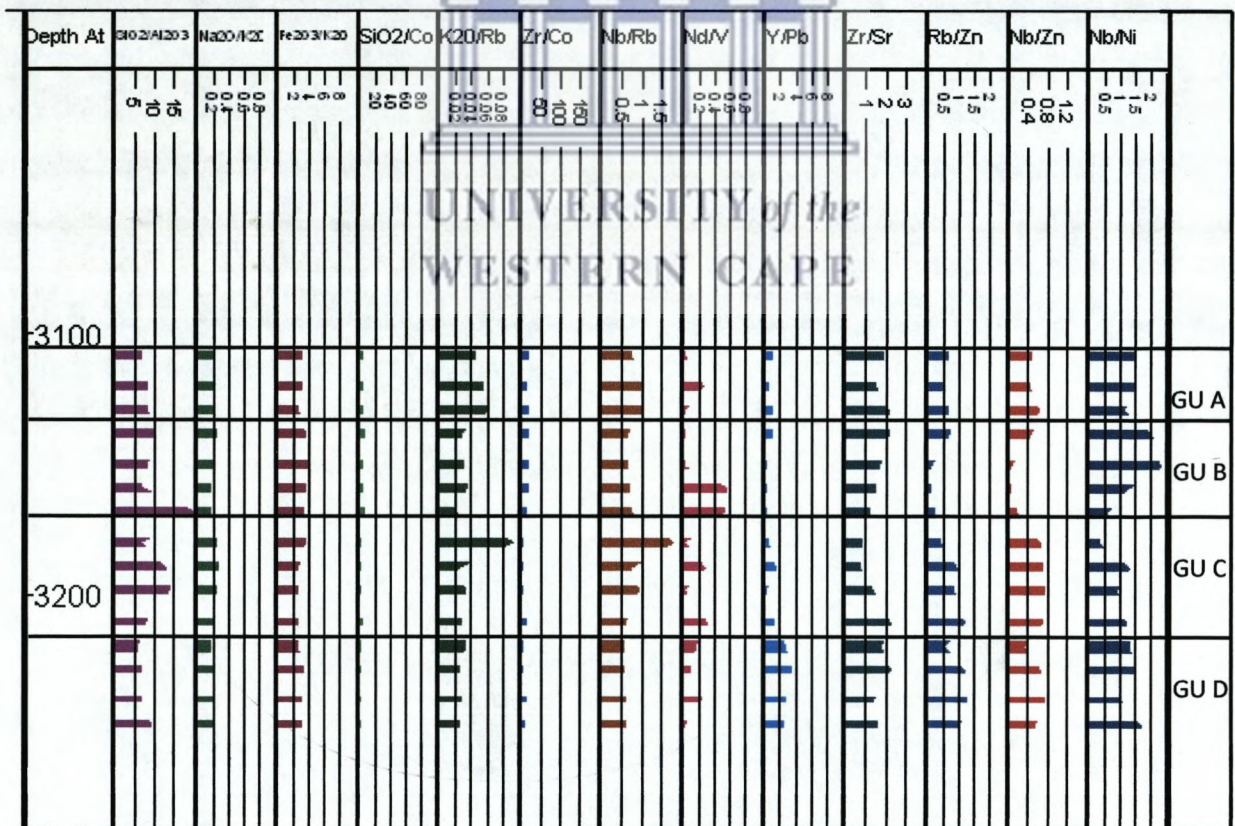


Figure 4.4.3 Element Ratio Profile for Well A-L1 (section 2)

Geochemical Unit 3 (GU3) (Refer to Fig. 4.4.2)

- $\text{SiO}_2/\text{Al}_2\text{O}_3$, $\text{Na}_2\text{O}/\text{K}_2\text{O}$ and SiO_2/Co display uniform values of approximately 4, 0.15 and 5 respectively for the unit.
- $\text{Fe}_2\text{O}_3/\text{K}_2\text{O}$ show values in the range 3 – 4.5 and display trends of slightly increasing towards the base of the unit.
- $\text{K}_2\text{O}/\text{Rb}$, Zr/Co , Zr/Sr and Nb/Rb have values in the ranges of patterns of increasing towards the base. The ratios reach an anomalous peak at the base of the unit.
- Nd/V , Rb/Zn and Y/Pb shows decreasing trends towards the base of the unit.

Geochemical Unit 4 (GU4) (Refer to Fig. 4.4.2)

- $\text{SiO}_2/\text{Al}_2\text{O}_3$ and SiO_2/Co have values in the ranges of 4 -12 and 5 - 30 respectively and displays decreasing downhole trends towards the base of the unit.
- $\text{Na}_2\text{O}/\text{K}_2\text{O}$ and Zr/Co have values of approximately 0.1 and 25 respectively. and exhibits fairly uniform patterns.
- $\text{Fe}_2\text{O}_3/\text{K}_2\text{O}$ along with $\text{K}_2\text{O}/\text{Rb}$, Nb/Rb , Nd/V , and Zr/Sr have values in the ranges 2 – 2.5, 0.3 – 0.4, 0.5 – 0.7, 0.5- 0.2 and 1-2 respectively and displays increasing trends towards the base of the unit.
- Rb/Zn and Nb/Zn have values in the ranges 1 – 1.5 and 0.5 – 0.9 respectively and displays similar dispersion trends. The trends that are exhibited by Rb/Zn and Nb/Zn are similar to those exhibited by $\text{Fe}_2\text{O}_3/\text{K}_2\text{O}$ along with $\text{K}_2\text{O}/\text{Rb}$, Nb/Rb , Nd/V and Zr/Sr .
- Nb/Ni displays patterns of cyclic increases followed by decreases.

4.4.2.3 Well A - U1

Geochemical Unit 1 (GU1) displays the following trends (Refer to Fig. 4.4.4):

- $\text{SiO}_2/\text{Al}_2\text{O}_3$, SiO_2/Co and Zr/Co have values in the ranges 4 – 7, 5 – 20 and 50 - 100 respectively and display similar patterns indicating decreasing trends towards the base of the unit.
- A slightly decreasing trend is exhibited by $\text{Na}_2\text{O}/\text{K}_2\text{O}$, $\text{K}_2\text{O}/\text{Rb}$ and Nb/Rb which have values falling in the range 0.3 – 0.4 for $\text{Na}_2\text{O}/\text{K}_2\text{O}$ and $\text{K}_2\text{O}/\text{Rb}$ and 0.5 – 0.75 for Nb/Rb . The trend displays by $\text{Na}_2\text{O}/\text{K}_2\text{O}$, $\text{K}_2\text{O}/\text{Rb}$ and Nb/Rb are similar to those displays by $\text{SiO}_2/\text{Al}_2\text{O}_3$, SiO_2/Co and Zr/Co .
- Rb/Zn and Nb/Zn has value sin the ranges 0.4 – 0.75 and 0.2 – 0.45 and displays increasing trends towards the base of the unit.
- $\text{Fe}_2\text{O}_3/\text{K}_2\text{O}$ exhibit fairly uniform values of approximately 3 for the unit.
- Nd/V displays values that fall in the range 0.1 to 0.4. The highest values are found at the top and bottom of the unit.
- Zr/Sr and Nb/Ni has values ranging from 1.9 – 4 and 1 – 2 respectively and displays trends of cyclic increases and decreases throughout the unit..

Geochemical Unit 2 (GU2) displays the following trends (Refer to Fig. 4.4.4):

- $\text{SiO}_2/\text{Al}_2\text{O}_3$ and $\text{Na}_2\text{O}/\text{K}_2\text{O}$ has values in the ranges 6 – 8 and 0.4 – 0.6 respectively and displays trends of increasing slightly towards the centre of the unit after which it decreases towards the base.
- SiO_2/Co and Zr/Co has values in the ranges 10 – 70 and 50 – 300 respectively and displays similar trends and shows overall trends of increasing towards the centre of the unit and decreasing rapidly towards the base of the unit.
- $\text{K}_2\text{O}/\text{Rb}$, Nb/Rb and Nb/Zn have values in the ranges 0.02 – 0.04, 0.4 – 0.6, 0.4 – 0.6 respectively and display similar patterns.
- $\text{Fe}_2\text{O}_3/\text{K}_2\text{O}$ exhibited fairly uniform patterns

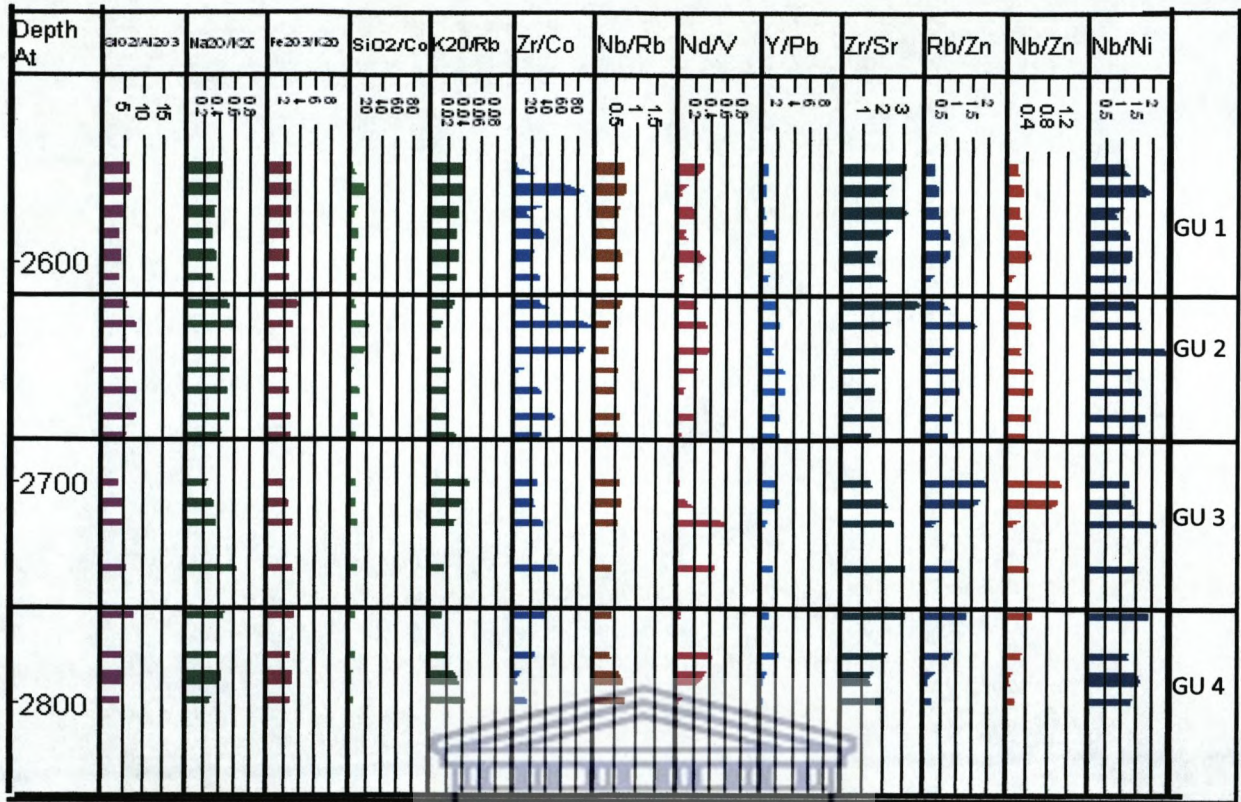


Figure 4.4.4: Element Ratio Profile for Well A-U1 (section 1)

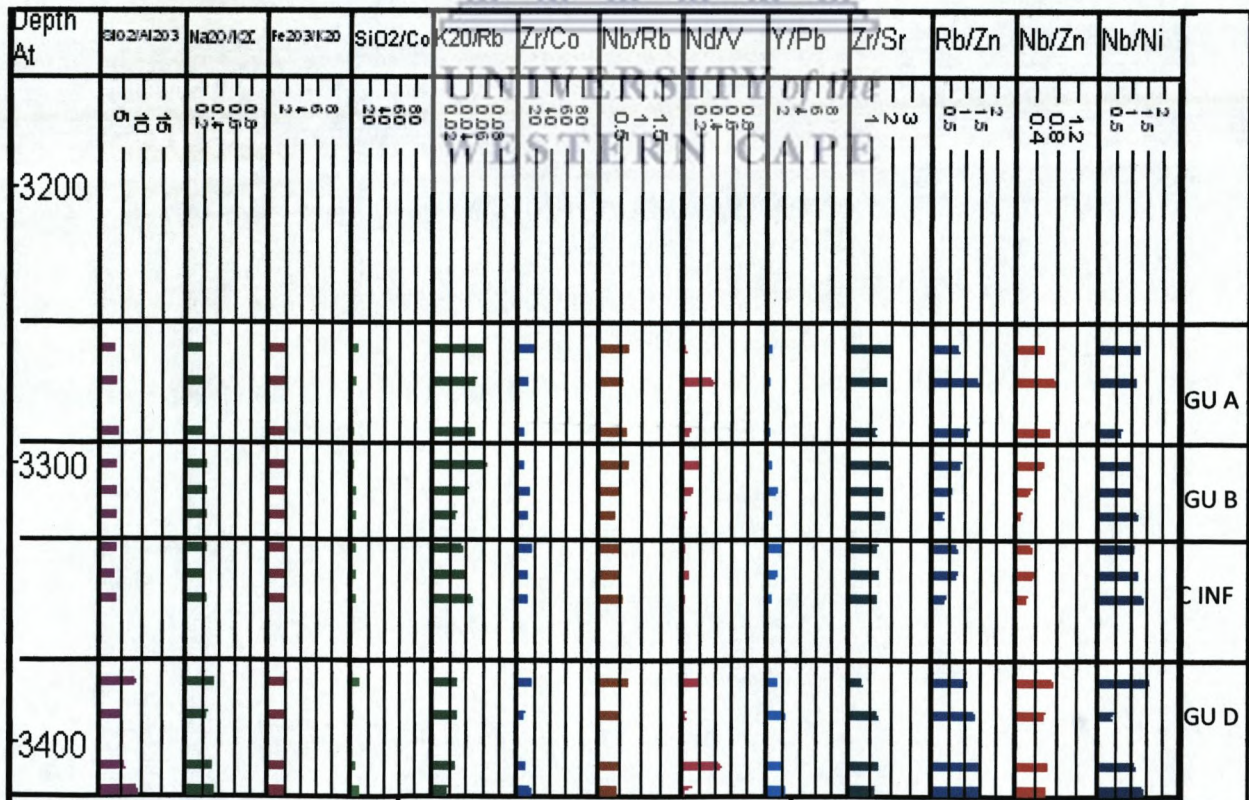


Figure 4.4.5: Element Ratio Profiles for Well A-U1 (section 2)

- Zr/Sr has values in the range 1.5 – 3 and displays a decreasing trend towards the base of the unit. Nb/Ni displays patterns of cyclic increases followed by decreases.

Geochemical Unit 3 (GU3) displays the following trends (Refer to Fig. 4.4.4):

- $\text{SiO}_2/\text{Al}_2\text{O}_3$, $\text{Na}_2\text{O}/\text{K}_2\text{O}$ and $\text{Fe}_2\text{O}_3/\text{K}_2\text{O}$ show values in the ranges 4 – 8, 0.3 – 0.6 and 2 – 3 respectively and display similar trends of increasing values towards the base of the unit.
- SiO_2/Co exhibited very low and uniform values of approximately 10 throughout.
- Zr/Co values vary from 40 – 55 and display a decreasing trend towards the base of the unit.
- $\text{K}_2\text{O}/\text{Rb}$, Nb/Rb , Rb/Zn and Nb/Zn has values that vary from 0.01 – 0.05, 0.4 – 0.6, 0.5 – 2 and 0.3 – 1.1 respectively and displays similar patterns that indicates a trend of decreasing values towards the base of the unit.
- Nd/V displays values that fall in the range 0.1 to 0.4. The ratio displays an overall decreasing trend towards the base of the unit.
- Zr/Sr has values that vary from 1 to 1.5 and displays trends of increasing values towards the base of the unit.

Geochemical Unit 4 (GU4) displays the following trends (Refer to Fig. 4.4.3):

- $\text{SiO}_2/\text{Al}_2\text{O}_3$, $\text{Fe}_2\text{O}_3/\text{K}_2\text{O}$ and Zr/Co displays uniform values of approximately 4, 3 and 20 respectively, throughout the unit.
- $\text{Na}_2\text{O}/\text{K}_2\text{O}$ has value in the range 0.3 - 0.4 and displays a decreasing trend towards the bottom of the unit.
- Rb/Zn, Nd/V and Y/Pb have values that are in the ranges 0.25 – 1, 0.01 – 0.4 and 0.5 – 2 respectively and displays patterns of decreasing towards the base of the unit. The trends displays by Rb/Zn, Nd/V and Y/Pb are similar to the trend displays by $\text{Na}_2\text{O}/\text{K}_2\text{O}$.

- SiO_2/Co has values that vary from 20 to 60 and exhibits a rapid increase in value towards the base of the unit
- $\text{K}_2\text{O}/\text{Rb}$, Nb/Rb and Zr/Sr have values in the ranges 0.02 – 0.04, 0.5 – 0.75 and 1.5 – 2 respectively and display similar dispersion trends. The patterns exhibited by $\text{K}_2\text{O}/\text{Rb}$ and Nb/Rb are inverse to those display by $\text{Na}_2\text{O}/\text{K}_2\text{O}$.

4.4.2.4 Well A-11

Geochemical Unit 1 (GU1) displays the following trends (Refer to Fig. 4.4.4):

- The element ratios $\text{SiO}_2/\text{Al}_2\text{O}_3$, $\text{Na}_2\text{O}/\text{K}_2\text{O}$, $\text{Fe}_2\text{O}_3/\text{K}_2\text{O}$, SiO_2/Co and Zr/Co displays uniform values of approximately 4, 2, 2, 5 and 20 respectively, throughout the unit .
- $\text{K}_2\text{O}/\text{Rb}$ displays patterns of increasing slightly towards the base.
- Nd/V has values that range from 0.4 – 0.1 and displays a pattern of decreasing towards the base of the unit.
- Rb/Zn , Zr/Sr , and Nb/Ni display trends of decreasing slightly, from 1.5 to 1, 1.5 to 1 and 1.25 to 1 respectively.

Geochemical Unit 2 (GU2) displays the following trends (Refer to Fig. 4.4.4):

- The element ratios $\text{SiO}_2/\text{Al}_2\text{O}_3$ (~4), $\text{Na}_2\text{O}/\text{K}_2\text{O}$ (~0.5), $\text{Fe}_2\text{O}_3/\text{K}_2\text{O}$ (~2), SiO_2/Co (~5) and Zr/Co (~20) displays uniform values throughout.
- The ratio Nd/V defined this unit. The ratio followed a pattern of cyclic increases and decreases throughout.
- Nb/Zn displays trend of decreasing slightly towards the base of the unit.

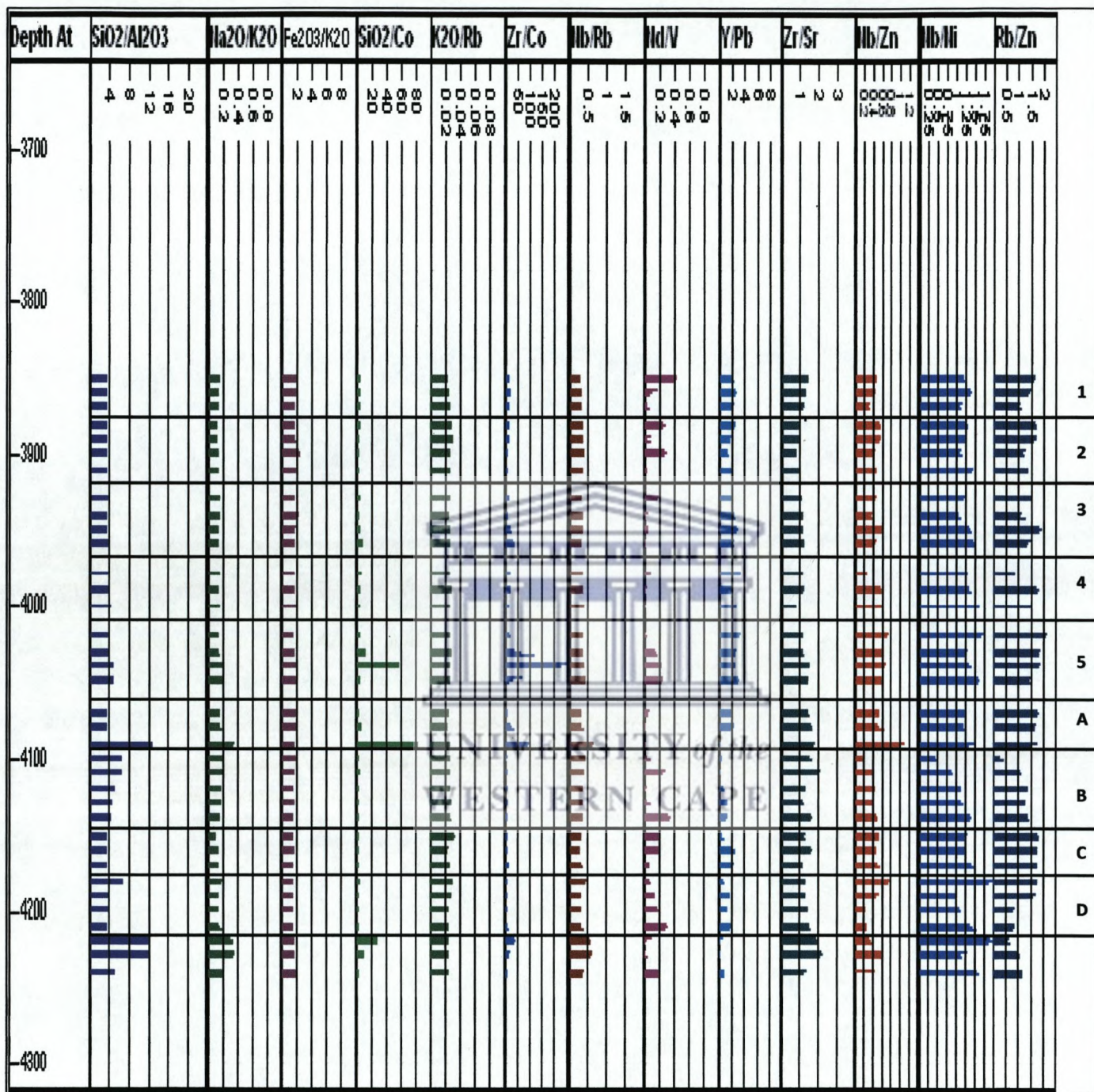


Figure 4.4.6: Element Ratio Profiles for Well A-11.

Geochemical Unit 3 (GU3) displays the following trends (Refer to Fig. 4.4.6):

- The element ratios SiO₂/Al₂O₃ (~4), Na₂O/K₂O (~0.5), Fe₂O₃/K₂O (~2), SiO₂/Co (~5) and Zr/Co (~20) displays uniform values throughout.
- The ratio Nd/V defined this unit. The ratio followed a pattern of decreasing values towards the base of the unit, from 0.2 to 0.05.

- Nb/Ni displays trend of increasing slightly towards the base of the unit while Rb/Zn decreases towards the base of the unit.

Geochemical Unit 4 (GU4) displays the following trends (Refer to Fig. 4.4.4):

- The element ratios $\text{SiO}_2/\text{Al}_2\text{O}_3$ (~4), $\text{Na}_2\text{O}/\text{K}_2\text{O}$ (~2), $\text{Fe}_2\text{O}_3/\text{K}_2\text{O}$ (~0.5), SiO_2/Co (~5) and Zr/Co (~20) displays uniform values throughout.
- The ratio Nd/V defined this unit. The ratio followed a pattern of decreasing values towards the base of the unit, from 0.1 to 0.02.
- Nb/Ni displays trend of increasing slightly towards the base of the unit while Rb/Zn displays patterns of increasing towards the centre followed by decreases towards the base of the unit.



Geochemical Unit 5 (GU5) (Refer to Fig. 4.4.4)

- The ratio $\text{SiO}_2/\text{Al}_2\text{O}_3$ displays slightly higher values (between 4 and 6) than it did for the previous units.
- SiO_2/Co shows a marked increase in the middle of this unit (~60) compared with the rest of the unit (values ranging between 5 and 10).
- Zr/Co displays a trend of increasing towards the middle of the unit and this is followed by a decreasing trend towards the base of the unit.
- Nb/Rb exhibited a trend of decreasing values while Nd/V revealed an increasing trend.

4.4.2.5 Correlated Units

The following units are found to correlate across the four wells:

Geochemical Unit A (GUA) (Refer to Figs. 4.4.1, 4.4.3, 4.4.5 and 4.4.6)

- $\text{SiO}_2/\text{Al}_2\text{O}_3$ for this unit had values ranging between 5 and approximately 12. The value for this ratio decreased towards the base.
- $\text{Na}_2\text{O}/\text{K}_2\text{O}$ (values ranging between: approx 0.3 to 0.8) shows an overall decreasing trend towards the base of the unit.
- $\text{Fe}_2\text{O}_3/\text{K}_2\text{O}$ values are fairly uniform throughout. SiO_2/Co has variable concentrations that range between slight increases and slight decreases.
- $\text{K}_2\text{O}/\text{Rb}$ displays relatively uniform values while Zr/Co displays a decrease (from 25 to 15) followed by an overall increasing trend (from 15 to approximately 45).
- Nb/Rb displays a decreasing trend while Nd/V increases throughout.
- Zr/Sr , Rb/Zn and Nb/Zn all displays decreasing trends for this unit.

This unit is characterized by the following ratios:

- Relatively low SiO_2/Co value
- Nd/V
- Rb/Zn
- Nb/Zn

Geochemical Unit B (GUB) (Refer to Figs. 4.4.1, 4.4.3, 4.4.5 and 4.4.6)

- $\text{SiO}_2/\text{Al}_2\text{O}_3$ had uniform values for this unit (approximately 6).
- The ratio $\text{Na}_2\text{O}/\text{K}_2\text{O}$ followed an increasing trend towards the middle of the unit which is then followed by a slight decrease towards the base.
- $\text{Fe}_2\text{O}_3/\text{K}_2\text{O}$, SiO_2/Co , $\text{K}_2\text{O}/\text{Rb}$ and Zr/Co displays fairly uniform values.
- Apart from the values being fairly consistent, SiO_2/Co values are also relatively low.
- Nb/Rb and Y/Pb displays trends of increasing followed by decreasing values.
- Nd/V displays consistent and low values (approximately 0.5).

This unit is characterized by the following ratios:

- $\text{Na}_2\text{O}/\text{K}_2\text{O}$
- Nd/V : Exceptionally low values when compared to GU5



Geochemical Unit C (GUC) (Refer to Figs. 4.4.1, 4.4.3 and 4.4.6)

- $\text{SiO}_2/\text{Al}_2\text{O}_3$ and $\text{Na}_2\text{O}/\text{K}_2\text{O}$ displays trends of slightly increasing towards the base of the unit while $\text{Fe}_2\text{O}_3/\text{K}_2\text{O}$, SiO_2/Co and $\text{K}_2\text{O}/\text{Rb}$ displays uniform, and in the case of SiO_2/Co low values throughout.
- Zr/Co is seen to display an increasing trend while Nd/V exhibited a decreasing trend. The values for Nd/V are much higher than for the preceding geochemical unit.
- Y/Pb exhibited a decreasing trend with values for this unit being much lower than for GU6.
- Rb/Zn and Nb/Zn exhibited trends of decreasing slightly towards the base and displays values of 1 and 0.4 respectively.

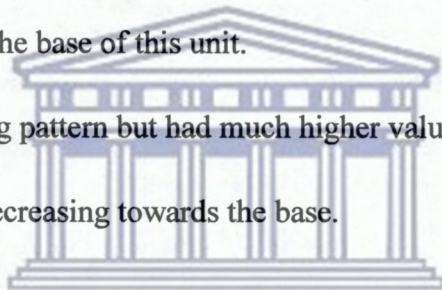
GUC could not be correlated across Well A-U1 since that part is not sampled. However, both GUB and GUD are present in Well A-U1 thus the position of GUD can be inferred.

This unit is characterized by the following:

- Decreasing Nd/V ratio and Rb/Zn

Geochemical Unit D (GUD) (Refer to Figs. 4.4.1, 4.4.3, 4.4.5 and 4.4.6)

- $\text{SiO}_2/\text{Al}_2\text{O}_3$ revealed an increasing pattern while $\text{Na}_2\text{O}/\text{K}_2\text{O}$ displays a decreasing pattern.
- $\text{Fe}_2\text{O}_3/\text{K}_2\text{O}$ and SiO_2/Co continued, as with GUA, B and C, to display uniform values, while $\text{K}_2\text{O}/\text{Rb}$, contrary to previous units, exhibited an overall decreasing trend.
- Zr/Co decreased towards the base of this unit.
- Nd/V displays a decreasing pattern but had much higher values than GUC.
- Zr/Sr revealed trends of decreasing towards the base.



UNIVERSITY of the
WESTERN CAPE

This unit is characterized by:

- Decreasing $\text{K}_2\text{O}/\text{Rb}$, Zr/Sr and Nd/V

4.4.3 DISCUSSION

4.4.3.1 Well A-A1

Geochemical Unit 1

The ratio $\text{SiO}_2/\text{Al}_2\text{O}_3$ decreased towards the base and therefore indicates that the unit is becoming increasingly argillaceous towards the base. The trend revealed by $\text{Na}_2\text{O}/\text{K}_2\text{O}$ is indicative of the fact that the feldspathic component in the samples decreased towards the base. SiO_2/Co ratio decreased towards the base of the unit and thereby corroborated the statement that the unit is becoming more argillaceous as Co is concentrated/ associated with the presence of clay minerals. The trends displayed by Zr/Co , Y/Pb provided further evidence to support the theory, by displaying decreasing trends towards the base.

Further evidence to support the above assumptions are the trend displays by the ratio Nd/V . Nd is depleted in sandstones and the concentration of V is a reflection of the abundance of detrital oxides and clay minerals that are present. Based on this the assumption is made that a low ratio would be indicative of the presence of sandstone. For this unit, the ratio increases towards the base, thus it indicates that the unit is becoming more argillaceous towards the base.

The XRF analysis done on the samples indicated that this unit had very high SiO_2 , Na_2O and Rb concentrations at the top of the unit. This along with the patterns displayed by the ratio could indicate the presence of arkose sandstone at the top of the unit. The elements mentioned above are associated with the presence of arkose sandstone (Tucker, 2001) and concentrations.

High Al_2O_3 , Fe_2O_3 , MnO , MgO and CaO concentrations are recorded for the lower half of the unit. These elements are associated with the presence of greywacke (Tucker, 2001). This corroborated the statement that the unit became clay rich towards the base.

Based on the above statements, the unit is described as arkose sands at the top and greywacke at the base.

Geochemical Unit 2

Geochemical Unit 2 displays trends that are consistent with those that would be displayed by a unit that is concentrated in clay minerals. The ratio $\text{SiO}_2/\text{Al}_2\text{O}_3$ decreased towards the base

and thus indicates that the unit is becoming increasingly arkose or argillaceous towards the base. This assumption is made on the basis that Al_2O_3 is commonly associated with the presence of clay minerals and is highly concentrated in greywacke (Tucker, 2001), (Ratcliffe et al, 2008).

The trend displayed by $\text{Na}_2\text{O}/\text{K}_2\text{O}$ indicates that the feldspathic components are decreasing towards the base. This assumption is based on the fact that the main source of Na_2O in detrital sedimentary rocks is detrital feldspar; hence a small ratio or decreasing ratio would indicate a decrease in the amount of feldspar present. This is consistent with the statement that the unit could be composed of greywacke as greywackes have low Na_2O concentrations (Tucker, 2001). $\text{K}_2\text{O}/\text{Rb}$ displays an increases trend towards the base of the unit and as K_2O is associated with clay minerals (Gentaneh, 2002) this further supported the assumption that the unit becomes more argillaceous.

Y/Pb and Zr/Sr displays trends that indicate a decrease toward the base of the unit. Y concentrations yttrium are predominantly determined by the excess of heavy resistate minerals, such as zircon (Baluz et al, 2000), xenotime and garnet in samples, while the concentrations of Pb are determined by the presence of primary detrital minerals such as feldspar, mica, sulphides and clay minerals. Hence it is assumed that a low concentration would indicate the latter. This corroborated the above statements. Sr is associated with the presence of carbonate minerals (Dypvik and Harris, 2001), (Cojan et al, 2002), (Gentaneh, 2002) thus the Zr/Sr indicates an increase in the amount of carbonate minerals and a decrease in the siliceous nature of the samples.

Zn/Rb and Zn/Nb shows increasing trends towards the base indicating that the unit is more arkose or argillaceous.

Contradictory to the above is the fact that the ratio Zr/Co indicates a trend of increasing towards the base. An increase in this ratio is associated with an increase in the siliceous nature of the samples, however all the other ratios indicate a decrease in the siliceous nature of the samples.

Base on the above this unit is termed as sandstone that becomes increasingly argillaceous at the base.

4.4.3.2 Well A-L1

Geochemical Unit 1

Geochemical Unit 1 is defined by $\text{SiO}_2/\text{Al}_2\text{O}_3$ values that increase towards the base, thereby signifying an increase in the siliceous nature of the unit. The ratio $\text{Na}_2\text{O}/\text{K}_2\text{O}$ displays relatively small values throughout the unit and thus indicates that the unit had very low feldspar content. The concentrations measured for the above elements, along with the patterns exhibited by the element ratios could have been an indication of the arkose nature of the sandstones. Arkose sandstones have high Na_2O and K_2O concentrations (Tucker, 2001), which would result in a low value for the ratio.

The trend displays by $\text{Fe}_2\text{O}_3/\text{K}_2\text{O}$ indicates a decrease in the concentration of iron minerals or clay mineral content. In this case it is assumed that it is indicative of a decrease in clay minerals. This assumption is made based on the fact that the major elements Al_2O_3 and TiO_2 displays the same downhole trends as $\text{Fe}_2\text{O}_3/\text{K}_2\text{O}$ and this element association is indicative of the presence of clay minerals (Deer et al, 1962). The ratios SiO_2/Co and Zr/Co both displays an anomalous peak at a depth of . This could possibly have indicates the presence of a clean sandstone unit. $\text{K}_2\text{O}/\text{Rb}$ decreases and this corroborated the statement that this unit had low feldspar content.

The lowest value for the ratio Nd/V is found at the base of the well thus confirming the assumption that the unit becomes cleaner towards the base. Zr/Sr displays trends of increase and decreases throughout the unit indicating layers with carbonates present and those without Sr as Sr is the main trace element for carbonates (Cojan et al, 2002). However and increase in this ratio corresponded to a decrease in the ratio Zr/Co .

Based on the major and trace element profiles and the element ratio patterns displays by this unit, the unit is classified as possibly arkose sandstone (low feldspar content and increases siliceous content) at the base and greywacke at the top (elevated concentrations of clay mineral group).

Geochemical Unit 2

The decreasing trends exhibited by the ratios $\text{SiO}_2/\text{Al}_2\text{O}_3$, SiO_2/Co and Zr/Co are indicative of a decrease in the siliceous nature of the unit towards the base. This is consistent with the decreasing concentrations observed for SiO_2 and Zr on the downhole profiles. $\text{Na}_2\text{O}/\text{K}_2\text{O}$ and $\text{Fe}_2\text{O}_3/\text{K}_2\text{O}$ display trends of marginally increasing towards the base. Increasing trends are

also displays for these elements on the downhole profiles. These ratios indicates an increase in the feldspathic nature the samples.

Rb/Zn and Nb/Zn trends indicate an increase in the clay minerals concentration towards the bottom of the well and are in line with the increasing trend displays by Rb and Zn on the downhole profiles. Y/Pb displays trends indicative of a decrease in the siliceous nature of the unit. This assumption is made on the basis that the concentration of yttrium is essentially determined by the abundance of heavy resistate minerals, such as zircon (*Barauz et al, 2000*), Contradictory to this is the fact that Nd/V displays trends that is indicative of an increase in the siliceous nature of the unit.

The measured concentrations for this unit along with the above patterns are indicative of the presence of greywacke sandstones with interbedded cleaner sandstones.

Geochemical Unit 3

The ratios $\text{SiO}_2/\text{Al}_2\text{O}_3$, SiO_2/Co , Zr/Co and Zr/Sr displays fairly uniform but rapidly decreased towards the base of the unit. This could be indicative of the presence of a cleaner sandstone layer at the base of the well. The top part of the unit is defined by clay rich sandstone. The feldspathic components remained fairly consistent throughout the well, however $\text{Fe}_2\text{O}_3/\text{K}_2\text{O}$ trends is indicative of an increase in the concentration of iron minerals towards the base of the unit.

Nb/Rb and Nd/V displays increasing trends towards the base of the rock, indicating an increase in the clay or feldspathic content of the unit. This however is contradictory to the trends displays by the above ratios.

Based on the above this unit is assumed to be composed of arkose or argillaceous sandstone at the top and clean sandstone at the base.

Geochemical Unit 4

The patterns exhibited by the ratios $\text{SiO}_2/\text{Al}_2\text{O}_3$, SiO_2/Co and Zr/Co are indicative of a decrease in the siliceous nature of the unit towards the base. Fairly uniform values are exhibited by $\text{Na}_2\text{O}/\text{K}_2\text{O}$ and thus indicate that the feldspathic component throughout the well remained the same.

On the other hand, $\text{Fe}_2\text{O}_3/\text{K}_2\text{O}$ displays an increase towards the base, thereby indicating an increase in the concentration of iron minerals towards the base, however, the values displayed by $\text{Fe}_2\text{O}_3/\text{K}_2\text{O}$ is lower than for the preceding unit.

Contradictory to the above evidence that supported the assumption that this unit is composed of more argillaceous rock towards the base, is the trend displayed by Zr/Sr . The pattern exhibited by this ratio is suggestive of an increase in the siliceous content of the unit.

4.4.3.3 Well A-U1

Geochemical Unit 1

The ratios $\text{SiO}_2/\text{Al}_2\text{O}_3$, $\text{Na}_2\text{O}/\text{K}_2\text{O}$, SiO_2/Co and Zr/Co display decreasing trends towards the base of the unit. This is suggestive of a decrease in the siliceous nature of the unit, a decrease in the feldspar components and an increase in the concentration of carbonate minerals.

$\text{Fe}_2\text{O}_3/\text{K}_2\text{O}$ display a fairly uniform pattern for this unit and are indicative of the fact that the concentration of iron minerals is constant throughout the unit.

Increasing trends are observed for the ratios Nd/V and Rb/Zn thus indicating an increase in the clay concentration towards the base.

Based on the above this unit is defined as being composed of feldspathic sandstone at the top and argillaceous or arkose sandstone at the base.

Geochemical Unit 2

$\text{SiO}_2/\text{Al}_2\text{O}_3$ shows lower values at the top and the bottom of this unit while the values are slightly higher and uniform for the rest of the unit. This indicates that the rocks are more arkose or argillaceous at the top and bottom of the unit and more siliceous for the rest of the unit.

$\text{Na}_2\text{O}/\text{K}_2\text{O}$ displays a uniform pattern for this well and also exhibited elevated values. This pattern is suggestive of the highly feldspathic nature of this unit. $\text{Fe}_2\text{O}_3/\text{K}_2\text{O}$ values are slightly more elevated than for the preceding unit, indicating an increase in the concentration of iron minerals for this unit.

SiO_2/Co followed the same trend as $\text{SiO}_2/\text{Al}_2\text{O}_3$, thus corroborating the statement that the middle section of the unit is more argillaceous than the top and the bottom. This is based on

the fact that Al_2O_3 and Co are associated with the presence of clay minerals (*Deer et al, 1962*)

and a concentration of these elements would result in a lower value for the ratio.

$\text{K}_2\text{O}/\text{Rb}$ displays an approximately uniform trend for the unit except for a slight decrease in the middle. Zr/Co displays decreased values at the top and bottom of the unit, but as the ratios $\text{SiO}_2/\text{Al}_2\text{O}_3$ and SiO_2/Co , peaked at the centre of the unit. This peak is assumed to be indicative of the presence of a clean or pure sandstone layer. This peak corresponded to a decrease in the ratios $\text{Fe}_2\text{O}_3/\text{K}_2\text{O}$ and $\text{K}_2\text{O}/\text{Rb}$. A decrease in those units is suggestive of a decrease in the amount of accessory minerals at that point, thus corroborating the assumption that a clean sandstone layer is present.

Based on the above, this unit is defined as feldspathic sandstone with interbedded clean sandstone.

Geochemical Unit 3

Lower $\text{SiO}_2/\text{Al}_2\text{O}_3$ values are present for this unit when compared to the preceding unit but the ratio increases towards the base of the well. $\text{Na}_2\text{O}/\text{K}_2\text{O}$ followed the same trend as $\text{SiO}_2/\text{Al}_2\text{O}_3$. The behaviour of these two ratios is indicative of the highly feldspathic nature of the unit.

It is assumed that there is an increase in the concentration of iron minerals present (from $\text{Fe}_2\text{O}_3/\text{K}_2\text{O}$ pattern). SiO_2/Co trends indicate a low silica concentration. $\text{K}_2\text{O}/\text{Rb}$ trends indicate that Rb replaced K in the feldspars.

Nd/V patterns indicate a decrease in silica content. This is consistent with trend exhibited by SiO_2/Co but contradictory to $\text{SiO}_2/\text{Al}_2\text{O}_3$. However Zr/Sr shows an increasing trend towards the base, indicating a decrease in the concentration of carbonates (*Cojan et al, 2002*) and a decrease in silica content. This is supportive of the fact that silica content increases toward the base of the unit.

Based on the above, Geochemical Unit 3 is assumed to be highly feldspathic sandstone.

Geochemical Unit 4

The patterns displays by $\text{SiO}_2/\text{Al}_2\text{O}_3$ and $\text{Na}_2\text{O}/\text{K}_2\text{O}$ indicate the presence of a highly feldspathic sandstone. SiO_2/Co indicates a peak in the middle of the unit, which would

indicate the presence of clean sandstone; however the ratio $\text{SiO}_2/\text{Al}_2\text{O}_3$ indicates no change in the siliceous nature of the unit. Contradictory to the pattern exhibited by SiO_2/Co Nd/V and Y/Pb displays trends that indicates a decrease in the siliceous nature of the samples. Rb/Zn also displays a decrease. Rubidium is concentrated in minerals where it substitutes for K-feldspar (*Gentaneh, 2002*). It usually substitutes for potassium in micas such as muscovite and in K-feldspars such as microcline and orthoclase. Rubidium is therefore present in K-feldspars, mica and clay minerals and is especially enriched in arkose and feldspathic sandstones (*Gentaneh, 2002*). This would thus support the assumption that the unit is a highly feldspathic sandstone.

Based on all of the above the unit could be classified as feldspathic sandstone that becomes increasing arkose towards the base.

4.4.3.4 Well A-11

Geochemical Unit 1

The ratios $\text{SiO}_2/\text{Al}_2\text{O}_3$, $\text{Na}_2\text{O}/\text{K}_2\text{O}$, $\text{Fe}_2\text{O}_3/\text{K}_2\text{O}$, SiO_2/Co , Zr/Co displays no discernible trends and hence no information could be gathered from them other than the fact that unit is siliceous.

$\text{K}_2\text{O}/\text{Rb}$, however, increases towards the base of the unit and is suggestive of the fact that Rb replaced K in the feldspar components. The ratio Nd/V indicates a decrease in the siliceous nature of the samples towards the base of the unit while Rb/Zn indicates a decrease in the feldspar components and an increase in the clay mineral concentration. The ratio Zr/Sr is indicative of a slight increase in the carbonate mineral concentration.

Based on the above this unit is classified as an argillaceous unit that became more clay rich towards the base.

Geochemical Unit 2

The ratios $\text{SiO}_2/\text{Al}_2\text{O}_3$, $\text{Na}_2\text{O}/\text{K}_2\text{O}$, $\text{Fe}_2\text{O}_3/\text{K}_2\text{O}$, SiO_2/Co , Zr/Co once again displays no discernible trends and hence no information could be gathered from them other than the fact that unit is siliceous.

Nd/V trends indicate the possible presence of alternating layers of argillaceous layers and less argillaceous layers or cleaner sandstone layers. Nb/Ni increases towards the base and thus suggested that the unit became more clay rich towards the base.

Geochemical Unit 3

As with the preceding unit, $\text{SiO}_2/\text{Al}_2\text{O}_3$, $\text{Na}_2\text{O}/\text{K}_2\text{O}$, $\text{Fe}_2\text{O}_3/\text{K}_2\text{O}$, SiO_2/Co , Zr/Co displays uniform patterns.

Nd/V decreased towards the base and is suggestive of the increase in the concentration of clay minerals towards the base of the unit. This is corroborated by the trends displays by Nb/Ni (which increases towards the base) and Rb/Zn (which decreased towards the base).

Geochemical Unit 4

As with the preceding unit, $\text{SiO}_2/\text{Al}_2\text{O}_3$, $\text{Na}_2\text{O}/\text{K}_2\text{O}$, $\text{Fe}_2\text{O}_3/\text{K}_2\text{O}$, SiO_2/Co , Zr/Co displays uniform patterns.

Nd/V decreased towards the base and is indicative of an increase in the concentration of clay minerals towards the base. This statement is corroborated by the pattern exhibit by Nb/Ni which shows an increase.

Rb/Zn trends indicate the presence of a highly feldspathic nature in the centre of this unit.

Geochemical Unit 5

$\text{SiO}_2/\text{Al}_2\text{O}_3$ displays higher values for this unit than the preceding units and is thus indicative of an increase in the siliceous nature of the samples. The highest value for this ratio is found at the base and indicates the possible presence of a clean sandstone unit.

However, SiO_2/Co displays a marked increase in the centre of the unit which could be suggestive of the presence of a cleaner sandstone unit, but $\text{SiO}_2/\text{Al}_2\text{O}_3$ did not exhibit any marked changes. Zr/Co displays the same trend as SiO_2/Co and thereby corroborated the statement that a more siliceous layer is found at the centre.

Nd/V increases towards the base and indicates an increase in the concentration of clay minerals towards the base,

Based on the above the unit is classified as alternating sandstones and argillaceous/ arkose sandstones and shales.

4.4.3.5 Correlated Units

Geochemical Unit A

$\text{SiO}_2/\text{Al}_2\text{O}_3$ trends are suggestive of a decrease in the siliceous nature of the unit towards the base, while SiO_2/Co trends suggested alternating layers of clean sandstone with an argillaceous or arkose layer. Zr/Co , however, indicates that the unit is cleaner in the middle and became more argillaceous at the top and bottom.

$\text{Na}_2\text{O}/\text{K}_2\text{O}$ trends revealed a decrease in the concentration of feldspathic components towards the base which corroborated the statement that the unit became more argillaceous towards the base.

Nb/Rb indicates a decrease towards the base which means that the Rb concentration increases. This is expected as Rb is associated with either the presence of feldspars or clay minerals. As the feldspar content decreased towards the base, it is most likely that it is associated with the presence of clay, thus explaining the decrease displays by the ratio (*Gentaneh, 2002*).

Nd/V displays an increase; hence it corroborated the statement that the ratio became more argillaceous towards the base as Nd is depleted in sandstones and V is associated with the presence of clays.

Zr/Sr indicates a decrease in the siliceous component and an increase in the carbonate components, while the ratio Rb/Zn indicates a decrease in rubidium concentration relative to the zinc concentration. Zn is associated with the presence of clays and substantiated the above statements.

This unit is classified as consisting of alternating layers of sandstone with sandstone of a more argillaceous nature.

Geochemical Unit B

$\text{SiO}_2/\text{Al}_2\text{O}_3$ trends are fairly uniform throughout this unit but are slightly higher than for the preceding unit thus indicating an increase in the siliceous nature of the samples. The trends displays by $\text{Na}_2\text{O}/\text{K}_2\text{O}$ are suggestive of an increase in the feldspathic components towards the base of the well.

$\text{Fe}_2\text{O}_3/\text{K}_2\text{O}$, $\text{K}_2\text{O}/\text{Rb}$, SiO_2/Co and Zr/Co displays relatively uniform trends for this well; however, SiO_2/Co values are extremely low and could be indicative of a very low siliceous

content. This is contradictory to the pattern displays by $\text{SiO}_2/\text{Al}_2\text{O}_3$ which indicates an increase in the siliceous nature of the rock when compared to the preceding unit.

The trends display by Nb/Rb and Y/Pb indicates the presence of alternating layers of feldspathic sandstone with clay rich sandstone or shales.

Nd/V displays consistently uniform and low values.

Based on the above information the assumption is made that the unit is composed of alternating layers of feldspathic sandstone with clay rich sandstone or shales.

Geochemical Unit C

$\text{SiO}_2/\text{Al}_2\text{O}_3$ and $\text{Na}_2\text{O}/\text{K}_2\text{O}$ displays similar trends, increasing towards the base of the unit. This could have been suggestive of the presence of feldspathic sandstone at the base. Contradictory to the increase displays by $\text{SiO}_2/\text{Al}_2\text{O}_3$, SiO_2/Co patterns exhibited low values which would be indicative of a low siliceous content for the unit.

Zr/Co, on the other hand, also displays an increasing trend towards the base which would be indicative of an increase in the siliceous nature of the rock; however, Y/Pb displays a trend that is inconsistent with the above statements. Y/Pb displays a decreasing trend which would be suggestive of low siliceous content but the concentration of yttrium is principally determined by the abundance of heavy resistate minerals, such as zircon. This meant that an increase in this ration would have been expected.

Based on the above this unit is classified as a highly feldspathic unit that became clay rich towards the base.

Geochemical Unit D

$\text{SiO}_2/\text{Al}_2\text{O}_3$ displays an increasing trend while $\text{Na}_2\text{O}/\text{K}_2\text{O}$ displays decreasing trends. This would be suggestive of alternating layers of clean sandstone with feldspathic sandstone.

$\text{K}_2\text{O}/\text{Rb}$ trends display a decrease in the feldspathic nature of the unit while Zr/Co, contradictory to $\text{SiO}_2/\text{Al}_2\text{O}_3$, displays a decrease in the siliceous nature of the unit. Zr/Sr indicates an increase in the concentration of carbonate minerals in the lower part of the unit. Sr is associated with the presence of carbonate minerals in particular calcite and aragonite or

with feldspar and biotite but at much lower concentrations. As the feldspar component of this unit decreased it is assumed that Sr is associated with the carbonate minerals.

The remainder of the ratios displays uniform patterns throughout the unit.

This unit is classified as consisting of alternating layers of sandstone, feldspathic sandstone and shale layers; however the sandstones in the lower part of the unit have higher carbonate minerals concentrations than the rest.



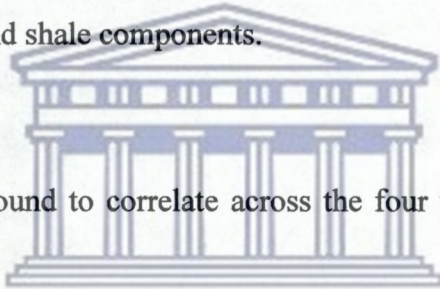
UNIVERSITY *of the*
WESTERN CAPE

4.4.4 SUMMARY

- Six geochemical Units are identified for Well A-A1, eight for Wells A-L1 and A-U1 and nine for Well A-I1.
- Geochemical Units 1 to 3 of Well A-A1 is defined as follows:
 - Geochemical Unit 1 is defined as consisting of arkose sandstones at the top and greywacke sandstones at the base
 - Geochemical Unit 2 is defined as pure sandstone at the top which became increasingly argillaceous towards the base.
- Geochemical Units 1 to 4 of Well A-L1 is defined as follows:
 - Geochemical Unit 1 is defined as possibly arkose sandstone at the base and greywacke at the top.
 - Geochemical Unit 2 is defined as consisting of greywacke components with interbedded cleaner sandstones.
 - Geochemical Unit 3 is defined as consisting of arkose or argillaceous sandstone at the top and cleaner sandstone at the base.
 - The trends displayed by the element ratio's for Geochemical Unit 4 is suggestive of the presence of sandstone that became increasingly argillaceous towards the base.
- Geochemical Units 1 to 4 of Well A-U1 is defined as follows:
 - Geochemical Unit 1 is defined as being composed of feldspathic sandstone at the top and an argillaceous or arkose component towards the base.
 - Geochemical Unit 2 is defined as a generally feldspathic unit with interbedded cleaner sandstones.
 - The element ratio's for Geochemical Unit 3 is suggestive of the presence of a highly feldspathic unit.
 - Geochemical Unit 4 is classified as feldspathic sandstone that becomes increasingly arkose towards the base.

• Geochemical Units 1 to 5 of Well A-I1 is defined as follows:

- Geochemical Unit 1 is classified as an argillaceous unit that became clay rich towards the base.
- Geochemical Unit 2 is defined as consisting of alternating layers of argillaceous layers and cleaner sandstone layers.
- Geochemical Unit 3 is defined as becoming increasingly argillaceous towards the base.
- Geochemical Unit 4 consisted of alternating layers of argillaceous layers with cleaner sandstone layers with a highly feldspathic layer found toward the centre.
- Geochemical Unit 5 is classified as consisting of alternating sandstone, argillaceous or arkose sandstone and shale components.



• Four units, Units A- D are found to correlate across the four wells. They are classified as follows:

- Unit A is defined as consisting of alternating layers of sandstone with an argillaceous component.
- Unit B is composed of alternating layers of feldspathic sandstone with clay rich sandstones or shales.
- Unit C is defined as a highly feldspathic unit that became increasingly clay rich towards the base.
- Unit D is classified as consisting of alternating layers of sandstone and shale layers. The sandstones at the base of the unit had a very high carbonate content.

The preceding chapter focused on the identification, correlation and discussion of chemostratigraphic units. This chapter focused on the identification, discussion and correlation of geophysical units i.e. units identified using well logs and well log attributes.

The well logs are discussed in the following sequence:

- At the beginning of the chapter a theoretical background (5.1) is given about the behaviour of logs and the principles on which they work.
- A general overview of the logs (5.2) produced for the each well is presented. The behaviour of the GR, Sonic, Neutron and Density logs are discussed and units identified.
- Neutron Density cross plots (5.3) are then created for each of the units that have been identified. These cross plots provided an indication of the possible lithology of the samples.
- M – N plots (5.4) are constructed such that the minerals constituting the make up of the samples could be identified and lithology inferred.
- A general correlation framework (5.5) is produced.

5.1 THEORETICAL BACKGROUND

In order to interpret well logs a basic understanding of the principles on which the work are necessary. This section aims to provide a concise introduction on the principles, applications and uses of the following logs: Gamma Ray (GR), Spontaneous Potential (SP), Neutron, Density, Sonic and Resistivity logs.

5.1.1 GAMMA RAY LOG (GR)

The GR log provides a record of the measure of radioactivity of the formations. The radioactivity measured originates from the radioactive elements that constitute the lithologies. These elements are normally uranium, thorium and potassium.

Shales most commonly contain the most radioactive elements and sandstone the least. The gamma ray log can thus be used as a tool to differentiate between pure sandstones and shales. The rule of thumb is that a kick to the left on the log indicates pure sandstone while a kick to the right is indicative of the presence of shale or a shaly layer.

The GR log is used to:

- identify shale layers
- lithological correlation and
- mineral identification



5.1.2 SPONTANEOUS POTENTIAL LOG

The spontaneous potential log is a measure of the natural potential differences between an electrode, the borehole and a reference electrode that is placed at the surface. (Rider, 2006)

There are 3 factors necessary to stimulate an SP current:

- A conductive fluid needs to be present
- A porous and permeable bed needs to be surrounded by an impermeable bed
- There needs to be a difference in salinity between the borehole fluid and formation water. (Rider, 2006)

The 0- value for the SP log is defined by the shale baseline that is a line along which there is no deflection and all values are related to this line. Shale displays a higher SP value than shaley-sand and sand. The SP log is also a very good indicator of facies. (Musset and Khan, 2000)

The main uses of the SP log include the calculation of formation – water resistivity, to indicate permeability and facies (Musset and Khan, 2000), (Rider, 2006), to estimate shale

volume, identification of depositional environments (*Krygowski, 2003*) and it is also used for correlation purposes.

The SP log will be used for this study in its capacity as a permeability indicator, facies indicator and most importantly for correlation purposes.

When correlating SP logs across the wells the following needs to be taken into consideration:

- The shale baseline has no interpretive meaning
- A difference in SP magnitude between wells could be as a result of a change in shaliness in a formation, a change in mud filtrate resistivity, the presence of hydrocarbons in a well and a change in the resistivity of the formation water.

(Krygowski, 2003)

5.1.3 NEUTRON LOG

The neutron log works on the principle of the bombardment of a formation with fast neutrons. Thus the log is expressed as a record of the formations reaction to this bombardment. The unit used to express this reaction is called neutron porosity units (npu). These units in turn are related to the hydrogen index of the formation. The hydrogen index is a measure of the amount of hydrogen that is present. (*Rider, 2006*)

In the event that formations are saturated with hydrogen they will quickly modify the neutrons. The hydrogen nuclei present within the formations are considered to originate from the water present and hence the tool can be used to determine the water saturation of a formation. (*Rider, 2006*)

The petroleum and sedimentology disciplines find that the water which acts as pore fillers are the most important type as this will then give an indication of the percentage of porosity for the formation. It is based on the above that the units of measurement, neutron porosity units are obtained.

The neutron log has the following uses:

- it measures porosity
- It aides the identification of the gross lithology (*Rider, 2006*)(*Krygowski, 2003*)

- When it is used in combination with the density log, it is a good indicator of subsurface geology.

For this specific study it is used in combination with the density log to support lithological identification of the units that are identified.

5.1.4 DENSITY LOG (RHOB)

The density log of a formation is a measure of the bulk density of the formation. Bulk density includes both the solid matrix and fluids that are enclosed in the pores.

The density log has the following uses:

- It can be used to calculate porosity
- It can be used to indicate lithology
- It can be used to identify certain minerals (*Rider, 2003*)

The density will be used to identify lithology and for correlation purposes. Lithology identification will be achieved by plotting neutron density and sonic-density cross plots. (*Krygowski, 2003*)

UNIVERSITY of the
WESTERN CAPE

5.1.5 SONIC LOG (Dt)

The sonic log displays the formations interval transit time (assigned the symbol Δt), which is the time it takes for a wave to travel a certain distance, proportional to the reciprocal wave velocity. The interval transit time of a formation depends on the following factors:

1. The type of lithology
2. The texture of the rock
3. Most importantly, porosity

(*Rider, 2003*)

For the purpose of this study, the sonic log will be used in comparison with the Neutron and Density data cross plots to identify lithologies. (*Krygowski, 2003*)

5.2 General Overview of Well Logs

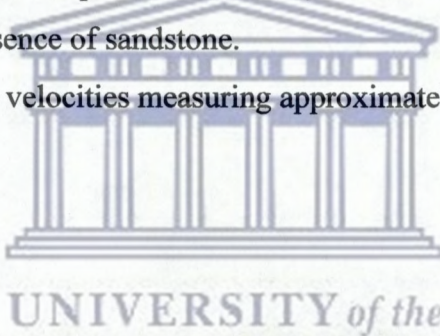
5.2.1 RESULTS

5.2.1.1 Well A – A1

The following patterns are displayed by the well logs (Refer to Figure 5.2.1):

- The GR log displays readings ranging between 80 API and 170API.
- The pattern exhibited by the SP log to a certain extent mimics the pattern displayed by the GR log.
- The neutron and density logs are plotted on the same track. This is to enable the recognition of cross over patterns. A cross over between these plots with the neutron log on the left indicates the presence of shale, while a cross over with the density in front indicates the presence of sandstone.
- The sonic log displays velocities measuring approximately 60US/F consistently.

5.2.1.2 Well A – I1



The well logs for Well A-I1 displays the following (Refer to Figure 5.2.2) :

- The GR log for Well A-I1 displays readings ranging between 30 API and 120API.
- The top part of the interval is defined by little or no deflections of the SP while the lower portion exhibits trends of positive and negative deflections.
- The neutron and density logs displays patterns that indicates the presence of units composed of shales and sandstones and alternating sandstones and shales.
- The sonic log displays velocities in the range 60 to 100 Us/Ft
- Resistivity logs can be used as a means of describing permeability. They do not however provide specific permeability values. The resistivity curves for this well indicates that poor permeability is found throughout the sampled interval.

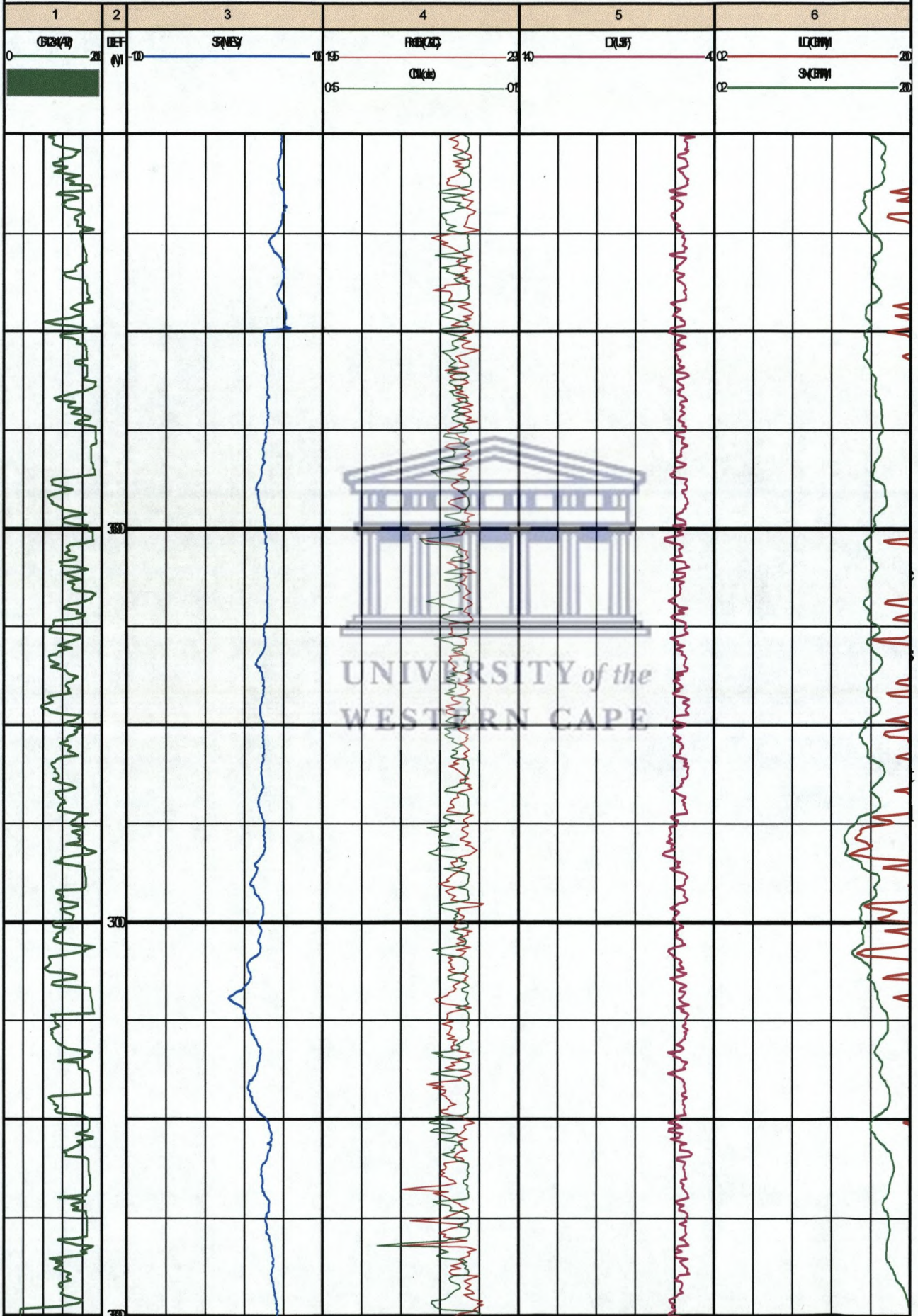
Scale: 1:100

AA

13m2

DEF (300m/300/20)

2000/03/03



No Samples

Scale : 1 : 1200

A-I1

DB : las (32)

DEPTH (3850.16M - 4210.16M)

2009/03/06 13:39

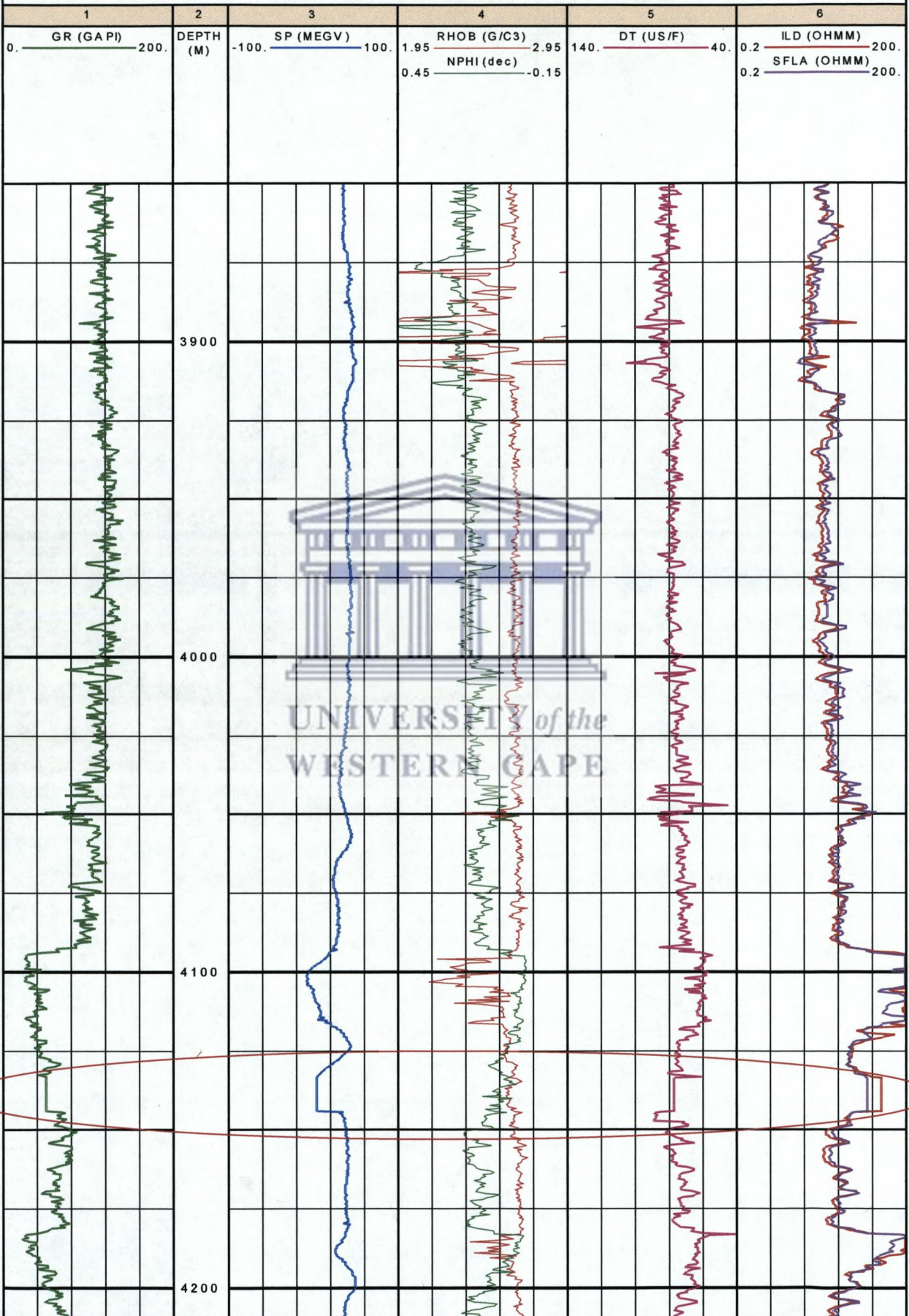


Figure 5.2.2 General Overview of the well logs for Well A-I1

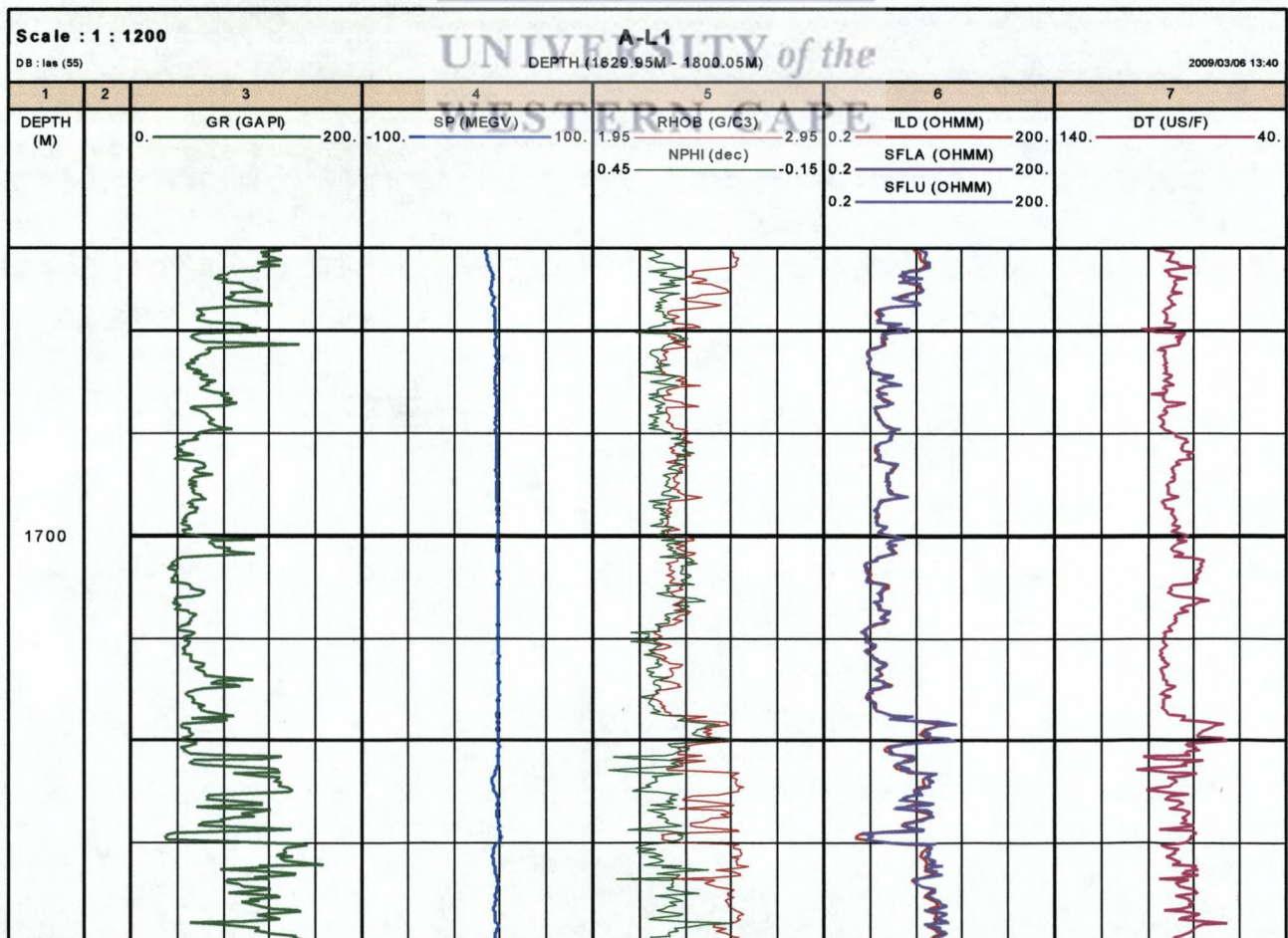
5.2.1.3 Well A – L1

Within Well A-L1 two areas of interest are identified. Thus the well logs are discussed for the first section (Depth: 1635m to 1800m) and then for the second section (Depth: 3100m to 3225m)

Well A-L1 (section 1) (Refer to Figure 5.2.3)

The well logs for this section display the following trends:

- The GR log displays readings in the range 40 API to 160 API. The readings decrease progressively towards the middle while the bottom of the section is defined by an increase in the readings.
- However, in contrast to the decrease in GR readings, the SP log shows no deflection.
- The neutron and density logs corroborate the trend shown by the SP
- The resistivity logs indicate a decrease in resistivity which corresponds to the decrease of the gamma ray log.
- A decrease in the sonic log is observed that corresponds to a decrease in the gamma and resistivity logs.



Well A-L1 (section 2)

The logs for Well A-L1 section 2 displays the following trends (Refer to Figure 5.2.4):

- GR readings for this section are much higher than for section 1.
- The neutron and density logs corroborate the preceding statement, indicating shaley sands, argillaceous sand and shales.
- Resistivity readings for this section are much higher than for the preceding section

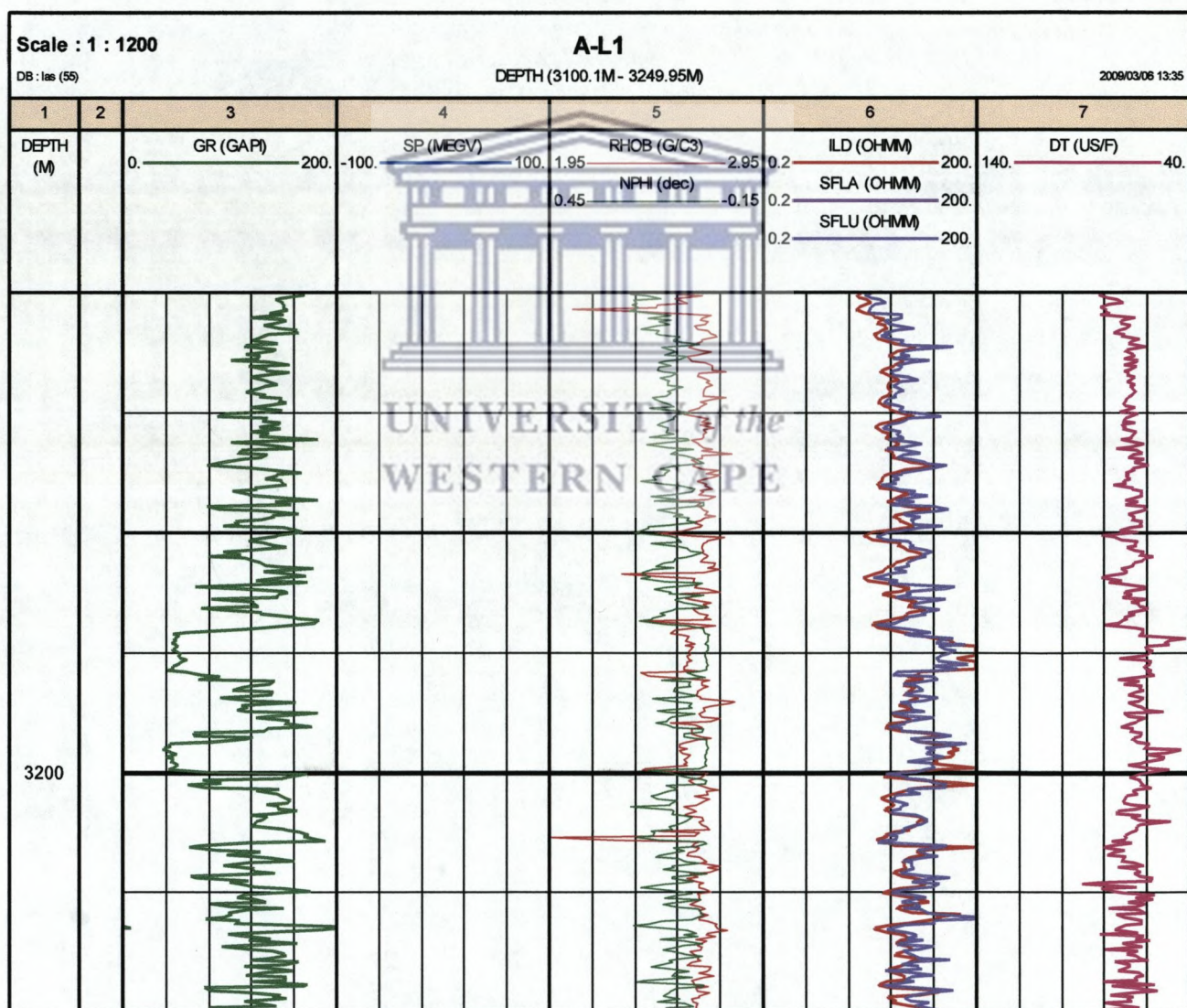


Figure 5.2.4: General Overview of the well logs for Well A-L1: Section 2

5.2.1.4 Well A-U1

The logs for section 1 of Well A-U1 displays the following trends (Refer to Figure 5.2.5):

- The GR log recorded readings that are in the range 40 API to 180 API.
- The SP log shows very little or no deflection for the interval.
- The Neutron and Density logs reveals cross over's that are interpreted to indicate the presence of sandstones and shales or silts.
- The resistivity log recorded relatively low resistivities for this section.
- The PEF log displays readings of approximately 1.8 consistently

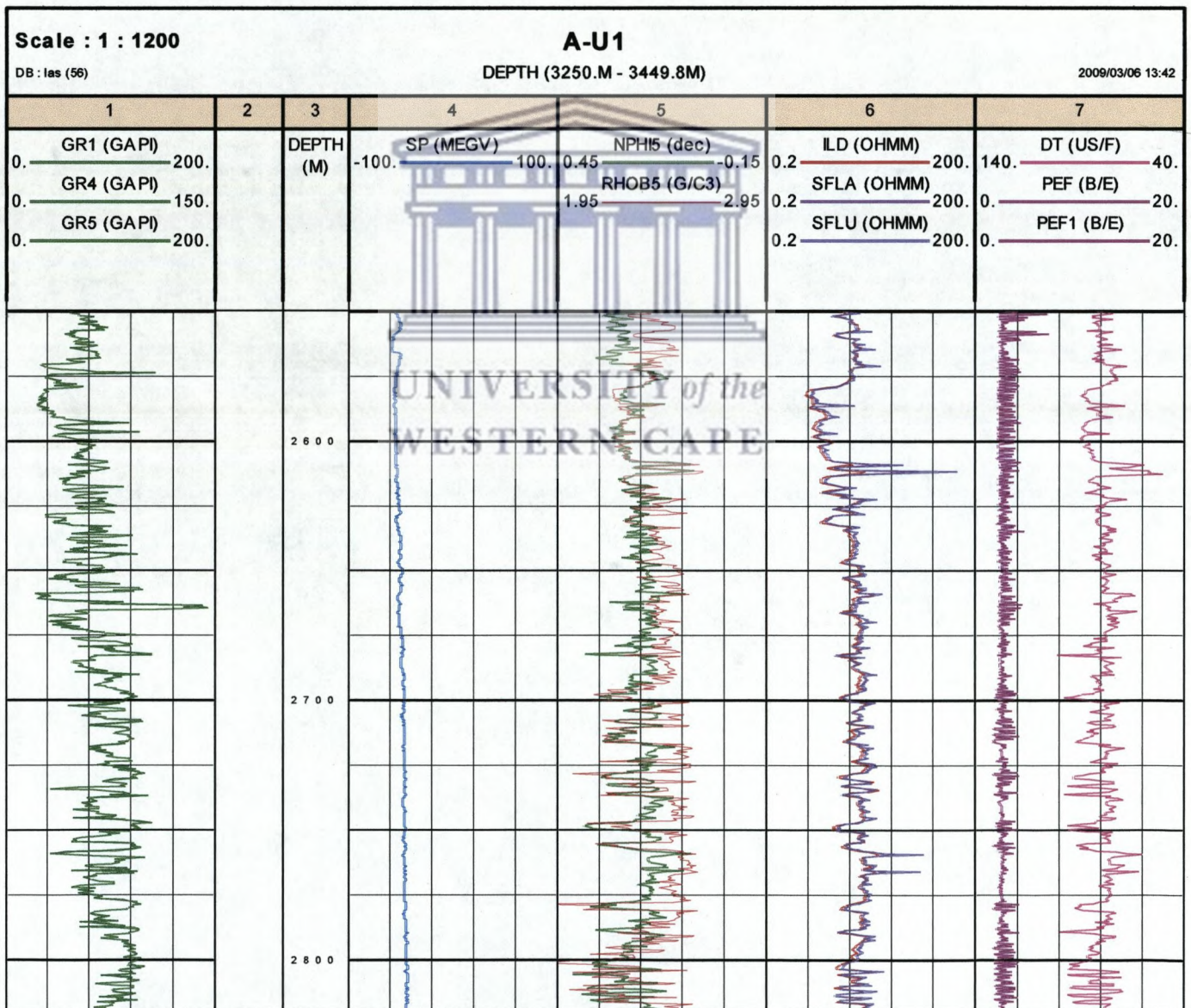
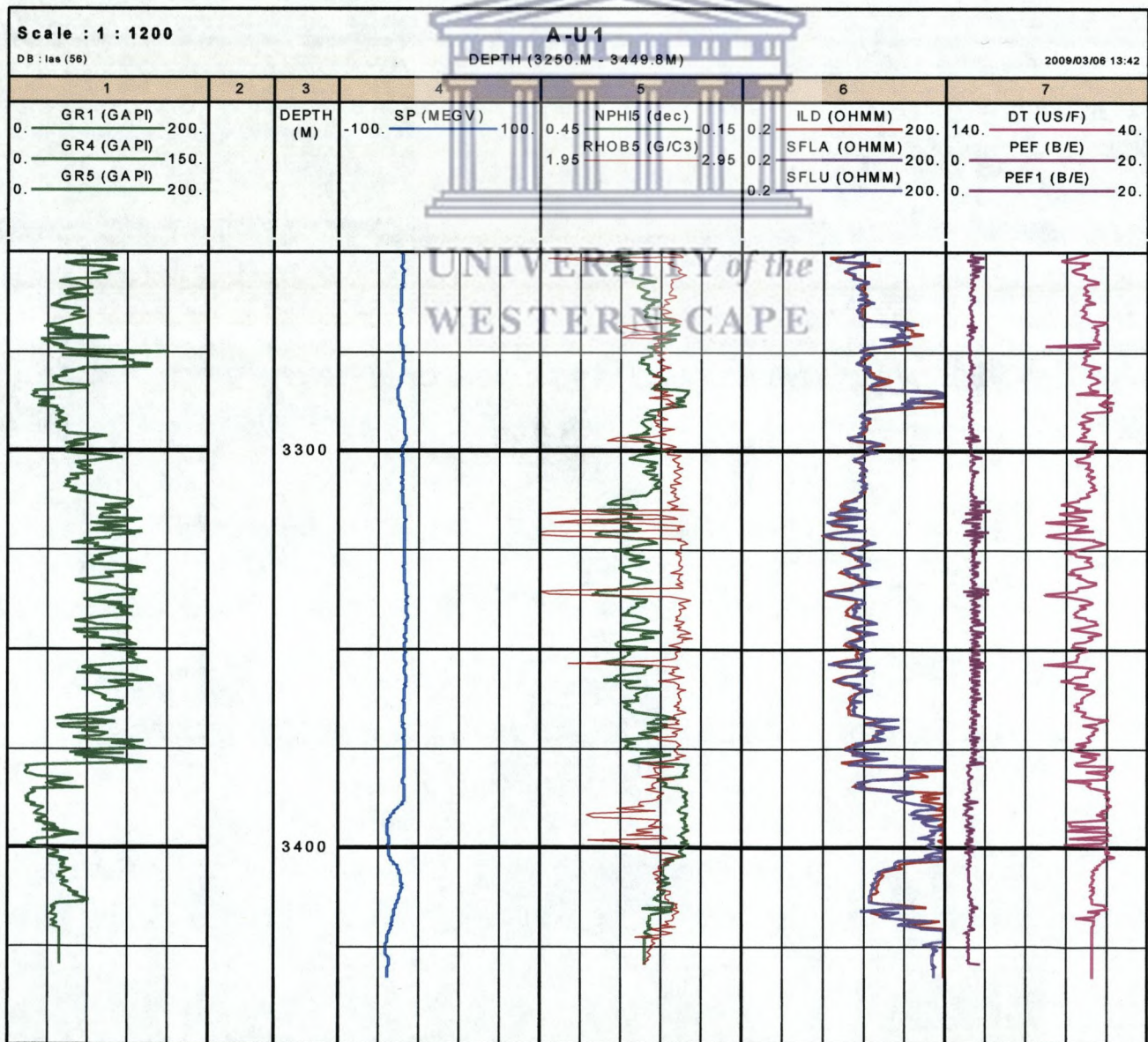


Figure 5.2.5 General Overview of the well logs for Well A-U1: Section 1

The well logs for Section 2 displays the following characteristics (Refer to Figure 5.2.6):

- GR readings are in the range 30API to 140API. The lowest readings are found at the top and the base of the section.
- The SP log shows little or no deflection up to a depth of 3390m after which it deflects to the left.
- Density- Neutron cross over's for this section indicates the presence of alternating lithologies or units.
- Resistivity readings are highly variable.
- The PEF log displays consistent values of 1.8 for the entire section.



5.2.2 DISCUSSION

5.2.2.1 Well A-A1

The GR log values for Well A-A1 are very high. This could be indicative of the presence of shales or clays (Rider, 2000). In this instance it is most likely that it is indicative of the presence of clay minerals and hence indicates the presence of argillaceous sandstones possibly alternating with shales.

The assumption that this unit is composed of alternating layers is made based on the pattern exhibited by the neutron and density patterns. However, at a depth of approximately 3605m the logs display a pattern that is generally assumed to indicate the presence of a limestone layer.

The SP log, to some extent mimics the pattern of the GR and indicates that this section is composed of alternating sequences of sandstone and shale. This interpretation is made on the basis that the SP log would deflect in the presence of sandstone and no deflection would be found along the log in the presence of shales (Rider, 2000). It is most likely that the section is composed of shale from a depth of 3500m to 3550m after which it is composed predominantly of alternating units of shaly – sand; this is based on the fact that shale displays a higher SP value than shaly sand (Musset and Khan, 2000).

Based on the log responses the area of interest for Well A-A1 is identified as consisting of alternating units of argillaceous sandstone and shales. Other properties exhibited by the log responses are the low permabilities that are present throughout the section (taken from the resistivity logs), and the high deep resistivity and low shallow resistivity measured for the section.

5.2.2.2 Well A-I1

The Gamma Ray log displays values of approximately 120 API up to a depth of 4000m after which it decreases towards the base of the section. It is assumed that the top part of the section is composed of argillaceous sandstones and clays or shales and that the section becomes progressively cleaner towards the base.

The Neutron and Density logs exhibit trends that are indicative of the presence of units of sandstone, alternating shales and sandstones and shales (Rider, 2000). The sonic log

measures approximately 80us/ft up to a depth of 4000m after which it increases towards the base of the section. The increase of the sonic log corresponds to a decrease in the GR log. This indicates that the lower part of the section is composed of more porous lithologies than the top part.

The resistivity curves for this well indicates that poor permeability is found throughout the sampled interval. The resistivity logs show an increase in resistivity towards the base of the well which corresponds with a decrease in GR readings and an increase in sonic readings.

The above responses indicate that the section is composed of sandstones alternating with shales units. The section becomes less compacted towards the base.

5.2.2.3 Well A-L1

Section 1

The GR log displays readings in the range 40 API to 160 API. The readings decrease progressively towards the middle of the section (from 1650m to 1750M), while the bottom of the unit is defined by increases in the readings. This is indicative of the presence of cleaner sandstones in the middle of the unit and sandstones of a more argillaceous nature at the top and bottom of the unit.

However, in contrast to the decrease in GR readings, the SP log shows no deflection, thereby indicating the presence of a shale or siltstone or it can also possibly indicate that the drilling fluids have invaded the formation.

The neutron and density logs corroborate the trend shown by the SP, also showing a pattern that will most probably be indicative of the presence of sandstone alternating with a shale unit or siltstone.

The resistivity logs indicate a decrease in resistivity which corresponds to the decrease of the gamma ray log (from 1650m to 1750M). This can be attributed to the presence of salt water in the formation as salt water is conductive and therefore has a low resistivity.

A decrease in the sonic log is observed that corresponds to a decrease in the gamma and resistivity logs.

Section 2

The GR log responses indicate the presence of either shale or argillaceous sands except for distinct sand units that are recognized at depths of 3174m to 3175m and 3192.5m to 3200m respectively.

The neutron and density logs corroborate the preceding statement, indicating shaly sands, argillaceous sand and shales. Resistivity readings for this section are much higher than for the preceding section.

5.2.2.4 Well A-U1

Section 1

The GR log recorded readings that are in the range 40 API to 180 API. The lowest readings are found at the top (up till a depth of 3317m) and towards the base (from a depth of 3375m) of the section. This is indicative of the presence of cleaner sands at these depths. The middle section (from 3317m to 3375m) is defined by sandstones of a more argillaceous nature.

The SP log shows very little or no deflection for the section and is presumably indicative of the presence of a shale component. The Neutron and Density logs reveals cross over's that are interpreted to indicate the presence of sandstones and shales or silts. The resistivity log recorded relatively low resistivities for this section. This can possibly be as a result of the presence of salt water.

The PEF log displays readings of approximately 1.8 consistently and this is in general an indication of the presence of sandstones (Rider, 2000).

5.3 GEOPHYSICAL UNITS

5.3.1 RESULTS

5.3.1.1 Well A-A1

The patterns exhibited by the well logs have led to the identification of eight units in the area of interest. Units A to D is found to correlate across the four wells and will be discussed later. Units 1, 2 and 3 are found only in Well A-A1.

- Unit 1 is defined by very high GR readings (80 API – 160 API). The top part of this unit displays readings of approximately 80 API while the readings at the base of the unit reach 160 API. The SP log shows a positive deflection at the top of the unit followed by a negative deflection at the base.
- Unit 2 is defined by higher GR values (160 API) than the preceding unit. This unit is however defined by a solitary peak of 120 API in the middle of the unit. This peak corresponds to a decrease in the density log. The neutron density cross over indicates that this unit is composed of sandstone.
- Unit 3 is defined by high GR values (range: 80 API – 120API). The SP log shows almost no deflection. Neutron- Density cross overs are indicative of presence of alternating units.

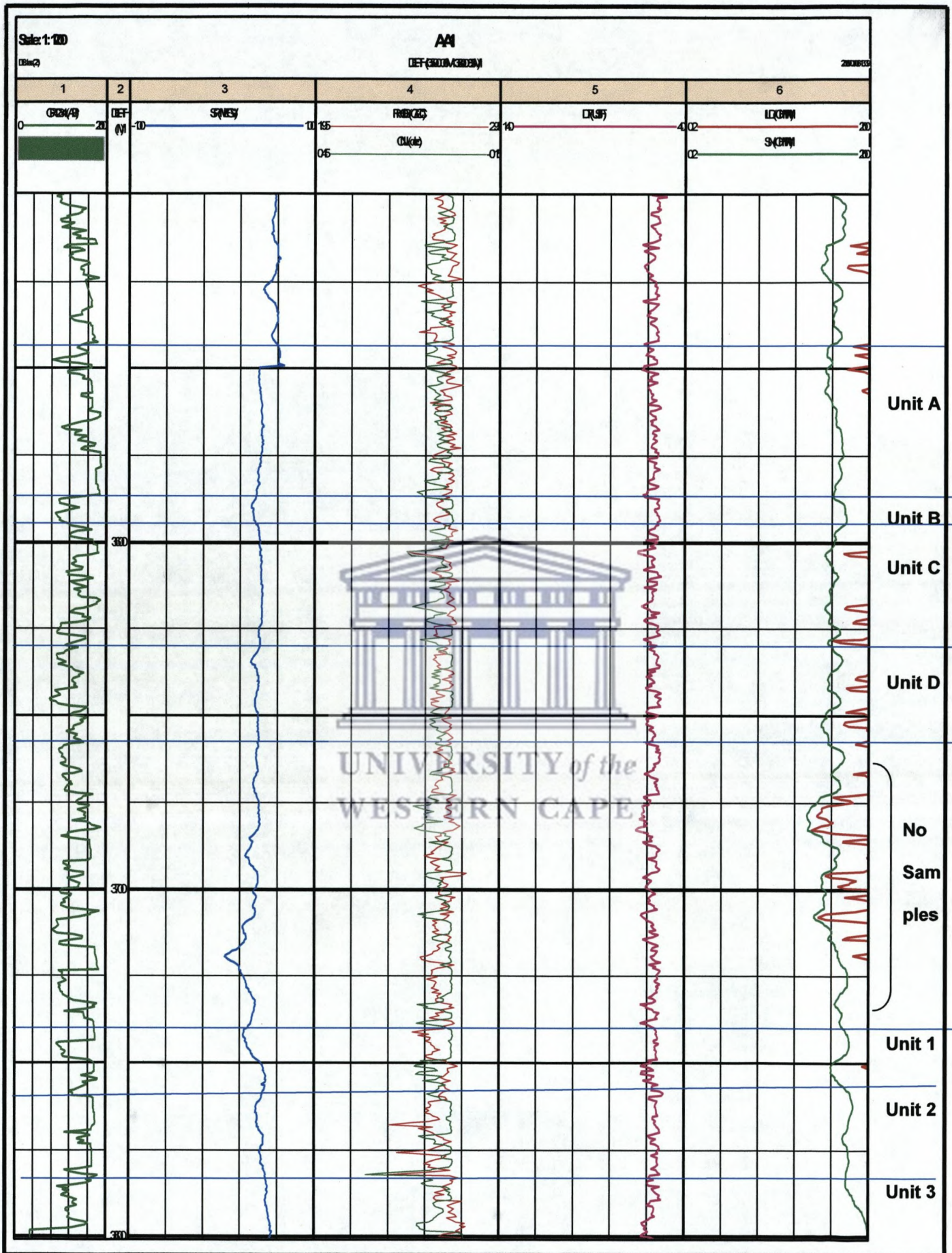


Figure 5.3.1: Geophysical units for Well A-A1

5.3.2.2 Well A-11

- Unit 1 is defined by GR readings of approximately 120 API. The SP log shows no deflection. The neutron and density logs displays patterns commonly associated with the presence of shales.
- Unit 2, same as with the preceding unit, displays GR readings of approximately 120 API and no deflection of the SP log, however, the neutron and density logs shows cross over patterns that indicates the presence of alternating layers of sandstone and shale.
- Unit 3, same as the preceding units, displays GR readings of approximately 120 API and no deflection of the SP log. The neutron and density logs displays trends associated with the presence of shale. This unit is also defined by an increase in resistivity and a decrease in velocity at the top of the unit.
- Unit 4 is defined by GR readings that fall in the range 100API to 120 API. Sonic velocities of approximately 80 us/ft are evident.
- Unit 5 is defined by lower GR readings (80 API – 120 API) than the preceding units. The GR log shows a decrease towards the base of the unit, thereby indicating that the units become progressively cleaner towards the base. However, the neutron and density cross over still indicates the presence of a shaly lithology.

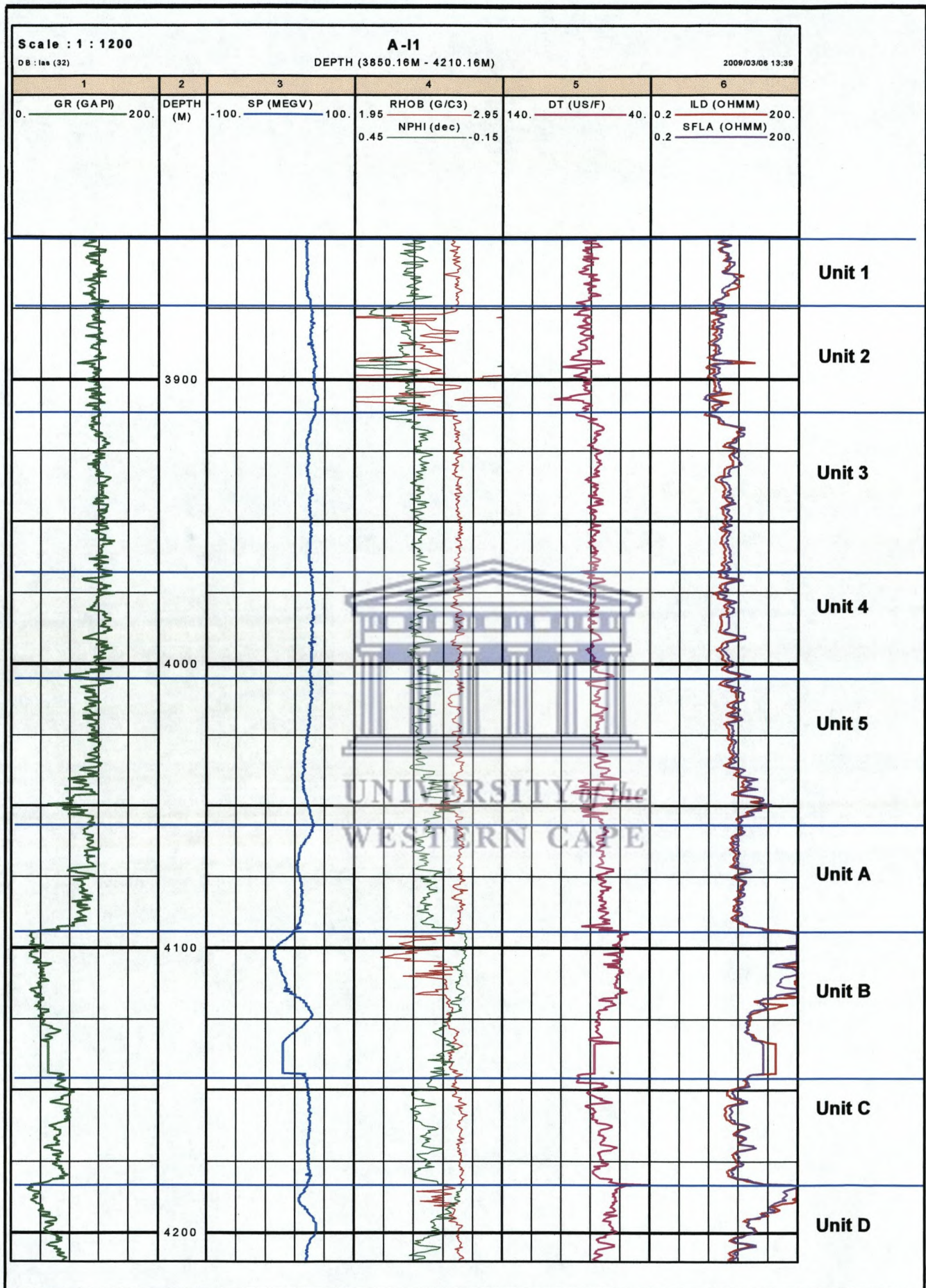
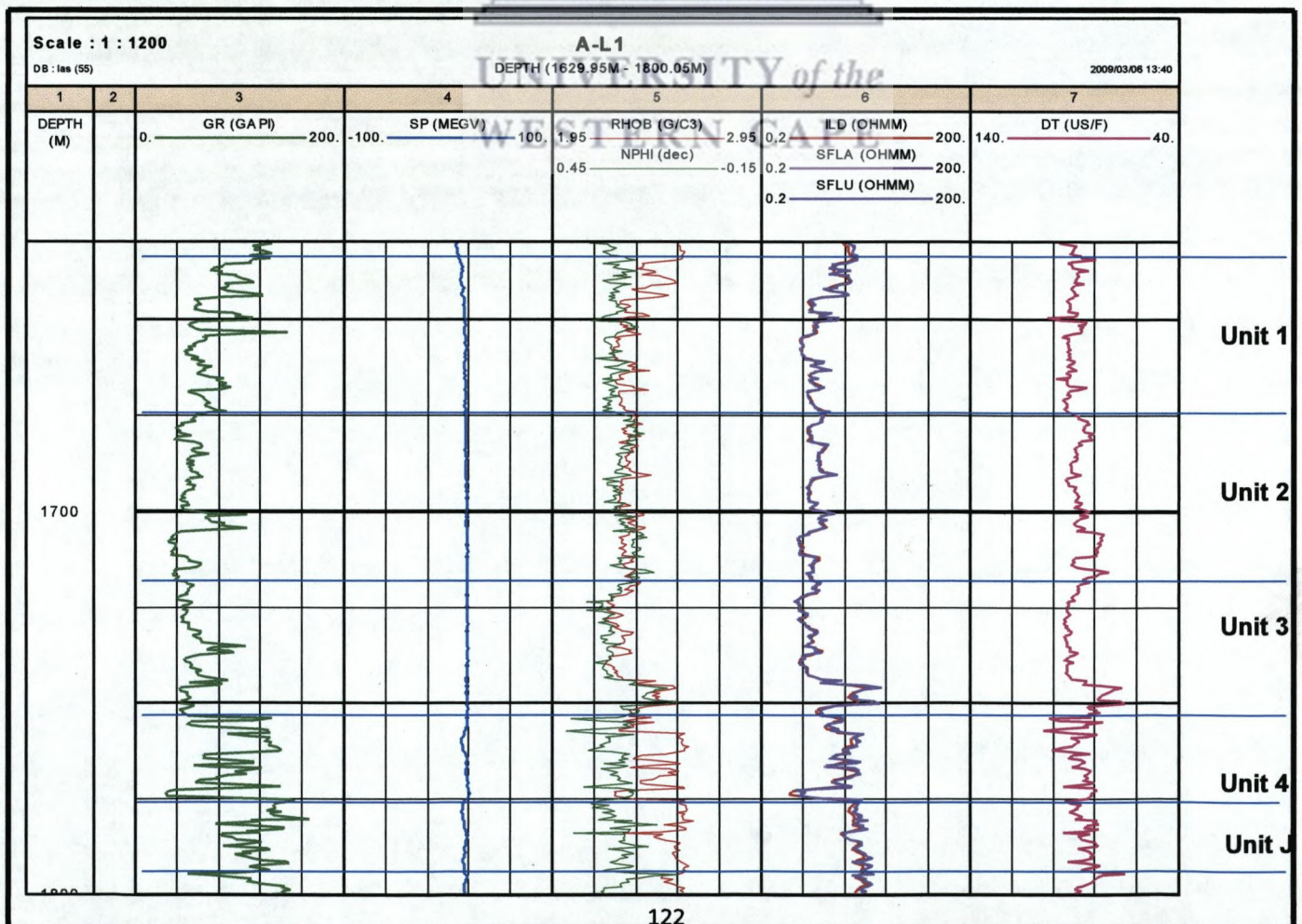


Figure 5.3.2: Geophysical units for Well A-11

5.3.1.3 Well A-L1

Four units have been defined in this section (Refer to Figure 5.3.3):

- Unit 1 is characterised by the SP log showing no deflection and the resistivity logs recording low resistivities.
- Unit 2 is defined by relatively high GR values and no deflection of the SP log. This unit displays low resistivity readings.
- Unit 3 is defined by a shalier unit than the preceding one. The SP log is defined by a straight line and the Resistivity log increases towards the base of this unit.
- Unit 4 is defined by higher GR readings than the preceding unit. The density and neutron logs indicate a shale unit with an interbedded sandstone unit. The resistivity for this unit is also higher than for the previous units.



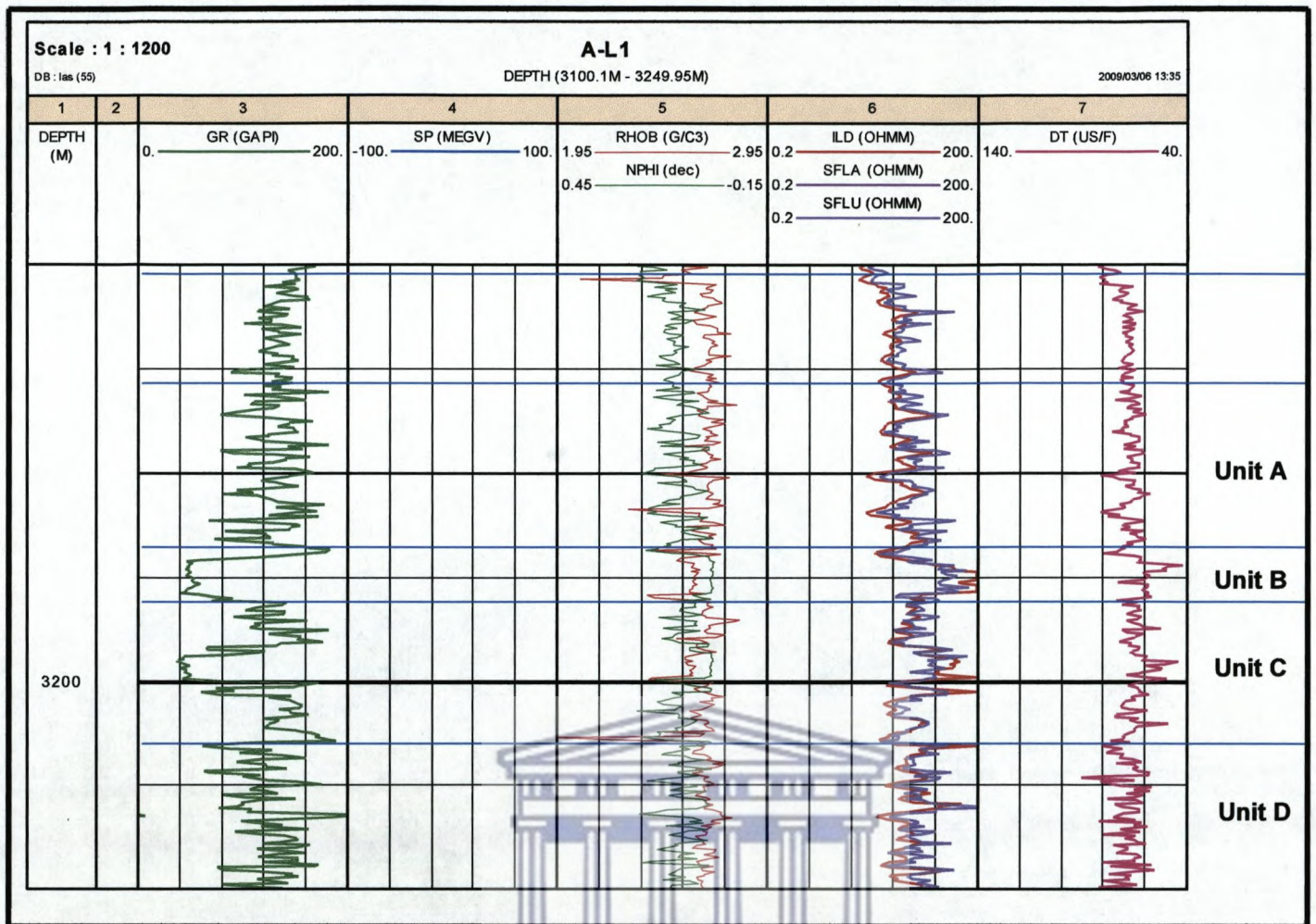


Figure 5.3.4: Geophysical units for Well A-L1: Section 2

5.3.1.4 Well A-U1

Four units are identified for Well A-U1:

- Unit 1 is characterised by GR readings in the range 40API to 60API. The Sp log only displays a deflection to the left at the top of the unit and no further deflections within the unit. Patterns that are displays by the Density- Neutron cross over are indicative of the presence of alternating lithologies or beds. Resistivity readings for this unit are extremely low.
- Unit 2 displays GR readings in the range 40API to 120API, except for an anomalous peak of 200API at a depth of approximately 2665m. The SP log shows no deflection for this unit while the Density – Neutron pattern indicates the presence of alternating units. High resistivities are found at the top of the unit and this is followed by low resistivities for the rest of the unit. The PEF log displays values of 1.8 consistently.
- Unit 3 is characterised by GR readings in the range 40API to 120API. The SP log shows no deflection while the cross over between the Neutron and Density logs indicates the presence of alternating units.

- Unit 4 displays GR readings in the range 80API to 120API while the SP log shows no deflection. The Neutron and Density logs indicate the presence of alternating layers. Resistivity readings fall in the medium range.

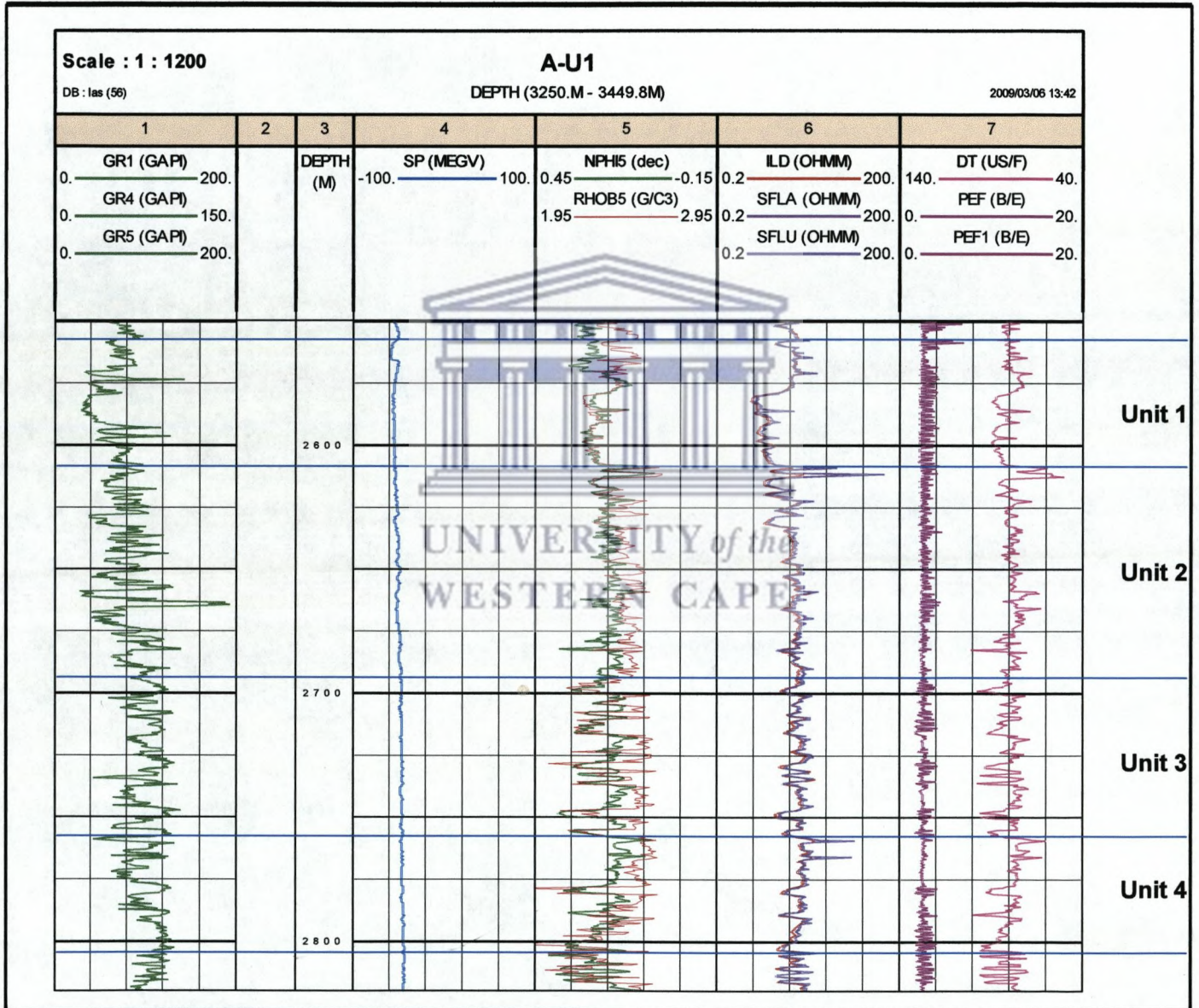


Figure 5.3.5: Geophysical units for Well A-U1: Section 1

Scale : 1 : 1200

A-U 1

DB : las (56)

DEPTH (3250.M - 3449.8M)

2009/03/06 13:42

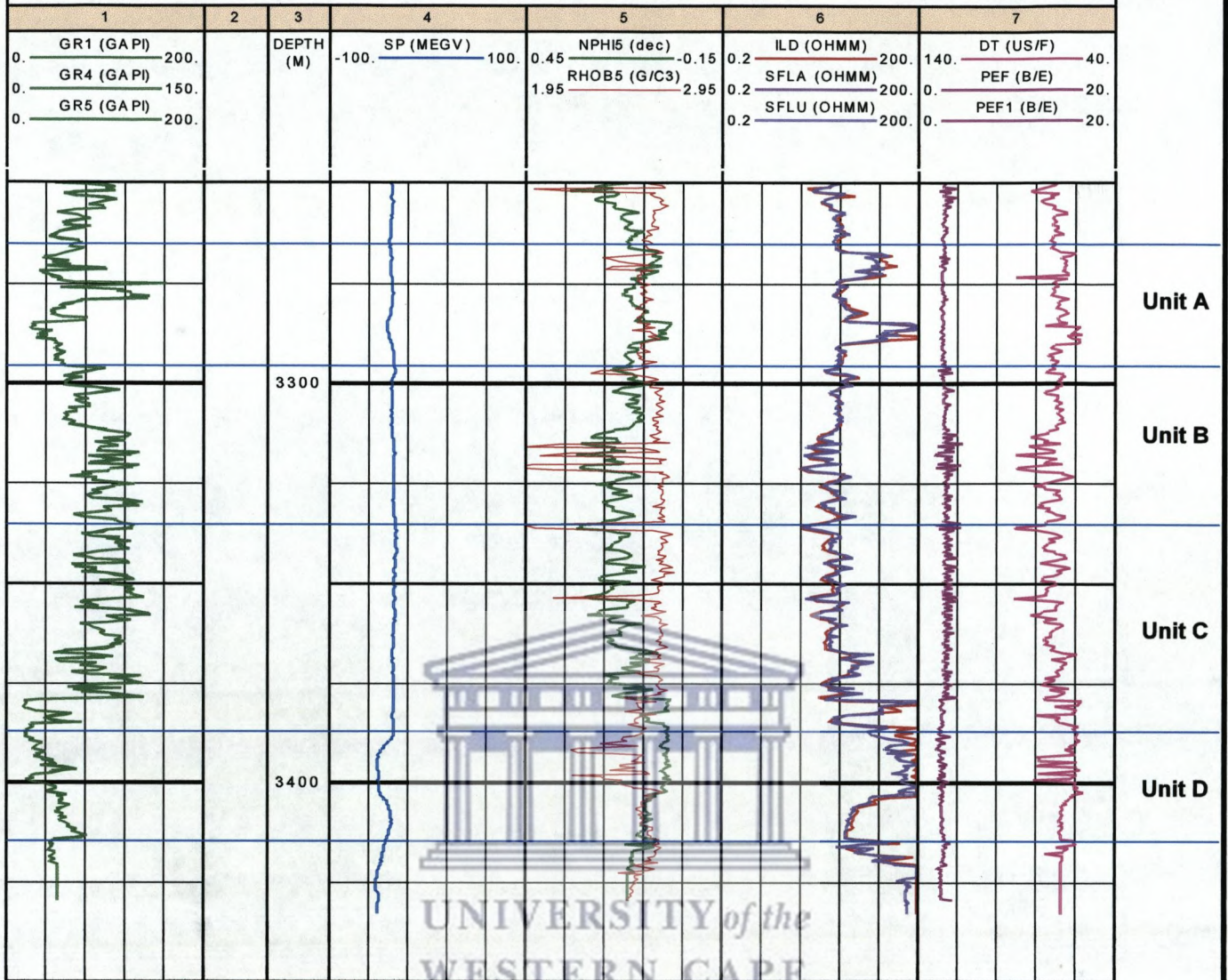


Figure 5.3.6: Geophysical units for Well A-U1: Section 2

5.3.2 DISCUSSION

5.3.2.1 Well A-A1

The patterns exhibited by the well logs have led to the identification of eight units in the area of interest. Units A to D is found to correlate across the four wells and will be discussed later.

Units 1, 2 and 3 are found only in Well A-A1. These units are defined by the following characteristics:

Unit 1

The GR log is defined by very high GR readings and this could indicate the argillaceous or clay rich nature of the samples. The top part of this unit displays readings of approximately 80 API while the readings at the base of the unit reaches 160 API, thus indicating that the unit is becoming increasingly radioactive towards the base.

The SP log shows a positive deflection at the top of the unit and this is followed by a negative deflection at the base. The above statements along with the density neutron plots indicates that this unit is composed of sandstone, however the sandstone is becoming more argillaceous towards the base.

Unit 2

This unit is defined by higher GR values (160 API) than the preceding unit and could thereby indicate the argillaceous nature of the lithology or it can possibly be indicative of the presence of shale. This unit is however defined by a solitary peak of 120 API in the middle of the unit. This peak corresponds to a decrease in the density log. The neutron density cross over indicates that this unit is composed of sandstone, most probably an argillaceous sandstone unit that is interbedded with a cleaner or more pure sandstone unit as depicts by the GR log.

Unit 3

Unit 3 is defined by high GR values (range: 80 API – 120API). The SP log shows almost no deflection. This along with the neutron and density logs suggests that the unit is composed of alternating sandstone and shale.

5.3.2.2 Well A-11

Based on the log responses for this well 9 units had been identified. Units A to D correlate with the other wells, while units 1 to 5 are found only in this well. They are defined by the following characteristics:

Unit 1

Unit 1 is defined by GR readings of approximately 120 API. This means that the unit is composed either of shale or argillaceous sandstones. The SP log shows no deflection which corroborates the fact that this unit is possibly composed of shale. The neutron and density logs display patterns that are commonly associated with the presence of shales. The resistivity logs indicate medium resistivity and no separation of the logs. The resistivity readings indicate that the unit is composed either of a conductive rock type or clays. High resistivity readings are obtained from the clays because they possess bound water (Serra, 1986).

Based on the log responses this unit is identified as being composed of argillaceous sandstones.

Unit 2

As with the preceding unit, GR readings of approximately 120 API are displayed and no deflection of the SP log. However, the neutron and density logs shows cross overs that indicate the presence of alternating layers of sandstone and shale. The resistivity logs indicate a high resistivity and no separation of the various resistivity curves. The high resistivity supplements the GR and Neutron and Density logs as it is assumed that the high resistivity is due to the presence of clays. The separation between the various resistivity tools is indicative of the porosity of the unit. No separation of the resistivity logs would indicate that the unit either possessed no porosity or no connected no porosity i.e. low permeability (Serra, 1986), in this case it is possibly indicative of the presence of low permeabilities.

Unit 3

Same as the preceding units, GR readings of approximately 120 API are displayed, thereby indicating the argillaceous nature of the unit. The SP log shows no deflection. The neutron and density logs displays trends associated with the presence of shale. This unit is also defined by an increase in resistivity and a decrease in velocity at the top of the unit.

Unit 4

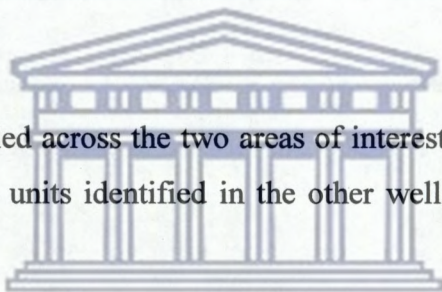
Unit 4 is defined by GR readings that fall in the range 100API to 120 API. The neutron and density logs along with the SP log indicate the presence of shale or silt. Sonic velocities of approximately 80 us/ft are displays.

Unit 5

Unit 5 is defined by lower GR readings (80 API – 120 API) than the preceding units. The GR log shows a decrease towards the base of the unit, thereby indicating that the units are becoming progressively cleaner towards the base. However, the neutron and density cross over pattern still indicates the presence of a shaly lithology.

5.3.2.3 Well A-L1

Eight units have been identified across the two areas of interest. The four units identified in section 2 correlated with the units identified in the other wells and will thus be discussed later.



UNIVERSITY of the
WESTERN CAPE

Unit 1

Unit 1 is defined as a mostly shaly unit with interbedded sandstones. The SP log shows no deflection and the resistivity log recorded a low resistivity. This could be an indication of the presence of drilling fluids in the formation.

Unit 2

The unit is defined by relatively GR values and no deflection of the SP log. The Neutron and Density logs indicate that the unit consists of alternating units of sandstone and shale, being sandier at the top and base of the unit. This unit displays low resistivity readings and this along with the SP log could possibly act as an indication that the drilling fluid has invaded the well.

Unit 3

Unit 3 is defined by a shalier unit than the preceding one. The SP log is defined by a straight line and the resistivity log increases towards the base of this unit. The increase in the resistivity log could be an indicator of the presence of hydrocarbons in the unit.

Unit 4

Unit 4 is defined by higher GR readings than the preceding unit. The density and neutron logs indicate the presence of a shale unit and interbedded sandstones. The resistivity for this unit is also higher than for the previous units.

5.3.2.4 Well A-U 1

Unit 1

The unit is defined by GR readings in the range 40 – 60 API, thus indicating that the rock contains a small amount of radioactive elements and in effect indicates that the unit is relatively clean. The patterns displays by the SP log are indicative of the presence of sandstone. Neutron and Density readings indicate the presence of shale or clay rich sandstone for the top half of the unit. The neutron density readings in the lower half of the unit, along with decreased resistivity readings and a straight SP line is indicative of the presence of limestone. However, it is most likely that this unit is composed of sandstone and that the pattern exhibited by the SP and the decrease in resistivity can be attributed to the presence of salt water in the formation.

Unit 2

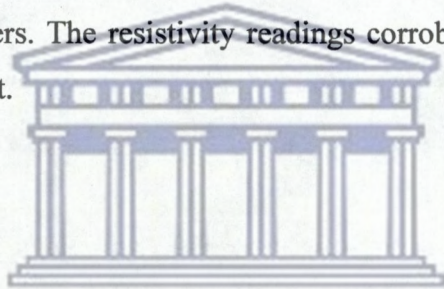
Unit 2 is defined by 40 – 120API. The pattern displays by the GR log is indicative of alternating layers of argillaceous or clay rich sandstone with a cleaner sandstone. This is corroborated by the pattern exhibited by the neutron and density logs. The resistivity measured is higher than for the preceding wells and indicates that the unit contains either conductive formations or clays. The bound water in clays possesses conductive surfaces (*Serra, 1986*). In this instance it is most likely that the resistivity readings are due to the presence of clays.

Unit 3

Gamma ray readings and patterns indicates the presence of alternating layers of argillaceous or clay rich sandstones with sandstones of a cleaner nature. The SP log shows no deflection and the readings are relatively low and are thus indicative of the presence of sandstone. Neutron and Density cross overs corroborates the pattern displays by the GR log, indicating alternating layers of argillaceous or clay rich sandstone with sandstone of a cleaner nature. The medium resistivity readings confirm the presence of clays within the unit.

Unit 4

The GR readings indicate the presence of a more clay rich sandstone than for the preceding units. The SP log displays relatively low values and is indicative of the presence of sandstone. The presence of alternating layers of clays/ shales and sandstones are indicates by the density neutron cross overs. The resistivity readings corroborate the statement that this unit has increases clay content.



UNIVERSITY *of the*
WESTERN CAPE

5.4 CROSS PLOTS

The preceding sections looked at well log responses and identified possible units from them. The log responses are partially used to identify lithology however log responses could be ambiguous. Thus Neutron – density cross plots are constructed for each unit.

The Neutron – Density cross plots are used for the identification of lithologies. The Neutron density Cross plot is composed of three lithology curves namely, sandstone, limestone and dolomite lithology curves. The location of the points of interest will thus indicate the lithology of the unit.

5.4.1 RESULTS

5.4.1.1 Well A-A1

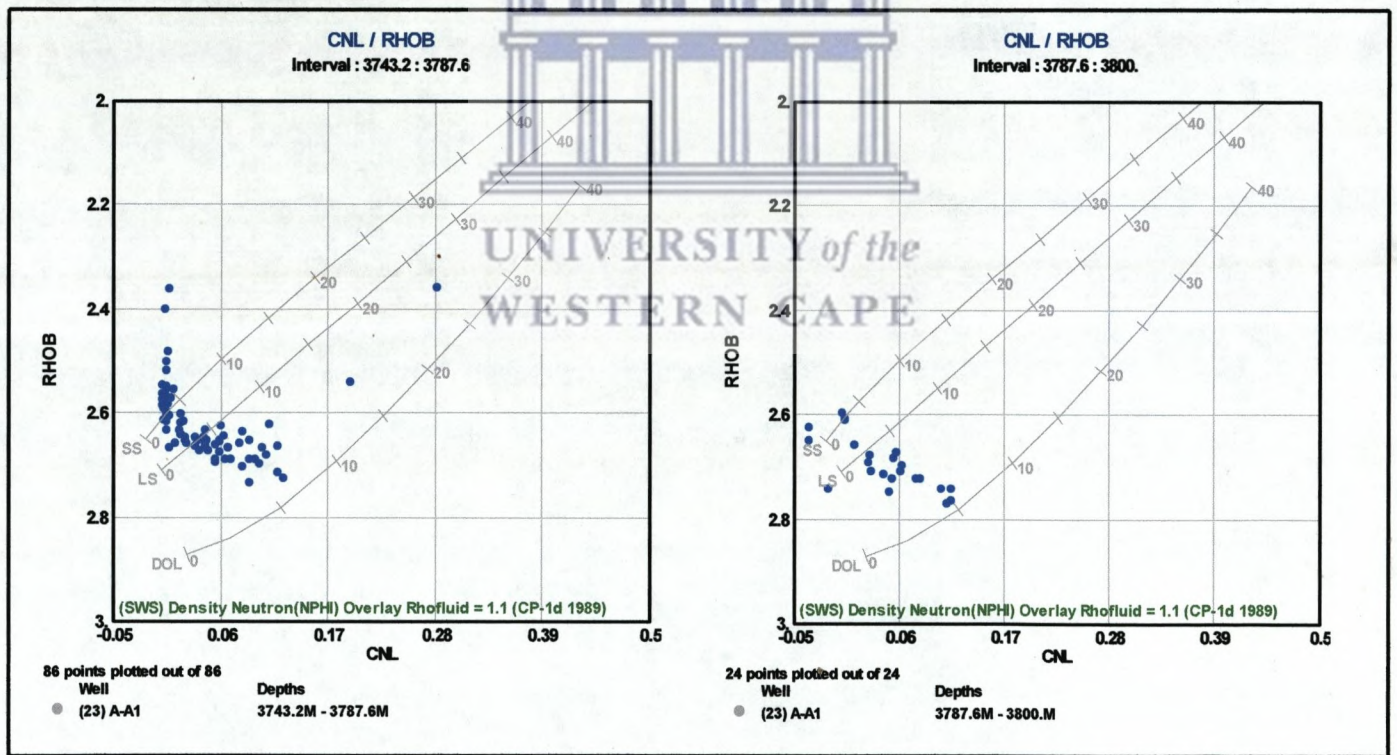


Figure 5.4.1: Neutron – Density Cross Plots for: (A) Unit 1 and (B) Unit 2 of Well A-A1.

The Neutron – Density Cross Plots for Well A-A1 displays the following trends:

- The points for Unit 1 plots across the three lithology curves. Unit 2 is also found to plot outside the sandstone lithology curve.
- The points for Unit 2 plots across the three lithology curves, but are concentrated between the limestone and dolomite lithology curves.

5.4.1.2 Well A-I1

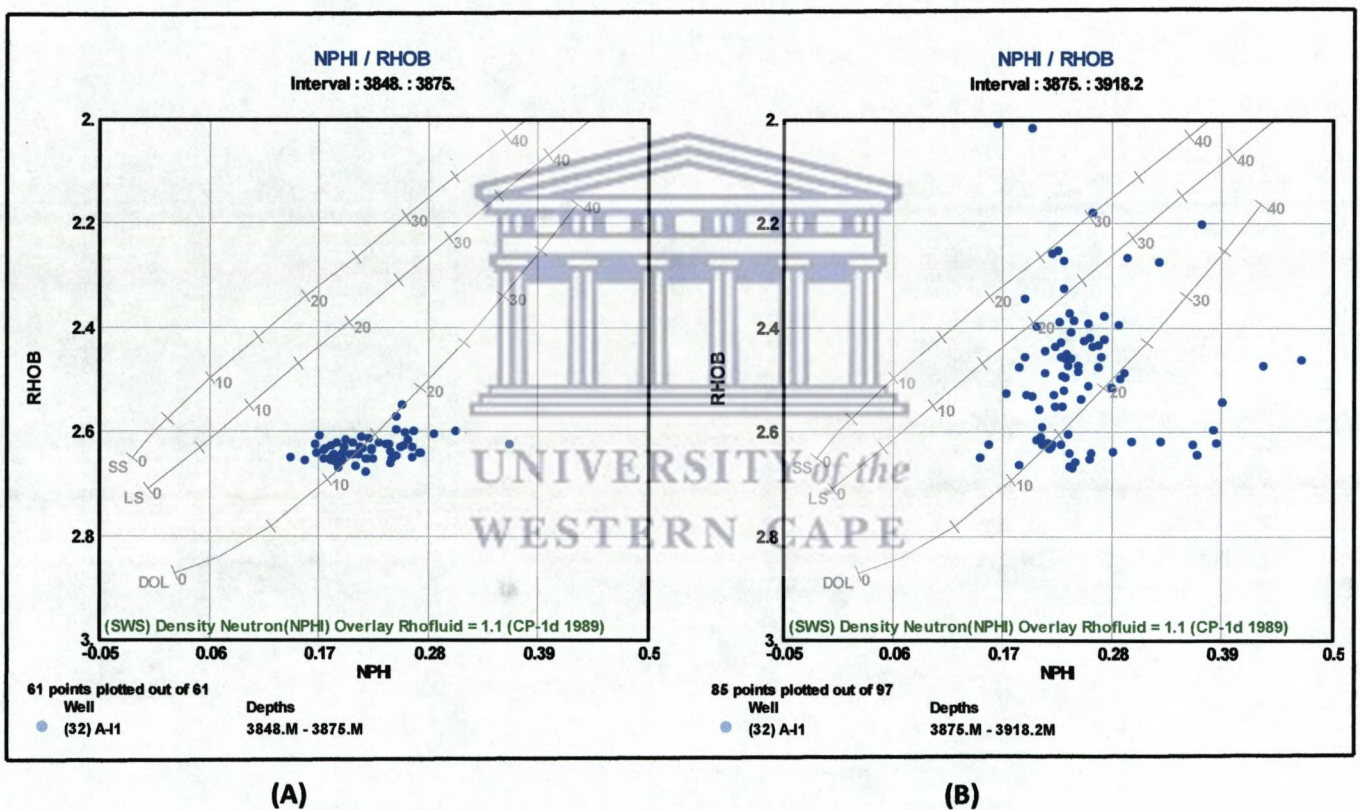
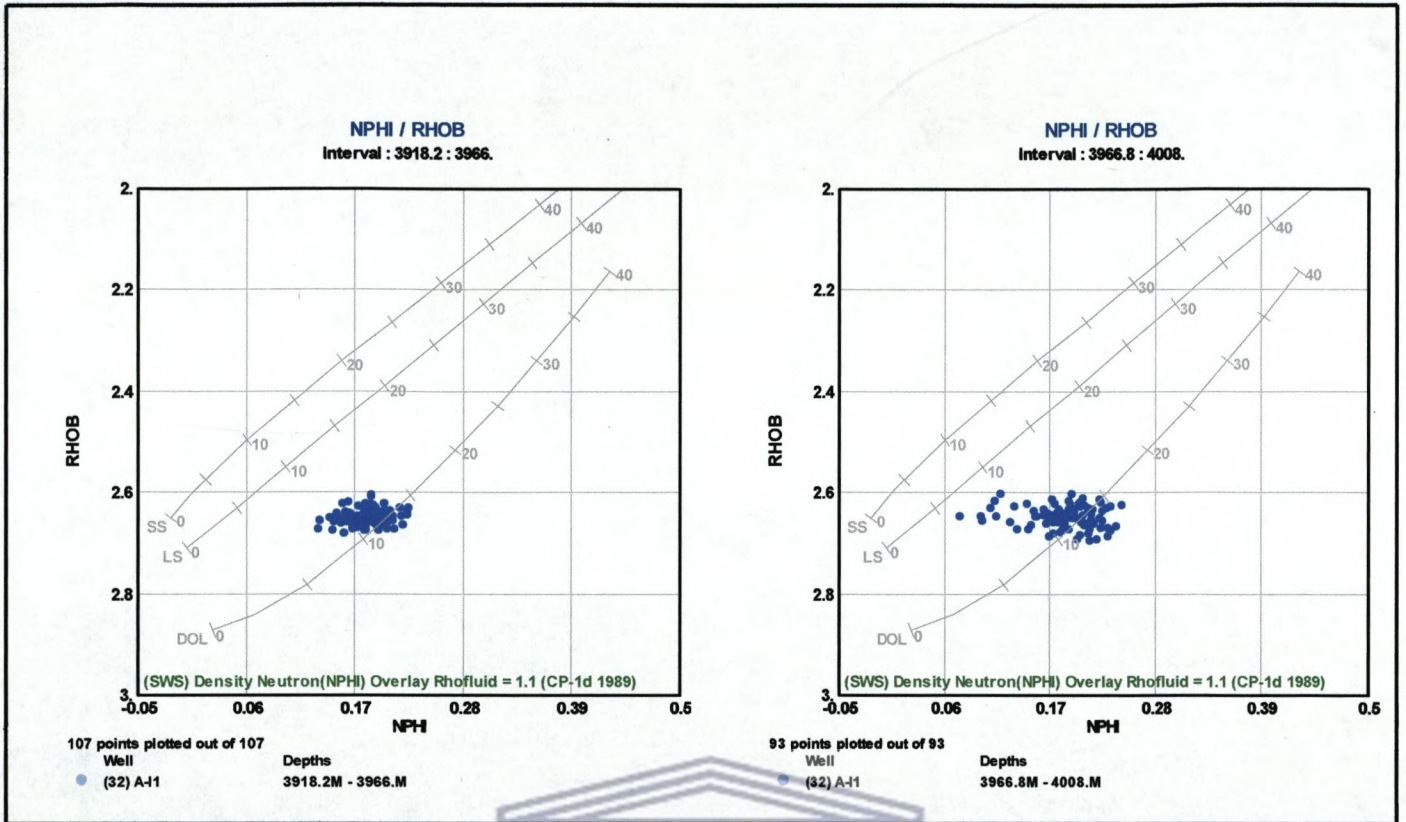
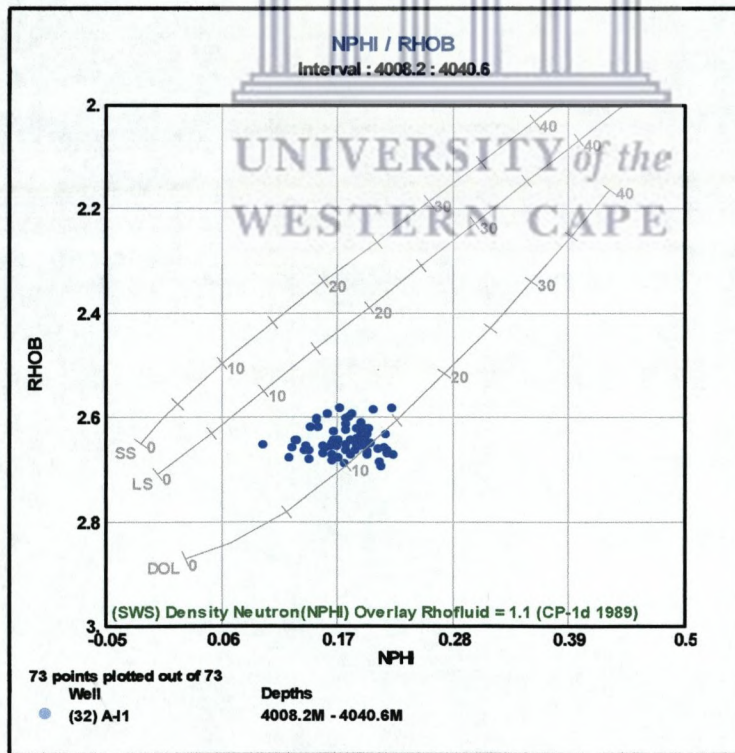


Figure 5.4.2: Neutron – Density Cross Plots for: (A) Unit 1 and (B) Unit 2 of Well A-I1.



(C)

(D)



(E)

Figure 5.4.3: Neutron – Density Cross Plots for: (C) Unit 3, (D) Unit 4 and (E) Unit 5 of Well A-11.

The Neutron – Density Cross Plots for Well A-I1 displays the following trends:

- Unit 1 is concentrated towards the dolomite lithology curve and is found to plot on the outside of the same curve.
- The points for Unit 2 are scattered across the top part of the plot across the three lithology curves but are concentrated between the limestone and dolomite lithology curves.
- Unit 3 clusters towards the dolomite lithology curve.
- The points for Unit 4 plot between the dolomite and limestone lithology curves but are concentrated towards the dolomite lithology curves.
- As with Unit 3, Unit 5 clusters towards the dolomite lithology curve.

5.4.1.3 Well A-L1

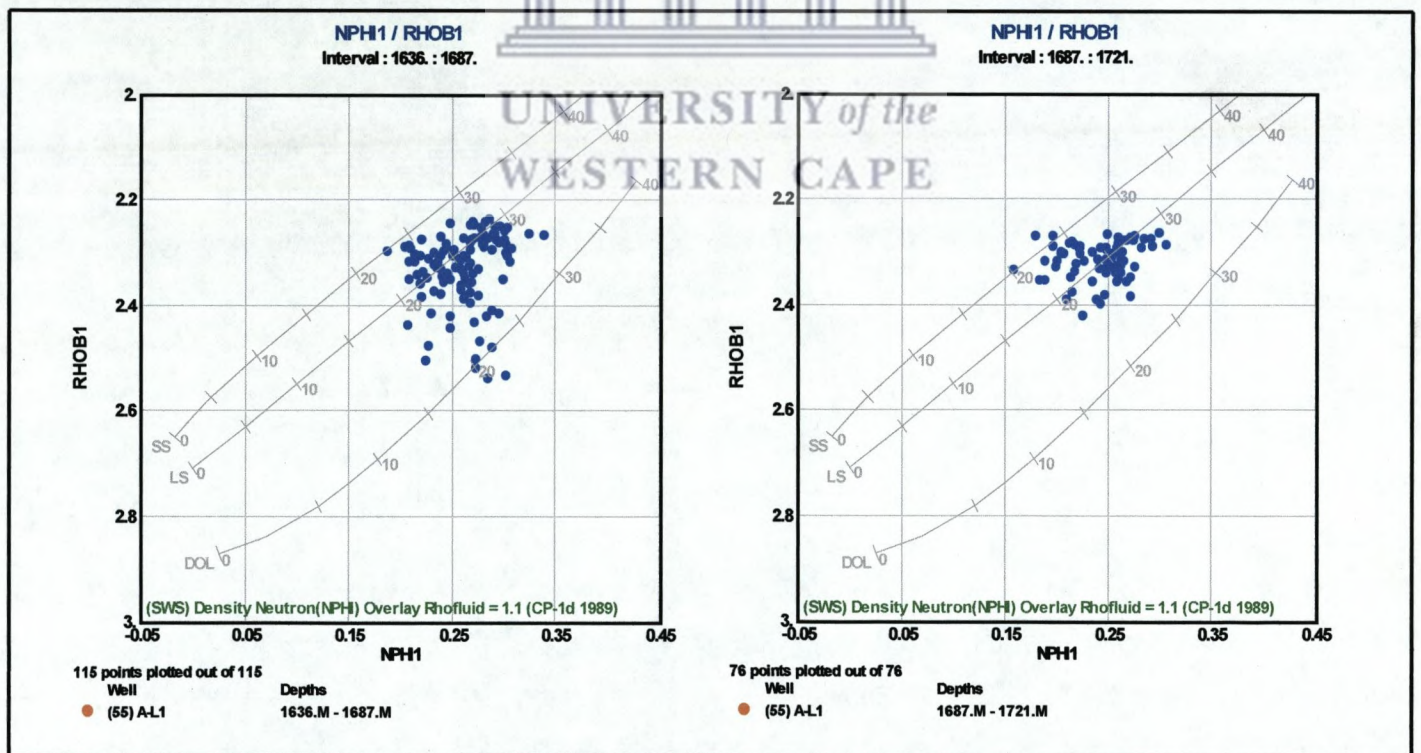


Figure 5.4.4: Neutron – Density Cross Plots for: (A) Unit 1 and (B) Unit 2 of Well A-L1

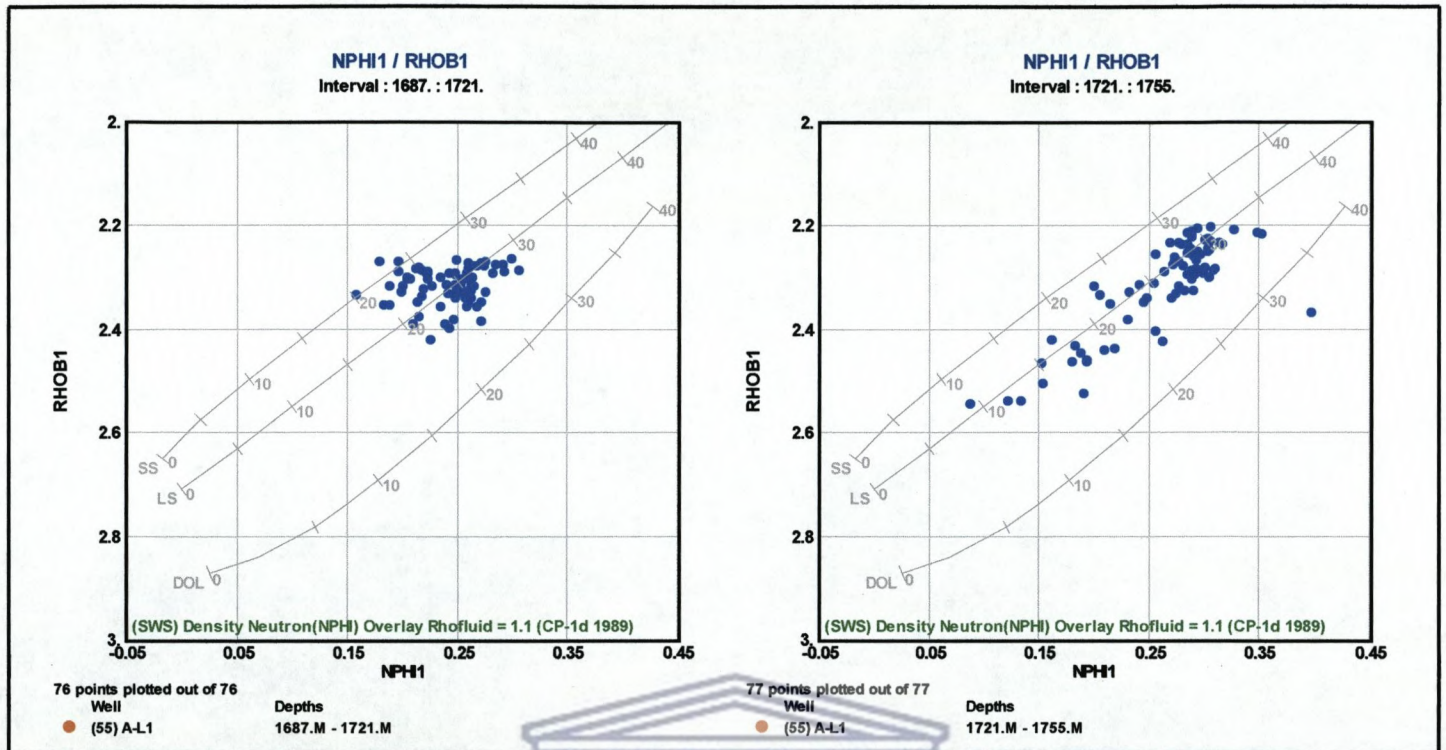


Figure 5.4.5: Neutron – Density Cross Plots for: (C) Unit 3, and (D) Unit 4 of Well A-L1.

The Neutron – Density Cross Plots for Well A-L1 displays the following trends:

- The points for Unit 1 are scattered across the three lithology curves but are concentrated across the limestone lithology curve.
- Unit 2 plots between the sandstone and limestone lithology curves but are found to be concentrated towards the limestone lithology curve.
- The points for Unit 4 are concentrated across the limestone lithology curve and appear to follow the limestone lithology curve.

5.4.1.4 Well A-U1

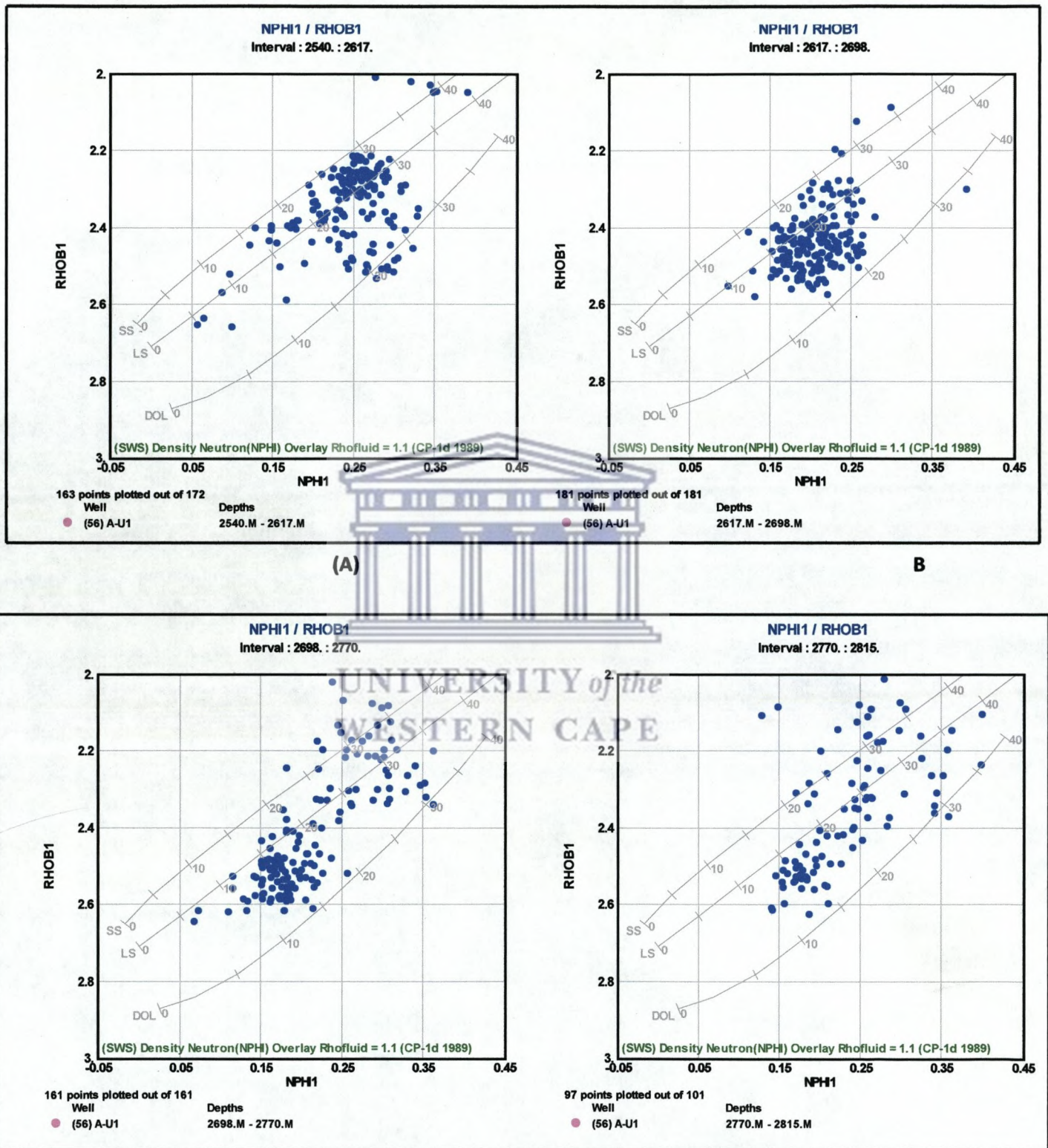
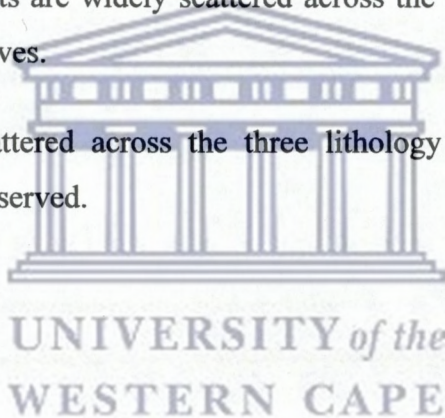


Figure 5.4.6: Neutron – Density Cross Plots for: (A) Unit 1, (B) Unit 2, (C) Unit 3, and (D) Unit 4 of Well A-U1

The Neutron – Density Cross Plots for Well A-U1 displays the following trends:

- The points for Unit 1 are scattered across the three lithology curves. A prominent cluster is found at the upper part of the plot between the sandstone and limestone lithology curves. The majority of the remainder of the points are scattered between the limestone and dolomite curves. Outliers are present at the top of the plot.
- Unit 2 is scattered across the three lithology curves. The points, however, appears to be concentrated between the limestone and dolomite lithology curves. Outliers are found outside the sandstone and dolomite lithology curves.
- The points for Unit 3 are scattered across the plot. A dominant cluster is found on the lower part of the plot between the limestone and dolomite lithology curves. The remainder of the points are widely scattered across the upper part of the plot across the three lithology curves.
- Unit 4 is widely scattered across the three lithology curves of the plot and no dominant cluster is observed.



5.4.1.5 Correlated Units

5.4.1.5.1 Unit A

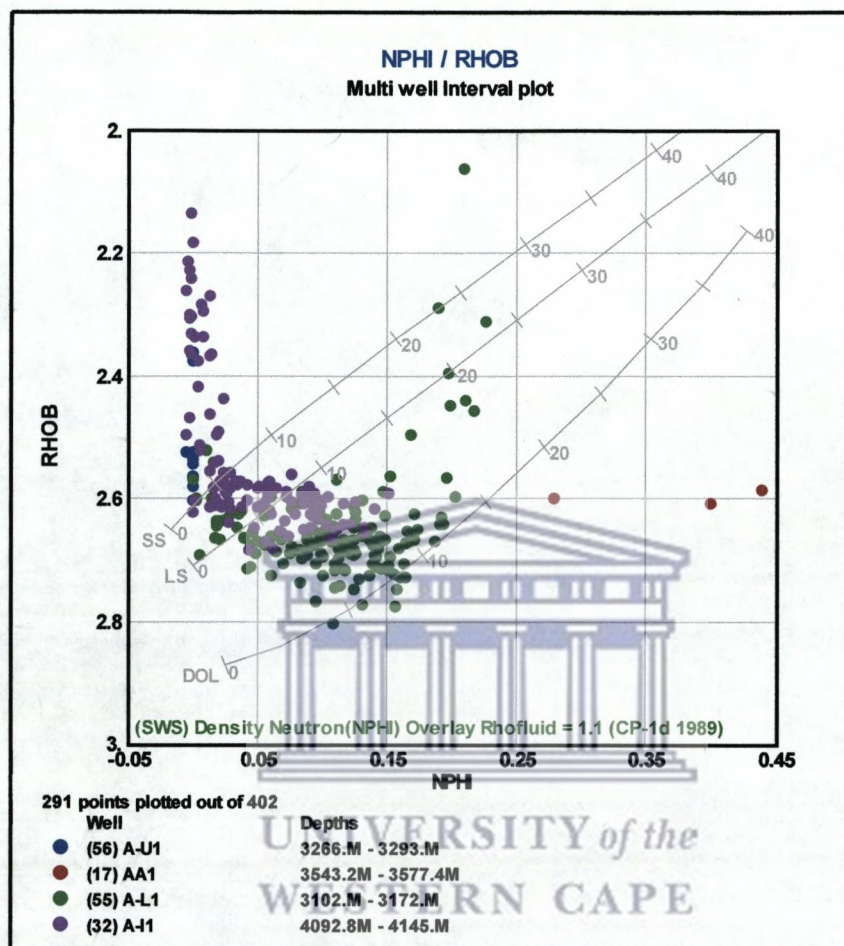


Figure 5.4.7: Neutron Density Cross plot for Unit A

The Neutron – Density Cross Plot for Unit A displays the following trends:

- The points for Well A-A1 plots outside the lithology curves.
- The points for Well A-I1 plots across the three lithology curves but are concentrated between the sandstone and limestone lithology curves and plots closer to the limestone curve than the dolomite curve. Some of the points plotted outside the lithology curves
- Points for Well A-L1 plots between the limestone and dolomite lithology curves
- The points for Well A-U1 follow the same trend as points for Well A-I1, plotting outside the three lithology curves.

5.4.1.5.2 Unit B

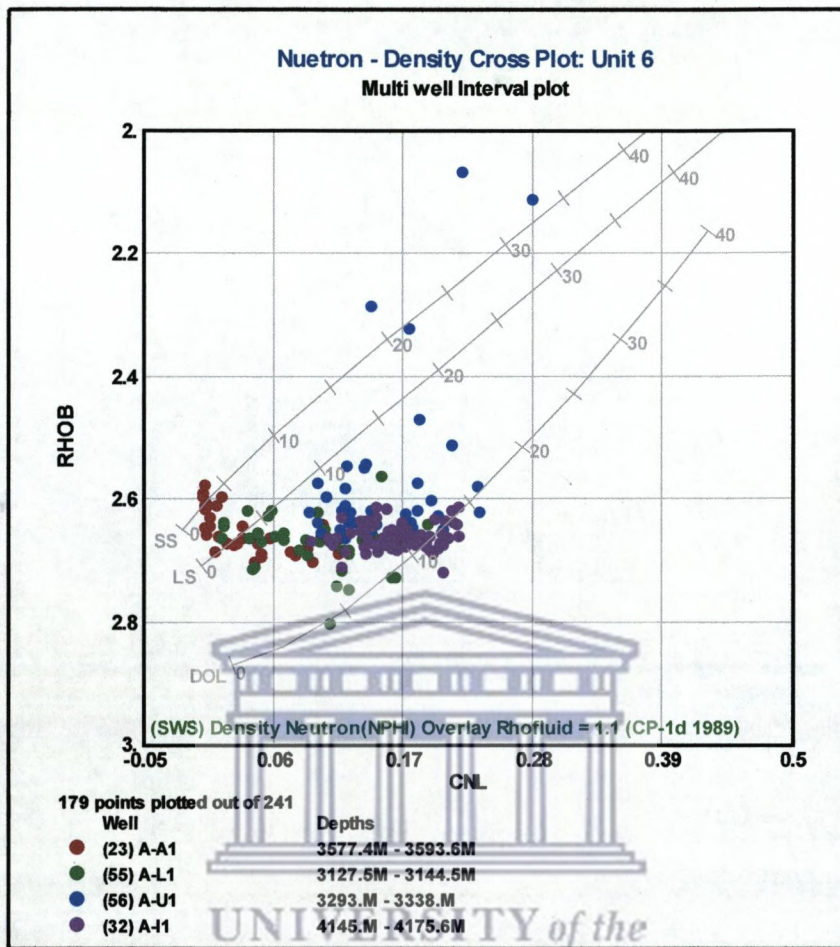


Figure 5.4.8: Neutron Density Cross plot for Unit B

The Neutron – Density Cross Plot for Unit B displays the following trends:

- Well A-A1 plots across all the lithology curves but is concentrated towards the sandstone curve.
- Well A-I1 is concentrated between the limestone and dolomite lithology curves.
- Well A-L1 follows a similar trend to Well A-A1; however it plots closer to the limestone curve than the dolomite lithology curve.
- Well A-U1 is concentrated towards the dolomite lithology curve.

5.4.1.5.3 Unit C

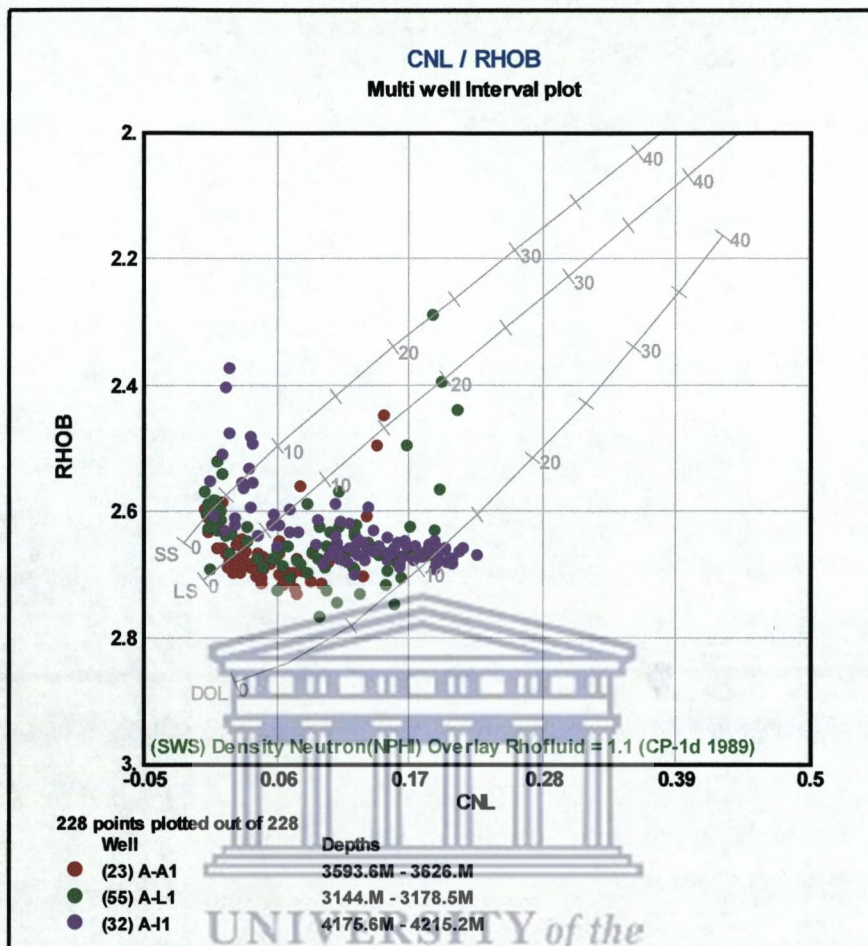


Figure 5.4.9: Neutron Density Cross plot for Unit C

The Neutron – Density Cross Plot for Unit C displays the following trends:

- The points for Well A-A1 plots across the sandstone and limestone lithology curves. A few points are scattered towards the upper corner of the plot between the limestone and sandstone lithology curves.
- Well A-L1 follows a similar dispersion pattern as A-A1, plotting across the limestone and sandstone lithology curves.
- Well A-I1 follows a very similar pattern as the previous wells; however some of the points are concentrated at the dolomite lithology curve.

5.4.1.5.3 Unit D

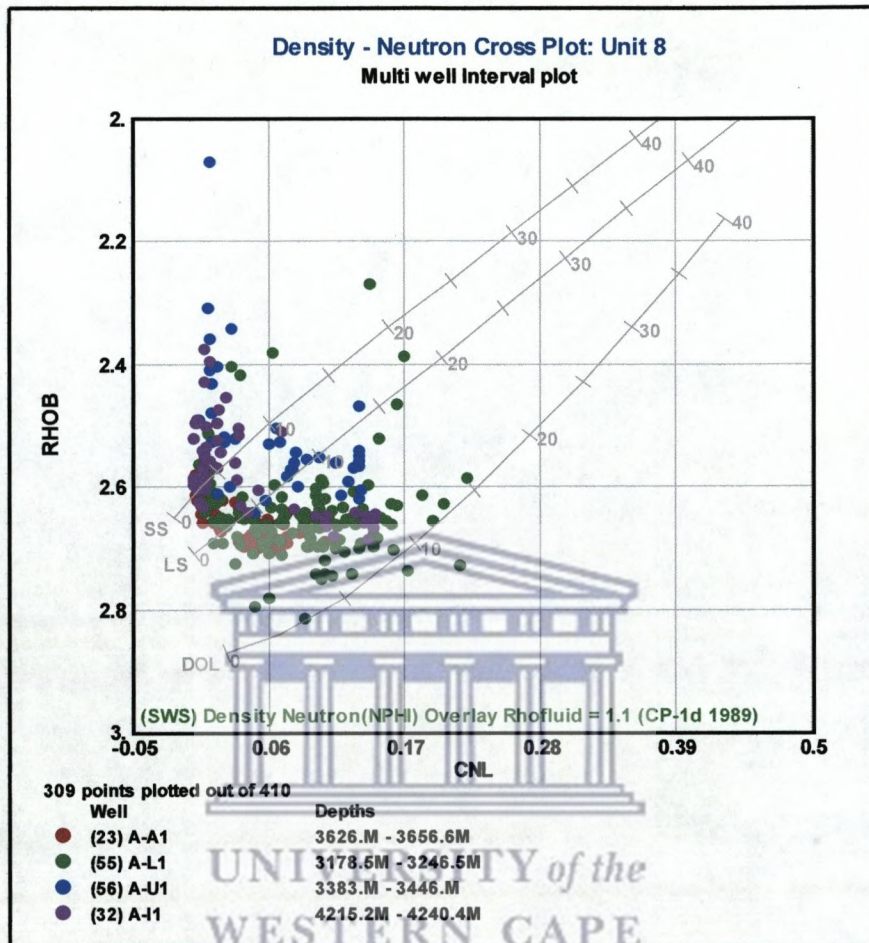


Figure 5.4.10: Neutron Density Cross plot for Unit D

The Neutron – Density Cross Plot for Unit D displays the following trends:

- Well A-A1 plots across the sandstone and limestone lithology curves. A few samples plotted on the left outer curve of the plot.
- Well A-L1 follows a similar dispersion pattern as Well A-A1.
- Well A-U1 plots across the same curves as the previous well however the points are located slightly higher on the curves as the points of the preceding wells.
- Well A-I1, as Wells A-A1 and A-L1, plots across the sandstone and limestone lithology curves. A number of the points are found to plot on the left outer curve of the plot.

5.4.2 DISCUSSION

5.4.2.1 Well A-A1

The neutron density plot indicates the presence of sandstones and either limestones or dolomite, but from the geochemistry it is known that the unit is not composed of either limestone or dolomite. It is thus inferred that the points plotting on the lower section of the plot between the limestone and dolomite lithology curves indicates the presence of calcareous shales. This corroborates the signatures obtained from the geochemistry which indicates an abundance of clay minerals while the CaO, MgO and MnO concentrations indicates the presence of carbonates.

Unit 2 of Well A-A1 plots across the three lithology curves. The points that plot towards the sandstone lithology line indicate the siliceous nature of the samples and corroborate the high SiO₂ concentration obtained by the whole rock analysis. The points between the limestone and dolomite lithology curves indicate the presence of shale or clay rich sandstone. This is in agreement with the results obtained from the geochemistry which indicates high concentrations of the elements associated with clays. The general overview of the well logs indicates that the well is composed of alternating layers of sandstone and shale or greywacke and this is reflected by the clustering of the points in the neutron density cross plot.

5.4.2.2 Well A-I1

Unit 1 clusters towards the dolomite lithology curve. The relative position of the points is indicative of the presence of shales or greywacke. This statement is substantiated by the geochemistry of the unit which displays a decrease in silica content (~ 50% SiO₂) and increase in the concentration of the elements associated with clays. CaO and Sr measures relatively high and indicate the calcareous nature of the samples. A small amount of the samples plotted outside the dolomite lithology curve and indicates the presence of calcareous shales.....

Unit 2 plots across the three lithology curves. The points that are located between the sandstone and limestone lithology curves are indicative of the siliceous nature of the unit and the presence of presumably sandstone while the samples that plot between the limestone and

dolomite lithology curves indicates the presence of a shale component, presumably calcareous shale. The geochemistry for this unit indicates the presence of alternating layers of siliceous units with argillaceous units. This trend is also observed from the well log responses. The relative positions of the samples confirm the above assumptions.

Unit 3 clusters towards the dolomite lithology curve. The relative positions of the points indicate the presence of shale. This confirms the results of the geochemistry and geochemical indices that reveals increasing clay content and low silica content. The log responses for this unit also substantiates the position of the samples on the neutron density cross plot by revealing high GR readings and a SP deflection that is associated with the presence of shale.

As with Unit 3, Unit 4 clusters towards the dolomite lithology curve, indicating the presence of a shale unit. This confirms the geochemistry and log responses that indicate the presence of a shale unit or a greywacke.

Unit 5 plots between the dolomite and limestone lithology curves but are concentrated towards the dolomite lithology curves. The movement of points towards the limestone curve could be indicative of an increase in the siliceous nature of the unit at places within the unit, as seen by the geochemical trends and log responses. The points that are clustered towards the dolomite curve are indicative of the presence of shale or greywacke component within the unit as observed from the geochemistry and log responses. Thus the positions of the points on the neutron density cross plot are indicative of the presence of alternating layers of sandstone, most probably of an argillaceous nature, with shales and confirms the trend displays by the geochemical profiles and log responses for the unit.

5.4.2.3 Well A-L1

Unit 1 plots across the three lithology curves. The points that are located between the sandstone and limestone curves are indicative of the presence of a siliceous rock, presumably sandstone, while the points located between the limestone and dolomite curves indicated the presence of a shaly sand or clay rich sand. This confirms the observation from the log responses which indicates the presence of alternating units of shale or clay rich sandstone. From the geochemistry the shaly sand is more accurately defined as argillaceous sand based on the element associations.

The points for Unit 2 plots on the upper section of the neutron – density cross plot across the three lithology curves. The relative positions of the points thus indicate the presence of sandstone and shaly-sands. The geochemistry of the unit supports the above assumptions by indicating the presence of a siliceous rock alternating with a more argillaceous unit. The log responses are also indicative of afore mentioned.

Unit 3 plots across the three lithology curves and indicates the presence of a sandstone unit as well as a shaly – sand component (indicated by the location of the points between the limestone and dolomite curves) for this unit. This corroborates the geochemical and well log responses that indicate the presence of alternating cleaner sandstone units with argillaceous unit and shalier units respectively.

Unit 4 plots across the three lithology curves on the neutron – density cross plot and thus indicates the presence of sandstones with porosities in the range 25% - 30%, a shale unit (points that follow the dolomite curve) and a shaly sand unit (points found between the limestone and dolomite curves). The neutron density plot thus results in the identification of three lithologies and confirms the geochemistry of the unit which indicates the presence of alternating sandstones with argillaceous units or shaly sands. The log responses for this unit substantiates the above assumption by displaying alternating layers of sandstone and shale or argillaceous sands.

UNIVERSITY of the
WESTERN CAPE

5.4.2.4 Well A-U1

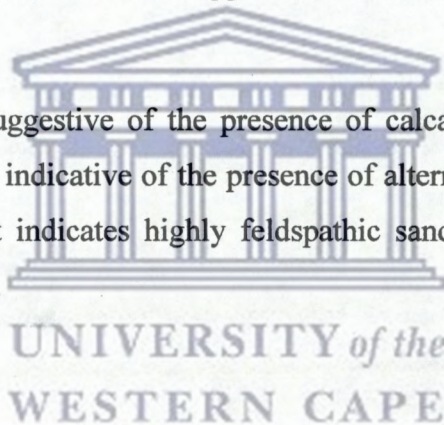
The points for Unit 1 on the neutron – density plot are scattered across the three lithology curves. A prominent cluster is found between the sandstone and limestone lithology curves which are indicative of the presence of sandstone, while the points that are located between the limestone and dolomite curves are suggestive of the presence of shaly- sand and minor shale components. The geochemical analysis confirms the above as it displays an increase in the concentration of clay minerals towards the base of the well thus indicating the presence of shale or clay rich sand at the base of the well.

Unit 2 plots across the three lithology curves but are concentrated between the limestone and dolomite lithology curves which are suggestive of the presence of calcareous shales. The remaining points are located between the sandstone and limestone lithology curves which indicate the presence of sandstone. The log responses for this unit substantiates the plotting

of the unit on the neutron – density cross plot by displaying patterns that are associated with the presence of argillaceous or clay rich sandstone and sandstone of a cleaner nature. The geochemistry, as the cross plot and log responses, is suggestive of the presence of arkose or argillaceous layers at the top and base of the unit and a highly siliceous rock for the rest of the unit.

The points for Unit 3 are scattered all over the neutron density plot. A prominent cluster is located between the limestone and dolomite lithology curves and the relative positions of the points are suggestive of the presence of calcareous shales or clays. The other lithologies identified using the plot included sandstones and shale components. The log responses confirms the above lithologies as the trends observed from the well logs are indicative of the presence of argillaceous or clay rich units alternating with sandstones of a cleaner nature. The geochemistry of the unit, however, is suggestive of a sandstone of a highly feldspathic nature.

Unit 4, as with Unit 3, is suggestive of the presence of calcareous clays, sandstones and shales. The log responses are indicative of the presence of alternating clays and shales while the geochemistry of the unit indicates highly feldspathic sandstone which becomes more argillaceous towards the base.



5.4.2.5 Correlated Units

5.4.2.5.1 Unit A

Well A-A1 plotted outside the lithology curves. This effect is associated with the presence of gas and is so termed the gas effect.

Well A-I1 plotted across the three lithology curves. The points which are concentrated towards the sandstone lithology curves are indicative of the siliceous nature of the unit, while the points clustered around the limestone curve could have indicates the presence of calcareous shales or clays as the composition of limestone and calcareous shales or clays or similar and they would be indistinguishable on a plot of this nature. Some of the points for Well A-I1 and Well A-U1 plotted outside the three lithology curves in a region which is indicative of the presence of gas.

Well A-L1 plotted between the limestone and dolomite lithology curves and thus reiterated the presence of calcareous shales in this unit.

Based on the Neutron- Density cross plots this unit is classified as consisting of sandstone and calcareous shale. This reiterated the geochemistry of the unit that indicates that the unit is composed of alternating layers of a siliceous component, most probably sandstone, and a more argillaceous component, in this case calcareous shale as seen on the Neutron –Density cross plots.

5.4.2.5.2 Unit B

Wells A-A1 and A-L1 plotted across the three lithology curves but are concentrated at the sandstone lithology curve indicating the highly siliceous nature of the unit. The points located between the limestone and dolomite lithology curves are suggestive of the presence of shales, presumably calcareous shales.

Wells A-I1 and A-U1 are clustered between the dolomite and limestone lithology curves and hereby indicates the presence of an argillaceous component in this unit.

The distribution and clustering of the points on the Neutron – Density cross plot corroborated the pattern exhibited by the geochemistry of this unit which indicates that the unit is composed alternating layers of feldspathic sandstone and clay rich sandstones or shales.

5.4.2.5.3 Unit C

Wells A-A1, A-L1 and A-I1 plotted across the three lithology curves. The clustering of points between the sandstone and limestone curves indicates the presence of a sandstone component in this unit, while the clustering of points between the limestone and dolomite curves are indicative of the presence of a calcareous component, most likely calcareous shale or clay in this unit. A large percentage of the points are found between the limestone and dolomite lithology curves and thus indicates that this unit is more clay rich than the preceding units.

The Neutron – Density cross plots mirrored the geochemistry of the unit which classified the unit as highly feldspathic and that it became more clay rich towards the base.

5.4.2.5.4 Unit D

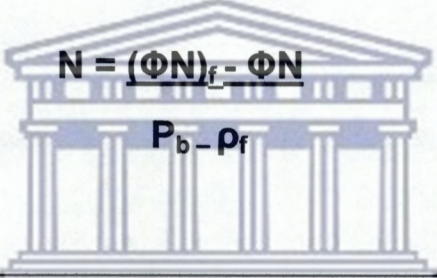
The Wells A-a1, A-L1, A-U1 and A-I1 plotted across the three lithology curves. The points for Well A-U1 plotted slightly higher than for the preceding units. The relative positions of these wells indicate the presence of a sandstone component and shale/ clay component, most likely of a calcareous nature.

The Wells A-I1, A-L1 and A-U1 plotted outside the sandstone lithology curve. This movement of points are usually the effect of gas on the lithology. The Neutron – Density cross plot thus indicates sandstone and shale components in the unit.

The Neutron –Density cross plot mirrored the geochemistry of the unit which indicates that the unit is composed of sandstone, feldspathic sandstone and shale layers. The geochemistry also indicates that the unit had a higher carbonate concentration than the preceding unit. This is also displays by the relative clustering of the point on the plot.

5.5 M-N PLOTS

The M-N cross plots is a method of constructing a lithology plot only by eliminating the effects of porosity, thus allowing the identification of mineral mixtures. The porosity, sonic and density logs are used to construct the M-N plot. The variables M and N are defined as follows:

$$M = \frac{t_f - t}{P_b - \rho_f} \times 0.003$$
$$N = \frac{(\Phi N)_f - \Phi N}{P_b - \rho_f}$$


UNIVERSITY of the
WESTERN CAPE

The values obtained for M and N are plotted against each other. The relative positions for certain minerals have thus been defined (see figure 5.5). Points for binary mixtures plot along a line which connects two mineral points while tertiary mixtures plot within a triangle which has been defined using the relative positions of calcite, dolomite and sandstone (refer to Figure 5.5).

Properties such as gas effect, secondary porosity and shaliness affect the M-N plot in such a manner that the points shift in the direction indicates by the arrows in Figure 5.5.

M-N Cross Plot

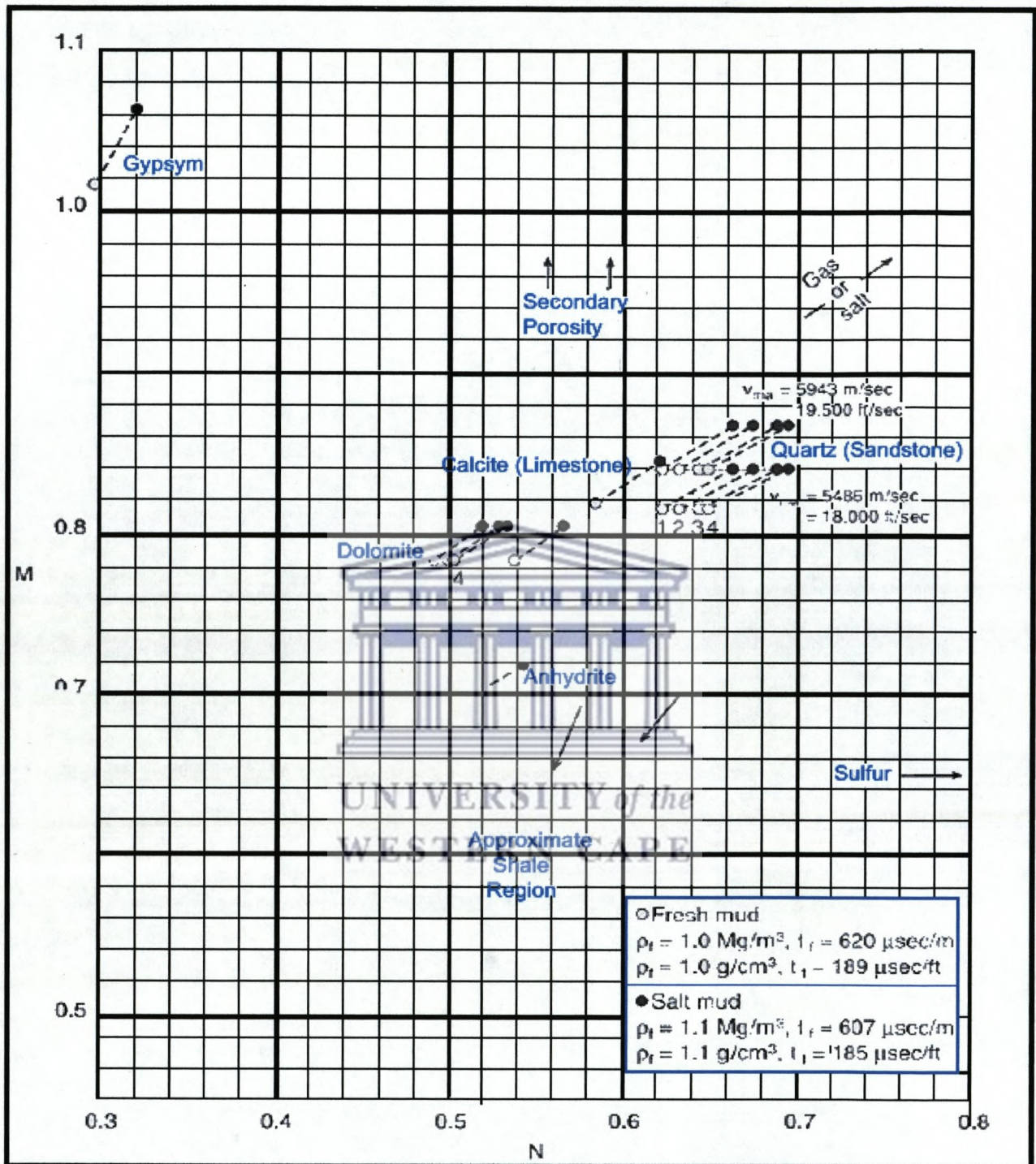
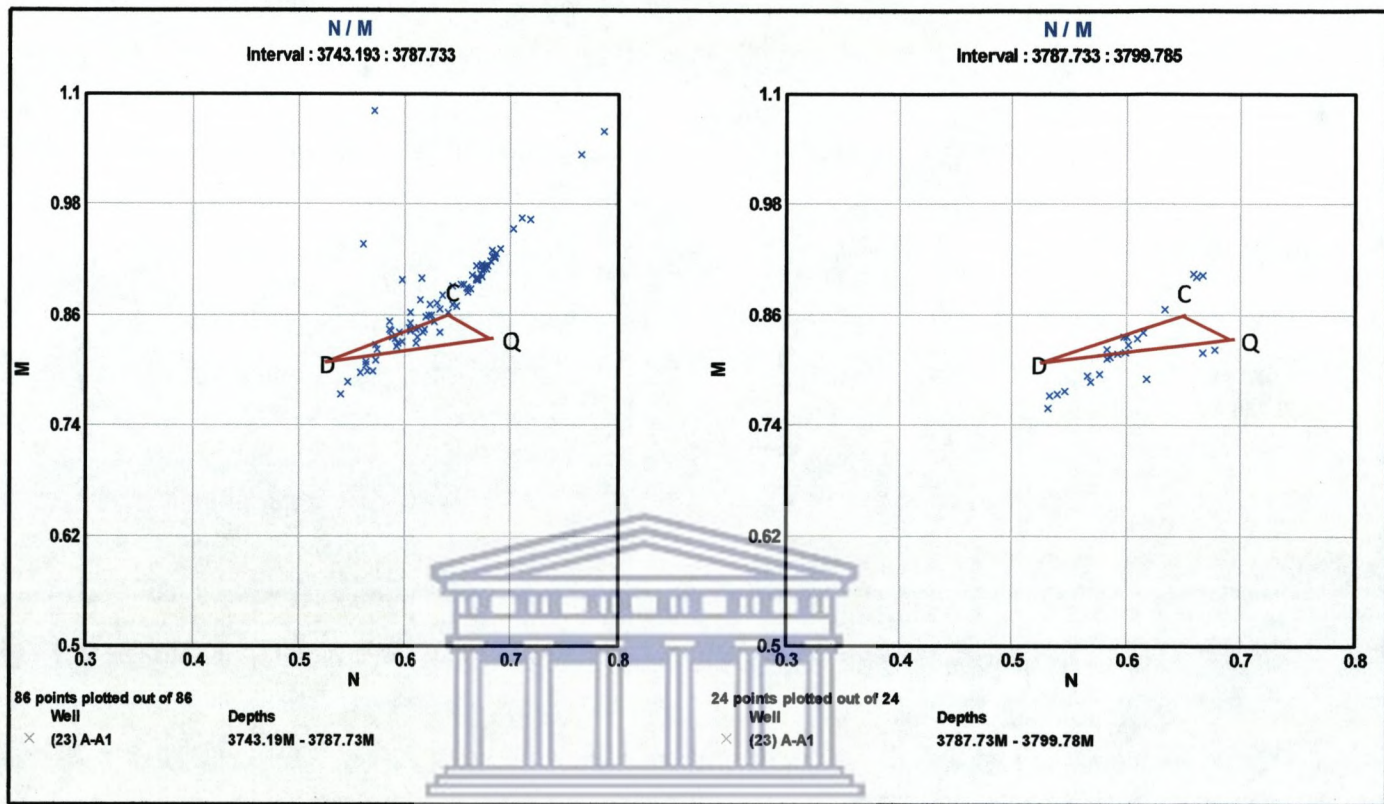


Figure 5.5: M-N Cross plots indicating the positions of minerals as defined by Schlumberger. (Modified from Schlumberger, 1995)

5.5.1 RESULT

5.5.1.1 Well A-A1



(A)

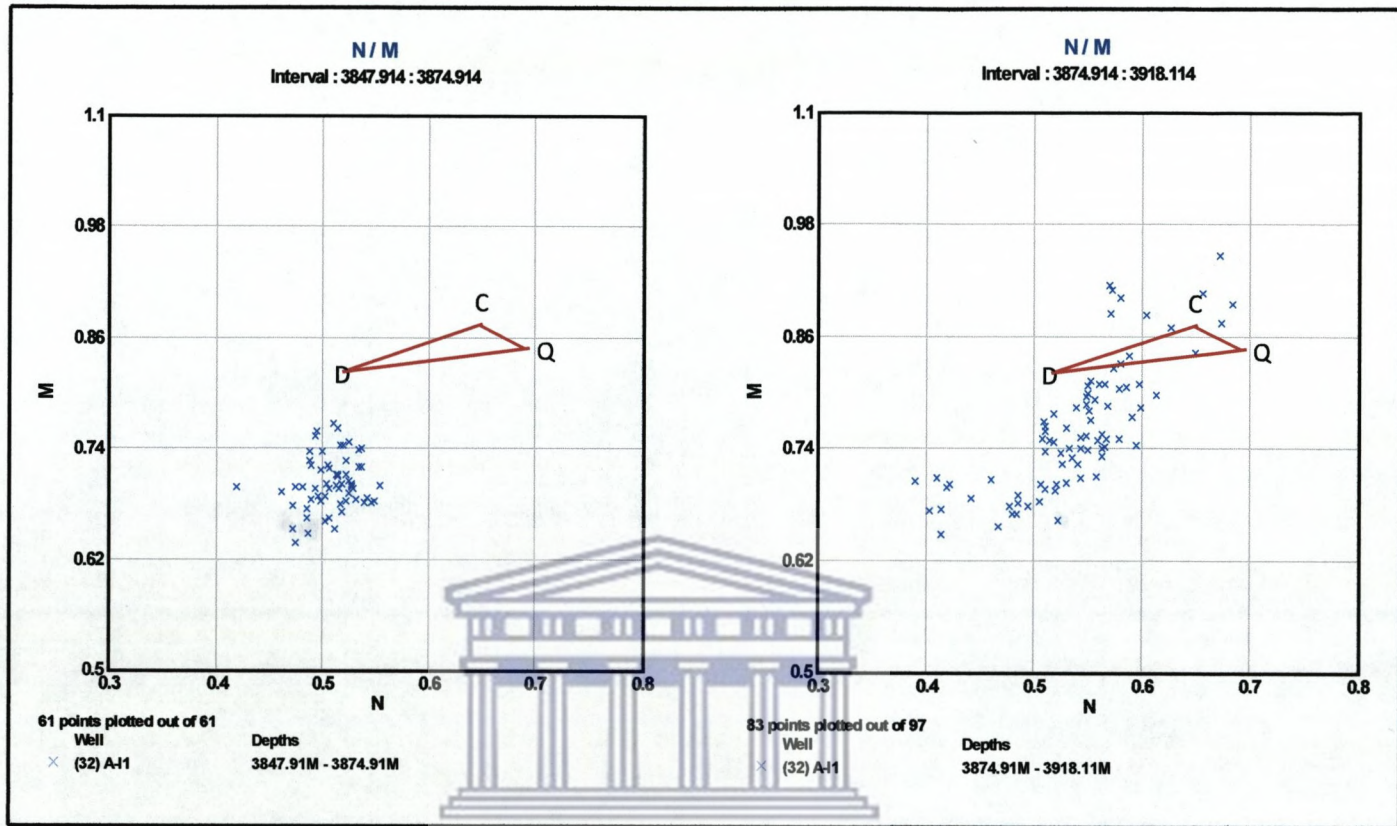
(B)

Figure 5.5.1: M/N plots for Unit 1 (A) and Unit (2) of Well A-A1.

The M-N Plots for Well A-A1 shows the following trends:

- The M-N plot for Unit 1 displays an upward movement of the points. The Points which plotted in the quartz-calcite-dolomite triangle are concentrated towards the region predefined as the calcite region. A minor amount of the points displays a downward shift.
- The points for Unit 2 plotted in the centre of the quartz-calcite-dolomite triangle, but show a tendency towards the calcite values. The Greater majority of the points shows a downward shift and plotted towards the predefined shale region.

5.5.1.2 Well A-I1



(A)

(B)

Figure 5.5.2: M/N plots for Unit 1 (A) and Unit 2 (B) of Well A-I1.

The M-N plots for Well A-I1 displays the following trends:

- The points for Unit 1 plotted in the lower half of the plot and display a downward shift. Points plotted in the region defined as the shale region.
- The points for Unit 2 are widely scattered across the M-N plot. An overall downward shift of points away from the basic quartz- calcite- dolomite triangle is observed. The points in the lower region clustered in the predefined shale region.

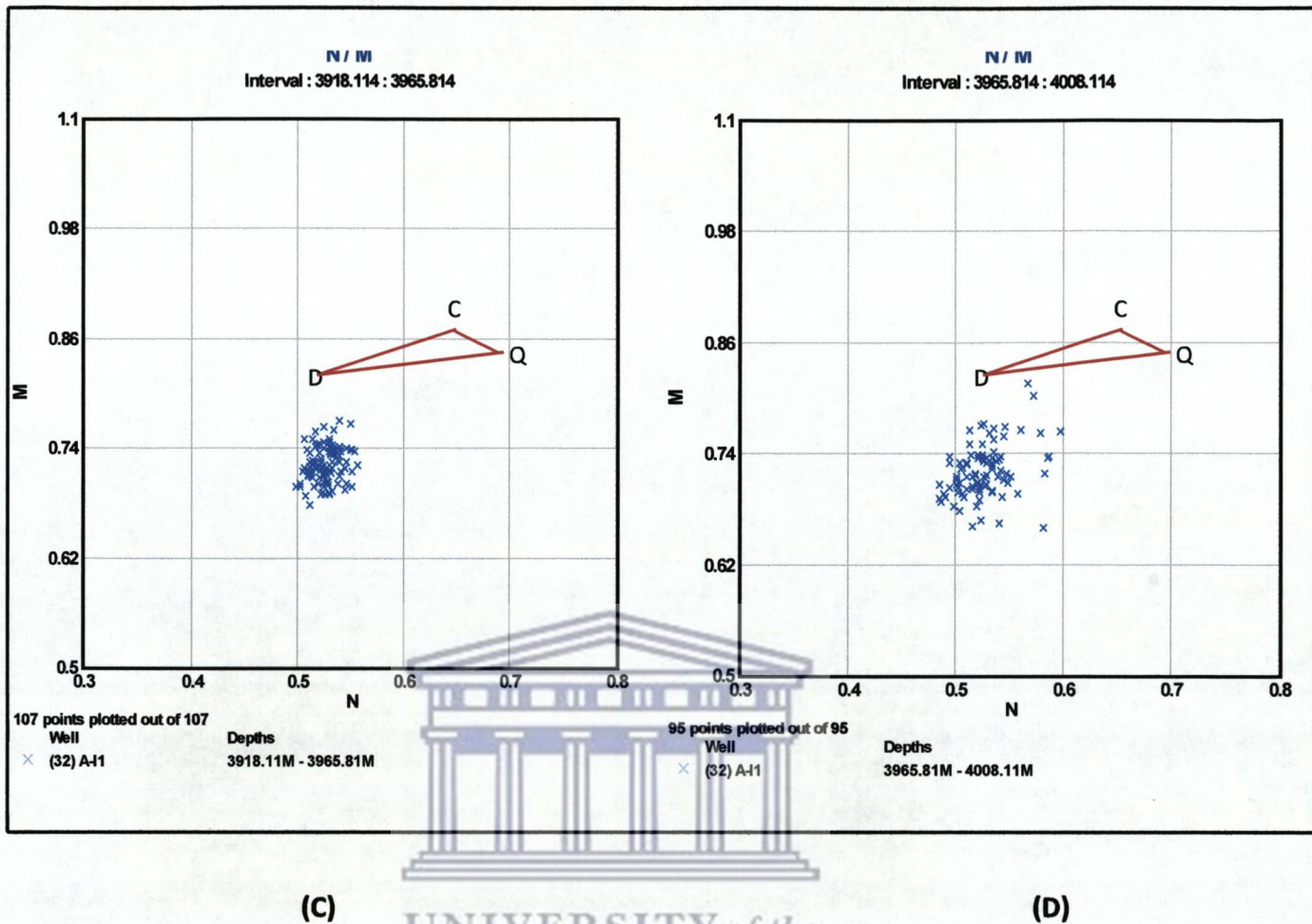
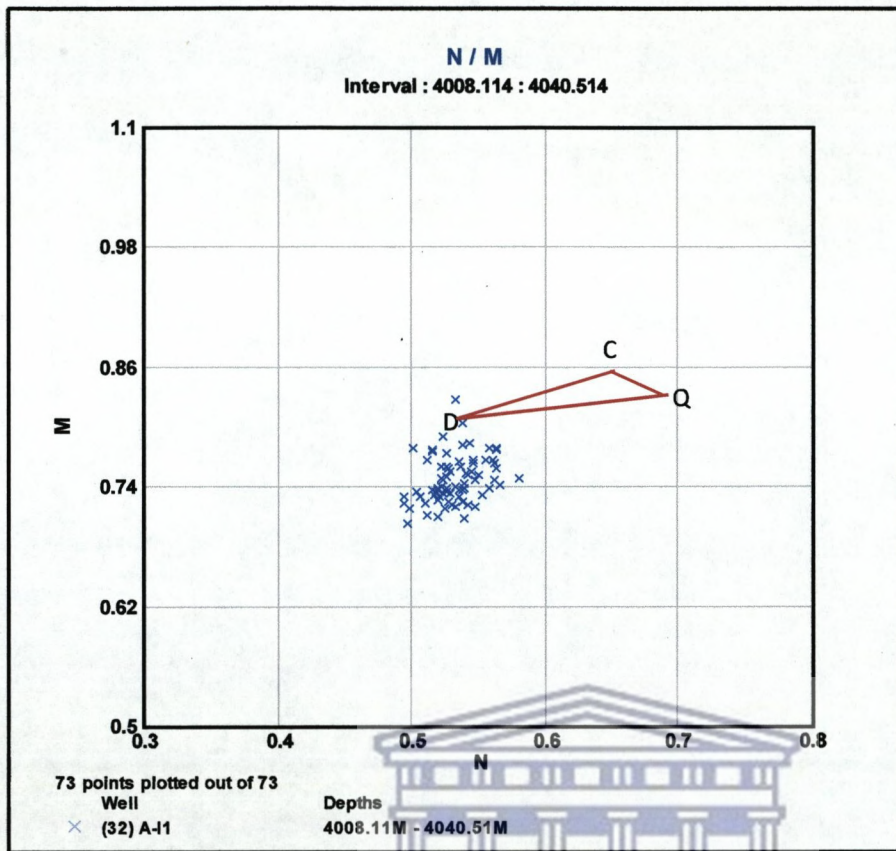


Figure 5.5.3: M/N plots for Unit 3 (C) and Unit 4 (D) of Well A-11.

- The points for Unit 3 plotted in the lower half of the M/N plot. They clustered in the region predefined as the shale region.
- The points of Unit 4, as with Unit 3 plotted in the lower half of the plot. The points are scattered in the shale region on the point.



(E)

Figure 5.5.4: M/N plot for Unit 5 (C) of Well A-I1.

- Unit 5 as with Units 3 and 4, plotted in the lower half of the plot in the region predefined as the shale region.

5.5.1.3 Well A-L1

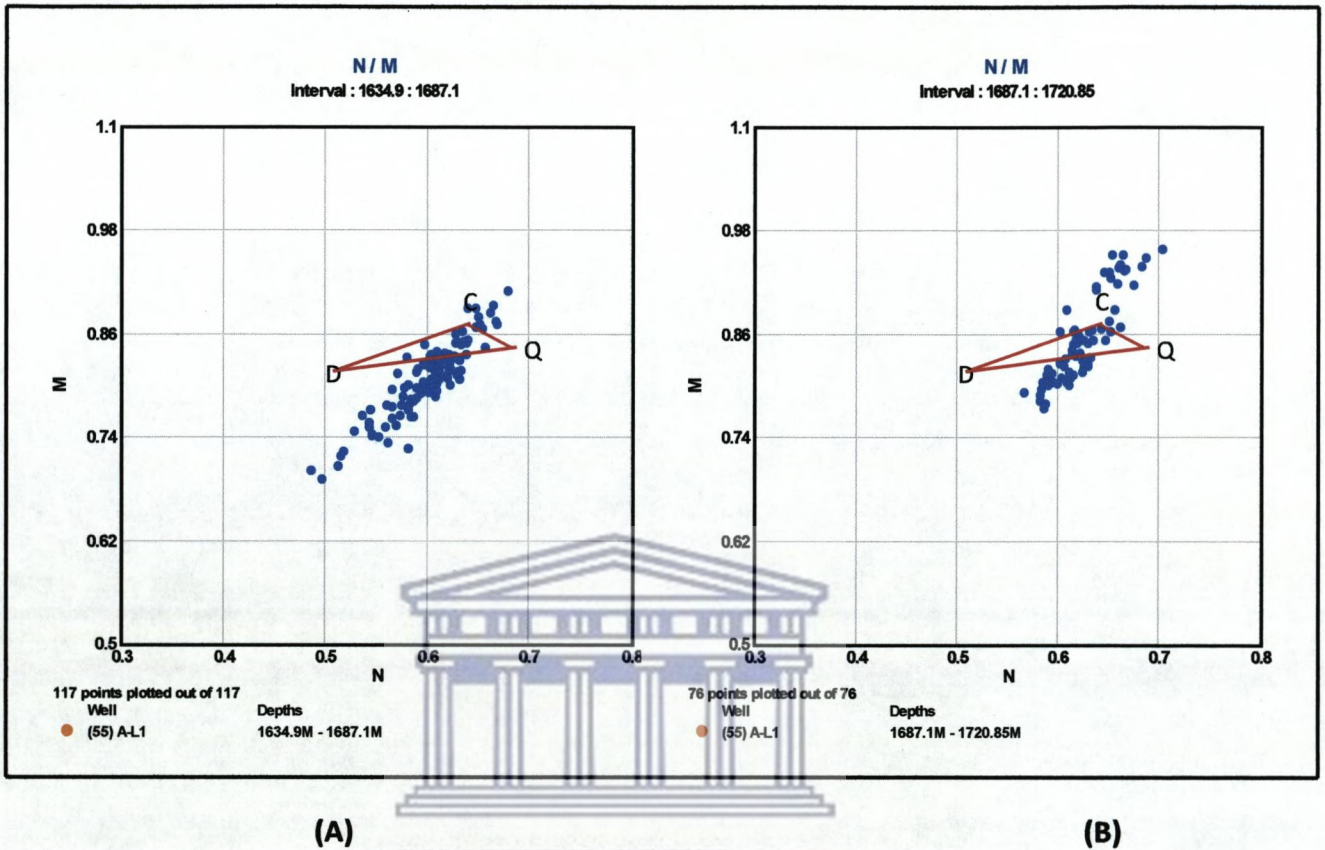
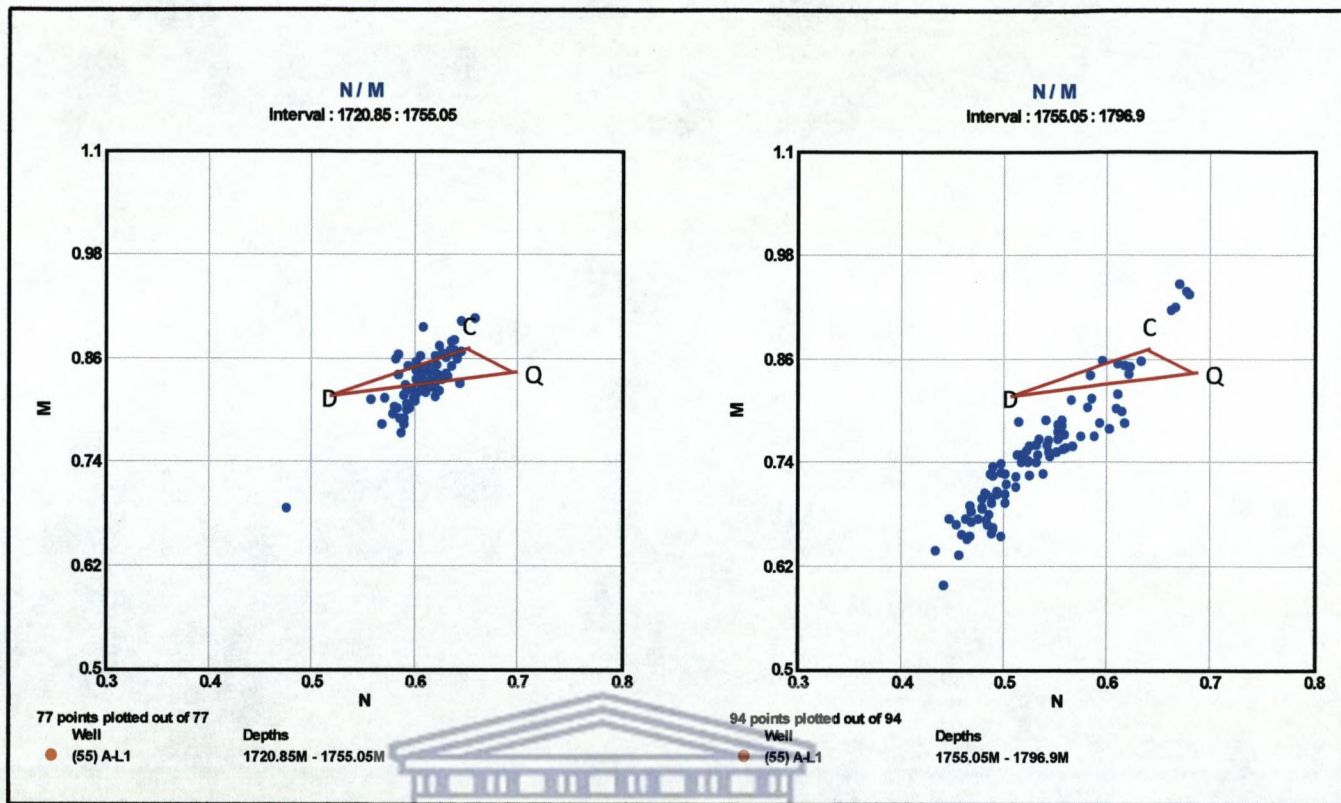


Figure 5.5.5: M/N plots for Unit 1 (A) and Unit 2 (B) of Well A-L1.

The M-N plots for Well A-L1 displays the following trends:

- The points for Unit1 clustered towards the calcite and quartz points. A downward shift of the points below the basic triangle formed by the quartz, calcite and dolomite pints are also observed.
- The M-N plot for Unit 2 displays a clustering of the points towards the quartz region. Minor cluster of points is also observed towards the calcite point. A small percentage of the points plotted above the basic triangle and a small percentage is situated just below the basic quart-calcite- dolomite triangle.



(C)

(D)

Figure 5.5.6: M/N plots for Unit 3 (C) and Unit 4 (D) of Well A-L1.

- The majority of points for Unit 3 clustered towards the predefined quartz region. A small percentage of points are found towards the calcite region as well as just below the basic triangle.
- The majority of the points for Unit 4 plotted below the quartz-calcite-dolomite triangle in the region predefined as the shale region. A small amount of points plotted inside the triangle while the remainder of the points plotted above the basic triangle in the region predefined as indicating the presence of salt or gas.

5.5.1.4 Well A-U1

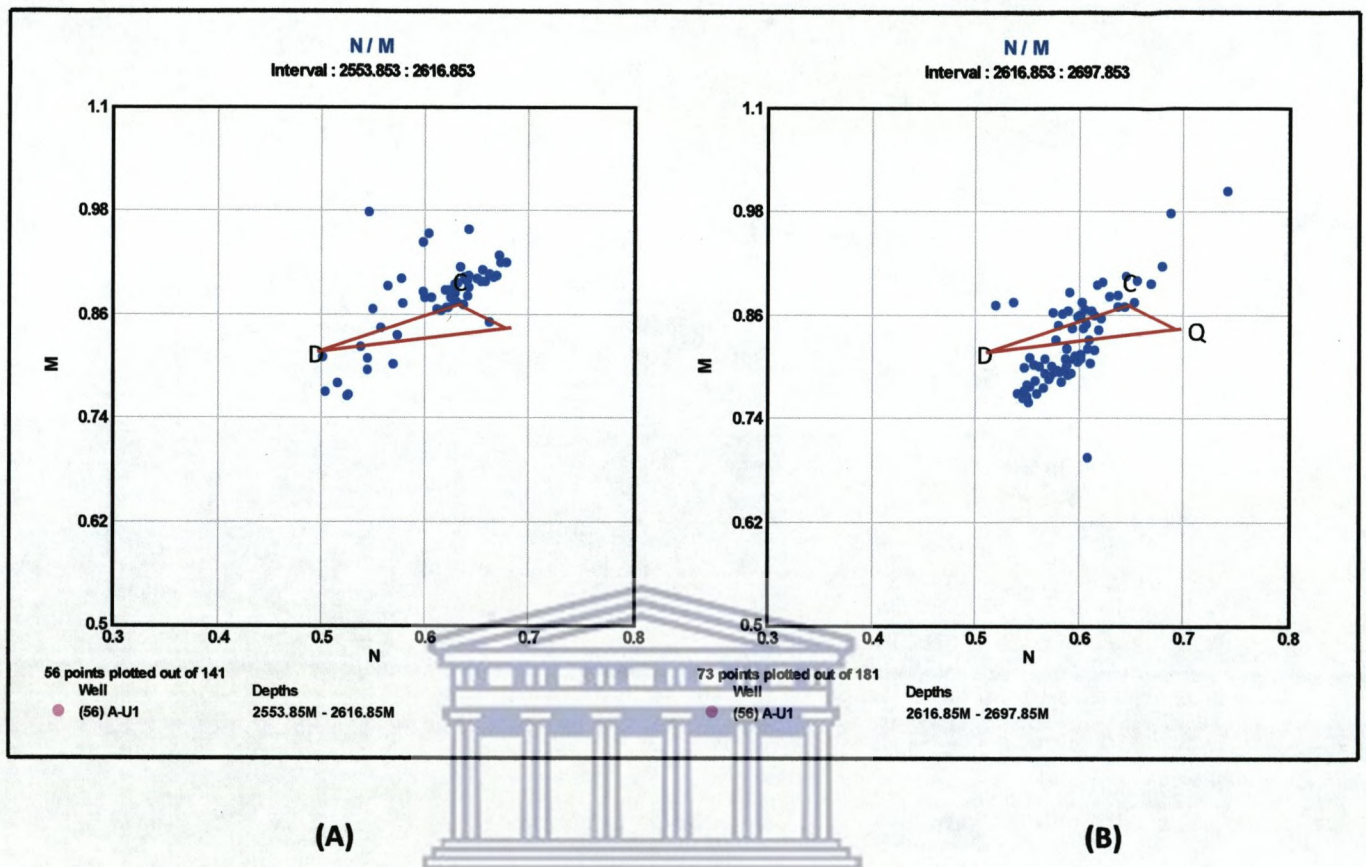
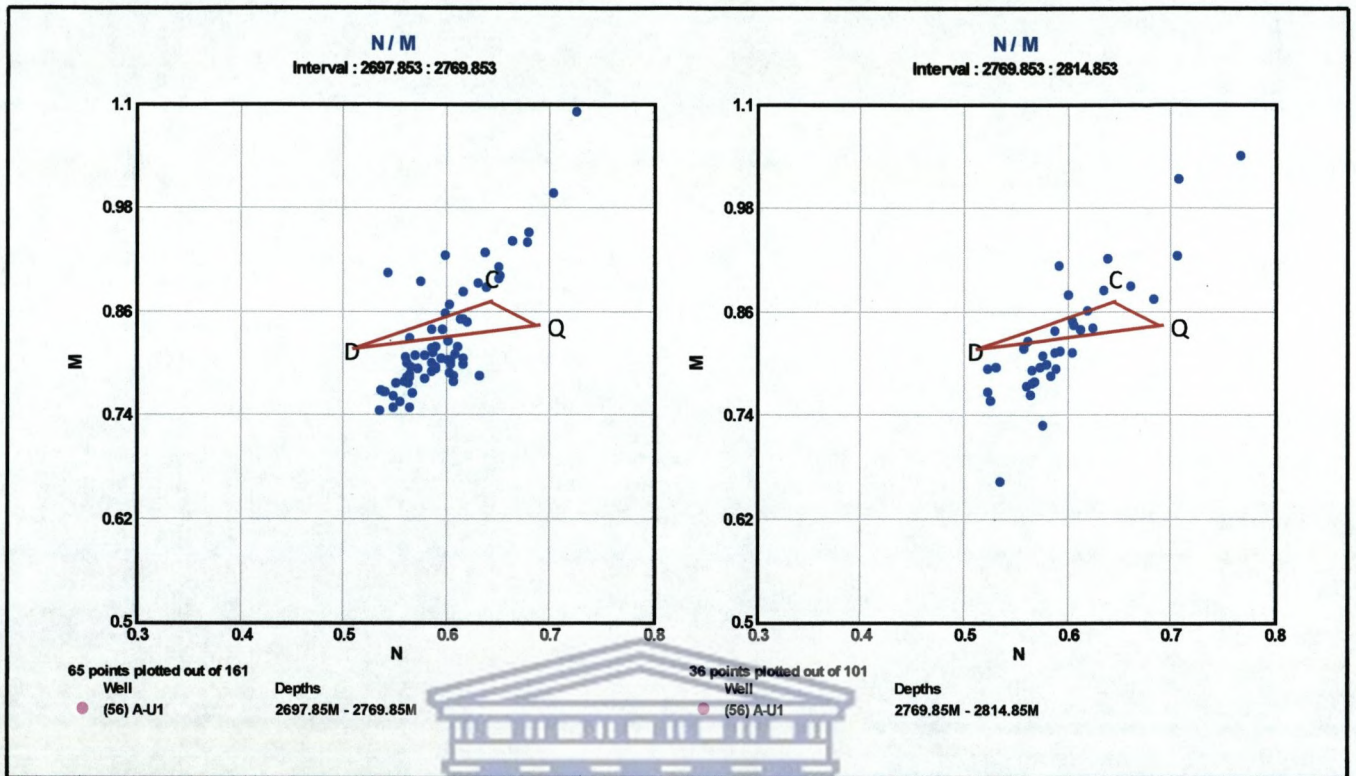


Figure 5.5.7: M/N plots for Unit 1 (A) and Unit 2 (B) of Well A-U1.

The M-N plots for Well A-U1 displays the following trends:

- Unit 1 of well A-U1 displays an upward shift of points, although these points still fall within the predefined shale region as well as cluster towards the calcite point.
- The bulk of the points for Unit 2 plotted either above or below the quart-calcite-dolomite basic triangle. The points below the basic triangle plotted in the region previously defined as the shale region while the points above the triangle still plotted in the predefined quartz region.



(C)

(D)

Figure 5.5.8: M/N plots for Unit 3 (C) and Unit 4 (D) of Well A-U1.

UNIVERSITY of the
WESTERN CAPE

- The majority of the points for Unit 3 show a downward shift. Then remainder of the points displays an upward shift and only a few points plotted in the quartz-calcite-dolomite triangle.
- The points for Unit 4 are widely scattered across the plot. A downward shift of points is observed in the lower half of the plot, while the remainder of the points displays an upward shift.

5.5.1.5 Correlated Units

5.5.1.1.1 Unit A

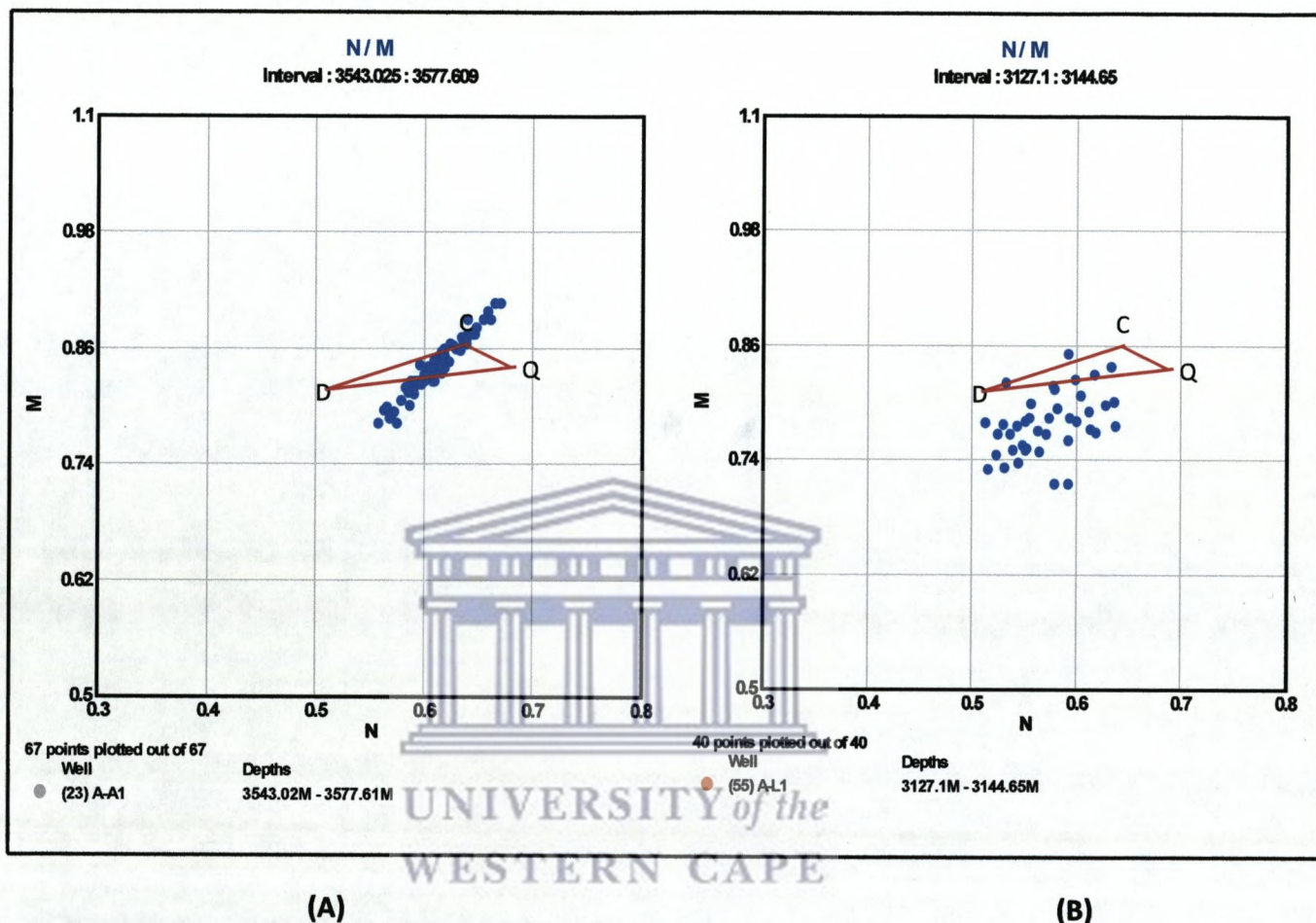


Figure 5.5.9: M/N plots for Well A-A1 (A) and Well A-L1 (B) of Unit A

Unit 1 displays the following trends:

- The points for Well A-A1 plotted both in the upper section as well as the lower region of the plot. The points in the upper region clustered towards the calcite region, while the points in the basic quartz-calcite-dolomite triangle plotted close to the predefined limestone region. The points in the lower half of the plot display a downward movement of points away from the basic triangle and plotted in the predefined shale region.
- For Well A-L1 the points in the basic quartz-calcite-dolomite triangle did not plot close to a definite point but is instead scattered throughout the triangle. However, a

general downward shift of the points is observed. The points for this well plotted in the shale and quartz regions.

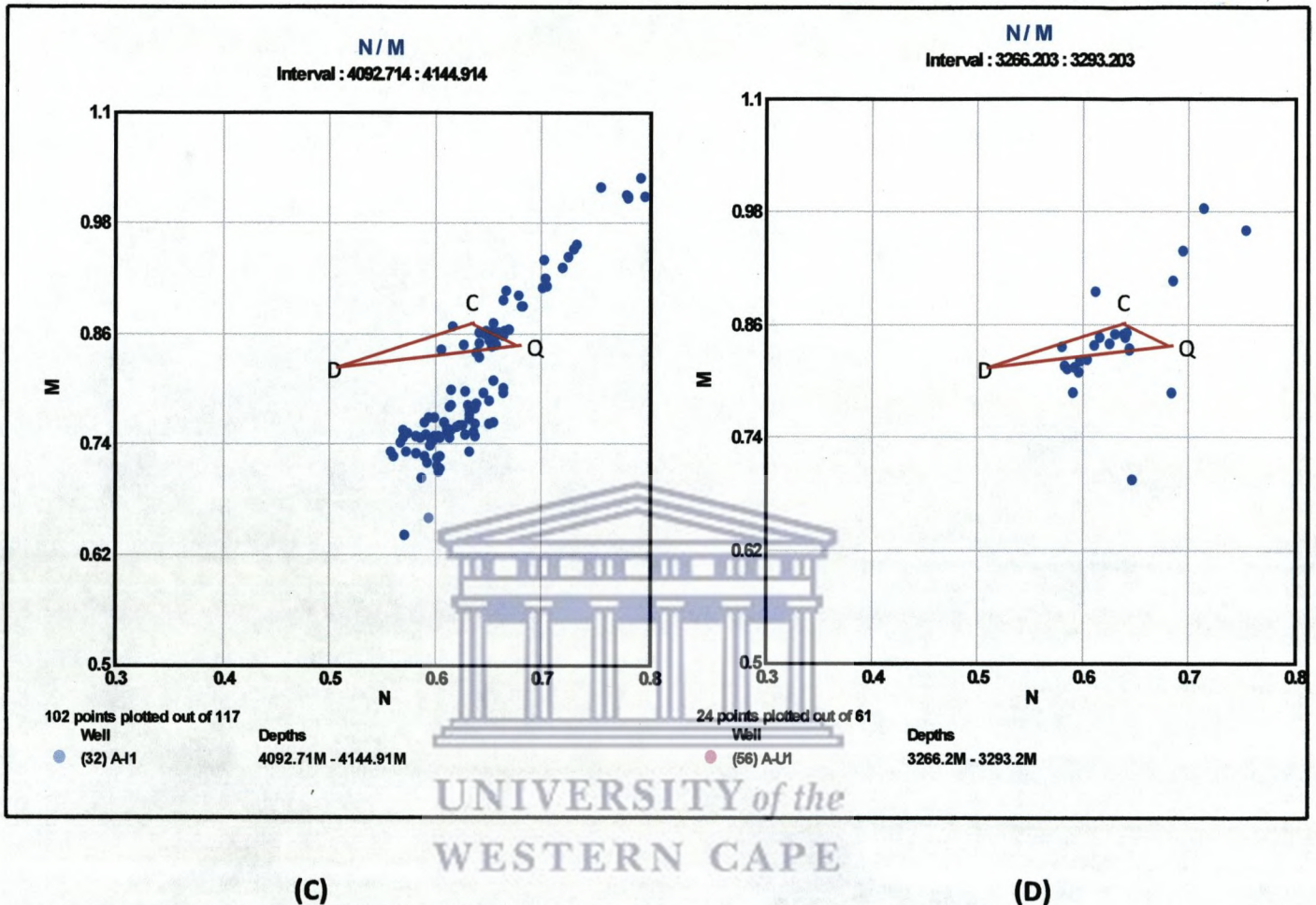


Figure 5.5.10: M/N plots for Well A-I1(C) and Well A-U1 (D) of Unit A.

- The points for Well A-I1 plotted across the upper and lower portions of the M-N plot. The points in the top half displays an upward movement of the points away from the basic triangle but still displays values associated with quartz. The points in the lower region plotted in the predefined shale region while the points in the basic triangle plotted close to the quartz point.
- Well A-U1 plotted across the M-N plot. The points in the basic triangle plotted close to the quartz points. A downward shift of points towards the shale region is observed. An upward shift of points is also observed but the values still fall in the quartz region.

5.5.1.5.2 Unit B

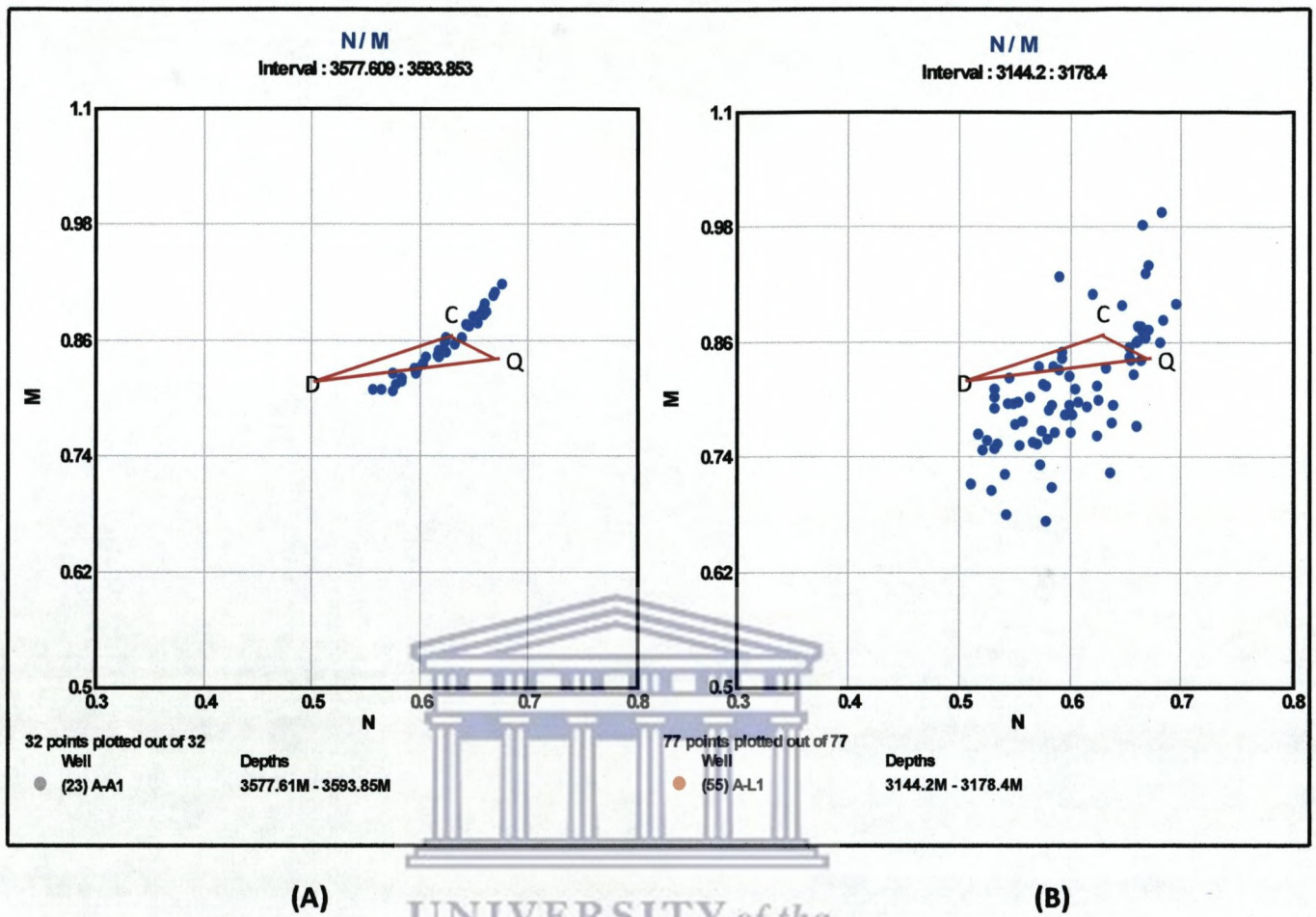


Figure 5.5.11: M/N plots for Well A-A1 (A) and Well A-L1 (B) of Unit B.

The M-N plots for Unit B displays the following patterns:

- The points of Well A-A1 displays an upward shift away from the quartz-calcite-dolomite triangle but still plotted in the quartz range. Th points in the triangle plotted in the calcite area.
- For Well A-L1 the points plotted across the plot. The points in the top half shows an upward movement of the samples away from the basic triangle but still plotted in the predefined quartz region. Points in the triangle plotted close to the calcite (limestone) values while the points in the bottom half of the plot clustered in the shale region.

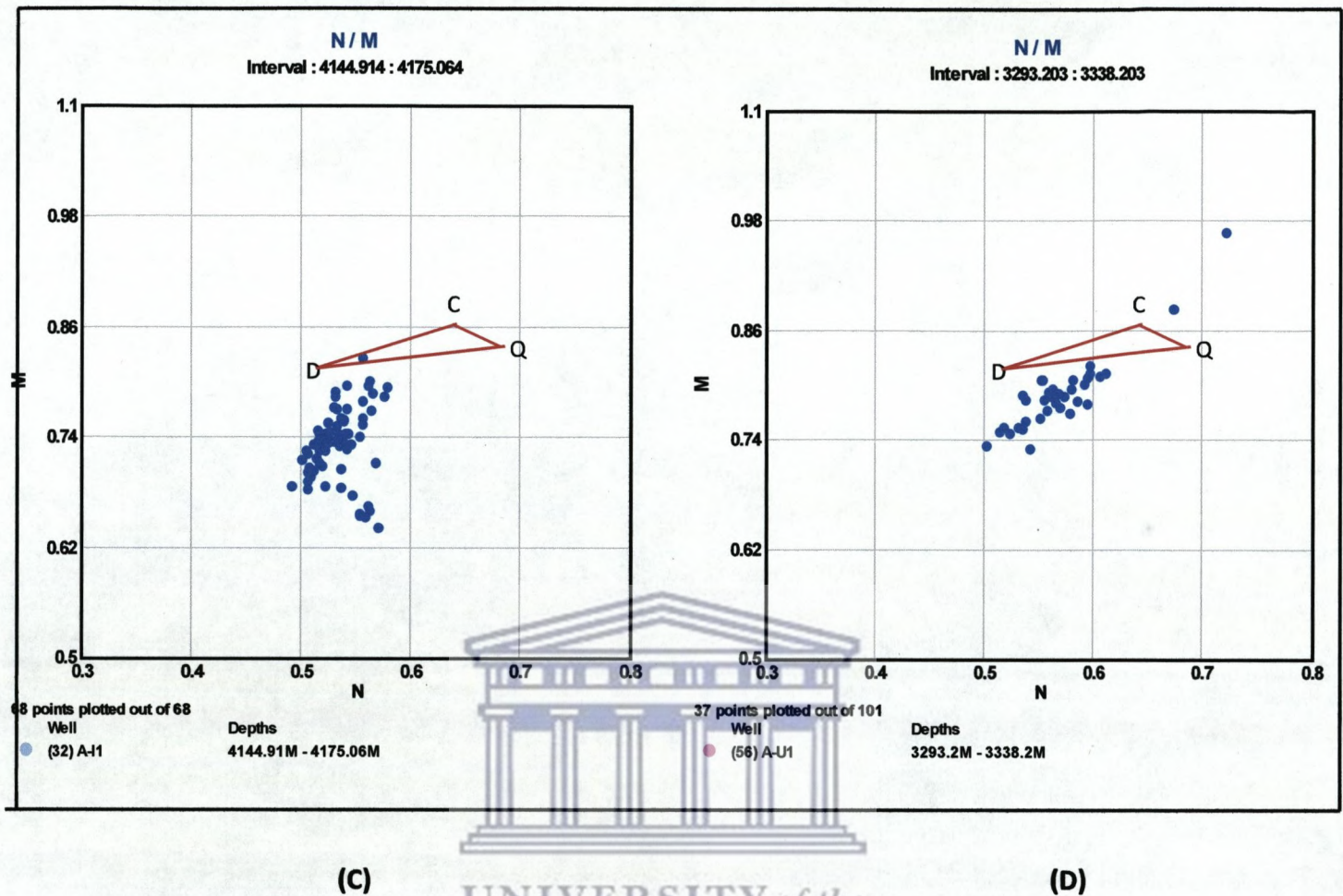


Figure 5.5.12: M/N plots for Well A-I1 (C) and Well A-U1 (D) of Unit B.

- Well A-I1 plotted in the lower half of the M-N plot. A general downward shift of the points away from the quartz-calcite-dolomite triangle. The points thus plotted in the predefined shale region. Anomalous point is observed towards the calcite point.
- A downward shift of the points away from the quartz-calcite-dolomite triangle is observed for Well A-U1. The points thus plotted in the shale region.

5.5.1.5.3 Unit C

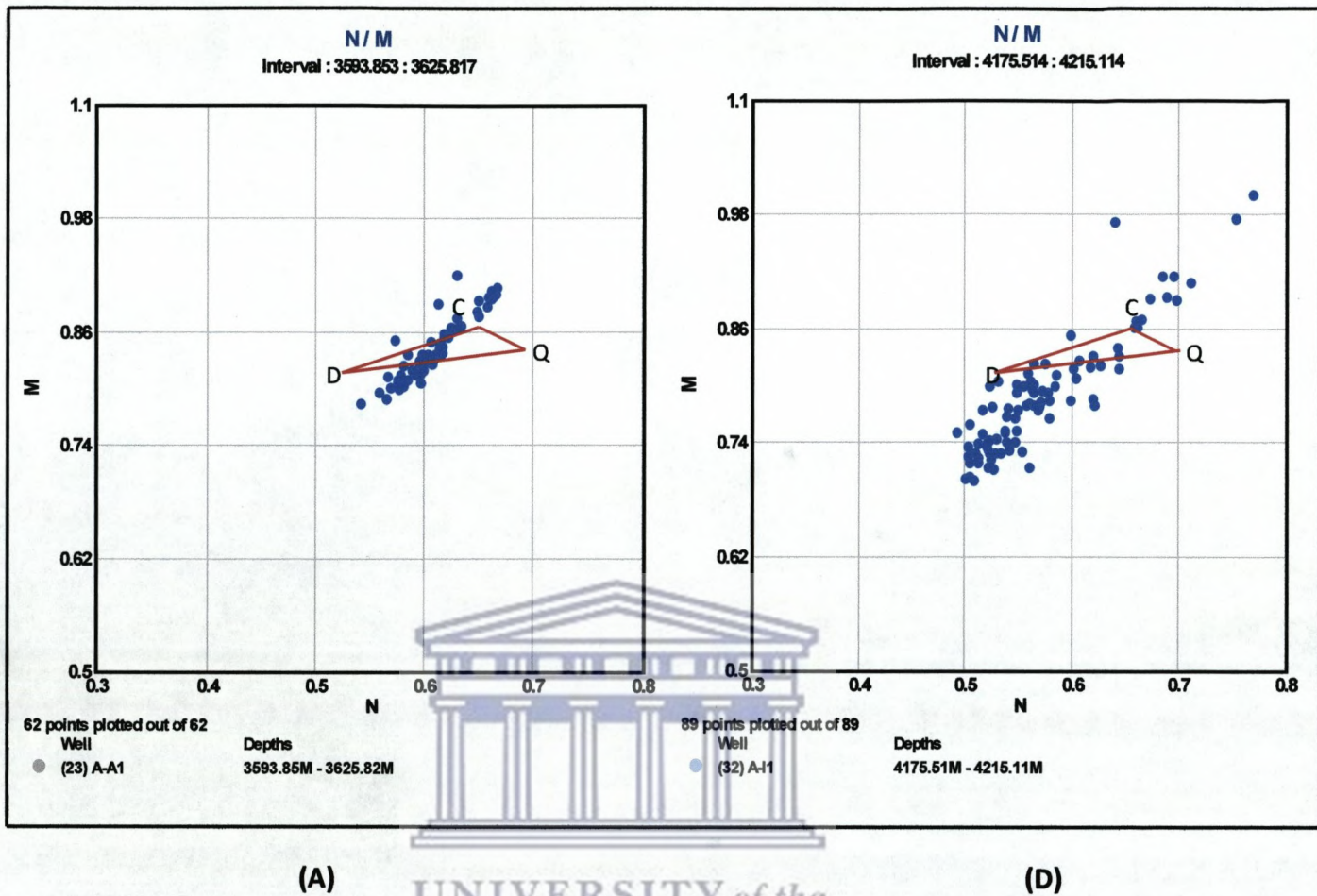
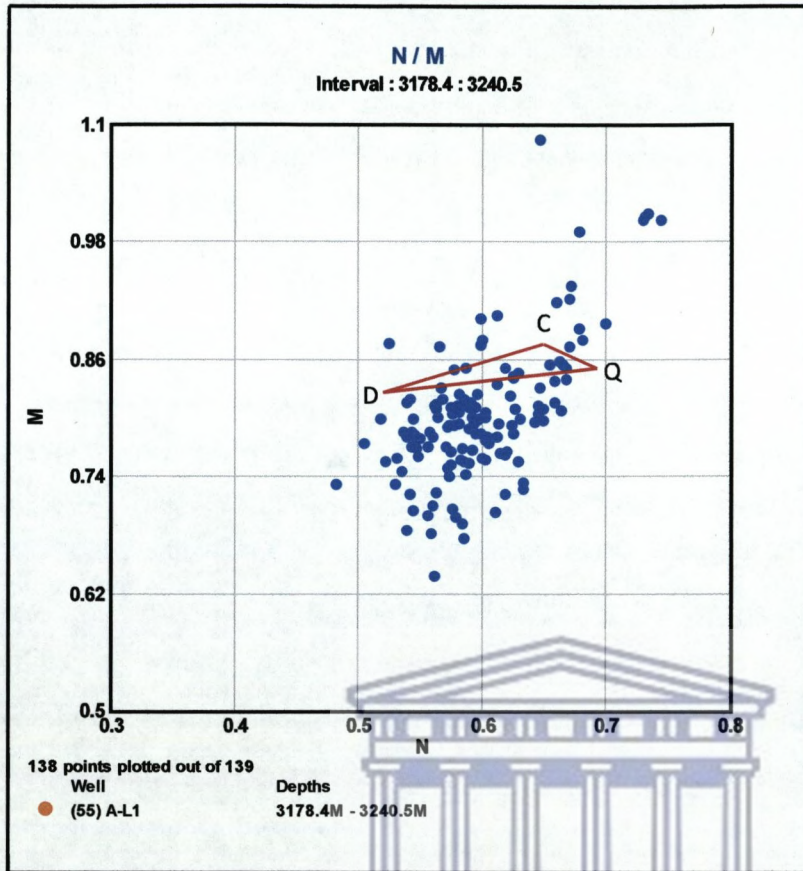


Figure 5.5.13: M/N plots for Well A-A1 (A) and Well A-I1 (B) of Unit C.

The M-N plots for Unit C displays the following trends:

- The points within the triangle for Well A-A1 plotted towards the calcite points. The points above the outer edges of the triangle plotted in a region defined as indicating quartz while the points on the lower outer edge of the triangle plotted in the shale region.
- The points for Well A-I1 are scattered across the M-N plot. Points displays an upward movement away from the basic triangle but still plotted in the region defined as indicating quartz. Points in the lower region plotted in the shale region.

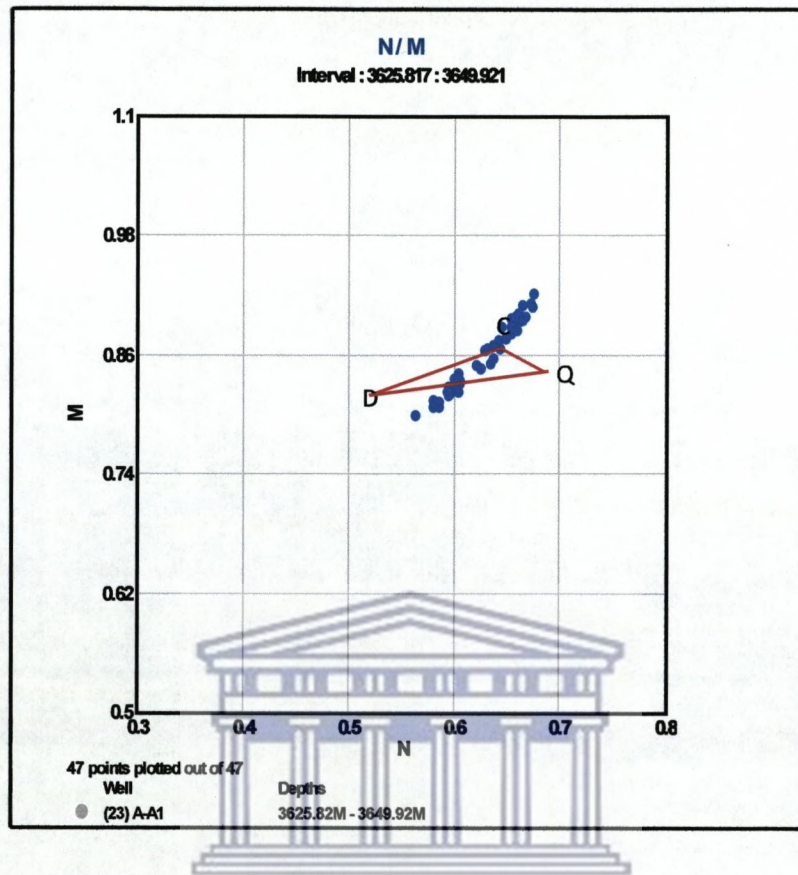


(C)

Figure 5.5.14: M/N plots for Well A-L1 of Unit C.

- Well A-L1 displays points that are scattered across the M-N plot. The points in the upper region shifted upwards from the basic triangle but still plotted in the quartz region. Points that are located in the lower half of the plot clustered in the area defines as the shale region.

5.5.1.5.4 Unit D



(A)

Figure 5.5.15: M/N plots for Well A-A1 (A) of Unit D.

- Well A-A1 displays an upward shift of points on the M-N plot but the points still fall in the region denoted as being indicative of quartz.
- The points for Well A-I1 are scattered across the M-N plot. Points on the upper right hand side plotted in the region predefined as indicative of quartz. Points on the lower half of the plot displays a downward shift away from the basic quartz-calcite-dolomite triangle and plotted in the region predefined as indicative of quartz.

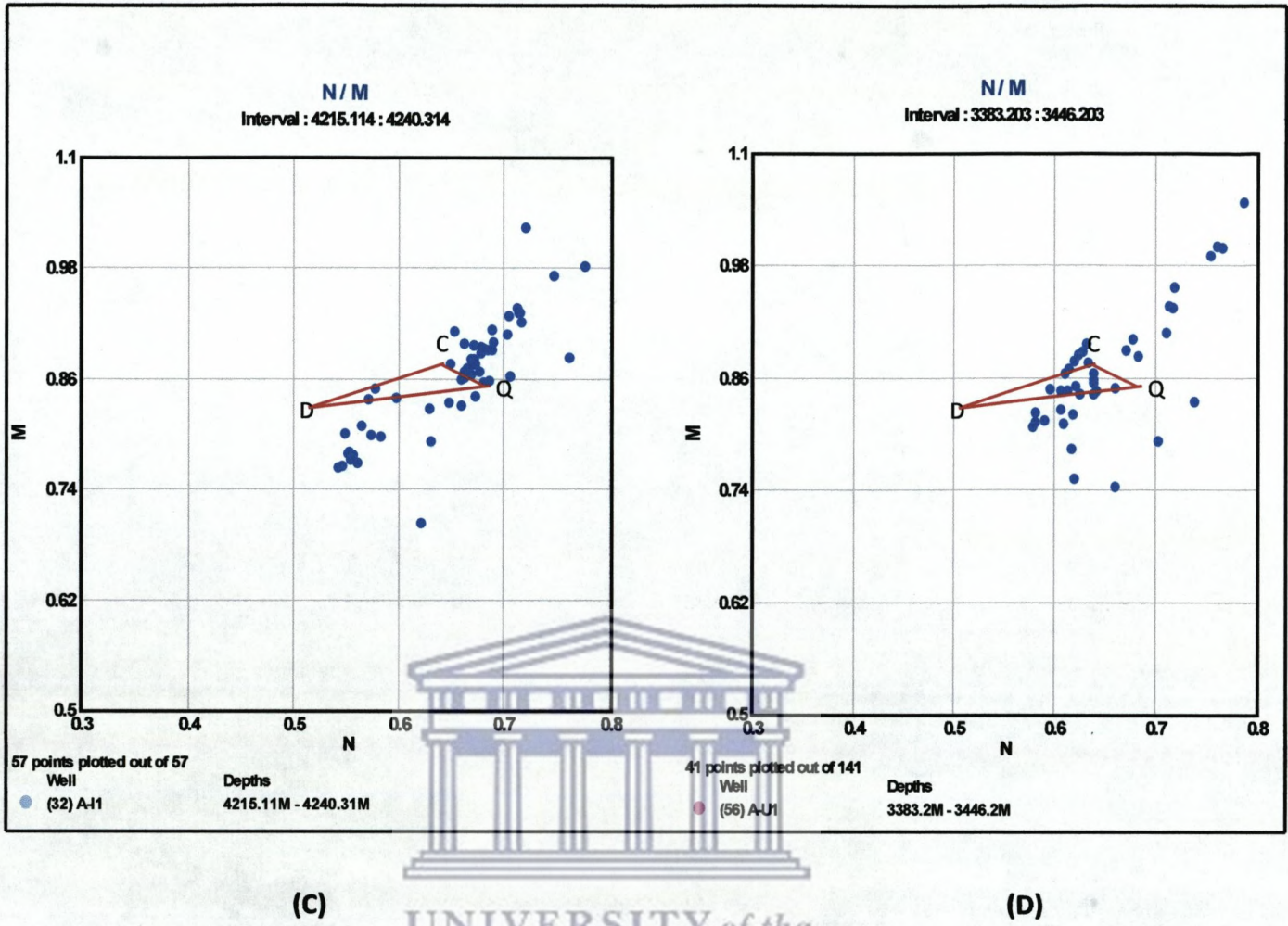


Figure 5.5.16: M/N plots for Well A-I1 (C) and Well A-U1 (D) of Unit D.

- The plot for Well A-U1 shows that the points are scattered across the plot. The points on the upper region of the plot, plotted in the region that is predefined as the being indicative of quartz. The points in the quartz-calcite-dolomite triangle plotted towards the quartz points. The remainder of the points for this well are scattered in the lower half of the plot.

5.5.2 DISCUSSION

5.5.2.1 Well A-A1

The upward movement of the points for Unit 1 could have been due to the formation of secondary porosity. The positioning of the points towards the calcite (limestone) region could have been as a result of the presence of calcareous clays and thus confirmed the neutron – Density cross plot and the geochemistry of the unit which mirrored the above. More support for the above mentioned statement is the downwards shift of the samples away from the quartz- calcite – dolomite triangle. This pattern is normally associated with the presence of shale.

Unit 2 shows a tendency towards the calcite values and hence could have been seen as an indicator for the presence of calcareous clays, as shown by the downwards shift of the points towards the shale region. The points are, however, also found close to the quartz region and this is thus as indication of the siliceous nature of the unit.

5.5.2.2 Well A-I1

Unit 1 plotted in the lower region of the plot, in the area defined as the shale region. This plotting of points in the shale region emulated the geochemistry of the unit which indicates that the unit consisted of an argillaceous component.

The points for Unit 2 are scattered across the M-N Plot. The points located in the upper region of the plot are indicative of the siliceous nature of the plot as this area is defined as representing the presence of quartz. The points in the lower half of the plot are indicative of the argillaceous nature of the unit. The relative positions of the samples on the plot reflected the geochemistry of the unit which indicates that the unit is composed of alternating layers of sandstone and a more argillaceous component, presumably greywacke.

Unit 3 of Well A-I1 plotted in the lower half of the M-N plot in the predefined shale region. This indicates that the unit either had an argillaceous or shale rich component. The geochemistry of the unit displays the same trend.

5.5.2.3 Well A-L1

Unit 1 clustered towards the calcite and quartz points. The points located in the quartz region represented the siliceous nature of the samples while the calcite component could have been indicative of the presence of shale, presumably calcareous shale as they possess a very similar composition to limestone. The downward shift of points away from the basic triangle confirmed the presence of shale in this unit. The M – N plot corroborated the patterns exhibited by the well logs for this area which indicates that this unit is composed mostly of shaly or argillaceous components interbedded with sandstones. The plotting of the points on the M – N plot is in line with the geochemistry of the unit that suggested the presence of sandstone and greywacke components.

Unit 2 mainly clusters towards the shale region while a minor cluster is observed towards the calcite region. Although the points clustered towards the calcite region, indicating the possible presence of a shale component, the unit is distinguishably less shaly than the preceding unit. The well log patterns for Unit 2 indicate relatively low GR values, while the neutron and density log indicates the presence of alternating layers of shale or an argillaceous component and sandstone. The geochemistry of the unit indicates that the unit is composed of greywacke sandstones with interbedded cleaner sandstones, thus the plotting of the points on the M – N plot emulated this assumption.

Unit 3, as with Unit 2, clustered predominantly towards the quartz region and therefore indicates that the unit had a highly siliceous component. A minute amount of points clustered towards the calcite region and indicates the possible presence of a very small shale component. Further evidence of the presence of a shale component in this unit is the downshift of the points away from the triangle. A shift such as this is predominantly associated with the presence of shale or an argillaceous component. The well logs suggested that this unit is predominantly shaly. The geochemistry of the unit, much as the M – N plots, indicates the presence of a cleaner sandstone unit and an argillaceous or arkose component (on the M – N plot this is indicated by the plotting of the points towards the calcite region).

The majority of points for Unit 4 plotted in the shale region and thereby indicate the presence of shale or an argillaceous component. The points that fall within the triangle indicate the siliceous nature of the unit. Some of the points plotted in the upper half of the plot and this effect is normally brought on by either the presence of gas or salt. In this

instance it is most likely that this effect is brought on by the drilling fluid which is composed of salt water. The geochemistry for this unit displays two patterns: the one trend indicates that the unit is composed of a mostly argillaceous component while the other suggested an increase in the siliceous nature of the unit. The M – N plot however, suggested that the former statement is more accurate.

5.5.2.4 Well A-U1

The plotting of the points on the M – N plot for Unit 1 indicates the presence of a shale or argillaceous component. A clustering of points is also observed towards the quartz region and thus indicates the siliceous nature of the unit. The location of the points on the M – N plots is in, line with the geochemistry of the unit which suggested the presence of feldspathic sandstone and argillaceous sandstone within the unit.

The points for Unit 2 indicate the dominance of quartz and a shale component within the unit. The geochemistry of the unit is suggestive of the presence of feldspathic sandstone and cleaner sandstone. This is reflected by the clustering of the points on the M - N plot.

The majority of the points for Unit 3 plotted in the lower region of the M – N plot and indicates the presence of shale or an argillaceous component. A minor cluster of points are observed in the triangle thus also indicating the siliceous nature of the samples. A few of the points shows an upward shift and this is presumably brought on by the development of secondary porosity in the unit. The clustering of the points on the M – N plot is in line with the geochemistry of the unit which is suggestive of the presence of a highly feldspathic sandstone.

Unit 4 is widely scattered across the M – N plot. However, the relative positions of the samples are indicative of two dominant components within the unit: the first component is quartz and the second component a shale or argillaceous rock type. The M – N plots reflected the geochemistry of the unit which suggested the presence of feldspathic sandstone that became increasingly arkose. The geochemistry of the unit is more specific as to the nature of the argillaceous component while the M – N plot purely suggested the presence of an argillaceous component.

5.5.2.5 Correlated Units

5.5.2.5.1 Unit A

Well A-A1 plotted in both the upper and the lower section of the plot. The relative positions of the points on the M – N plot is indicative of the presence of presumably shales and quartz.

The WellA-L1 plotted in such a manner that a general cluster could not be defined. However the points plotted in the region of quartz and that indicates the siliceous nature of the unit. The points also display a downward shift and this is indicative of the presence of shale.

Well A-I1 indicated, as with the previous wells, the presence of shale or an argillaceous component and the presence of quartz. However in this well an upward shift of the points is observed and this could possibly have been brought on by the development of secondary porosity.

Well A-U1 also indicates the presence of shale or an argillaceous component and the presence of quartz thus indicating the siliceous nature of the unit. Well A-U1, as with Well A-I1, displays an upward movement of the points, which could have been associated with the development of secondary porosity.

The M – N plots for this unit indicates the presence of a siliceous component and the presence of shale or an argillaceous component within the unit. This emulated the geochemistry of the unit which is suggestive of the presence of cleaner sandstone with sandstone of a more argillaceous nature.

5.5.2.5.2 Unit B

Well A-A1 displays two trends on the plot. The first is the plotting of the point in the quartz region thus indicating the siliceous nature of the unit. The second trend saw the points plot in the triangle towards the calcite region which presumably indicates the presence of calcareous clays or shales.

Well A-L1 is scattered across the M – N plot but still displays the presence of three dominant components: quartz (indicates by the plotting of the points towards the upper region of the plot), calcareous shale or calcite rich minerals (indicates by the plotting of the points towards

the calcite values) and a shale or argillaceous component (indicated by the points located in the lower half of the plot).

Wells A-I1 and A-U1 predominantly plotted in the lower half of the plot. The downward movement of the points, as mentioned previously, is associated with the presence of shale or an argillaceous component.

The M – N plots for this unit indicates the presence of a siliceous and a shale or argillaceous component. This is in line with the geochemistry of the rock unit that suggested the presence of feldspathic sandstones and either clay rich sandstones or shales.

5.5.2.5.3 Unit C

The relative positions of the points for the Well A-A1 on the M – N plot is indicative of the presence of shale or an argillaceous component and the siliceous nature of the unit.

Well A-I1, as with Well A-A1, indicates the presence of shale or argillaceous component and the siliceous nature of the unit.

Well A-L1, as with the preceding wells, plotted in a manner that is suggestive of the siliceous nature of the samples and the presence of shale or an argillaceous component.

The M – N plots for this unit is suggestive of the presence of two dominant components within this unit. The plotting of the points on the M – N plot mirrored the geochemistry of the unit which suggested the presence of a feldspathic component and a clay component in the unit. The geochemistry however, is capable of classifying the argillaceous unit into a feldspathic component and an argillaceous component.

5.5.2.5.4 Unit D

The relative positions of the points for Well A-A1 of Unit D are indicative of the siliceous nature of the samples by plotting in the quartz region. Well A-I1 indicates the siliceous nature of the samples as well as the presence of a more argillaceous component; this is indicated by the downward shift of the points away from the quartz-calcite-dolomite triangle, an effect that is brought on by the presence of shales or clays. The Well A-U1 displays the same trends as Well A-I1 and thus is indicative of the presence of a quartz rich or siliceous

rock unit as well as the presence of a slightly more argillaceous component. Some of the points for the four wells plotted close in proximity to the calcite region as well.

The patterns exhibited by the M-N plots are similar to the Neutron density plots which indicate the presence of sandstone and possibly calcareous clays in the unit. These patterns emulated the geochemistry of the unit which is suggestive of the presence of sandstones alternating with more feldspathic sandstones and shales. The geochemistry of the unit is also suggested an increase in the carbonate mineral content towards the base of the unit. This confirms the plotting of the points on the Neutron – Density cross plot towards the limestone region and the M-N plots towards the calcite region. The carbonate minerals presence could thus be indicative of the presence of calcareous clays within this unit.



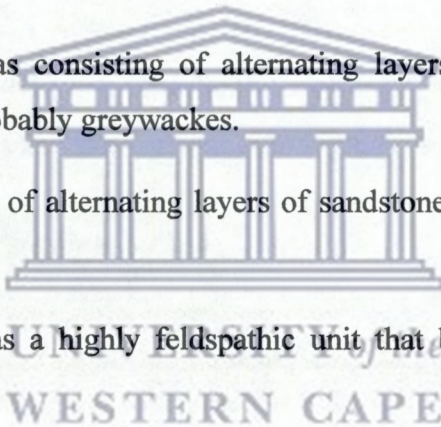
UNIVERSITY *of the*
WESTERN CAPE

5.6 SUMMARY

The Petrophysical analysis of Wells a-A1, A-I, A-L1 and A-U1 led to the identification of 33 Units. Four units were found to correlate across the four wells.

- Units 1 to 3 of Well A-A1 is defined as follows:
 - Unit 1 is defined as consisting of calcareous shales or clays and sandstones.
 - Unit 2 is defined as consisting of sandstones and shales or greywackes
- Units 1 to 4 of Well A-L1 is defined as follows:
 - Unit 1 is defined as possibly arkose sandstone at the base and greywacke at the top.
 - Unit 2 is defined as being composed of shales or argillaceous components with interbedded sandstones.
 - Unit 3 is defined as consisting of arkose or argillaceous sandstone at the top and cleaner sandstone at the base.
 - The petrophysical results of Unit 4 are suggestive of the presence of sandstone that became increasingly argillaceous towards the base.
- Units 1 to 4 of Well A-U1 is defined as follows:
 - Unit 1 is defined as being composed of sandstones at the top and an argillaceous or arkose component towards the base.
 - Unit 2 consists of argillaceous layers with interbedded cleaner sandstones.
 - Unit 3 is composed of sandier units and either argillaceous or arkose components.
 - Unit 4 is classified as feldspathic sandstone that became increasingly argillaceous towards the base.
- Geochemical Units 1 to 5 of Well A-I1 is defined as follows:
 - Unit 1 is defined as being highly argillaceous, most probably being composed of greywacke.

- Unit 2 is defined as consisting of alternating layers of argillaceous layers, most probably clay rich sandstones and cleaner sandstone layers.
 - The petrophysical results of Unit 3 suggest the presence of argillaceous sandstones and shales.
 - Unit 4 consists of greywackes and shales.
 - Unit 5 is classified as consisting of alternating sandstone, argillaceous or arkose sandstone and shale components.
- Four units, Units A- D are found to correlate across the four wells. They are classified as follows:
 - Unit A is defined as consisting of alternating layers of sandstone with clay rich sandstones, most probably greywackes.
 - Unit B is composed of alternating layers of sandstones with clay rich sandstones or shales.
 - Unit C is defined as a highly feldspathic unit that became increasingly clay rich towards the base.
 - Unit D is classified as consisting of alternating layers of sandstone and calcareous shale layers.



CHAPTER 6 COMPARISON OF CHEMOSTRATIGRAPHIC AND PETROPHYSICAL RESULTS

6.1 General Overview and Comparison of the Chemostratigraphic and Petrophysical Characteristics of Wells A-A1, A-I1, A-L1 and A-U1

6.1.1 Results

6.1.1.1 Well A-A1

6.1.1.1.1 Chemostratigraphic Results

The Chemostratigraphic results can be summarised as follows (*refer to table 4.1.1*):

SiO₂ is the dominant constituent with concentrations above 50% and clusters with Zr on the PCA plot. TiO₂, SO₃, Fe₂O₃, K₂O and MgO CaO concentrations are in the range 1% - 5% and along with Al₂O₃, clusters on the PCA plot. Co displayed the lowest concentrations with a range of 4ppm – 27ppm. Much higher concentrations are exhibited by Ni, V, Nb and Y (40ppm – 160ppm). Zr, Sr and Rb contents ranged between 160ppm – 350ppm. The highest average concentrations for these samples were a function of the elements Zn and Ba.

The results of the Major and Trace element profiles can be summarized as follows:

SiO₂ and Na₂O display similar dispersion concentrations and have concentrations in the ranges 60% - 75% and 0.4% - 1.8% respectively. Al₂O₃, K₂O and Fe₂O₃ displays similar dispersal trends downhole with concentrations in the ranges 10% to 16%, 1% to 5% and 0.4% - 9% respectively. CaO, MgO and MnO displays similar dispersal trends and have concentrations that falls in the ranges 4% -7%, 2.1% - 2.9% and 0.08% - 0.12% respectively. Co concentrations showed great variation falling in the range 3.5ppm – 22.5ppm. Ni concentrations were in the range 10ppm to 140ppm. Zr displayed high values throughout the sampling interval with values that range between 225ppm and 300ppm. Zn, Pb, Ba and Sr displays similar downhole dispersion patterns, with concentrations that fall in the ranges 116ppm – 8900ppm, 90ppm -1280ppm, 423ppm – 3150ppm and 100ppm – 225ppm

respectively. Zn displays diametric correlations with the refractory elements Ni, Y, Nb and Rb.

6.1.1.12 Petrophysical Results

The GR log displays readings ranging between 80 API and 170API. The pattern exhibited by the SP log to a certain extent mimics the pattern displayed by the GR log. The pattern displayed by these logs are

The neutron and density logs were plotted on the same track. This was to enable the recognition of cross over patterns. A cross over between these plots with the neutron log on the left indicates the presence of shale, while a cross over with the density in front indicates the presence of sandstone.

The sonic log displays velocities that measures approximately 60US/F consistently



6.1.1.2 Well A-I1

6.1.1.2.1 Chemostratigraphic Results

The Chemostratigraphic results can be summarized as follows:

SiO₂ is the dominant constituent with concentrations ranging above 50% but in contrast to the previous well SiO₂ clusters alone on the PCA plot. Al₂O₃ and Fe₂O₃ concentrations are relatively high and display average concentrations of 13.2% and 6.8% respectively. These elements along with the elements TiO₂, K₂O, MnO, MgO and P₂O₅ trace elements Ce, Nb, V, Zr and Sr cluster together on the PCA plot.

The remainder of the elements is grouped into three clusters. The second cluster is composed of the elements Ni, Co, Zn, Pb and Ba. The third cluster is composed of the elements CaO and SO₃. LOI plots between the 1st cluster and the 3rd cluster.

The major and trace element profiles display trends that are indicative of the dominance of SiO₂ with concentrations in the range 55% to 90%. Al₂O₃, Fe₂O₃, MnO, MgO, K₂O and TiO₂ displays similar dispersal trends and has concentrations that ranges between..... respectively. This element cluster group however, displays an inverse relationship with SiO₂. CaO concentrations are in the range 1% to 9% and as with the previous elements, display a diametric relationship with SiO₂. Na₂O concentrations are relatively uniform throughout the

interval. The trace elements Co and Ni display similar dispersal patterns and have concentrations in the ranges 10ppm – 60ppm and 20ppm – 140ppm respectively. V, Zr and Sr display similar dispersal trends and has concentrations in the ranges 60ppm – 80ppm and 75ppm – 225ppm respectively. Ni, Co, V, Zr and Sr trends are characterized by marked changes below a depth of 4125m. Co and Ni trends display rapid increases while Zr, Sr and V trends are characterized by marked decreases.

6.1.1.2 Petrophysical Results

The GR log readings range between 30 API and 120 API. The top part of the interval displays no deflection of the SP curve while the lower half of the curve is characterised by positive and negative deflections of the SP curve. The pattern displayed by the Neutron and Density curves is suggestive of the presence of units of sandstone, shale and alternating layers of sandstone and shale. The sonic log displays values in the range 60Us/f to 100Us/f thereby indicating the presence of alternating units of porous and less porous units.

6.1.1.3 Well A-L1

6.1.1.3.1 Chemostratigraphic Results

SiO₂ is the dominant constituent of the samples for Well A-L1 with concentrations above 50%. The elements Al₂O₃ and Fe₂O₃ also display relatively high concentrations of 8.4% and 6.1% respectively. Zr is the dominant trace element, followed by Zn and Rb with concentrations averaging 155.3, 111.3 and 92.7ppm respectively.

The PCA plots for Well A-L1 highlights three element clusters. The first cluster is composed of the elements Fe₂O₃, K₂O, Ni and Zr and is indicative of the presence of clays. The second cluster consists of the elements MnO, SO₃, P₂O₅ and Na₂O₃ and this element association is commonly associated with the presence of clays and feldspars. The elements CaO and SiO₂ are indicative of the presence of carbonates and the siliceous nature of the samples respectively.

The major and trace elements profiles show the dominance of SiO₂ with concentrations ranging between 60% and 75%. Al₂O₃, Fe₂O₃, MnO and MgO display similar dispersal trends and have concentrations in the ranges 6% - 12%, 4%- 10%, 0.14% - 0.18% and 1%-

2% respectively. Na₂O and MgO display similar dispersal trends and have concentrations in the range 0.1% - 0.55% and 0.5% - 1.5% respectively. Co has concentrations in the range 1ppm – 30ppm and displays inverse relationships with Sr, Zn, Zr and Pb. Ni and V follows similar dispersion trends while Zr displays inverse relationships with Co, Fe₂O₃, MnO and MgO. Nb, Rb and Y display similar downhole trends.

6.1.1.3.2 Petrophysical Results

The interval was divided into two sections for the well log interpretation. The first interval is from a depth of 1635m to 1800m and the second interval is from 3100m to 3225m.

The GR readings for section 1 are in the range 40API to 160API. The readings decrease progressively towards the middle of this section after which it increases towards the base of this section. In contrast, the SP log shows no deflection and is indicative of the presence of a large shale unit. A decrease in the sonic log which correlates to a decrease in the GR log and resistivity logs is observed.

The GR readings for section 2 are much higher than for the top section. The cross over patterns between the Neutron and Density logs are indicative of the presence of shaly – sand, argillaceous sandstones and shales. Section 2 also has higher resistivity readings than section 1.

6.1.1.4 Well A-U1

6.1.1.4.1 Chemostratigraphic Results

The Chemostratigraphic results for Well A-U1 shows a dominance of the major elements SiO₂, Al₂O₃ and Fe₂O₃ with concentrations ranging from 60% to 80%, 10% - 18% and 7% respectively. The trace elements are dominated by Zr, Zn, Sr, V and Rb averaging 279.7ppm, 166ppm, 142ppm, 108ppm and 95ppm respectively.

CaO and MnO display similar downhole trends and have concentrations ranging from 3% to 13% and 0.01% to 0.04% respectively. Al₂O₃, K₂O and TiO₂ cluster together on the PCA plot and display similar downhole dispersion patterns. The trace elements Co, Ni and V display similar dispersion patterns. Ni and V are found in the same cluster on the PCA while

Co clusters with the major elements CaO, SO₃, MnO and P₂O₅. Co, Ni and V display an inverse relationship with Zr.

6.1.1.4.2 Petrophysical Results

The interval is divided into two sections. The first section does not correlate across the wells and will be discussed below.

The well log patterns for Well A-U1 display GR readings ranging between 40 API and 180API. The SP log, as with the previous well, follows a straight line curve and shows no deflections. The Neutron and Density logs reveal patterns which are associated with the presence of sandstones and shale or siltstones.



UNIVERSITY *of the*
WESTERN CAPE

6.1.2 Discussion

6.1.2.1 Well A-A1

SiO₂ is the dominant constituent for this well and is thus suggestive of the highly siliceous nature of the samples. Al₂O₃ concentrations are relatively high and could be an indicator of the presence of clay minerals. This is inline with the trend displayed by the GR log which recorded relatively high values and which usually is indicative of the presence of shales or clays.

The principal component analysis plots led to the identification of four element association clusters. The first cluster, SiO₂ and Zr is indicative of the siliceous nature of the samples. This corroborates the trends displayed by the GR and SP logs. The remainder of the elements clusters indicated groups that are associated with the presence of clays, feldspars and carbonate minerals. SiO₂ however, displays a diametric relationship with the clay mineral cluster and thus supports the trends displayed by the GR, SP and Neutron and Density logs which are indicative of the presence of alternating layers of sandstone, argillaceous sandstone and possibly shales or clays.

Overall, Well A-A1 is interpreted by both the well logs and Chemostratigraphic results as being composed of alternating layers of sandstone with sandstone of a more argillaceous nature or possibly shales.

6.1.2.2. Well A-I1

SiO₂ is the dominant constituent and is indicative of the siliceous nature of the samples. The high concentrations of Fe₂O₃ may be seen as in indicator for the presence of iron minerals. Al₂O₃ concentrations are relatively high and are associated with the presence of clay minerals. This trend is also displayed by the GR log which displays values up to 120 API.

Nb concentrations are high and suggest that the samples possibly have high concentrations of clays and Ferro magnesium silicates. The PCA plots led to the identification of three element clusters. These elements clusters indicates the presence of a clay mineral cluster, a carbonate cluster and the clustering of elements that are associated with the presence of either detrital ferromagnesium silicate minerals, detrital Fe-oxides or clay minerals. In this instance it was most likely that these elements were associated with the presence of clays.

The downhole element profiles and the log responses both suggest that the sandstone/ unit become cleaner towards the base of the interval. This is confirmed by a decrease in GR readings, increase in SiO₂ concentrations and an increase in the sonic log readings which is indicative of a more porous unit.

The Chemostratigraphic results and the well log response of Well A-I1 are both indicative of the presence of alternating units of shales and argillaceous sandstone and the presence of cleaner sandstone towards the base of the interval.

6.1.2.3 Well A-L1

The high SiO₂ concentrations are indicative of the siliceous nature of the unit. Al₂O₃ displays an inverse relationship with SiO₂ as seen on the PCA plot. This is indicative of the presence of alternating sandier units with clay rich or feldspathic units. The clustering of Fe₂O₃, MnO and MgO suggests the presence of argillaceous components in the unit, as these elements are associated with clay minerals. CaO concentrations indicate an increase in the amount of carbonate minerals at the top of section 1 and the bottom of section 2. Na₂O and MgO display similar trends and their association is commonly indicative of the presence of feldspars. However, on the PCA plot, Na₂O plots close to the clay mineral cluster as well as the carbonate cluster.

The GR log displays trends of decreasing progressively towards the middle of section 1. This corresponds to an increase in SiO₂ concentrations on the geochemical profiles. The base of section 1 is defined by higher GR readings that correspond to an increase in the concentrations of Al₂O₃, Fe₂O₃ and TiO₂. The Sp log along with the GR log, displays patterns indicative of the presence of shale, sandstone and possibly siltstone, which is in line with the trend displayed by the geochemistry of the sections.

The GR for section 2 display higher readings and indicates the presence of predominantly shale or an argillaceous unit, except for the distinct sand units which are recognized at depths of 3174m to 3176m and 3192.5m and 3200m respectively. The low Gamma readings are consistent with sharp increases for the ratio SiO₂/Al₂O₃.

The well log responses corroborate the geochemical results which indicate the presence of alternating sandier units and argillaceous units.

6.1.2.4 Well A-U1

The high concentrations of SiO_2 and Zr are indicative of the siliceous nature of the samples while Al_2O_3 , Zn, V and Rb concentrations are indicative of the feldspathic nature of the samples. The high Sr concentrations are indicative of the presence of most likely calcite. Four element clusters are recognized on the PCA plot. The first cluster is composed of elements that are predominantly associated with the presence of clays while the third cluster is composed of the refractory elements. The second cluster, however, is composed of elements associated with clays (P_2O_5 and Co) and elements associated with carbonates (CaO, MnO and SO_3). The fourth cluster is representative of the feldspathic nature of the samples and includes the elements Na_2O , SiO_2 and Nb.

Na_2O and SiO_2 display inverse downhole trends suggesting the presence of alternating layers of feldspathic sandstone with cleaner sandstone. Al_2O_3 , Co and Ni display inverse relationships with SiO_2 and Zr. These element patterns indicate the presence of sandstones, shales and feldspathic sandstones.

The GR log indicates the presence of highly radioactive units and sandier units in this section. The Neutron and Density cross overs, as with the geochemical profiles, are indicative of the presence of alternating units within the section. The SP log in contrast, displays no deflection and is thus indicative of the presence of shale in the entire section. However, the PEF log displays readings of 1.8 consistently and thus indicates the presence of sandstones, in line with the geochemical results.

6.2 Comparison of the Chemostratigraphic and Petrophysical Units of Wells A-A1, A-II, A-L1 and A-U1

6.2.1 Well A-A1 (Refer to Figure 6.1)

Unit 1

The results of the Chemostratigraphic analysis and the Petrophysical analysis were fairly consistent. The unit appears to become increasingly argillaceous towards the base. This trend was displayed both by the decrease in the ratio $\text{SiO}_2/\text{Al}_3\text{O}_3$ towards the base of the unit and increase in the GR logs towards the base of the unit.

The geochemistry of the unit indicated the presence of a feldspathic component in the unit and subsequently indicated that this component decreased towards the base of the unit. The well logs and subsequent plots could not adequately distinguish this trend.

The neutron density plot for Unit 1 indicated the presence of sandstone and either limestone or dolomite, but from the geochemistry it was known that the unit was not composed of either limestone or dolomite. It is thus inferred that the points plotting on the lower section of the plot between the limestone and dolomite lithology curves indicates the presence of calcareous shales. This corroborates the signatures obtained from the geochemistry which indicates an abundance of clay minerals while the CaO, MgO and MnO concentrations indicates the presence of carbonates.

The upward movement of the points observed for Unit 1 on the M-N plot could be due to the formation of secondary porosity. The positioning of the points towards the calcite (limestone) region could be as a result of the presence of calcareous clays and thus confirms the Neutron – Density cross plot and the geochemistry of the unit which mirrors the above. More support for the above mentioned statement was the downwards shift of the samples away from the quartz- calcite – dolomite triangle. This pattern is normally associated with the presence of shale.

Unit 2

The geochemistry and the Petrophysical properties for this unit were fairly consistent. Both methods indicated the presence of clays in the unit by displaying high GR readings and high Al_3O_3 concentrations. The geochemistry of the unit could be capable of narrowing down the

sources of the high Al_3O_3 and displayed trends that indicates the presence of an argillaceous or arkosic sandstone.

Unit 2 of Well A-A1 plotted across the three lithology curves on the Neutron – Density cross plot. The points that plotted towards the sandstone lithology line indicated the siliceous nature of the samples and corroborate the high SiO_2 concentration obtained by the whole rock analysis. The points between the limestone and dolomite lithology curves indicate the presence of shale or clay rich sandstone. This is in agreement with the results obtained from the geochemistry which indicates high concentrations of the elements associated with clays. The general overview of the well logs indicates that the well is composed of alternating layers of sandstone and shale or greywacke and this is reflected by the clustering of the points in the neutron density cross plot.

A tendency towards tendency towards the calcite values was observed for the M-N plot and this underlines the geochemistry which indicated an increase in Sr and as explained previously Sr is commonly associated with the presence of carbonate minerals. This could be seen as an indicator for the presence of calcareous clays, as shown by the downwards shift of the points towards the shale region. The points are, however, also found close to the quartz region and this was thus as indication of the siliceous nature of the unit thus confirming the high SiO_2 concentrations observed for this unit.

6.2.2 Well A-I1 (Refer to Figure 6.2)

Unit 1

The majority of the geochemical ratio's, with the exception of $\text{K}_2\text{O/Rb}$, Nd/V and Rb/Zn , displays no discernible trends and no information can be gathered from them.

High Al_2O_3 concentrations suggest that this unit has high concentrations of clay minerals. This trend is also displayed by the chemostratigraphic ratio Nd/V which is indicative of a decrease in the siliceous nature of the unit towards the base. The ratio Rb/Zn displays a trend which is suggestive of an increase in the concentration of clay minerals towards the base of the unit.

The well log responses are fairly consistent with the Chemostratigraphic results and indicate that the unit is composed of either shale or an argillaceous sandstone unit. The SP log shows

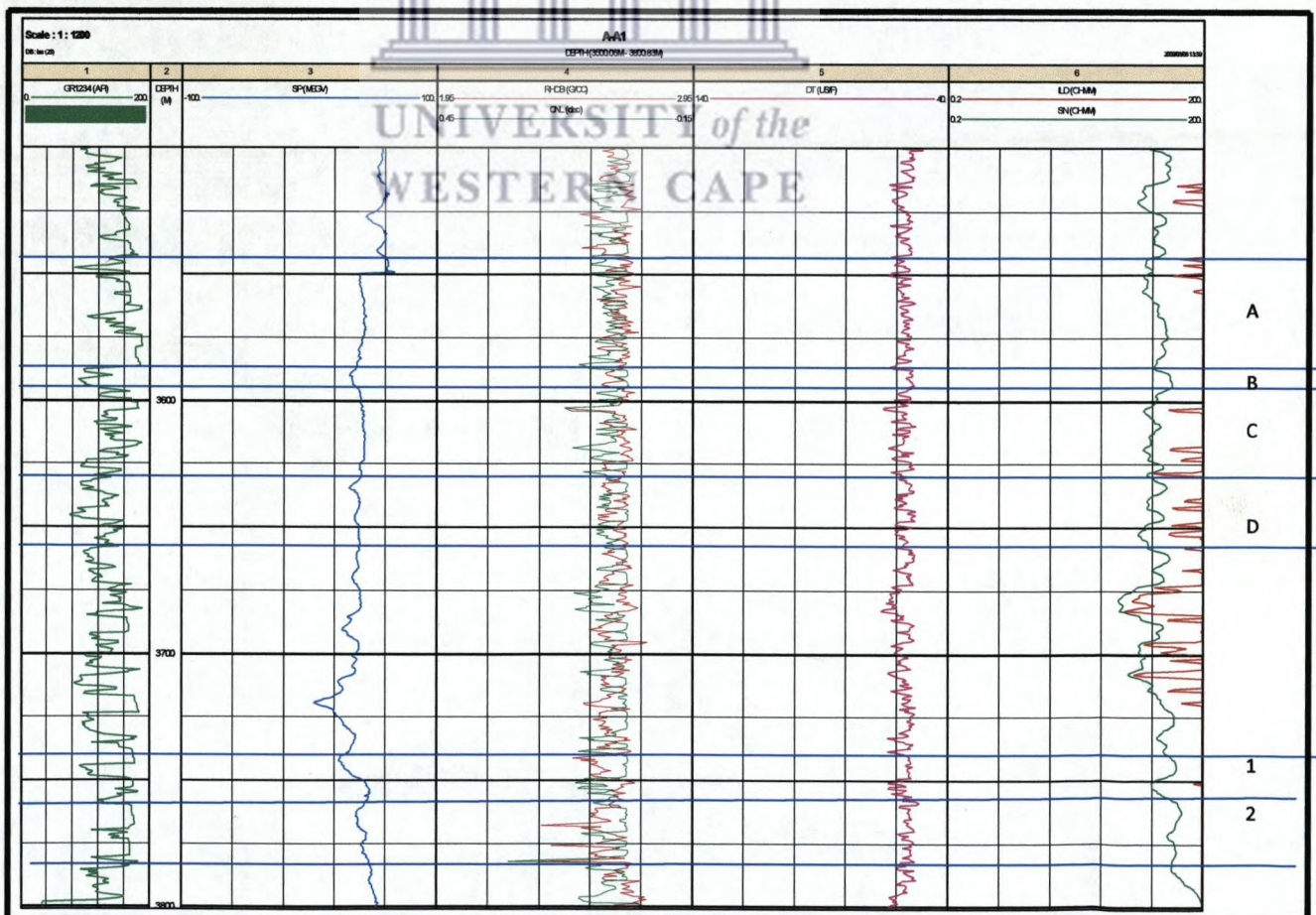
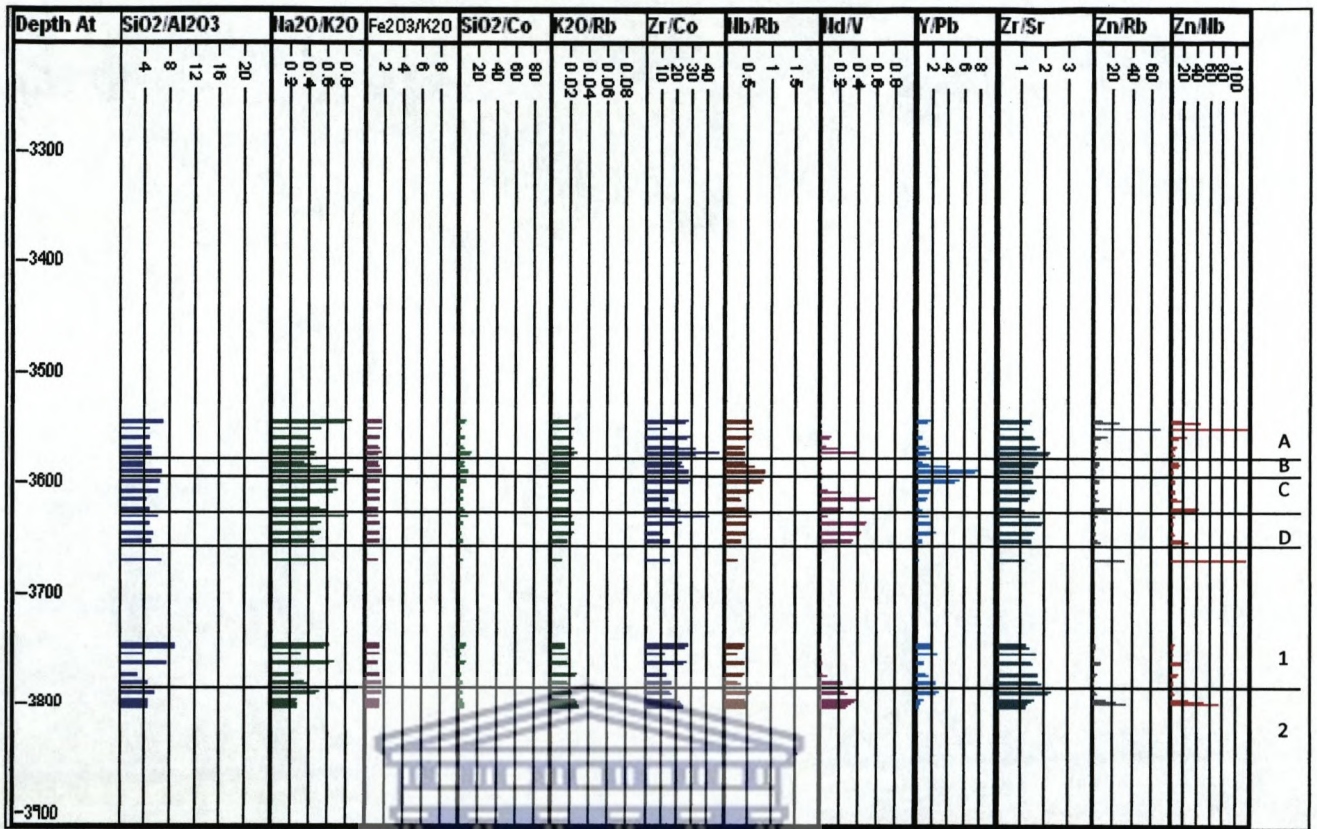


Figure 6.1 Comparison of the Chemostratigraphic Units (A) and Petrophysical Units (B) for Well A-A1

no deflection and reiterates the above assumption. The resistivity logs indicate that the unit is composed of either a conductive rock type or clays, in this case, most likely clays.

Unit 1 clusters towards the dolomite lithology curve on the Neutron-Density cross plot. The relative position of the points is indicative of the presence of shales or greywacke. This statement is substantiated by the geochemistry of the unit which displays a decrease in silica content (~50% SiO₂) and an increase in the concentration of the elements associated with clays. CaO and Sr measures relatively high and is indicative of the calcareous nature of the unit.

On the M-N plot Unit 1 plots in the lower region of the plot in the predefined shale region. The plotting of the points on the M-N plot emulates the geochemistry and well log responses of the log which indicates that the unit consists of argillaceous sandstone.

Unit 2

The chemostratigraphic ratio Nd/V suggests the presence of alternating layers or units of argillaceous sandstone and cleaner sandstone units. Nb/Ni increases towards the base of the unit and suggests that the unit becomes clay rich towards the base.

The well log responses for this unit displays relatively high GR readings of approximately 120 API. This along with the straight line curve displayed by the SP log and the pattern displayed by the Neutron and Density logs indicated the presence of a shale or argillaceous sandstone.

On the Neutron Density cross plot unit 2 plots across the three lithology curves and thus indicates the presence of sandstone and the calcareous shale. The geochemistry of this unit indicates the presence of alternating layers of siliceous units with argillaceous units and this trend as observed from the log response and indicated by the positions of the samples on the cross plot.

The points for Unit 2 were scattered across the M-N plot and is located in regions that suggest the presence of quartz and shale. The relative positions of the samples on the plot reflect the geochemistry of the unit which indicates that the unit is composed of alternating layers of sandstone and a more argillaceous component, presumably, greywacke.

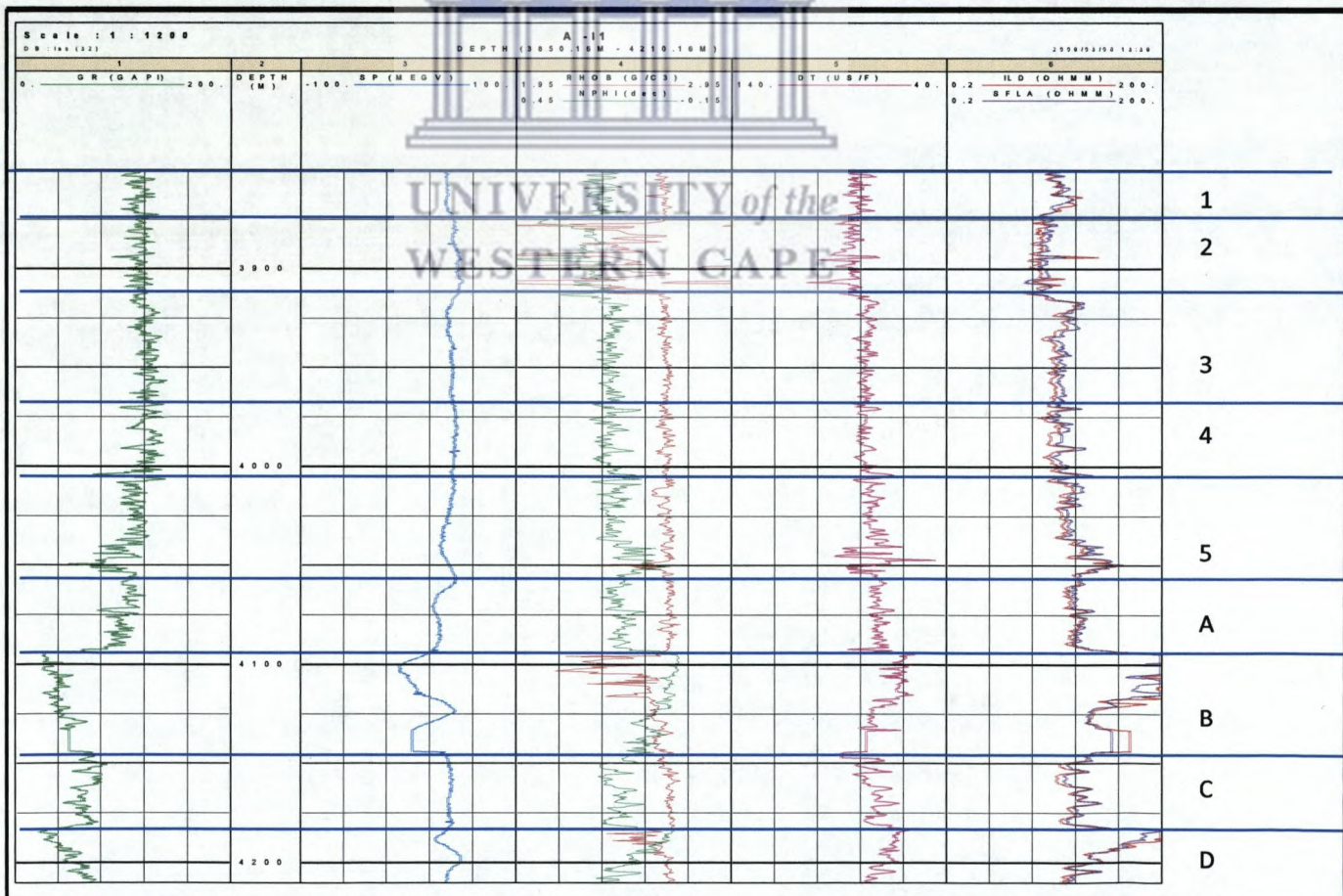
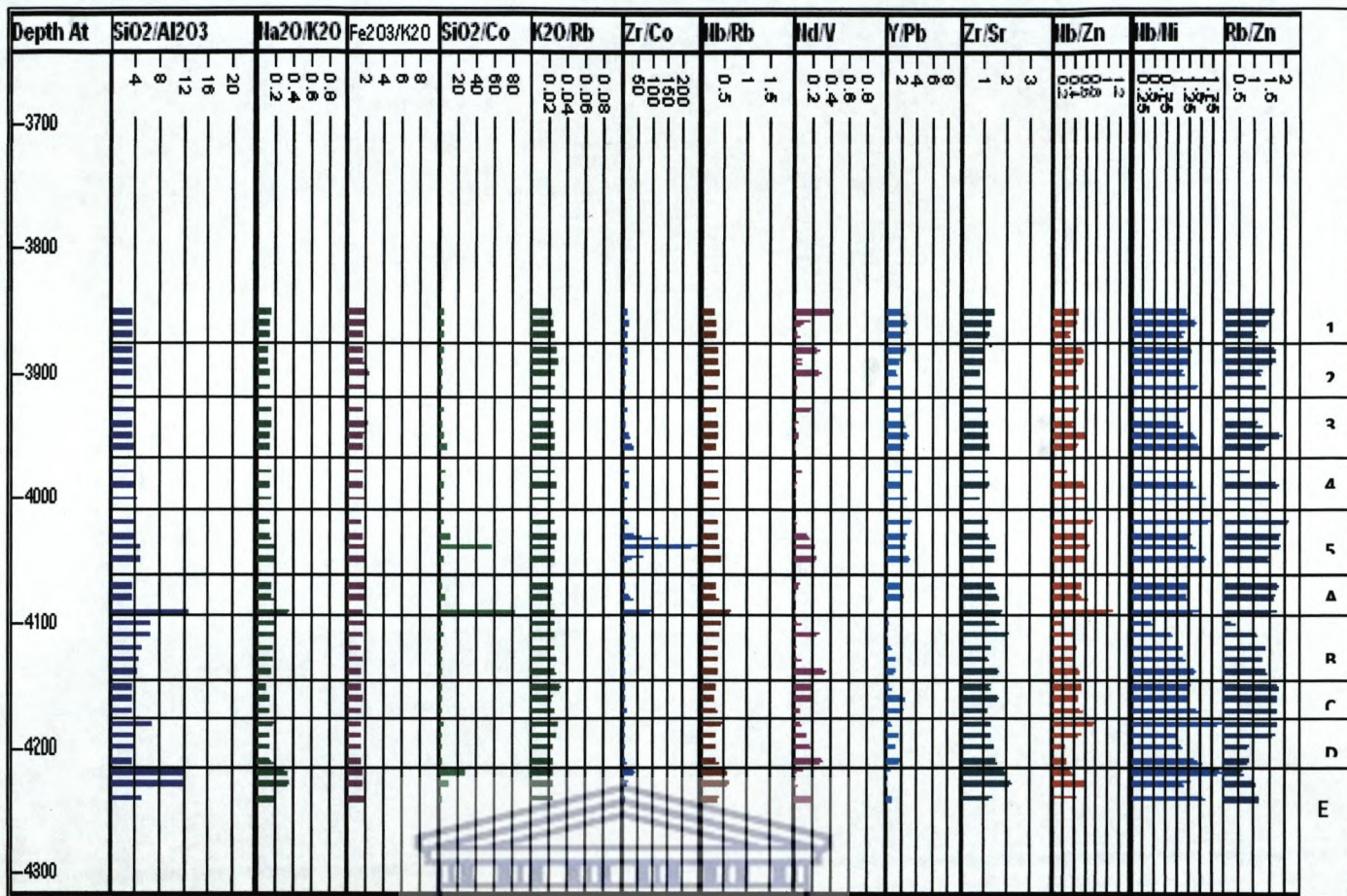


Figure 6.2 Comparison of the Chemostratigraphic Units (A) and Petrophysical Units (B) for Well A-11.

Unit 3

The chemostratigraphic indices Nd/V and Nb/Ni were the only ratios to display discernible trends. The trends displayed by the ratios are suggestive of an increase in the concentration of clay minerals towards the base of the unit. This corroborates the high concentrations of Al_2O_3 that was measured for the unit and the decreasing trend displayed by SiO_2 .

The well logs responses confirmed the geochemical results by displaying GR readings of approximately 120 which is indicative of the presence of either argillaceous sandstones or shales. This statement is further supported by the straight line curve displayed by the SP log and the cross over pattern displayed by the Neutron and Density logs. The unit also displayed a decrease in velocity which would support the above statements.

Unit 3 clusters towards the dolomite lithology curve on the Neutron-Density cross plot. The relative position of the points is indicative of a lithology of an argillaceous nature. This confirms the results of the geochemistry and geochemical indices that revealed increasing clay content and low silica content.

On the M-N plot unit 3 plotted in the predefined shale region and therefore concur with the geochemistry and the well logs which indicated the presence of either argillaceous sandstone or shale.

Based on the petrophysical and geochemical results Unit 3 is characterized as being composed of argillaceous sandstones alternating with shales.

Unit 4

The SiO_2 content indicated the siliceous nature of the samples. The chemostratigraphic indices Nd/V and Nb/Ni characterized this unit. They displayed increasing trends towards the base of the unit. The middle of the unit is characterized by the presence of a highly feldspathic layer as indicated by the Rb/Zn ratio.

The well log responses, as with the chemistry and chemostratigraphic results, indicate the presence of a shale or argillaceous unit. The Sonic log decreases towards the base of the unit, indicating that the unit becomes more compacted towards the base. This corroborates the trends displayed by the chemostratigraphic ratios which indicated an increase in the argillaceous nature of the unit towards the base.

Unit 4 clusters towards the dolomite lithology curve in a position that is presumably indicative of the presence of shales and on the M/N it plots towards the predefined shale region. This confirms the geochemical results and the well log responses which were indicative of the presence of shale or greywacke.

Unit 5

The chemostratigraphic indices for Unit 5 indicate an increase in the siliceous nature of the interval (increase in $\text{SiO}_2/\text{Al}_2\text{O}_3$). The highest value for this ratio was found at the base of the unit and indicates the presence of a clean sandstone unit. The elements ratios SiO_2/Co and Zr/Co display the same trend indicating a peak in the centre and are suggestive of the presence of a sandier layer towards the centre of the unit. Although the unit is sandier than the preceding units, the shale component is still present as seen by the concentrations of Al_2O_3 and TiO_2 .

Unit 5 was defined by lower GR readings than the preceding units and thus confirms the geochemical assumption that this unit is sandier than the preceding units. The GR log indicates a decreasing towards the base which correlates to the increasing trend displayed by $\text{SiO}_2/\text{Al}_2\text{O}_3$. Although lower GR readings are found in this unit the pattern exhibited by the Neutron and Density logs and the high GR readings at places indicates that a shale component is still present in the unit.

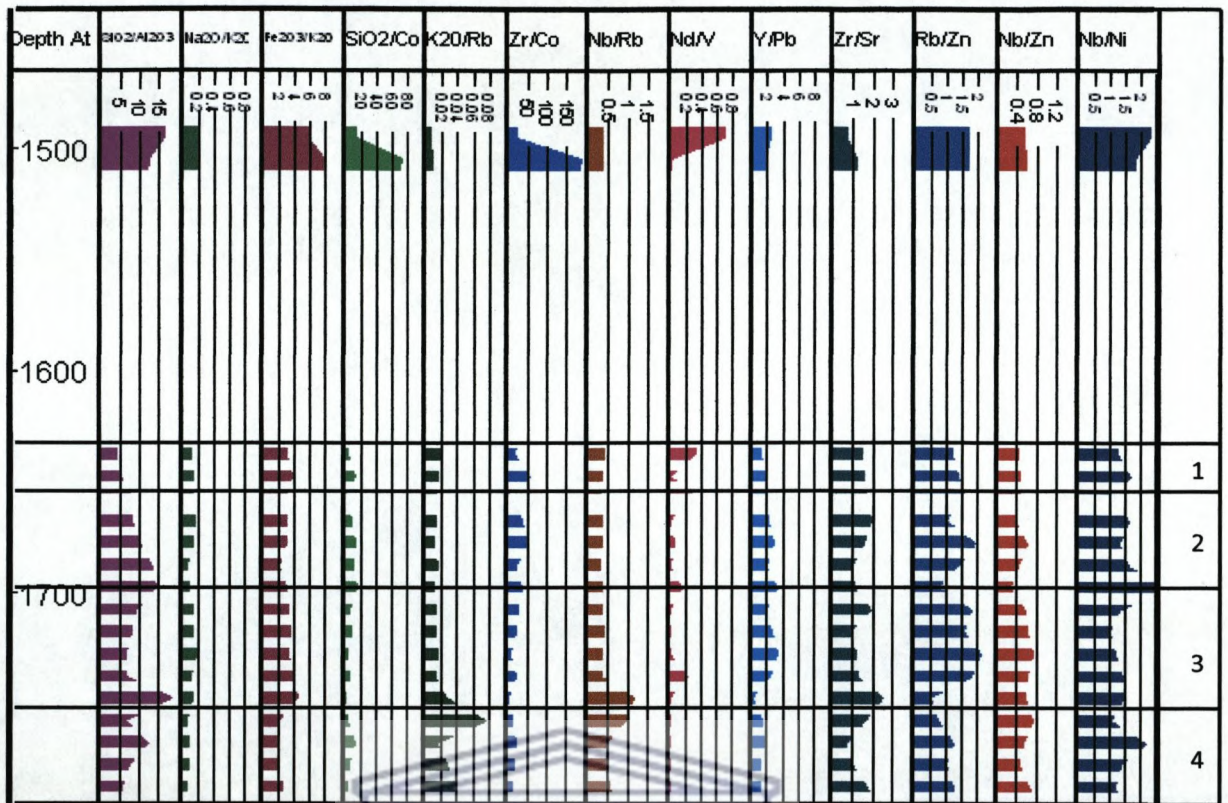
On the Neutron – Density cross plot the unit plots between the limestone and dolomite lithology curves and the movement of the points towards the limestone curve could be indicative of an increase in the siliceous nature of the unit as seen by the geochemical and petrophysical results. As with the geochemistry and well logs responses the M-N plots indicates the presence of a shale components in this unit.

The geochemistry and petrophysical results both suggest that this unit is composed of alternating unit of sandstone (in places argillaceous) and shale.

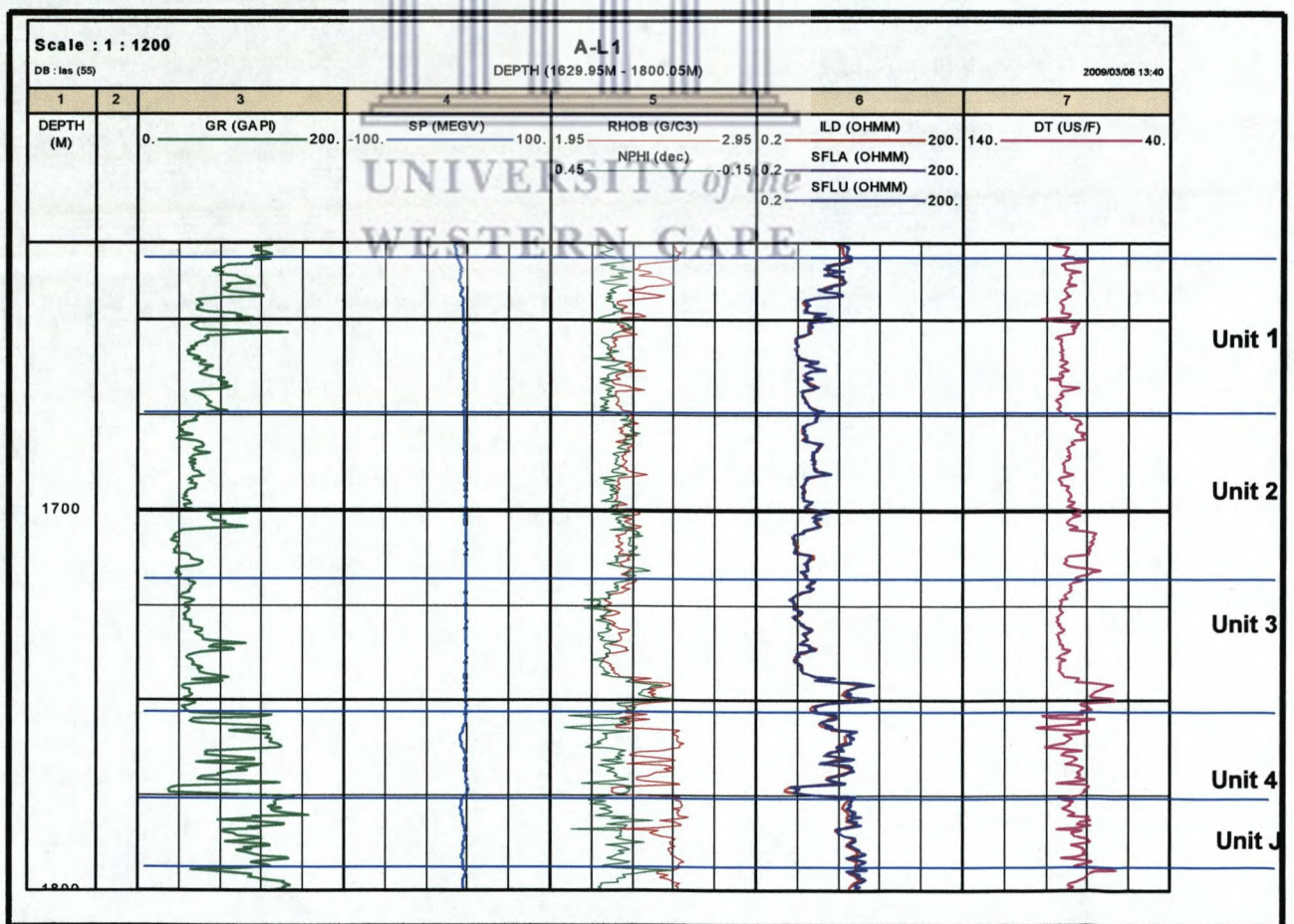
6.2.3 Well A-L1 (Refer to Figure 6.3)

Unit 1

Unit 1 displays high $\text{SiO}_2/\text{Al}_2\text{O}_3$ values and low uniform values for $\text{Na}_2\text{O}/\text{K}_2\text{O}$. The above signifies the highly siliceous nature of the samples and along with the pattern displayed by



(A)



(B)

Figure 6.3 Comparison of the Chemostratigraphic Units (A) and Petrophysical Units (B) for Well A-L1 (section 1).

$\text{Na}_2\text{O}/\text{K}_2\text{O}$ and the decreasing trend displayed by $\text{K}_2\text{O}/\text{Rb}$, are suggestive of the presence of arkosic sands. Decreasing trend displayed by the ratio $\text{Fe}_2\text{O}_3/\text{K}_2\text{O}$ and major elements Al_2O_3 and TiO_2 suggests a decrease in the clay mineral content downhole. Based on the geochemistry the unit is defined as arkose sands that become cleaner towards the base.

The well log responses are suggestive of the presence of a mostly shaly unit with interbedded sandstones. From the geochemistry it is known that the shaly unit is composed of arkosic sands. On the Neutron – Density cross plot the unit plots across the three lithology curves and this is indicative of the presence of a siliceous rock, presumably sandstones and the presence of a clay rich or shaly sand. This clustering of the points confirms the geochemistry and well log responses.

Unit 1 on the M-N plot clusters towards the calcite and quartz regions, thereby indicating the siliceous nature of the section and the presence of presumably calcareous shales. The M-N plot corroborates the patterns exhibited by the well logs and the geochemistry for this area which indicates that the unit is composed mostly of shale or argillaceous components interbedded with sandstones.

Unit 2

The chemostratigraphic ratios $\text{SiO}_2/\text{Al}_2\text{O}_3$, SiO_2/Co , Zr/Co and Y/Pb reveals decreasing trends, thereby suggesting a decrease in the siliceous nature of the unit towards the base. This is consistent with decreasing concentrations measured for SiO_2 and Zr. The geochemistry also indicates an increase in the feldspathic component (increasing trends displayed by $\text{Fe}_2\text{O}_3/\text{K}_2\text{O}$ and $\text{Na}_2\text{O}/\text{K}_2\text{O}$) downhole and an increase in the clay mineral content downhole (increasing trends displayed by Rb/Zn and Nb/Zn). In summary the geochemistry and the chemostratigraphic indices suggests that the unit is composed of greywacke sandstones and interbedded cleaner sandstones.

The well log responses emulates the geochemistry which indicates the the unit consists of alternating units of sandstone and shale or presumably greywacke. The relative positions of the points on the Neutron – Density cross plot indicates the presence of sandstone and shaly sands or greywackes. This supports the results obtained from the geochemistry.

The points for Unit 2 on the M-N plot display clusters that are indicative of the presence of sandstones and shaly sands or greywackes. Although the points cluster towards the calcite region this unit appears to be less shaly than the preceding unit. The petrophysical results

indicate that Unit 2 consists of alternating layers of shale or an argillaceous component and thus emulating the geochemical results.

Unit 3

The geochemical results are indicative of a unit that has a fairly shaly composition but begins to become cleaner towards the base of the unit. The chemistry suggests that the unit is composed of a clay rich or argillaceous component for most part but that cleaner sandstone layers are present throughout. The chemostratigraphic ratios display two contradictory trends. The first trend suggests that the unit becomes cleaner towards the base i.e. sandier. The second trend is suggestive of an increase in the clay mineral content towards the base of the unit. The downhole patterns propose a sequence of alternating layers of sandier units with argillaceous units.

The well log responses indicate patterns that as a rule are indicative of the presence of shale or argillaceous components. The Neutron – Density cross plot signifies the presence of a sand component and a shale component. The M-N plot clusters predominantly towards the quartz region while a minute cluster is found towards the shale region. This would imply that the unit has a highly siliceous nature but that a shaly component is still present.

The petrophysical results suggest that the unit is composed of sandstones and argillaceous/arkose components. The well log patterns indicates that the unit is becoming cleaner towards the base of the unit and suggest that the first chemostratigraphic trend is most likely accurate. The geochemistry in turn narrows down the M-N plot suggestion that the unit has either an arkosic or argillaceous component into a definite argillaceous component.

Unit 4

The geochemical results for this unit show a decrease in the siliceous nature of the unit towards the base and shows that the feldspathic component remains fairly constant throughout the unit. Although the iron mineral content increases towards the base of the unit it is still less than for the preceding unit. As with the previous well, the chemostratigraphic indices provide conflicting trends. Overall the ratios indicate that the unit becomes increasingly argillaceous towards the base, but the ratio Zr/Sr indicates the opposite. However, based on the fact that only one ratio is indicative of an increase in the siliceous nature, it is most likely not the case.

The well log responses emulate the chosen chemostratigraphic theory that the unit becomes increasingly argillaceous by displaying GR readings that suggest a highly radioactive unit. The neutron and density logs display patterns that are indicative of the presence of alternating units and this conforms to the pattern exhibited by the downhole geochemical profiles.

The Neutron- Density cross plot is suggestive of the presence of three lithologies namely, sandstone, shale or an argillaceous lithology and shaly-sand. This supports the above results which are indicative of alternating units and the fact that the unit becomes increasingly radioactive towards the base.

On the M-N plot the unit plots in regions that are associated with the presence of a highly argillaceous or shale component and a minor siliceous component. This emulates the results obtained from the geochemistry and the well logs and reiterates the assumption that the first chemostratigraphic tendency is more accurate.

6.2.4 Well A-U1 (Refer to Figure 6.5)

Unit 1

The chemostratigraphic ratios for Unit 1 are indicative of a decrease in the siliceous nature of the units, a decrease in the feldspathic components and an increase in the carbonate mineral content towards the base of the unit. The concentration of iron minerals appears to be more or less constant through the unit based on the pattern exhibited by the ratio Fe_2O_2/K_2O . Nd/V and Rb/Zn displays inverse trends to SiO_2/Al_2O_3 , SiO_2/Co and Zr/Co which would imply that there is an increase in the concentration of clay minerals downhole. Based on the geochemical results the unit is defined as consisting of alternating layers, with the layers at the top of the unit being composed of more feldspathic lithologies while the layers at the bottom of the unit is composed of an argillaceous unit, presumably calcareous shale. The last statement is based on the increase of carbonate minerals towards the base of the unit.

Interpretation of the petrophysical results has led to the unit being classified as being fairly sandy based on the GR readings and the pattern displayed by the SP log. The Neutron and Density logs, however, display trends associated with the presence of alternating layers of sandstone and shale within the unit. Towards the base of the unit, however, the SP log displays a straight line which as a rule is interpreted as being indicative of the presence of shale or an argillaceous unit, as proposed based on the geochemistry of the unit.

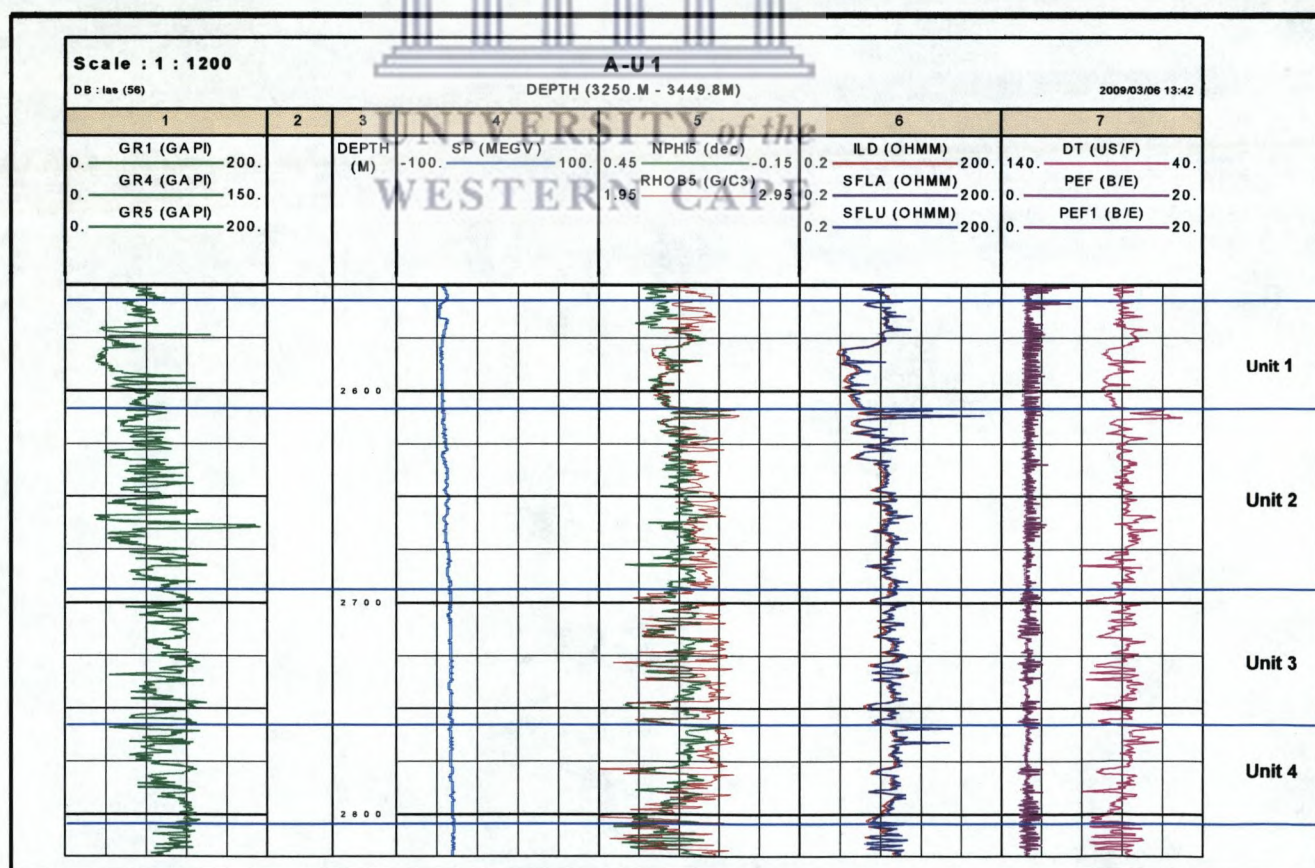
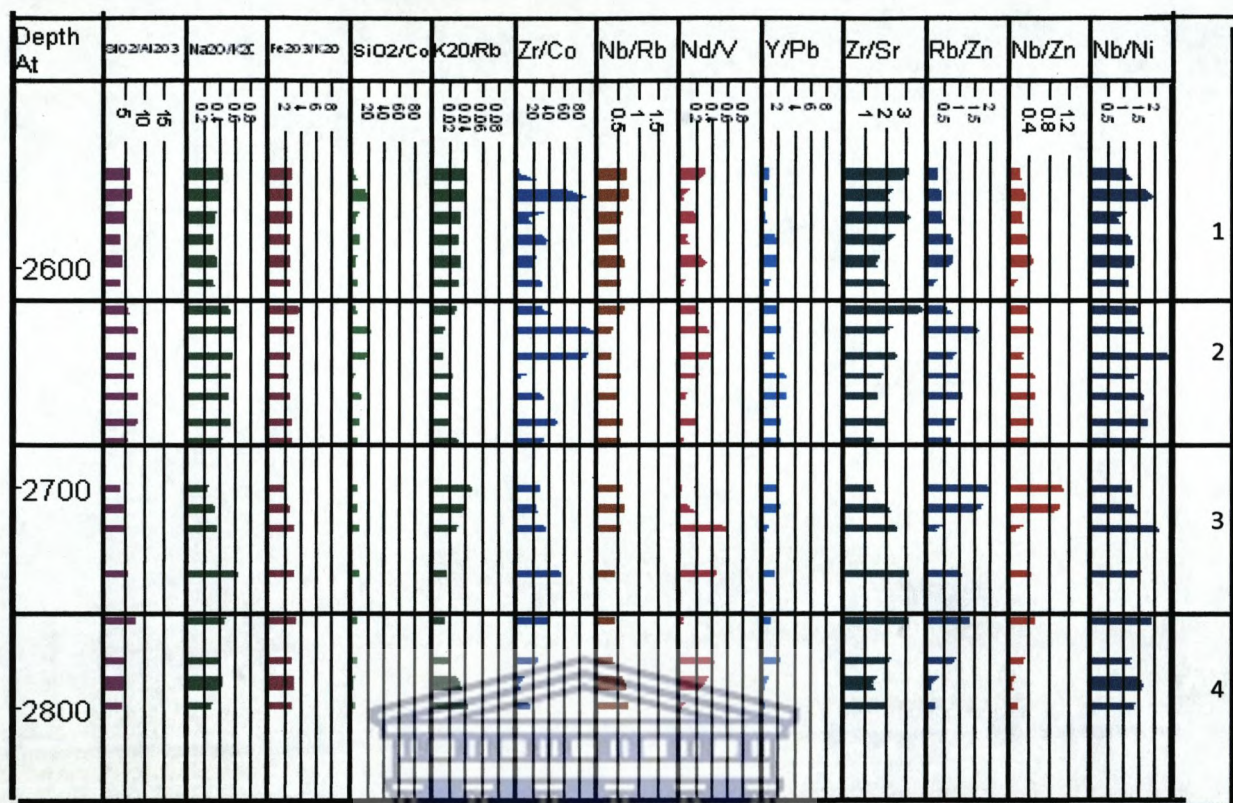


Figure 6.5 Comparison of the Chemostratigraphic Units (A) and Petrophysical Units (B) for Well A-U1 (section 1).

The Neutron – Density plot for this unit indicates the presence of sandstones as well as a shale or argillaceous component and thus corroborates the trends observed from the geochemistry. The M-N plot mirrors the geochemical results by plotting in the quartz and calcite regions thus indicating the presence of sandstones and calcareous shale.

Unit 2

The chemostratigraphic results indicate that the top and the bottom of the unit are slightly more argillaceous than the rest of the unit. The pattern displayed by $\text{Na}_2\text{O}/\text{K}_2\text{O}$ and Fe_2O_3 is suggestive of a lithology that is highly feldspathic and has a higher concentration of iron minerals than the preceding unit. The chemostratigraphic ratios are also indicative of the presence of very clean sandstone in the centre of the unit (at a depth of 2630m to 2640m). The peak corresponds to a decrease in the ratios $\text{Fe}_2\text{O}_3/\text{K}_2\text{O}$ and $\text{K}_2\text{O}/\text{Rb}$ thereby indicating a decrease in the amount of accessory minerals present at that point. Based on the geochemistry, this unit is defined as feldspathic sandstones with interbedded cleaner sandstones.

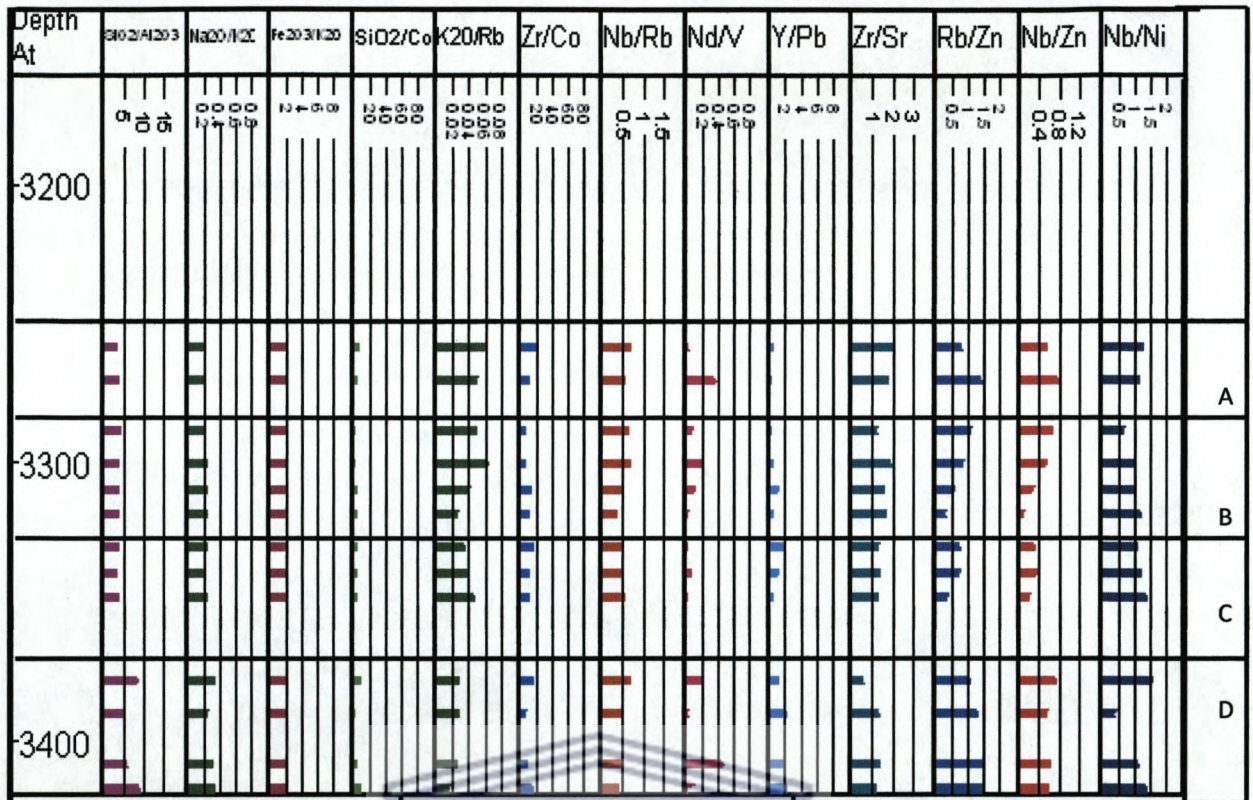
The GR log is indicative of the presence of alternating layers of argillaceous or clay – rich sandstones with cleaner sandstones. This pattern was reiterated by the Neutron and Density logs. The relative positions of the unit on the Neutron-Density cross plot and on the M-N plot is suggestive of the presence of sandstones and calcareous shales.

Unit 3

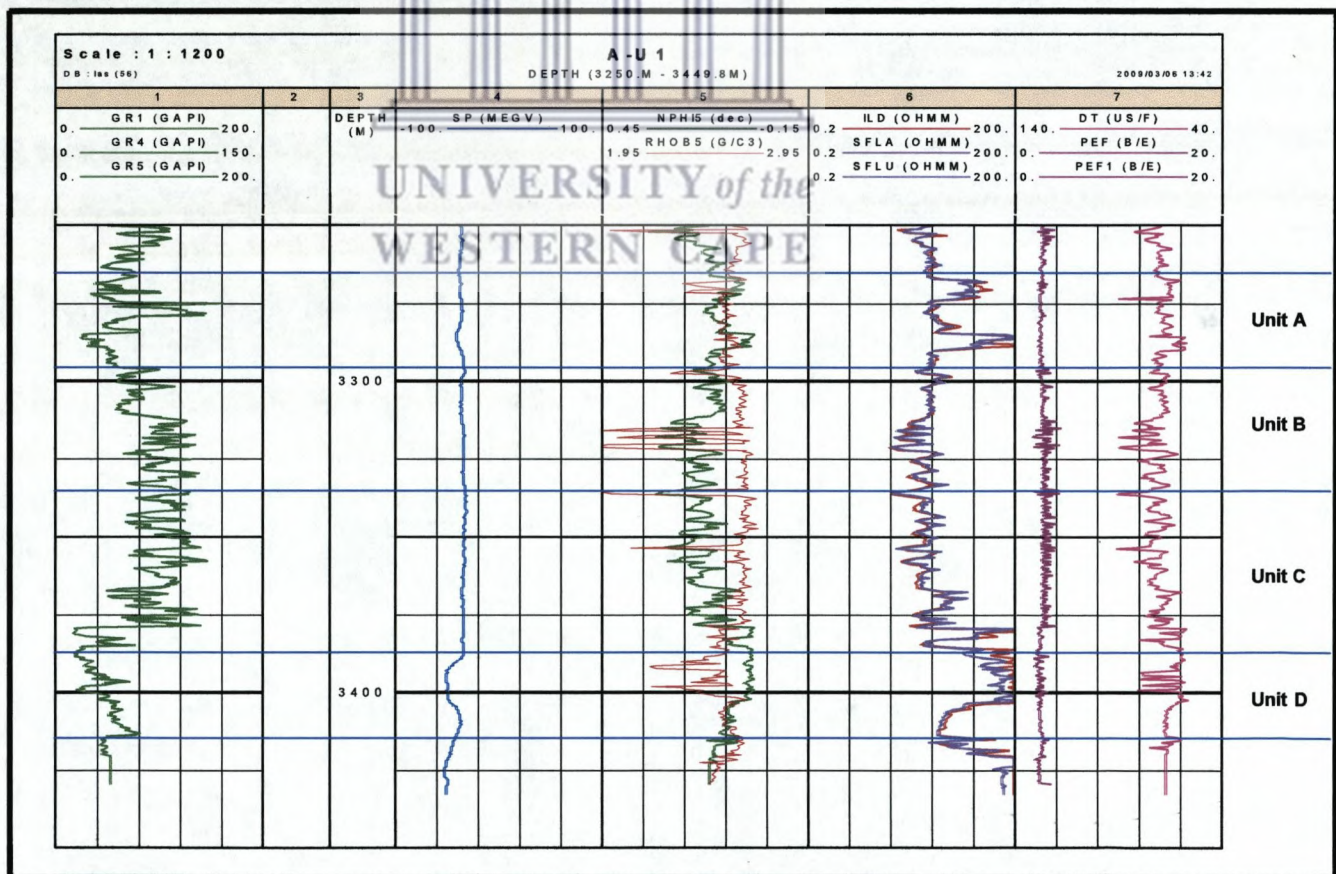
The unit is characterised by lower $\text{SiO}_2/\text{Al}_2\text{O}_3$ values than the preceding unit. The ratio, however, follows an increasing trend towards the base and is therefore indicative of an increase in the siliceous nature of the sample downhole. The trend displayed by $\text{Na}_2\text{O}/\text{K}_2\text{O}$ suggests an increase in the feldspathic component downhole. Based on the behaviour of these two ratios it can be assumed that the unit is composed of feldspathic sands which become increasingly feldspathic downhole.

The GR readings and other well log responses are indicative of the presence of argillaceous units, alternating with sandier units. This trend is also displayed by the geochemical profiles. From the geochemistry it is known that the argillaceous unit is most probably composed of highly feldspathic sands.

The Neutron – Density cross plot reveals the presence of calcareous shales or clays, sandstones and shales. The plotting of the points in the region identified as being indicative



(A)



(B)

Figure 6.6 Comparison of the Chemostratigraphic Units (A) and Petrophysical Units (B) for Well A-U1 (section 2).

of the presence of calcareous clays could instead be indicative of the presence of plagioclase feldspars as it is known from the geochemistry, the unit is highly feldspathic.

On the M-N plot the relative positions of the points indicate the presence of shale or an argillaceous component, now assumed to be indicative of the presence of feldspars, and a siliceous component. The clustering of the unit on the M-N plot thus mirrors the geochemistry of the unit.

Based on the geochemical results and the well log responses this unit is classified as consisting of alternating layers of feldspathic sandstone and sandier units.

Unit 4

As with the previous units, $\text{SiO}_2/\text{Al}_2\text{O}_3$ and Na_2O are indicative of the presence of highly feldspathic sandstone. The remainder of the ratios provide contradictory evidence. The ratio SiO_2/Co indicates a peak in the centre of the unit at a depth ofm which would usually be indicative of the presence of a cleaner sandstone layer, however, the ratios Nd/V and Y/Pb displays trends that indicates an increase in the clay mineral content. In support of the statement that the unit is highly feldspathic is the trend displayed by $\text{K}_2\text{O/Rb}$ which displays trends that's associated with the presence of K-feldspars such as microcline or orthoclase. Based on the above the unit can be confidently described as highly feldspathic.

The GR readings for this unit are indicative of the presence of a clay-rich unit, presumably the feldspathic component based on the geochemistry. The SP log displays trends associated with the presence of sandstone, further support for the characterization of this unit as consisting of feldspathic sandstones. The neutron and density logs display trends that imply that the unit consists of alternating layers.

The Neutron - Density cross plot exhibits patterns that are associated with the presence of calcareous clays, which are assumed to demonstrate the presence of plagioclase feldspars, shales and sandstones. The M-N plot is suggestive of the presence of quartz, shale and an argillaceous component, which is presumably the feldspathic component.

The petrophysical results reflect the geochemistry of the unit which suggest the presence of feldspathic sandstones that become increasingly argillaceous towards the base of the unit.

6.2.5 Correlated Units

(Refer to Figures 6.1.1 to 6.1.6)

6.2.5.1 Unit A

The geochemistry of Unit A suggests that there is a decrease in the siliceous nature of the unit towards the base. The trend displayed by the ratio SiO_2/Co is indicative of the presence of alternating layers of sandier units with clay rich units. A trend of decreasing feldspathic content is also observed. Based on the geochemical trend displayed by the chemostratigraphic indices the unit is classified as consisting of alternating layers of sandstone with sandstone of a more argillaceous nature, probably greywacke.

On the Neutron – Density cross plot, some of the points for this unit plots outside the three lithology curves and this effect is normally associated with the presence of gas. Only Well A-L1 did not plot in this area. The remainder of the points plotted in areas that are usually indicative of the presence of sandstones and shales or an argillaceous component.

The M-N plots for this unit indicates the presence of a siliceous component and the presence of a shale component. This emulates the geochemistry of the unit which is suggestive of the presence of cleaner sandstones with an argillaceous component, presumably greywacke.

6.2.5.2 Unit B

The chemostratigraphic ratio $\text{SiO}_2/\text{Al}_2\text{O}_3$ displays fairly uniform trends throughout this unit but the values are slightly higher than for the previous unit. This means that the silica content remains more or less constant throughout the unit. However, the ratio $\text{Na}_2\text{O}/\text{K}_2\text{O}$ indicates an increase in the concentration of orthoclase feldspar towards the base of the unit. Nb/Rb and Y/Pb trends show that the unit consists of alternating layers.

Based on the geochemistry, the unit is characterised as being composed of alternating layers of feldspathic sandstone with clay rich sandstones or shales.

On the Neutron – Density cross plot for this unit, two distinct trends are visible. The first trend is the clustering of Wells A-A1 and A-L1, which reveals the presence of both a siliceous components and an argillaceous component. This emulates the geochemistry of the unit. In contrast to this the second trend, which involves the clustering of Wells A-U1

and A-I1, indicates the presence of an argillaceous component only. A possible explanation for this discrepancy could be based on the geographical locations of the wells. Well A-U1 and A-I1 are located further from land than Wells A-L1 and A-A1; this means that it is more likely that they will contain finer grained materials.

The M-N plots for this unit indicates the presence of a siliceous and a shale or argillaceous component. Based on the geochemistry it is most likely that the argillaceous component is in fact feldspar, presumably K-feldspar.

6.2.5.3 Unit C

The chemostratigraphic analysis of the unit displays trends which are consistent with the presence of feldspathic sandstones. The ratios are suggestive of an increase in the argillaceous or feldspathic components downhole and this in turn can be interpreted as being indicative of a decrease in the siliceous nature of the unit. This is corroborated by the decreasing trend displayed by the ratio SiO_2/Co . Contradictory to the above mention trends is the pattern displayed by the ratio Zr/Co . The pattern displayed by this ratio is suggestive of an increase in the siliceous nature of the samples downhole. As this pattern is only displayed by one ratio it is highly unlikely that this is the situation.

Based on all the geochemical results this unit can be confidently described as a highly feldspathic unit that becomes increasingly argillaceous towards the base. The M-N plots for this unit is suggestive of the presence of two dominant components within this nit. The plotting of points on the M-N plot mirrors the geochemistry of the unit which suggests the presence of a feldspathic component and a clay component.

6.2.5.4 Unit D

The Chemostratigraphic and geochemical results are indicative of the presence of alternating layers of sandy units and feldspathic units. $\text{SiO}_2/\text{Al}_2\text{O}_3$ displays trends indicative of an increase in the siliceous nature of the unit towards the base. However, the feldspathic content decreases downhole as indicated by the ratios $\text{Na}_2\text{O}/\text{K}_2\text{O}$ and $\text{K}_2\text{O}/\text{Rb}$. The ratio Zr/Sr and Sr concentrations for this unit are indicative of an increase in the concentration of carbonates towards the base of the well.

Based on the geochemical chemostratigraphic analysis of the unit it can be classified as consisting of alternating layers of sandstone, feldspathic sandstones and shales.

The Neutron – Density cross plot mirrors the geochemistry of the unit, which indicates that the unit is composed of sandstones, feldspathic sandstones and shale layers. This is corroborated by the relative clustering of the points on the plot. The geochemical results are also indicative of increased carbonate concentrations for this unit and this is reflected by clustering of points towards the limestone lithology curve.

The patterns exhibited by the M-N plots are similar to the Neutron – Density plots that indicate the presence of sandstone and possibly calcareous clays in the unit. These patterns emulate the geochemistry of the unit which is suggestive of the presence of sandstones alternating with more feldspathic sandstones and shales. The geochemistry of the unit is also suggestive of an increase in the carbonate mineral content towards the base of the unit. This is confirmed by the plotting of the points on the Neutron – Density cross plot towards the limestone region and on the M-N plot towards the calcite region. The carbonate minerals present could be indicative of the presence of calcareous clays within the unit.

The comparison for the Chemostratigraphic and petrophysical results for the wells is fairly competitive. The results appear to mirror each other.

UNIVERSITY of the
WESTERN CAPE

6.3 Correlation Framework

The Petrophysical and Chemostratigraphic results led to the identification of four units that could be correlated across the wells. The results obtained were fairly similar in terms of unit division and correlation. The methods complimented each other such that where no samples were available the logs provided a response and where the logs malfunctioned the samples provided a Chemostratigraphic signature.

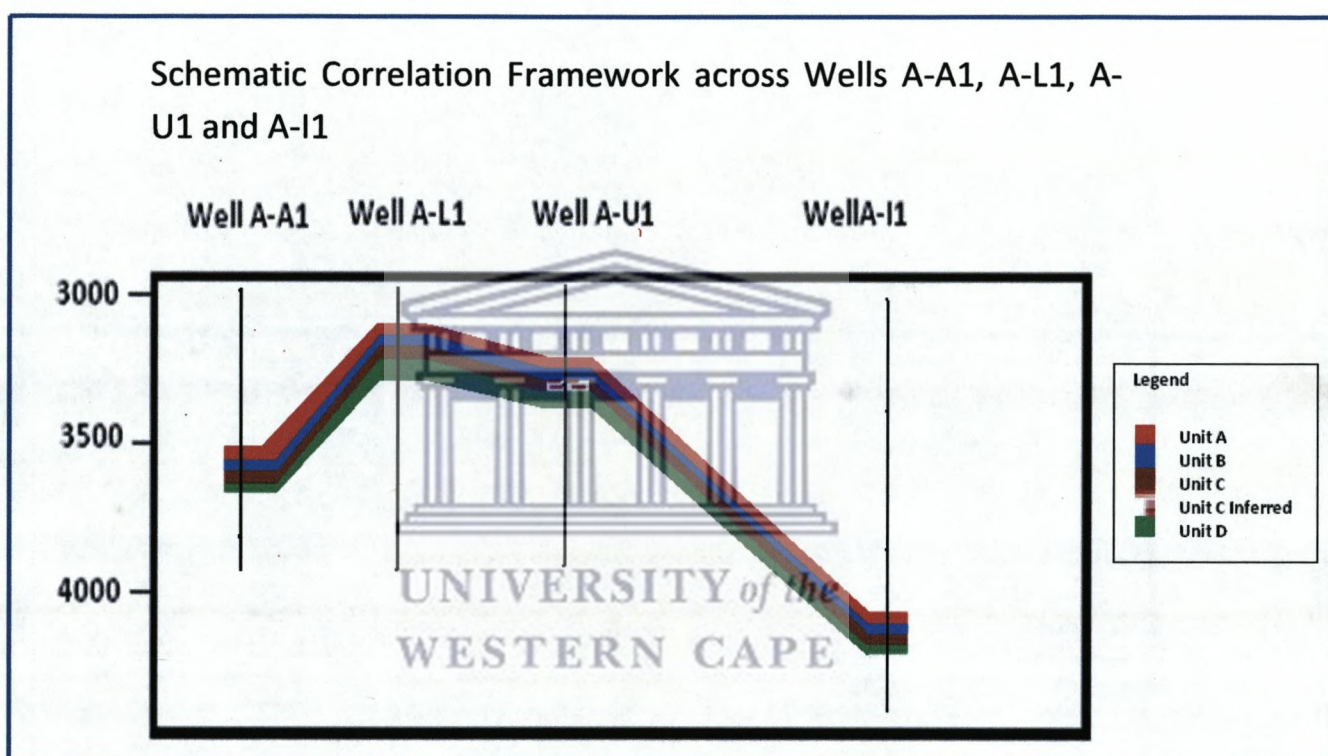


Figure 6.7: Schematic Correlation Framework across Wells A-A1, A-L1, A-U1 and A-I1, constructed using the Chemostratigraphic results.

The correlation framework (refer to **Figure 6.3.1**) displays the following:

- The thickness of Unit A is slightly more in Well A-A1 than in Wells A-L1, A-U1 and A-I1 in which it is more uniform.
- Unit B appears to be uniform throughout the four wells.
- Unit C was inferred across Well A-U1 because no samples were available for that section hence no Chemostratigraphic results were available.
- Unit D appears thickest in Wells A-L1 and A-U1 and much thinner in Wells A-A1 and A-I1.

SECTION 3

Chapter 7 Conclusions and Recommendations



UNIVERSITY *of the*
WESTERN CAPE

CHAPTER 7 CONCLUSIONS AND RECOMMENDATIONS

7.1 CONCLUSIONS

7.1.1 CHEMOSTRATIGRAPHY

The conclusions of the Chemostratigraphic analysis can be summarized as follows:

The Principal Component Analysis Plots (*refer to Chapter 4.2*) produced element groupings that indicate the presence of alternating units of non-feldspathic sandstone, feldspathic sandstone, calcareous clays, and non-calcareous clays or shales.

The elements associated with the presence of carbonates and the elements associated with the presence of clay minerals plots close to each other for all the wells and thus indicate the presence of calcareous clays or shales within the wells. The samples for Well A-U1 are highly feldspathic when compared to the other wells. The elements that displayed diametric relationships on the PCA plots (*refer to Chapter 4.2*) were used to formulate the following ratios: $\text{SiO}_2/\text{Al}_2\text{O}_3$, $\text{Al}_2\text{O}_3/\text{K}_2\text{O}$, $\text{Na}_2\text{O}/\text{K}_2\text{O}$, $\text{K}_2\text{O}/\text{Rb}$, SiO_2/Co , Fe_2O_3 , Nd/V , Zr/Co , Zr/Sr , Y/Pb , Nb/Zn and Nb/Ni . The geochemical fingerprints produced by these ratios led to the identification of 31 geochemical units across the four wells.

Based on the element distribution patterns (*refer to Chapter 4.1*), Principal Component Analysis plots (*refer to Chapter 4.2*) and the Major and Trace element down hole profiles (*refer to Chapter 4.3*) the ratios were classified as being indicative of the presence of (a) cleaner or pure sandstones (b) clays (c) feldspathic components and (d) carbonates.

It is concluded that the presence of pure sandstones are indicated by high values for the ratios $\text{SiO}_2/\text{Al}_2\text{O}_3$, SiO_2/Co , Zr/Co , Y/Pb and Nd/V ; the presence of clays or shale are indicated by low values for $\text{SiO}_2/\text{Al}_2\text{O}_3$, $\text{Fe}_2\text{O}_3/\text{K}_2\text{O}$, SiO_2/Co , Zr/Co and Y/Pb and high values for the ratios Nb/Rb and Rb/Zn and the presence of feldspathic sandstones are indicated by high values for the ratio $\text{Na}_2\text{O}/\text{K}_2\text{O}$ and low values for the ratio Zr/Sr . (*Refer to section 4.4.1*)

Based on the Chemostratigraphic analysis (*refer to Chapter 4.4*) six geochemical units are identified for Well A-A1, eight for Wells A-L1 and A-U1 and nine for Well A-I1. Of the 31 units identified across the wells, four units termed A-D correlates across Wells A-A1, A-L1, A-U1 and A-I1.

The remaining units for Well A-A1 (*refer to sections 4.4.2.1 and 4.4.3.1*) are concluded to be composed of arkosic sandstones, greywackes, sandstones, clean sandstones and argillaceous components. As for Well A-I1 (*refer to sections 4.4.2.4 and 4.4.3.4*), the dominant rock types are concluded to be sandstones, arkose sandstones, argillaceous components and shales. The rock types in the four remaining units for Well A-L1 (*refer to sections 4.4.2.2 and 4.4.3.2*) are concluded as being arkose sandstones, greywacke and argillaceous sandstones. In Well A-U1 (*refer to sections 4.4.2.3 and 4.4.3.3*) it is concluded that the remaining 4 units are composed of cleaner or pure sandstones, feldspathic sandstones, arkose sandstones and argillaceous components.

Based on the Chemostratigraphic analysis the correlated units, A-D, are defined as follows (*refer to sections 4.4.2.5 and 4.4.3.5*);

Unit A is defined as consisting of alternating layers of sandstone with more argillaceous components. Unit B is composed of alternating layers of feldspathic sandstones with clay rich sandstones or shales. Unit C is a highly feldspathic unit that becomes increasingly clay rich towards the base of the section. Unit D is defined as consisting of alternating layers of sandstone and a more feldspathic component. The unit has increased carbonate content towards the base.

In conclusion, the dominant rock types in Wells A-A1, A-L1, and A-U1 and A-I1 appear to be pure sandstones arkose sandstones, feldspathic sandstones, calcareous clays and shales.

7.1.2 PETROPHYSICAL

The conclusions of the Petrophysical analysis can be summarized as follows:

A general overview of the well log responses led to the following conclusions:

Well A-A1 (*refer to section 5.2.1.1 and 5.2.2.1*) consists of alternating units of argillaceous sandstones and shales. It is also concluded that the section displays relatively low permeabilities. Well A-I1 (*refer to section 5.2.1.2. and 5.2.2.2.*) is composed of sandstones and shales. The well becomes increasingly compacted towards the base. Well A-L1 (*refer to sections 5.2.1.3 and 5.2.2.3*) is defined by sandstones and the presence of more argillaceous components such as shaly sands and shales. Well A-U1 (*refer to sections 5.2.1.4 and 5.2.2.4*) is defined as consisting of sandstones and argillaceous components such as shale.

Based on the well log responses six units are identified for Well A-A1, nine for Wells A-L1 and A-I1 and eight for Well A-U1. Of the 33 units identified across the wells four were found to correlate across the wells. Neutron – Density cross plots and M-N plots were constructed for each unit.

Based on the general overview of the well logs, Neutron – Density cross plots and M-N plots for each unit the following conclusions are made:

Units 1 to 3 of Well A-A1 consist of calcareous clays, sandstones and greywackes. Units 1 to 5 of Well A-I1 are defined as consisting of greywackes, sandstones, argillaceous sandstones and greywackes. The dominant rock types for Units 1 to 4 of Well A-L1 is concluded to be shales, sandstones, arkosic sandstones and argillaceous components. Units 1 to 4 of Well A-U1 are composed of the rock type's sandstones, shales, argillaceous sandstones and feldspathic sandstones.

Based on the general overview of the well logs, Neutron – Density cross plots and the M-N plots for the correlated units, A-D, the following conclusions were made:

In conclusion Unit A is defined as consisting mainly of sandstones and greywackes, while Unit B consists of sandstones and either shales or clay-rich sandstones. Unit C is composed of feldspathic sandstones and argillaceous components. Unit D is defined as being composed of sandstones and calcareous shales or clays.

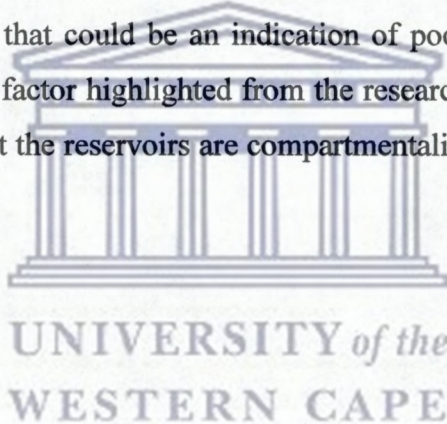
7.1.3 DISCUSSION OF CHEMOSTRATIGRAPHIC AND PETROPHYSICAL CONCLUSIONS

The Chemostratigraphic and Petrophysical results produced accurate and comparable results. However, the Chemostratigraphic analysis provided finer details regarding the lithology of the units. Based on the well log responses no distinction could be made between highly feldspathic sandstone, arkosic and argillaceous sandstone, while these distinctions were possible when analyzing the samples using Chemostratigraphy.

The geochemistry was capable of providing signatures in areas where the wireline tools malfunctioned. The logs, on the other hand, sheds light on properties such as porosity and permeability of the rocks which cannot be obtained accurately from the geochemistry.

When comparing the correlation capabilities of these two techniques, the one based on geochemical signatures and the other based on the responses obtained from wireline tools, it is important to acknowledge that both these techniques has strengths and weaknesses. The best of both these techniques can only be fully utilised when either technique is used in conjunction with other techniques.

In terms of the study area, the Orange Basin, offshore South Africa, it can be concluded that the dominant lithologies in the basin are sandstones, argillaceous sandstones, shales, feldspathic and arkosic sandstones and clays. In terms of petroleum prospectivity the sandstones in Wells A-A1, A-I1, A-U1 and A-L1 could possibly be considered to be reservoirs and the shales could be considered to be seals or source rocks, depending on the organic matter content. On the down side, the sandstones display relatively poor permeabilities and the porosities are variable. The density logs indicate that the sandstones are highly compacted and that could be an indication of poor porosities but more research needs to be done. Another factor highlighted from the research is the presence of alternating lithologies. This means that the reservoirs are compartmentalised and that the area has a high degree of heterogeneity.



7.2 RECOMMENDATIONS

Based on the conclusions of the Chemostratigraphic and Petrophysical analysis of Wells A-A1, A-I1, A-L1 and A-U1 in the Orange Basin, offshore South Africa, the following recommendations are made

- Chemostratigraphic analysis

It is recommended that instead of ditch cuttings, as was used for this study, core samples should be used. Alternatively a smaller sampling interval should be set for the sampling of ditch cuttings. This will enable more detailed correlations to be made. Another recommendation would be that ICP-MS is used for the sample analysis. The reason for this being that ICP-MS has a lower detection level than the XRF instruments and would thus be able to measure REE concentrations in the sample. This would further enhance the use of chemostratigraphy as at the same time as performing Chemostratigraphic analysis it would be possible to determine the provenance of the samples.

Highly recommended is the application of Chemostratigraphy as an industry standard. This would benefit the industry for a number of reasons. Chemostratigraphy is a cost efficient technique, it is highly accurate for lithology and provenance determination and it has the ability to work in any depositional setting.

- Petrophysical analysis

It is recommended that well logs always be run in conjunction with another correlation technique because the results tend to be ambiguous at times and comparison with other methods is necessary to eliminate the ambiguity. The well logs also tend to fail at times and data would then be lost. Another reason why well logs should always be used in conjunction with another technique would be the fact that it is not possible to determine lithology accurately.

- Orange Basin

The Orange Basin, offshore South Africa, is a relatively under explored basin with huge petroleum potential. To best understand the basin it is recommended that a basin-wide Chemostratigraphic study is undertaken. This will enhance the knowledge of the lithologies within the basin and also the provenance of the basin. Understanding these topics will better help to understand the petroleum elements within the basin.



UNIVERSITY *of the*
WESTERN CAPE

REFERENCES

1. Barton, K.R, Muntingh, A, Noble, R.D.P., 1993, Geophysical and Geological Studies Applied to the Hydrocarbon Exploration on the West Coast Margin of South Africa, Extended Abstracts of the third International Congress of the Brazilian Geological Society, Rio De Janeiro, 1993.
2. Broad, D.S, Jungslager, E.H.A, McLachlan, I.R, Roux, J., 2007, *Offshore Mesozoic Basins*, Geology of South Africa, pp 553 – 565.
3. Broad, D.B., Mills., S.R., 1993, South Africa offers exploratory potential in variety of basins. Oil and Gas publications, 6, pp 38-44
4. Carey, P., 2007, Introduction to Petroleum Geology, unpublished.
5. Clemson, J., Cartwright, J.A., Booth, J., 1997, Structural segmentation and the influence of basement structure on the Namibia passive margin, Journal of the geological Society of London, 154, pp 447 - 482
6. Cojan, I., Renard, M., 2002, Sedimentology, Taylor and Francis, pp 156 – 214.
7. Corbett, I.A., Burrell, B., 2001, The earliest Pleistocene Orange River fan-delta: an example of successful exploration delivery aided by Quaternary research in diamond placer sedimentology and palaeontology, Quaternary International, Volume 82, pp 63 – 73.
8. Dale, D.C., McMillan, I.K., 2003, the rising and falling of the African continent, the rising and falling of global sea-level and changing shoreline positions through time, Earthyear, Journal of Sustainable Development, 3, pp 58 – 59.
9. Davis, J.C, 2002, Statistics and Data Analysis in Geology, Third Edition, Blackwell Publishing
10. Dingle, R.V., 1993, Structural and Sedimentary development of the continental margin of southwestern Africa, Communications of the Geological Survey of Namibia, 8, pp 35 – 43
11. Doveton, J.H., 1992, Geological Applications of Wireline Logs: A synopsis of Development Trends, The Log Analyst, Volume 33, number 3, pp 286 - 303

12. Doveton, J.H., Merriam, D.F., 2004, Borehole petrophysical chemostratigraphy of Pennsylvanian black shales in the Kansas subsurface, *Chemical Geology*, Volume 206, pp 249 – 258.
13. Dypvik, Harris., 2001, Geochemical Facies Analysis of Fine Grained Siliciclastics using, Th/U, Zr/Rb and (Zr+Rb)/Sr ratio's. *Chemical geology*, Volume 181, pp 131 - 146
14. Eagles, G., 2007, *New angles on the South Atlantic opening*, *Journal of Geophysics*, Volume 168, Issue 1, pp 353 – 361.
15. Ehrenberg, S.N., Siring, E., 1992, Use of bulk chemical analysis in Stratigraphic correlation of sandstone: an example from the Statford Nord Field, Norwegian continental shelf, *Journal of Sedimentary Petrology*, 52, 318- 330
16. Fouke, B.W., Schlager, W., Vandamme, M.G.M., Henderiks, J., Van Hilten, B., 2005, *Sedimentary Geology*, Volume 175, pp 297-314.
17. Gale, A.S., Jenkyns, H.C., Kenned, W.J., Corfield, R.M., 1993, *Journal of the Geological Society, London*, Volume 150, pp 29 – 32.
18. Gallagher, K., 1999, Brown, R., *Denudation and Uplift at Passive Margins: the record on the Atlantic Margin of Southern Africa*, *The Royal Society of London*, 335, pp 835 – 859.
19. Gerrard, I., Smith G.C., 1982, Post-Paleozoic Succession and Structure of the Southwestern African Continental Margin, *Studies in Continental Margin Geology*, AAPG memoir 34, pp 49 – 74.
20. Gladzenko, T.P., Hinz, K., Eldholm, O., Meyer, H., Neben, S., Skogseid, J., 1997, South Arlantic Volcaniv Margins, *Journal of the Geological Society of London*, Volume 154, pp 465 – 470.
21. Gomez Peral, L.E., Poire, D.G., Strauss, H., Zimmerman, U., 2007, Chemostratigraphy and diagenetic constraints on Neoproterozoic carbonate successions from the Sierras Bayas Group, Tandilia System, Argentina, *Chemical Geology*, Volume 23, pp 109 – 128.

22. Hussain, M., 2007, Elemental Chemistry as a tool for Stratigraphic correlation: A case study involving lower Paleozoic Wajid, Saq and Qasim formations in Saudi Arabia, *Marine and Petroleum Geology*, Volume 24, pp 91 – 108.
23. Jarvis, I., Moreton, J., Gerard, M., 1998, *Chemostratigraphy of the Madeira Abyssal Plain Miocene-Pleistocene Turbidites, Site 950*, Proceedings of the Ocean Drilling Program, Scientific Results, Volume 157, pp 535 – 542.
24. Jarvis, I., Murphy, A.M., Gale, A.S., 2001, Geochemistry of pelagic and hemipelagic carbonates: criteria for identifying systems tracts and sea level change, *Journal of the Geological Society, London*, Volume 158, pp 685 – 696.
25. Jenkyns, H.C., Jones, C.E., Grocke, D.R., Hesselbo, S.P., Parkinson, D.N., 2002, Chemostratigraphy of the Jurassic System: applications, limitations and implications for palaeoceanography, *Journal of the Geological Society, London*, Volume 159, pp 351 – 378.
26. Jungslager, E.A., 1999, *Petroleum Habitats of the Atlantic Margin of South Africa*. In: Cameron, N.R., Bate, R.H., Clure, V.S. (Eds), *The Oil and Gas Habitat of South Atlantic*, London: Special Publications, Geological Society of London, pp 153 – 168.
27. Krygowski, D., 2003, *Guide to Petrophysical Interpretation*,
28. Kuhlmann, G., Paton, D., di Primio, R., van der Spuy, D., Horsfield, B., 2007, Modelling hydrocarbon generation and migration within a passive continental margin setting, Orange Basin (South Africa), *Geochemical Research Abstracts*, Volume 9.
29. Laudon, R., 1996, *Principles of Petroleum development Geology*, Pentrice Hall Petroleum Engineering Series, New Jersey.
30. Lawrence, S., 1995, Shelf North Of Falklands May Be New South Atlantic Petroleum Province, *Oil and Gas Journal*, pp 52 – 55.
31. Lovell, M.A., Pezard, P.A., Harvey, P.K., 1992, Chemical Stratigraphy of boreholes in the Izu Bonin Arc from in situ measurements, Proceedings of the Ocean Drilling Program, Scientific Results, Volume 126.

32. Lyons, C., Zaba, J., 1996, Standard Handbook of Petroleum and Natural Gas Engineering, Gulf Publishing Company, Volume 2,
33. Macdonald, D., Gomez – Perez, I., Franzese, J., Spallet, L., Lawver, L., Gahagan, L., Dalziel, i., Thomas, C., Trewin, N., Hole, M., Paton, D., 2003, Mesozoic break of south western Gondwana: implications for regional hydrocarbon potential of the south Atlantic, Marine and Petroleum Geology, Volume 20, 287 -308.
34. McMillan, I.K., 2003, Foraminiferally defined biostratigraphic episodes and sedimentation patterns of the Cretaceous drift successions in seven basins on the South African and southern Namibian Continental Margin, South African Journal of Science, Volume 99, pp 537 – 575.
35. Muntingh, A., 1993, Geology, prospects in the Orange basin offshore western South Africa, Oil and Gas Journal, Volume 25, pp 106 – 109.
36. Muntingh, A., 1991, Sequence Stratigraphy of the Orange Basin, Western Offshore South Africa, AAPG, Volume 73, Issue 3, pp 48 – 49.
37. Muntingh, A., Brown, L.F., Sequence Stratigraphy of Petroleum Plays, Post – Rift Cretaceous Rocks (Lower Aptian to Upper Maastrichtian), Orange Basin, Western Offshore, South Africa, AAPG, Volume XX, Chapter 4, pp 71 – 98
- ✓ 38. Pearce, T., Besly, B.M., Wray, D.S., Wright, D.K., 1999, Chemostratigraphy: a method to improve interwell correlation in barren sequences - a case study using onshore Duckmantian/Stephanian sequences (West Midlands, UK): Sedimentary geology < Volume 124, pp 197 – 220.
39. Pettijohn, F.J., Potter, P.E., Siever, R., 1987, Sand and Sandstone, Springerlink, Second Edition, pp
40. Rangel, A., Parra, P., Nino, C., 2000, The La Luna Formation: chemostratigraphy and organic facies in the Middle Magdalena Basin, Organic Geochemistry, Volume 31, pp 1267 -1284.
- ✓ 41. Ratcliffe et al, 2003, Enhanced reservoir characterisation of the Triassic Argilo Gresex - Inferieur, Algeria using high resolution chemostratigraphy, Extended Abstract, AAPG Conference, Salt Lake City, Utah.

- ✓ 42. Rider, 2006, The Geological Interpretation of Well Logs, Second Edition, Whittles Publishing.
43. Scopelleti, G., Bellanca, A., Neri, R., Baudin, F., Coccioni, R., 2006, Comaprive High Resolution Chemostratigraphy of the Bonarelt Level from the reference Bottacione section and from an equivalent section in NW Sicily: Consistent and contrasting responses to the OAE2, Chemical Geology, 228, pp 266 – 285.
- ✓ 44. Serra, O., 1984, Fundamentals of Well Log Interpretation, developments in Petroleum Science, Elsevier
45. Stevenson, I.R., McMillan, I.K., 2004, Incised valley fill Stratigraphy of the Upper Cretaceous succession, proximal Orange Basin, Atlantic margin of southern Africa, Journal of the Geological Society of London, Volume 161, pp 185 – 208.
46. Tucker., 2001, Petrology, Blackwell Science, Third Edition, Chapters 2 and 3 arkose sandstones
47. Van der Spuy,D., 2003, Aptian source rocks in some South African Cretaceous basins, Petroleum geology of Africa: New Thenes and Developing technologies. Geol. Soc., London, Special Publications. The Geological Society of London.
48. Vickery, C., 1960, The Chemistry of yttrium and scandium, International series of monographs on inorganic chemistry, Volume 2, Pergamon Press, pg17
49. Wright. J.B., South Atlantic Continental Drift and the Benue Trough, Tectonophysics, Volume 6, Issue 4, pp 301 – 310.

APPENDIX A: XRF Analysis – Major Elements



UNIVERSITY *of the*
WESTERN CAPE

Sample name	SiO ₂	Al ₂ O ₃	Fe ₂ O ₃	MnO	MgO	CaO	Na ₂ O	K ₂ O	TiO ₂	P ₂ O ₅	SO ₃
	Si	Al	Fe	Mn	Mg	Ca	Na	K	Ti	P	S
	(%)	(%)	(%)	(%)	(%)	(%)	(%)	(%)	(%)	(%)	(%)
S-NIM-S	68.776	17.963	1.476	0.017	0.711	0.682	0.432	15.82	0.045	0.097	0.05
A-A1 3544-46	68.619	9.996	4.124	0.112	2.661	5.909	2.165	2.485	0.615	0.074	0.164
A-A1 3550-52	54.517	11.746	5.331	0.142	2.814	6.956	1.532	3.109	0.731	0.086	0.241
A-A1 3558-60	60.663	13.437	5.723	0.127	3.093	5.362	1.628	4.004	0.908	0.093	0.204
A-A1 3566-68	63.867	13.303	5.191	0.105	2.559	4.505	1.761	3.837	0.826	0.082	0.164
A-A1 3582-84	57.252	15.019	5.582	0.108	2.574	4.689	1.384	4.201	0.878	0.084	0.242
S-S10	60.025	11.77	4.975	0.111	1.494	0.951	0.129	0.545	0.419	0.055	0.047
A-A1 3588-90	72.122	10.842	4.341	0.088	2.401	4.212	2.338	2.658	0.614	0.069	0.132
A-A1 3598-3600	67.141	10.565	4.166	0.113	2.626	6.373	2.038	2.881	0.595	0.072	0.117
A-A1 3614-16	56.179	14.076	6.055	0.122	2.549	5.959	1.53	4.145	0.837	0.081	0.213
A-A1 3606-08	65.721	10.692	4.308	0.111	2.638	5.878	2.076	2.864	0.612	0.077	0.143
A-A1 3622-24	60.276	12.969	4.921	0.105	2.322	4.903	1.786	3.661	0.714	0.078	0.171
S-SARM49	117.829	0.223	0.041	-0.002	0.176	-0.021	0.04	-0.01	0.009	0.032	0.013
A-A1 3630	71.924	11.706	3.961	0.07	1.841	3.22	2.401	2.862	0.572	0.069	0.175
A-A1 3636-38	63.542	13.363	5.104	0.103	2.482	5.295	1.733	3.502	0.762	0.075	0.252
A-A1 3644-46	62.24	11.995	4.95	0.106	2.718	5.569	1.755	3.277	0.735	0.082	0.229
A-A1 3652-54	57.836	11.876	5.023	0.131	3.369	8.174	1.597	3.554	0.738	0.077	0.173
A-A1 3772-74	53.612	19.233	6.412	0.088	1.605	1.758	0.884	4.561	1.107	0.083	0.304
S-SY-2	66.767	13.453	6.4	0.3	2.955	8.428	4.564	5.087	0.134	0.269	0.041
A-L1 3137-40	75.25	7.654	6.336	0.12	1.006	3.208	0.423	1.883	0.499	0.077	1.159
A-L1 3149-52	68.129	8.361	7.67	0.153	1.277	5.354	0.376	1.999	0.502	0.097	1.341
A-L1 3158-61	61.815	9.405	8.74	0.172	1.305	6.223	0.424	2.549	0.559	0.093	2.014
A-L1 3167-70	90.428	4.458	3.49	0.065	0.655	1.716	0.194	1.14	0.257	0.059	0.921
A-L1 3179-82	69.136	10.899	8.472	0.15	1.17	2.084	0.563	2.525	0.596	0.091	1.34
S-FK	100.411	7.835	0.313	0.007	0.574	0.091	0.325	4.863	0.07	0.077	0.03
A1-3670-72	71.283	10.995	4.058	0.083	1.797	2.758	1.815	3.093	0.673	0.091	0.212

	Si	Al	Fe	Mn	Mg	Ca	Na	K	Ti	P	S
	(%)	(%)	(%)	(%)	(%)	(%)	(%)	(%)	(%)	(%)	(%)
A1-3746-48	78.788	9.151	3.831	0.068	2.277	2.643	1.691	2.694	0.651	0.083	0.171
A1-3754-56	58.317	15.585	5.699	0.148	1.949	5.029	1.151	4.057	0.878	0.081	0.349
A1-3762-64	68.356	9.378	3.432	0.056	1.484	2.019	1.717	2.534	0.559	0.077	0.193
A1-3780-82	57.25	13.411	5.95	0.146	3.298	5.984	1.234	3.724	0.941	0.166	0.211
S-NIM-S	69.861	18.456	1.495	0.016	0.698	0.686	0.442	15.87	0.044	0.097	0.048
A-A1 3788-90	68.833	12.509	5.2	0.091	2.384	2.946	1.629	3.201	0.831	0.145	0.184
A-A1 3796-98	66.023	15.234	6.464	0.1	2.784	1.821	1.172	4.586	0.869	0.12	0.09
A-A1 3800-02	65.684	15.184	6.648	0.11	3.014	2.122	1.319	4.642	0.837	0.114	0.079
A-L1 1490-1500	85.582	5.235	4.065	0.069	0.859	0.987	0.148	0.715	0.278	0.048	0.686
A-L1 1500-1510	78.435	6.304	7.704	0.127	1.496	2.518	0.172	0.967	0.394	0.07	0.432
S-S-10	60.003	11.66	5.018	0.111	1.481	0.957	0.13	0.548	0.419	0.055	0.047
A-L1 1635-40	58.221	15.257	10.201	0.107	1.79	2.962	0.39	3.483	0.806	0.077	2.019
A-L1 1645-50	57.917	12.21	9.203	0.106	1.706	3.354	0.315	2.541	0.658	0.075	1.415
A-L1 1655-60	69.664	9.42	6.278	0.068	1.277	2.352	0.273	2.095	0.534	0.061	1.444
A-L1 1665-70	70.472	8.726	5.767	0.07	1.21	2.129	0.311	1.932	0.519	0.061	1.209
A-L1 1675-80	74.398	7.569	5.583	0.071	1.142	2.334	0.237	1.905	0.429	0.091	1.261
S-SARM49	117.951	0.224	0.04	-0.001	0.178	-0.021	0.043	-0.01	0.009	0.031	0.011
A-L1 1685-90	75.426	5.733	4.611	0.062	0.937	2.181	0.141	2.328	0.291	0.1	2.224
A-L1 1695-1700	84.326	5.889	4.59	0.057	0.846	1.104	0.13	1.613	0.319	0.073	1.083
A-L1 1705-10	76.757	8.553	6.574	0.072	1.093	1.393	0.293	2.043	0.492	0.07	0.667
A-L1 1715-20	70.405	9.011	6.247	0.085	1.347	1.985	0.235	1.779	0.456	0.083	0.971
A-L1 1725-30	66.724	10.016	6.932	0.089	1.592	2.191	0.384	2.223	0.509	0.072	0.857
S-FK	100.681	7.89	0.315	0.005	0.595	0.091	0.335	4.866	0.07	0.077	0.03
A-L1 1735-40	64.783	9.853	8.148	0.094	1.689	2.011	0.234	2.151	0.515	0.076	0.853
A-L1 1745-50	58.254	3.208	3.621	0.081	0.928	17.09	0.12	0.83	0.23	0.059	0.476
A-L1 1755-60	53.793	8.331	6.675	0.098	1.145	10.23	0.201	3.183	0.47	0.068	4.051
A-L1 3248-51	75.974	8.444	5.984	0.107	1.091	2.544	0.414	2.046	0.502	0.076	1.177
Sample name	SiO ₂	Al ₂ O ₃	Fe ₂ O ₃	MnO	MgO	CaO	Na ₂ O	K ₂ O	TiO ₂	P ₂ O ₅	SO ₃

	Si	Al	Fe	Mn	Mg	Ca	Na	K	Ti	P	S	
	(%)	(%)	(%)	(%)	(%)	(%)	(%)	(%)	(%)	(%)	(%)	
A-L1 4149-52		51.77	15.422	8.121	0.065	1.982	2.967	0.604	5.488	0.822	0.087	2.962
A-L1 4197-4200		53.928	15.931	7.622	0.061	2.065	2.366	0.636	5.034	0.868	0.077	1.263
A-II 4218-21		85.074	7.019	2.691	0.027	0.988	0.858	0.579	1.7	0.297	0.053	0.629
S-SARM49		117.536	0.223	0.041	-0.001	0.18	-0.021	0.039	-0.01	0.009	0.032	0.013
A-II 3909-12		50.863	15.482	9.525	0.078	2.084	5.239	0.613	4.797	0.831	0.084	3.004
A-II 3978		52.361	15.036	7.822	0.072	2.034	4.556	0.685	4.804	0.817	0.084	3.346
A-II 3999-4000		51.585	12.686	7.117	0.072	1.853	9.156	0.532	3.592	0.678	0.093	3.04
A-II 4047-50		61.866	13.215	7.524	0.072	1.87	3.798	0.654	3.716	0.704	0.08	1.245
A-II 4089-92		85.036	6.7	2.651	0.024	1.006	1.433	0.556	1.622	0.291	0.053	0.596
S-NIM-S		70.014	18.479	1.493	0.016	0.707	0.686	0.426	15.87	0.044	0.097	0.048
A-L1 3188-91		85.974	6.734	4.025	0.075	0.746	0.674	0.398	1.581	0.355	0.057	0.718
A-L1 3197-3200		86.62	6.215	3.837	0.062	0.713	0.693	0.349	1.492	0.364	0.054	0.751
A-L1 3239-41		68.252	10.489	7.22	0.14	1.2	3.685	0.459	2.521	0.61	0.094	1.239
A-L1 3209-12		74.581	9.825	5.616	0.117	0.913	0.624	0.495	2.314	0.577	0.059	0.618
A-L1 3218-22		63.638	11.268	7.321	0.118	1.222	1.89	0.436	2.845	0.622	0.086	1.54
S-SY-2		67.042	13.556	6.396	0.301	2.917	8.444	4.534	5.092	0.134	0.272	0.043
A-L1 1785-90		62.997	11.212	7.836	0.125	1.189	1.889	0.169	3.202	0.675	0.077	2.087
A-L1 1795		66.313	11.862	7.098	0.092	1.013	1.402	0.147	3.093	0.702	0.07	2.397
A-L1 3107-10		58.026	9.434	7.971	0.158	1.307	7.494	0.526	2.669	0.613	0.127	2.229
A-L1 3119-22		71.966	8.817	6.836	0.144	1.017	3.437	0.477	2.286	0.521	0.095	1.749
A-L1 3128-31		71.931	8.964	6.433	0.105	1.04	2.325	0.472	2.505	0.57	0.076	1.684
A-II 4169-70		53.945	15.905	7.882	0.063	2.092	3.124	0.667	5.278	0.865	0.081	1.96
A-II 4179-82		68.815	10.367	4.538	0.045	1.492	3.356	0.595	3.078	0.508	0.066	1.079
A-II 4188-91		57.547	14.668	6.815	0.054	1.877	1.822	0.6	4.858	0.744	0.076	1.628
A-II 4197-4200		55.183	16.054	7.731	0.059	2.102	2.641	0.657	4.964	0.872	0.075	1.255
A-II 4239-42		64.406	12.945	6.63	0.062	1.742	2.573	0.696	3.735	0.675	0.078	1.14
S-SY-2		64.81	12.702	6.278	0.297	2.899	8.372	4.474	5.061	0.133	0.27	0.044
Sample name	SiO ₂	Al ₂ O ₃	Fe ₂ O ₃	MnO	MgO	CaO	Na ₂ O	K ₂ O	TiO ₂	P ₂ O ₅	SO ₃	

	Si	Al	Fe	Mn	Mg	Ca	Na	K	Ti	P	S
	(%)	(%)	(%)	(%)	(%)	(%)	(%)	(%)	(%)	(%)	(%)
S-FK	98.536	7.466	0.31	0.005	0.565	0.088	0.326	4.843	0.069	0.075	0.03
A-II 4098-4101	69.492	11.114	6.196	0.054	1.565	1.266	0.608	3.018	0.531	0.077	0.703
A-II 4119-21	61.635	12.616	5.653	0.051	1.759	2.813	0.609	3.68	0.634	0.074	1.111
A-II 4128-30	60.317	13.763	6.309	0.055	1.896	3.318	0.634	4.018	0.697	0.076	1.031
A-II 4137-40	60.227	14.744	6.362	0.052	1.895	2.048	0.631	4.217	0.744	0.074	1.248
A-II 4149-52	43.582	12.914	7.795	0.076	1.653	2.563	0.501	5.041	0.775	0.081	2.424
S-NIM-S	69.879	18.353	1.49	0.016	0.704	0.685	0.436	15.87	0.045	0.098	0.049
S-NIM-S	69.85	18.41	1.492	0.015	0.697	0.686	0.434	15.87	0.044	0.097	0.049
A-I 3927-30	51.24	14.939	8.326	0.075	1.984	4.615	0.691	4.909	0.839	0.081	3.434
A-A1 3572-74	51.263	14.968	8.338	0.075	1.979	4.617	0.673	4.915	0.84	0.081	3.437
A-I 4209-12	55.847	16.711	8.027	0.064	2.103	2.007	0.659	5.12	0.891	0.077	1.49
A-I 3849-52	53.627	16.25	9.153	0.079	2.063	3.332	0.66	4.652	0.843	0.08	2.796
A-I 3858-61	52.561	16.105	8.871	0.081	2.067	3.808	0.663	4.973	0.864	0.079	2.347
A-I 3867-70	50.584	15.388	8.329	0.08	2.03	4.363	0.637	5.094	0.875	0.079	2.082
S-NIM-S	70.247	18.53	1.502	0.015	0.691	0.687	0.443	15.88	0.045	0.098	0.049
A-U1 2595-2600	56.821	14.062	7.189	0.069	1.828	2.035	1.02	2.821	0.851	0.077	1.075
A-U1 2606-09	46.356	13.244	6.994	0.072	1.703	2.669	0.85	2.743	0.824	0.086	0.935
A-U1 2618-21	56.134	10.52	7.432	0.115	1.774	5.985	1.057	2.017	0.635	0.099	1.26
A-U1 2627-30	67.41	8.687	5.061	0.074	1.432	2.949	0.993	1.72	0.514	0.077	1.048
A-U1 2657-60	70.494	8.89	4.637	0.071	1.292	3.16	0.94	1.833	0.51	0.077	0.809
S-SY-2	64.774	12.637	6.268	0.295	2.897	8.377	4.503	5.059	0.134	0.274	0.044
A-U1 2639-42	67.364	8.776	4.638	0.066	1.307	2.042	1.037	1.901	0.55	0.081	0.989
A-U1 2648-51	65.768	9.656	4.725	0.055	1.381	2.037	1.114	2.097	0.556	0.067	0.872
A-U1 2565-70	62.551	9.493	5.12	0.062	1.445	4.033	0.817	1.97	0.522	0.081	2.269
A-U1 2669-72	69.652	8.699	4.871	0.06	1.269	2.262	0.933	1.762	0.604	0.073	0.899
A-U1 2699-2702	54.314	16.2	7.042	0.069	1.943	1.605	0.93	4.002	0.823	0.077	1.094
A-U1 3257-60	54.133	17.057	6.995	0.049	1.969	0.898	0.895	4.194	0.891	0.068	1.046
Sample name	SiO ₂	Al ₂ O ₃	Fe ₂ O ₃	MnO	MgO	CaO	Na ₂ O	K ₂ O	TiO ₂	P ₂ O ₅	SO ₃

	Si	Al	Fe	Mn	Mg	Ca	Na	K	Ti	P	S
	(%)	(%)	(%)	(%)	(%)	(%)	(%)	(%)	(%)	(%)	(%)
A-U1 3269-72	55.401	16.473	6.778	0.047	1.925	0.895	0.826	4.051	0.851	0.066	1.11
S-S-10	59.89	11.753	4.963	0.109	1.48	0.954	0.137	0.548	0.417	0.054	0.05
A-I 3879-82	50.967	15.821	8.858	0.079	2.022	3.953	0.626	5.494	0.843	0.082	2.534
A-I 3888-91	47.563	14.671	9.082	0.082	1.971	6.185	0.589	5.181	0.807	0.081	3.025
A-I 3897-3900	47.239	14.076	11.019	0.092	1.978	6.757	0.591	4.497	0.741	0.099	4.889
A-I 3939-42	50.979	15.141	9.459	0.086	2.002	4.875	0.612	4.282	0.829	0.084	2.62
A-I 3948-51	50.599	14.951	8.072	0.069	1.968	4.976	0.659	4.916	0.809	0.081	3.973
S-SARM49	118.016	0.208	0.039	-0.002	0.171	-0.024	0.036	-0.01	0.009	0.032	0.012
A-II 3957-60	49.103	14.088	7.602	0.073	1.855	6.088	0.603	4.725	0.768	0.09	SO3
A-II 3987-90	49.384	13.84	7.869	0.076	1.88	5.384	0.635	4.747	0.779	0.087	S
A-II 4017-20	54.154	14.761	7.356	0.066	1.922	6.196	0.639	4.693	0.782	0.087	(%)
A-II 4029-32	54.413	15.816	8.157	0.065	2.04	4.915	0.654	5.168	0.847	0.084	
A-II 4038-40	59.74	12.6	6.807	0.064	1.779	5.76	0.719	3.813	0.72	0.083	5.033
S-FK	100.813	7.881	0.314	0.005	0.563	0.089	0.327	4.87	0.07	0.076	4.246
A-II 4068-71	53.898	15.834	8.584	0.071	2.079	3.314	0.661	4.551	0.876	0.08	4.077
A-II 4077-80	55.359	16.419	8.311	0.069	2.113	2.962	0.657	4.539	0.891	0.08	3.291
A-II 4107-10	69.04	11.186	4.876	0.041	1.558	1.108	0.553	2.996	0.547	0.065	1.986
A-II 4158-61	56.328	17.17	8.665	0.069	2.16	1.562	0.665	5.051	0.9	0.084	0.029
A-II 4227-30	85.34	7.171	2.766	0.028	0.977	1.272	0.606	1.757	0.307	0.053	1.069
S-SY-2	67.184	13.58	6.403	0.301	2.932	8.437	4.517	5.093	0.135	0.274	0.869
A-U1 1760	47.194	12.302	13.107	0.175	2.175	6.351	0.66	2.367	0.793	0.163	0.756
A-U1 1770	48.414	13.292	11.82	0.148	2.192	5.318	0.737	2.574	0.873	0.141	1.059
A-U1 1880	42.126	11.574	9.658	0.194	1.888	10.87	0.644	2.239	0.798	0.186	0.532
A-U1 1890	45.776	10.73	9.63	0.185	1.826	10.19	0.493	2.087	0.744	0.171	0.045
A-U1 2555-60	58.575	10.366	5.89	0.075	1.538	5.977	0.92	2.129	0.597	0.085	2.693
S-SARM49	115.9	0.21	0.039	-0.003	0.169	-0.022	0.042	-0.01	0.009	0.031	2.1
A-U1 3287-90	55.329	14.461	6.427	0.05	1.781	1.771	0.775	3.555	0.765	0.068	5.028
Sample name	SiO2	Al2O3	Fe2O3	MnO	MgO	CaO	Na2O	K2O	TiO2	P2O5	SO3

	Si	Al	Fe	Mn	Mg	Ca	Na	K	Ti	P	S
	(%)	(%)	(%)	(%)	(%)	(%)	(%)	(%)	(%)	(%)	(%)
A-U1 3299-3302	54.838	16.716	6.816	0.047	1.951	0.795	0.91	4.164	0.889	0.067	4.414
A-U1 3308-11	55.154	16.849	6.819	0.046	1.964	0.823	0.944	4.212	0.906	0.073	3.441
A-U1 3317-20	54.11	16.204	6.934	0.057	1.942	1.561	0.936	4.014	0.877	0.083	0.013
A-U1 3329-32	54.299	16.406	7.071	0.051	1.928	1.155	0.901	4.074	0.887	0.069	1.435
S-FK	99.992	7.748	0.311	0.004	0.563	0.089	0.336	4.861	0.07	0.075	1.125
A-U1 3338-41	54.493	17.13	6.802	0.053	2.028	1.565	0.89	4.192	0.904	0.069	1.167
A-U1 3347-50	53.692	16.419	6.919	0.055	1.913	1.364	0.937	4.035	0.893	0.074	1.259
A-U1 3377-80	74.802	8.854	3.221	0.029	1.151	0.577	0.604	1.846	0.409	0.054	1.237
A-U1 3389-92	63.817	13.617	5.882	0.044	1.642	0.607	0.732	3.183	0.677	0.066	0.986
A-U1 3416-19	73.847	8.175	3.216	0.029	1.104	1.487	0.591	1.785	0.389	0.056	0.724
S-NIM-S	70.107	18.456	1.495	0.015	0.71	0.686	0.431	15.87	0.046	0.098	0.048
A-U1 2708-11	57.888	13.207	7.167	0.087	1.667	4.944	1.024	2.971	0.668	0.081	3.721
A-U1 2717-20	60.413	12.493	7.767	0.098	1.672	4.639	0.948	2.709	0.645	0.083	2.557
A-U1 2738-41	59.941	10.702	6.482	0.084	1.445	4.588	1.39	2.211	0.584	0.092	2.102
A-U1 2759-62	53.967	7.333	5.453	0.094	1.273	13.45	0.803	1.707	0.487	0.093	2.772
A-U1 2777-80	57.737	12.946	7.817	0.093	1.726	5.001	1.137	2.846	0.698	0.098	2.639
S-S-10	60.284	11.76	5.027	0.11	1.493	0.956	0.133	0.549	0.42	0.055	0.051
A-U1 2786-92	57.448	13.182	7.727	0.086	1.656	3.989	1.164	2.695	0.695	0.078	2.824
A-U1 2798-2801	56.191	14.585	8.586	0.087	1.767	3.307	0.907	3.049	0.787	0.088	2.955
A-U1 3407-10	69.348	12.812	5.5	0.043	1.616	1.364	0.9	2.924	0.656	0.065	1.148

Appendix B: XRF Analysis – Trace Elements



UNIVERSITY *of the*
WESTERN CAPE

Sample name	Co Co (ppm)	Ni Ni (ppm)	V V (ppm)	Zr Zr (ppm)	Sr Sr (ppm)	Zn Zn (ppm)	Ba Ba (ppm)	Pb Pb (ppm)	Ce Ce (ppm)	Nd Nd (ppm)	Nb Nb (ppm)	Y Y (ppm)	Rb Rb (ppm)
S-NIM-S	-1	38	8	17	76	15	2768	9	-89	-23	46	-4	598
A-A1 3544-46	9	84	83	245	176	218	1003	20	-96	-21	65	37	116
A-A1 3550-52	20	82	91	227	225	8963	3162	1286	-37	-3	75	66	131
A-A1 3558-60	10	74	106	288	192	1197	1093	116	18	12	102	88	179
A-A1 3566-68	18	60	100	299	170	609	864	62	-57	-11	77	73	182
A-A1 3582-84	15	85	107	321	194	974	1226	176	-62	-10	79	70	199
S-S10	28	225	102	216	42	50	191	16	-47	-9	40	8	30
A-A1 3588-90	8	70	80	283	162	211	938	26	-138	-34	73	39	129
A-A1 3598-3600	8	61	78	317	164	225	1041	28	107	39	63	47	137
A-A1 3614-16	18	71	105	269	193	855	1611	126	97	36	65	71	200
A-A1 3606-08	14	85	104	273	172	125	755	24	137	47	63	57	131
A-A1 3622-24	20	66	90	277	166	700	1124	63	-62	-10	67	67	168
S-SARM49	-4	-5	2	5	5	-3	23	9	-101	-28	32	-27	5
A-A1 3630	7	62	77	286	126	232	780	24	42	18	72	70	133
A-A1 3636-38	16	77	99	278	189	1076	1547	95	115	40	68	71	169
A-A1 3644-46	27	107	95	246	203	6155	2067	272	65	26	71	57	151
A-A1 3652-54	17	78	91	286	204	1131	1159	95	-19	2	68	75	165
A-A1 3772-74	23	114	149	244	221	8193	1807	401	-46	-7	70	76	259
S-SY-2	9	10	58	289	198	183	456	-87	36	16	60	196	139
A-L1 3137-40	16	23	82	282	126	64	511	33	107	36	49	54	74
A-L1 3149-52	16	18	80	220	182	64	452	29	46	19	49	57	75
A-L1 3158-61	15	41	91	223	216	134	626	42	3	9	52	66	94
A-L1 3167-70	14	79	53	153	102	63	354	22	-116	-31	39	18	42
A-L1 3179-82	88	156	87	269	142	755	921	74	88	32	50	72	93
S-FK	-14	24	7	32	46	6	716	20	-133	-37	24	-23	81
A1-3670-72	16	78	104	230	162	647	1247	19	-64	-13	110	100	136
A1-3746-48	11	109	86	270	167	334	1084	27	-39	-3	71	48	120
A1-3754-56	21	128	118	267	205	280	1727	54	202	69	67	69	221
A1-3762-64	11	92	95	217	146	292	993	9	-63	-15	114	71	135
A1-3780-82	14	155	122	247	318	3419	1508	203	66	28	80	66	196
S-NIM-S	5	49	8	26	81	14	2751	10	-205	-56	38	-5	622
A-A1 3788-90	18	157	118	304	250	195	1282	30	-41	-4	72	54	177
A-A1 3796-98	14	131	131	240	145	152	641	19	-71	-15	59	50	221
A-A1 3800-02	10	137	130	226	135	167	690	21	84	31	58	52	219
A-L1 1490-1500	6	26	57	121	56	62	149	101	-113	-28	36	1	31
A-L1 1500-1510	1	31	83	191	96	55	181	24	-117	-29	41	31	42
S-S-10	27	234	107	220	43	51	192	16	-70	-16	38	3	30
A-L1 1635-40	16	46	121	269	202	106	592	42	-33	-3	56	67	133
A-L1 1645-50	5	36	102	286	180	95	523	42	-25	-1	45	46	97
A-L1 1655-60	-1	56	95	290	136	66	380	33	-104	-23	43	36	83
A-L1 1665-70	8	35	93	295	125	51	469	21	38	17	46	11	71
A-L1 1675-80	5	44	84	248	149	98	484	31	-126	-31	43	30	59
S-SARM49	-14	12	1	2	2	-3	23	13	-177	-50	33	-28	5
A-L1 1685-90	7	33	58	143	178	94	351	27	50	20	41	11	40
A-L1 1695-1700	5	21	65	172	129	66	397	25	-104	-28	40	20	40
A-L1 1705-10	11	43	87	299	131	98	629	35	-57	-10	45	34	71
A-L1 1715-20	8	55	88	183	134	1490	1082	229	-57	-10	41	33	68

Sample name	Co Co (ppm)	Ni Ni (ppm)	V V (ppm)	Zr Zr (ppm)	Sr Sr (ppm)	Zn Zn (ppm)	Ba Ba (ppm)	Pb Pb (ppm)	Ce Ce (ppm)	Nd Nd (ppm)	Nb Nb (ppm)	Y Y (ppm)	Rb Rb (ppm)
A-L1 1755-60	13	40	89	160	254	75	442	29	25	16	52	36	71
A-L1 1765-70	6	26	64	136	142	56	513	26	-175	-46	42	6	46
A-L1 1775-80	12	34	94	177	147	70	530	24	63	24	48	27	82
S-S-10	33	209	95	219	44	43	194	18	-51	-12	37	12	28
A-L1 3227-30	106	36	80	270	201	125	1427	37	116	41	59	68	93
A-L1 3248-51	43	26	68	231	104	147	1424	28	42	19	49	52	78
A-L1 4149-52	17	57	138	168	149	126	1124	36	67	30	56	71	204
A-L1 4197-4200	19	54	144	192	139	268	1209	55	74	30	55	66	202
A-I1 4218-21	3	19	54	110	57	122	1702	38	-102	-26	38	-12	69
S-SARM49	0	6	1	2	5	-1	24	10	73	24	31	-31	6
A-I1 3909-12	23	41	143	167	180	132	441	38	-43	-6	59	74	182
A-I1 3978	10	47	133	191	171	232	436	21	13	10	60	71	182
A-I1 3999-4000	16	34	116	170	222	92	329	25	-27	0	55	64	142
A-I1 4047-50	16	36	120	201	142	97	421	18	76	28	58	56	141
A-I1 4089-92	1	26	63	99	55	34	376	17	-142	-36	38	-6	59
S-NIM-S	-1	35	7	15	75	17	2764	14	-227	-64	47	4	620
A-L1 3188-91	43	41	56	172	100	229	1106	32	80	27	41	24	59
A-L1 3197-3200	49	49	63	198	133	147	1306	37	-44	-8	43	14	57
A-L1 3239-41	32	52	90	305	141	741	1619	102	-37	-4	54	64	104
A-L1 3209-12	25	42	79	330	67	224	928	48	45	20	46	8	84
A-L1 3218-22	65	38	97	243	120	145	1413	38	1	6	52	57	107
S-SY-2	1	16	60	286	194	176	452	-89	205	68	56	188	136
A-L1 1785-90	21	36	100	238	140	174	624	25	28	15	49	64	91
A-L1 1795	21	32	99	259	120	85	362	17	1	5	54	58	101
A-L1 3107-10	20	30	92	277	230	70	357	28	50	21	51	72	87
A-L1 3119-22	20	27	81	260	147	80	236	23	-77	-17	44	53	78
A-L1 3128-31	16	36	83	277	126	98	618	28	-61	-12	46	49	84
A-I1 4169-70	20	41	151	193	172	112	1161	28	8	9	56	64	197
A-I1 4179-82	23	23	86	173	134	60	2402	23	-9	4	46	9	107
A-I1 4188-91	24	59	130	180	145	106	2281	30	35	18	54	46	180
A-I1 4197-4200	25	54	152	200	141	271	794	65	71	26	57	66	203
A-I1 4239-42	26	33	129	187	158	134	2785	52	75	27	54	39	154
S-SY-2	11	8	55	281	188	175	458	-91	236	75	62	174	137
S-FK	-1	24	5	32	43	5	715	17	-90	-23	22	-23	76
A-I1 4098-4101	63	155	98	133	91	966	1304	294	-58	-11	47	34	115
A-I1 4119-21	33	42	103	144	115	106	1717	29	-32	-3	47	11	143
A-I1 4128-30	35	45	116	168	148	120	2034	35	-97	-22	49	37	151
A-I1 4137-40	34	40	117	222	138	116	3859	39	117	40	56	46	161
A-I1 4149-52	20	41	134	144	120	97	999	32	58	25	52	1	176
S-NIM-S	-6	44	9	21	78	16	2762	5	-11	0	42	7	625
S-NIM-S	7	49	10	22	74	14	2767	5	-178	-48	40	9	591
A-I 3927-30	17	46	138	188	180	118	430	37	62	26	56	71	181
A-A1 3572-74	4	40	139	188	179	116	423	32	156	53	58	66	179
A-I 4209-12	25	44	152	195	135	250	1164	39	137	47	61	69	208
A-I 3849-52	13	47	154	178	127	123	362	36	200	65	55	73	203
A-I 3858-61	11	41	154	180	144	137	391	28	18	12	58	75	199
A-I 3867-70	14	51	160	186	162	207	579	33	-176	-43	55	65	194

Sample name	Co Co (ppm)	Ni Ni (ppm)	V V (ppm)	Zr Zr (ppm)	Sr Sr (ppm)	Zn Zn (ppm)	Ba Ba (ppm)	Pb Pb (ppm)	Ce Ce (ppm)	Nd Nd (ppm)	Nb Nb (ppm)	Y Y (ppm)	Rb Rb (ppm)
A-U1 2627-30	3	36	84	290	136	346	2260	57	-56	-10	52	11	71
A-U1 2657-60	7	33	87	236	145	73	882	19	1	7	47	-10	77
S-SY-2	17	16	55	274	173	172	457	-91	-61	-10	58	168	135
A-U1 2639-42	4	22	80	349	99	94	1438	35	-57	-11	49	15	72
A-U1 2648-51	1	42	86	297	111	59	1208	24	155	53	45	-3	84
A-U1 2565-70	3	22	81	264	131	48	475	19	16	10	49	41	79
A-U1 2575-80	22	62	104	216	107	515	888	138	170	60	54	46	101
A-U1 2585-90	7	42	123	257	123	135	722	54	111	39	56	68	139
S-S-10	27	218	100	220	39	45	192	17	25	11	41	2	28
A-U1 2678-81	10	36	101	309	134	194	1291	46	33	16	50	53	109
A-U1 2669-72	10	33	86	492	103	81	1328	30	74	28	44	11	67
A-U1 2699-2702	9	41	127	260	126	741	1877	120	-72	-14	55	39	173
A-U1 3257-60	12	40	146	196	94	254	442	36	-35	-5	53	10	206
A-U1 3269-72	17	41	143	194	85	171	411	24	15	9	56	16	198
S-S-10	25	207	101	223	40	42	194	17	-89	-23	41	31	25
A-I 3879-82	13	47	149	164	180	109	448	32	112	40	60	74	186
A-I 3888-91	18	45	146	150	170	101	421	42	-77	-15	56	67	172
A-I 3897-3900	35	55	136	139	186	140	324	54	117	40	58	65	162
A-I 3939-42	23	56	140	172	151	170	346	31	-53	-7	56	65	171
A-I 3948-51	11	43	138	175	163	94	353	26	-14	4	58	77	181
S-SARM49	-8	-1	0	1	7	-1	23	8	-71	-18	28	-39	6
A-I1 3957-60	6	36	132	182	153	125	373	33	-118	-28	53	64	172
A-I1 3987-90	11	41	138	177	151	95	340	29	-41	-5	55	54	172
A-I1 4017-20	14	33	136	185	165	77	355	20	-191	-49	57	68	163
A-I1 4029-32	5	49	139	189	174	97	382	29	39	20	58	67	176
A-I1 4038-40	0	39	121	246	168	77	384	22	69	27	52	54	143
S-FK	1	28	7	32	46	7	714	16	-73	-19	22	-24	80
A-I1 4068-71	23	44	159	188	131	104	394	32	2	6	54	57	190
A-I1 4077-80	11	49	158	185	116	119	359	30	-37	-4	58	65	198
A-I1 4107-10	25	51	104	151	72	109	1060	33	75	28	43	-8	115
A-I1 4158-61	24	45	163	185	115	122	460	33	99	34	55	77	214
A-I1 4227-30	8	39	58	94	43	67	334	16	-54	-10	41	-4	71
S-SY-2	9	17	59	282	185	175	464	-91	197	64	60	173	137
A-U1 1760	30	45	142	165	166	107	210	24	32	17	55	69	103
A-U1 1770	26	45	150	190	156	111	230	27	-9	5	54	78	116
A-U1 1880	28	34	128	241	238	123	259	31	33	17	57	67	98
A-U1 1890	20	33	126	233	242	146	251	31	-48	-5	53	61	97
A-U1 2555-60	9	38	89	319	184	46	643	22	-95	-21	51	35	92
S-SARM49	-3	6	1	4	4	0	23	11	-147	-41	30	-38	5
A-U1 3287-90	35	76	127	172	93	152	357	27	49	20	54	33	161
A-U1 3299-3302	32	44	142	204	97	195	367	38	50	22	51	20	209
A-U1 3308-11	16	49	140	208	92	223	606	35	-87	-19	56	24	206
A-U1 3317-20	20	48	141	205	104	131	591	32	62	25	56	22	196
A-U1 3329-32	14	50	145	211	105	142	510	29	-84	-19	56	27	205
S-FK	8	29	5	32	47	10	707	19	-227	-63	22	-21	80
A-U1 3338-41	21	47	149	214	103	104	447	34	32	16	57	16	206
A-U1 3347-50	23	36	148	214	108	118	436	28	-88	-20	55	23	199

Sample name	Co (ppm)	Ni (ppm)	V (ppm)	Zr (ppm)	Sr (ppm)	Zn (ppm)	Ba (ppm)	Pb (ppm)	Ce (ppm)	Nd (ppm)	Nb (ppm)	Y (ppm)	Rb (ppm)
A-U1 2708-11	12	38	105	285	164	172	582	33	-91	-20	52	59	127
A-U1 2717-20	8	26	102	275	157	156	413	43	0	6	54	52	118
A-U1 2738-41	7	37	87	387	175	290	1132	80	-68	-13	49	26	91
A-U1 2759-62	9	28	90	345	325	72	354	30	23	14	52	33	76
A-U1 2777-80	12	43	104	316	166	94	512	26	-63	-11	51	56	125
S-S-10	27	210	106	222	43	43	194	16	-120	-32	36	21	25
A-U1 2786-92	-1	34	107	300	145	86	534	32	163	54	51	52	121
A-U1 2798-2801	18	40	123	274	123	99	378	33	-26	0	57	73	141
A-U1 3407-10	26	47	117	203	113	183	372	35	111	37	53	2	144



UNIVERSITY of the
WESTERN CAPE